Vector Controlled Induction Motor Drive Systems

by

Aravind S. Bharadwaj

Dissertation submitted to the faculty of the
Virginia Polytechnic Institute and State University
in partial fulfillment of the requirements for the degree of

DOCTOR OF PHILOSOPHY

in

Electrical Engineering

APPROVED:

Dr. Krishnan Ramu, Chairman

Dr. William T. Baumann

Dr. Jaime De La Ree Lopez

Dr. John W. Layman

Dr. Charles E. Nunnally

February 18, 1993

Blacksburg, Virginia

Vector Controlled Induction Motor Drive Systems

by

Aravind S. Bharadwaj

Committee Chairman: Dr. Krishnan Ramu

Department of Electrical Engineering

(ABSTRACT)

Over the years, dc motors have been widely used for variable speed drives for numerous industrial applications despite the fact that ac machines are robust, less expensive, and have low inertia rotors. The main disadvantage of the ac machines is the complexity in control and the cost of the related circuitry. With the advent of vector control, ac machines have overcome this disadvantage and are being employed in different applications where dc motors were traditionally used. The *d-q* modeling, simulation and analysis of the different vector control strategies are presented with the results for different configurations of the drive system. A Computer Aided Engineering (CAE) package has been developed to serve as a modeling tool for the entire drive system including the motor, converter, controller and the load. This package provides a user friendly environment to perform an interactive dynamic simulation to assess the torque ripple, losses, efficiency, torque, speed, and position responses and their bandwidth and evaluates the suitability of the drive system for a particular application. By utilizing the similarity between the vector controlled induction motor drive and the separately excited dc motor, a method for the design and study of the speed controller for the speed/position drive is formulated. This results in the simplicity of the design approach and helps in improving the performance of the drive system. Finally, a novel sensorless vector control scheme which eliminates the position transducer is formulated. The only input for this control scheme is the stator current measured by current transducers. The modeling, simulation and analysis for the different schemes is performed using the CAE package and experimental verification is performed with the aid of a DSP based drive system.

ACKNOWLEDGEMENTS

In the name of God, I would like to thank my advisor, Dr. Krishnan Ramu, who has been a constant source of support and guidance throughout my graduate studies. I am very grateful for his training which will be a valuable resource in my professional career.

I owe it to Dr. Nunnally for his advice and concern, especially during my first year of graduate school. His generous encouragement and support throughout my stay here has been a great source of inspiration. I am also deeply indebted to Dr. De La Ree for helping me in my employment search and would never forget his timely help and concern for my well being. I also wish to thank Dr. Baumann and Dr. Layman, for consenting to be in my committee and for their input.

I would like to thank Mr. Dean Lloyd of Lloyd Electric Company, Mr. Herb Johnson of A.O. Smith Corporation, Mr. Iftikhar Khan and Dr. William Gordon of Texas Instrument, Inc., Mr. Tom Battely of Teknic, Inc., Mr. Bob Lineberry for helping me with the resources to accomplish this work. I also acknowledge the help and cooperation of Dr. Geun-hie Rim, Krishna Chintam, Ralph Bedingfield, Prasad Ramakrishna, and all the members of the Motion Control Systems Research Group, past and present.

I am very grateful to all my friends and my family who have been a great source of support and comfort. In particular, words fail to express my gratitude to Kannan, Partha and Ravi. All this would not have been possible but for the support, inspiration and encouragement of my parents. I am grateful to my parents, sisters, and in-laws, for their patience and understanding.

Most of all, I would like to express my deep indebtedness to my wife, Radha, who has been a constant pillar of support and understanding. I dedicate this dissertation to her for all her sacrifices to help me get this work accomplished.

TABLE OF CONTENTS

LIST OF FIGURES

Chapter 1
INTRODUCTION

1.1 OVERVIEW

Variable speed motor drives are essential in a variety of applications ranging from textile mills, rolling mills, paper mills, traction, coal industry to robots, machine tools, and fan and pump applications. Over the years, dc motors have been predominantly employed for variable speed drives for high performance applications. The ac motor drives, such as the induction motor drives have the following advantages over their dc counterpart [286, 156]:

1. Absence of commutators or brushes eliminates commutator problems due to heavy loading or high $\frac{di}{dt}$ effects.
2. Their simple and robust construction requires less maintenance.
3. Higher motor efficiency results in higher overall drive system efficiency.
4. Lower moment of inertia leads to the reduction in the acceleration of power.
5. Higher voltage capability of the motors reduces the cable size of the main circuit.
6. In some applications such as the mine hoist drives, the capability of stall or zero speed operation minimizes the application of mechanical brake. This results in shorter trip times and better utilization of the equipment. Also, sensing the load torque direction would enable the application of the starting torque in the right direction realizing a smooth start.

In spite of all the above mentioned advantages of the ac drives, there was a major reluctance on the part of the industry to replace the existing dc drives. This can be attributed

to the following reasons [167, 166]:

1. The cost of the ac power converter far exceeded that of a phase controlled, line commutated reversible converter for the dc machine.

2. While the mechanical construction of the dc motor is complicated, their control is simple due to the orthogonal field and armature axis. On the other hand, the ac machines are multi-variable non-linear structures and the rotor currents are inaccessible. The torque is given as a function of the stator and rotor currents. Since the rotor currents are not accessible without modifications to the machine structure, the control has to be performed through the stator voltages and currents. Hence a complex control scheme is required to match the converter fed dc drive. This requires sensing devices, nonlinear electronic components and other devices which increases the cost and decreases the reliability of the overall drive system.

The recent advances made in the field of semiconductor technology and microelectronics, has reduced the impact of these constraints. With the advent of vector control, the control of the induction motor is achieved similar to that of a separately excited dc motor by providing independent channels for torque and flux control, induction machines are fast replacing the dc drives for these applications in the industry [22, 90].

This chapter is organized as follows. The next section describes in detail the evolution of the vector control principle and discusses the various vector control strategies. Several examples involving the application of vector control technique in different industrial applications will be cited to demonstrate its growing popularity. A comprehensive literature survey is performed to get an insight into the development of this technique and also to identify the areas in which more research has to be performed. This is followed by the scope of this dissertation in Section 1.3. The various issues to be resolved are identified in this section and the organization of the dissertation is described in the subsequent section.

1.2 STATE OF THE ART

The complexity of the control associated with the induction machines was alleviated by the advent of vector control in the early '70s [25, 90]. The main difference between vector control and the existing schemes for induction machines, such as the constant volts/hertz or slip frequency control, is that the frequency, and voltage or current imposed on the motor are controlled without neglecting the phase relationships [129]. Without appropriate phase angle control, vector control degenerates into conventional slip frequency control resulting in poor dynamic characteristics [353]. Vector control was compared with the slip frequency control and found to have a faster torque response [122]. Quick torque response is achieved even if a load is applied and the drive system reaches steady state instantaneously. A comparative study of vector control with the torque angle control and synchronous control has been performed and the advantages of vector control highlighted [148]. Vector control is also known as decoupling control since the stator currents are decoupled into separate torque and flux producing channels. It is also known as field oriented control due to the fact that the control is based on the field orientation of stator currents.

1.2.1 Classification

Two vector control strategies were formulated during the late '60s and decoupling of the stator currents was achieved either by the direct measurement of the flux [24] or by estimation from the motor model [88]. Both these methods are based on the space phasor modeling of the induction machines [221]. The measurement technique is also known as flux detection control [162] or flux feedback control [226, 225] since the flux is measured and fed back into the control circuit. On the other hand, the estimation technique is known as flux feedforward control or slip frequency control due to the fact that the slip frequency is calculated from the model for flux estimation.

The flux feedback control uses Halls sensors or search coils to sense airgap flux. Alternately the rotor flux is estimated based on the stator current vector, voltage vector and/or

rotor speed. The flux feedforward control determines the rotor flux from the stator current signals and rotor speed. An alternate method uses the terminal voltages and line currents for determining the stator flux derivatives which are then integrated to obtain the flux. Or else, the terminal voltage, line currents and rotor speed are used as observer quantities to determine rotor flux [4].

1.2.2 Direct Vector Control

The direct measurement technique was popular in the earlier stages due to the sensitivity of the estimation techniques to motor parameter variations [23]. This technique also provided instantaneous and well damped control of torque. The earlier forms of this type of control involved the measurement of the airgap flux. Field sensing devices utilizing Hall effect were installed at two or more places within the airgap of the motor to measure the airgap flux [169]. The mechanical and thermal stresses on these semiconductor devices caused problems in measurement. The rotor slot harmonics are filtered and only the fundamental components are extracted. A detailed description of the placement of the sensing coils for airgap flux measurement has been presented in [251]. Amorphous microcore sensors were also used to detect the magnetic field and to sense the torque and rotor currents [219].

Various schemes have been proposed for the sensing of airgap flux. A method for flux control independent of stator resistance variation based on the magnetizing current is presented in [1]. This measurement technique performs satisfactorily up to 1 Hz but the performance degrades at lower speeds. Another method for the measurement of the airgap flux used the tapped stator windings of the motor [357, 46]. An airgap flux sensing method was proposed using search coils and providing an open loop flux estimator using the predictor corrector algorithm [73]. The major disadvantage of airgap flux oriented control is that the system becomes unstable above a certain critical load [12].

The problem of instability is overcome by using the rotor flux instead of the airgap flux. Since the rotor flux is not directly accessible, the measurement techniques are even more complex [9]. A torque drive vector control using the rotor flux orientation presented

problems with the integrator adjustment for obtaining the field angle using LEM transducers [16]. Another method which measures the stator and rotor flux using Halls sensors to obtain the field angle and rotor flux, achieved four quadrant operation for fast torque response [63].

The measurement of the rotor flux is dependent on the leakage inductance. A method using the measurement of the stator flux has been proposed to overcome this effect [340]. The maximum torque capability of this orientation was found to be equal to that of a properly tuned flux feedforward vector control system. The limitation of the stator flux is that for low speed operation, it is difficult to obtain a good performance [80]. This is due to the fact that the stator resistance has to be known or estimated in order to calculate the stator flux from the terminal voltages.

The rotor flux measurement technique is the most widely used for the flux feedback vector control strategy. It can be noted that the major disadvantage of the various flux measurements using different methods is the deterioration of performance at low speeds, i.e., 3-5% of the rated speed [113]. Also, the delay time in signal processing affects the dynamic behavior of the drive system because it results in stator current coupling [11]. This effect can be reduced by employing simplified decoupling circuits for the machine and the inverter. The main effort in research towards this direction is the elimination of the transducers and parameter insensitivity.

1.2.3 Indirect Vector Control

Despite the strong incentives such as the absence of transducers and wide speed range operation, acceptance of the flux feedforward technique has been slow due to its dependence on the rotor parameters. With the advent of various parameter adaptation schemes to alleviate this problem, it has gained more attention and is widely used for different industrial applications. A nonlinear model for the saturated induction machines is also derived to take into account the saturation effects on the parameters [320]. The rotor flux is estimated from the stator currents and rotor speeds, or from line voltage and current measurements. The field angle is obtained from the induction motor model in synchronously rotating reference

frames.

The components of the rotor flux are also estimated using the state observer technique and its dynamic and steady state behavior analyzed [14]. In another method, the flux is estimated using the state observer technique by having the rotor speed and the dc link voltage as measured quantities [154, 153]. This method for the current source inverter generates the commanded currents from which the rotor flux and the electromagnetic torque are estimated. A dual observer technique is employed which simplifies the speed controller design [44]. Torque control is achieved by using a predictive observer and employing separate torque and flux feedback loops [89].

An analytic method was presented to detect the spatial position and magnitude of the rotor flux based on the machine structure using voltage sensors [103]. Another approach which calculates the speed from the structure of the motor and the measured stator phase voltages is presented [105, 106]. This method is independent of electromagnetic parameter variation but is not valid for low speed operation. The effects of the machine structure on the torque pulsations were studied and the slot rotor structure is found to be unsuitable for vector control due to problems at low frequencies [312]. Vector control for special motor structures such as the twin stator induction motor has been proposed [305]. Airgap flux control for a double cage motor with a current controlled inverter drive was proposed [50]. This provides deep bar compensation to avoid rotor resistance sensitivity and improve the transient performance [48]. Current control for a doubly fed induction motor was proposed in [323]. Vector control has been employed for spindle applications with wide constant power range using dual winding motor [159]. A larger operation range before employing field weakening is achieved by winding changeover.

1.2.4 Parameter Sensitivity and Adaptation

The major disadvantage of the indirect vector control scheme is that it is machine parameter dependent since the model of the motor is used for flux estimation. The machine parameters are affected by variations in the temperature and the saturation levels of the

machine [140, 189]. Parameter sensitivity of the indirect vector controlled induction motor results in steady state errors in torque and flux and enhanced losses reducing the output of the drive system and transient oscillations in flux and torque. The incorporation of parameter adaptation schemes is required to offset these effects. Numerous parameter adaptation schemes have been proposed earlier. Most of the schemes are themselves dependent on some machine parameters and hence produce different steady state errors which can be used as a criterion for evaluation of these schemes. The manner in which a scheme affects the dynamic behavior in terms of bandwidth and stability can be used to assess the advantages of one scheme over the other. These schemes are classified depending on the extent of the use of the induction motor model, shown in Fig. 1.1. Parameter adaptation schemes are classified into direct and indirect methods [135].

Direct Compensation Schemes

The direct method of compensation schemes can be broadly classified into two categories based on the measurement of the parameters, i.e., either by injecting an external signal and measuring the parameters or by measuring directly the relevant parameters. They can further be classified depending on their use of additional transducers or on their dependency on the motor parameters.

Injection of signals using additional transducers

In the first category, the compensation signal is measured by the injection of some test signals. Some of these schemes use additional transducers other than the current and speed sensors required in an indirect vector control scheme [278, 287, 288, 326]. The scheme proposed in [287] uses the Model Reference Adaptive System (MRAS). A sinusoidal signal is injected into the flux producing axis of the stator current so that the rotor resistance is compensated, even when the flux producing current is zero, by satisfying the Popov's integral inequality. A similar approach is adopted in [278] and the compensation is provided by combining a high frequency ac component to the stator current. Both these methods are influenced by the variation of the stator resistance and require transducers such as search

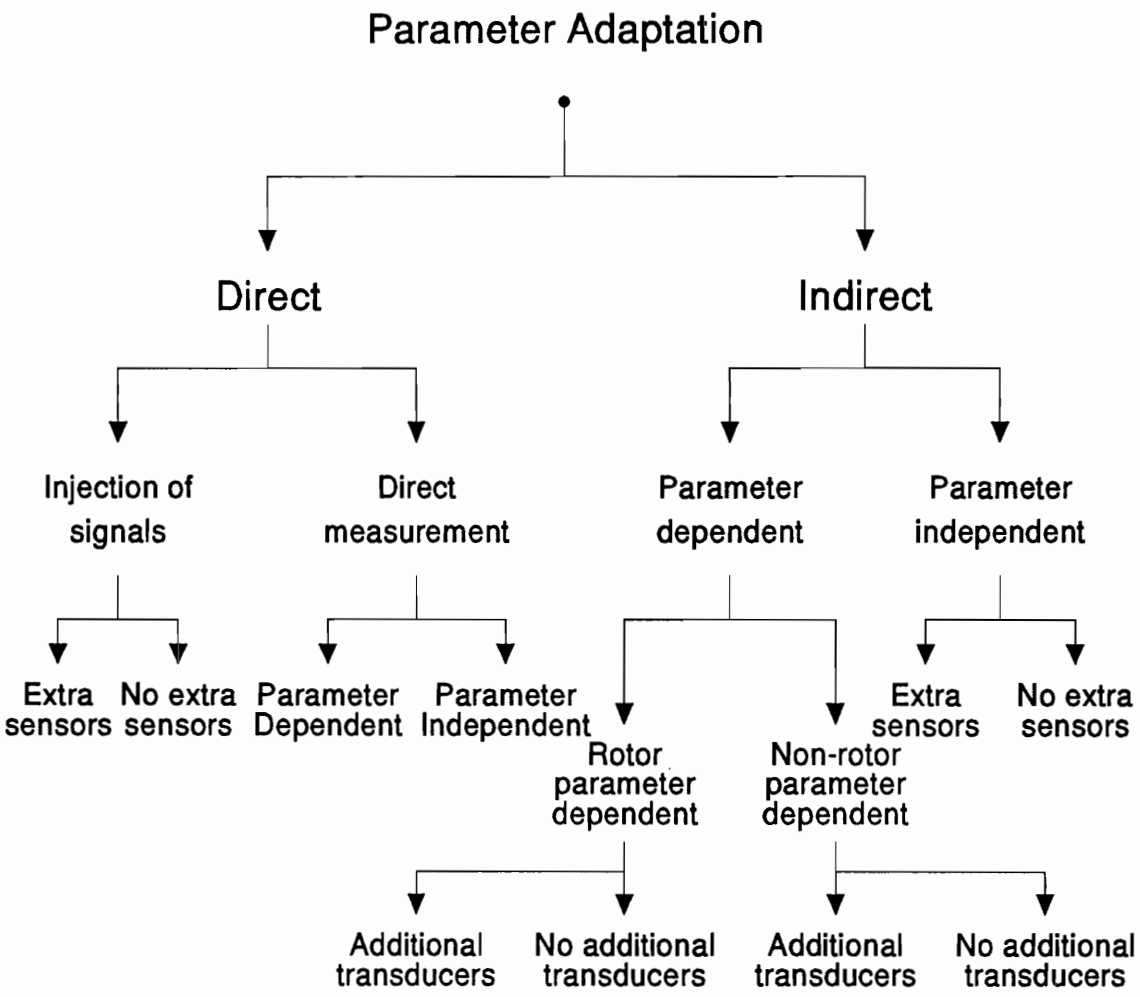

Figure 1.1: Classification of Parameter Adaptation Schemes

coils. In the scheme proposed in [288] for identification of rotor resistance including zero speed operation, a high frequency ac component is injected in the field component of the stator current to produce a high frequency ripple in the rotor flux. By measuring the ac component of the rotor flux, a change in the rotor resistance is detected which is used for parameter compensation. A low cost scheme useful in low performance applications has been proposed to set the controller gain automatically without the need for extensive testing [326]. In this scheme, the only additional signal required is the feedback signal from one of the motor line to line voltages. The rotor time constant is measured by injecting a single phase ac current and the voltage transient that occurs when this test current is switched to dc is observed.

Injection of signals without additional transducers

The requirement of additional transducers is undesirable as it increases the complexity and cost of the scheme and reduces its reliability. This disadvantage is eliminated in other schemes which inject a test signal and sense the corresponding output to provide compensation [68, 197, 198, 264]. One of the earliest methods used a level characteristic signal, similar to the white noise having an impulse shaped correlation function, and correlated with the output to check for error [68]. But the disadvantage of this scheme is that it is difficult to identify the rotor resistance when the induction motor has zero steady state torque. Also the injected signal may cause undesirable interference with the performance of the drive. Direct monitoring of the alignment of the flux and torque producing stator current component axes is also performed by injecting a negative sequence current perturbation signal [197, 198]. In this scheme, the voltage corresponding to the negative sequence is sensed and resolved into d and q axes components. Here the parameters are determined on-line. Another scheme superimposes a test signal on the voltage reference and the compensation is provided by monitoring the instantaneous electromagnetic energy and this scheme is independent of the stator resistance [264].

Direct Measurement and parameter dependent

In the other class of schemes of the direct method, the compensation signal is generated

by the direct monitoring and measurement of motor parameters and alignment of the flux and torque axis [119, 167, 349]. The scheme proposed in [349] employs additional transducers and the compensation signal is generated by the direct measurement of the induced voltage. The compensation signal is dependent on the rotor inductance and this reduces the reliability of the scheme. The compensation signal can also be generated by using either the magnitude or the phase of the induced voltages. In the scheme proposed in [167], the error function is generated by using the vector product of the measured and the calculated values of the induced voltages. A modified method proposed in [119] uses only the phase of the measured and calculated values of the induced voltages. Both these methods are parameter dependent and require additional transducers for compensation.

Direct Measurement and parameter independent

The major disadvantage of the schemes in the previous section is their dependency on the machine parameters which reduces their reliability. A simple method was proposed for rotor flux control valid both in steady state and transient operation based on the indirect measurement through the rotor and stator currents [191]. The rotor currents are directly measured using two Hall's transducers placed in quadrature on the shields in front of the rotor ring. The stator reference currents are derived from these measurements which maintain the rotor flux constant.

Indirect Compensation Schemes

Due to the difficulty in directly measuring all the parameters, the indirect methods have gained more attention in practical applications. In the indirect method a variable other than L_r, R_r and L_m can be measured and tracked and the error due to the difference with its commanded value provides an estimate of the deviation of the parameter from its nominal value. For example, the variables may be reactive power, modified reactive power, airgap power, temperature, etc.

Parameter Dependent

Most of these schemes are dependent on the machine parameters. The variations in

these parameters affect the accuracy of the parameter adaptation method itself. Various schemes have been proposed based on the Model Reference Adaptive Control (MRAC) technique and most of them fall in this category. In these schemes, the motor adapts to the changes in the motor parameters after the initial identification. The adaptation functions by creating an error signal between the motor model reference and an estimated quantity based on motor outputs. This error will modify the gain in the system until the error is driven to zero. A tuning algorithm based on this principle was proposed using the torque model of the controller [184].

Rotor Parameter Dependent using additional transducers

Some of the compensation schemes are dependent on the rotor parameters. A subset of these schemes use additional transducers [72, 95, 103, 131]. One of the earliest schemes proposed for rotor time constant compensation is not affected by the stator resistance but dependent on the leakage inductances [72]. The compensation is provided by defining a function, modified reactive power in this case, which is computed using the stator currents and voltages. A variation of this scheme which does not require any more additional transducers and some integration of key signals was proposed later [131]. The scheme proposed in [95] is based on the evaluation of the stator current trajectory from a dynamic response of the induction motor to the PWM switching sequence and this requires additional voltage transducers. An analytic method was presented to detect the spatial position and magnitude of the rotor flux based on the machine structure using voltage sensors [103]. In this scheme, the parameters are identified by observing the stator voltage corresponding to a stator ramp current.

Rotor Parameter Dependent without additional transducers

Several schemes which eliminated the requirement of additional transducers were also proposed [6, 231, 236, 237, 283, 313, 314, 351]. A scheme was proposed for the estimation of parameters applicable to both steady state and transient operation [6]. In this scheme, parameter compensation is accomplished by a set of correction factors obtained from the sensitivity analyses of the performance characteristics. The correction factors are generated

using the partial derivatives of the variables with respect to the parameters. In the scheme proposed in [283], the compensation signal is generated from the error in the estimation of the flux and the rotor current component without any additional transducers. This scheme is dependent on the mutual and the rotor inductances. A scheme using the Kalman filter with the white noise component contained in the three phase PWM switching sequence was proposed [351]. In this scheme, the result is computed in less than a minute, given an accurate value of the magnetizing inductance. The limitation of this scheme is that the load conditions should change gradually and is valid only beyond 0.05 p.u. speed for the effective functioning of this compensation scheme. Another method based on the discrete MRAC for identification and compensation of the rotor resistance was proposed [313, 314]. Instead of the direct compensation for the rotor resistance the slip frequency can also be adjusted. One such scheme is implemented in a microprocessor by simulating the constant parameter motor in parallel with the actual motor [231]. Another scheme in which the flux is sensed from the motor terminal voltages and currents, without Hall sensors or sensing coils was also proposed in [236, 237]. But this scheme is also dependent on the rotor parameter.

Non-Rotor Parameter Dependent using additional transducers

The major disadvantage of the schemes discussed in the previous section is that the error function controlling the compensation itself is dependent on the motor parameters directly affected by the temperature and saturation. A novel scheme has been proposed which eliminates this problem and is dependent only on the stator resistance [41, 42]. This scheme uses airgap power equivalence for compensation and does not need any additional transducers for sensing parameter variation. This scheme is one of the simplest to implement and has the speed of response required for many high performance industrial applications. Another scheme dependent only on the stator resistance requiring voltage transducers is based on the terminal voltages, currents and shaft speed [290]. In this scheme, the rotor resistance is estimated using tables for mutual inductance and measured terminal quantities.

Non-Rotor Parameter Dependent without additional transducers

Several schemes were proposed which were dependent on non-rotor parameters and

require no additional transducers [7, 104, 222, 224, 256]. The schemes proposed in [7] and [104] are based on the instantaneous input power and electromagnetic torque, respectively. These schemes are derived from a knowledge of the stator inductance and are valid only in steady state operation. A simple scheme using the dc link power measurement to estimate the steady state torque and its use in the analytic calculation of the rotor time constant was proposed [224]. This is more applicable to steady state than under dynamic operation. A correlation method using system information from the stator current trajectory to derive the error angle between the actual flux axis and that of the model using differential equations and dependent on the stator resistance was proposed [222]. Another MRAC scheme which is dependent on the stator inductance and stator resistance requiring no additional transducers was also proposed [256].

Parameter Independent with additional transducers

Some schemes which are independent of the machine parameters were also proposed and some of them require additional transducers [60, 201, 235, 321, 322]. The scheme proposed in [235] is based on the slip frequency control with the torque producing current which is calculated from the stator voltages and currents. The magnitude of the rotor flux is derived from the magnetic energy independent of the stator resistance and without any flux transducers. Another algorithm using the hierarchical recursive algorithm to estimate the stator speed and parameters by measuring the stator currents and voltages has been presented [201, 321, 322]. In this scheme, the nonlinear model is transformed into a linear regression model and the variation of parameter is tracked to provide compensation. This scheme has been verified by simulation but is yet to be implemented. The motor parameters are also identified by exciting a normal model and the trajectory sensitive model with the torque component of the stator current and measuring the actual torque [60].

There are numerous variations of the conventional vector control scheme depending on the application involved. These techniques will be discussed in the following paragraphs.

1.2.5 Variations of Vector Control

A variation in the conventional indirect vector control schemes employs the rotor reference frame model for estimating the rotor flux [276, 275]. This facilitates easier monitoring of the rotor speed and the motor transfer function exhibits minimum variation with the rotor speed. This technique has been used for torque control of high performance applications such as mine hoist drives. The main disadvantage of this system is the sensitivity to the rotor time constant.

The field acceleration method has been proposed as an alternative for vector control [347]. It is identical to vector control in basic principle and provides fast torque control [117]. It is based on the equivalent circuit modeling and was attempted for traction applications [343]. The magnetic field in the airgap is kept at constant amplitude and the speed is controlled to produce a desired value of torque. By accelerating or decelerating the rotation of the airgap flux, fast torque control is achieved. A comparative study showed equivalent transient response for vector control and field acceleration methods [91].

A cycloconverter fed simulator following vector control for a wide speed range has been proposed for rolling mills [88, 100]. The comparison of current is performed in the d-q reference frame instead of the three phase reference to eliminate phase delay. This system is characterized by high speed accuracy, quick response, high power factor and a wide range of field weakening operation. A Model Reference Adaptive System was also presented for extending the operation in the field weakening mode [123]. Another variation of the vector control theory was proposed to achieve quick torque response by controlling the motor and the inverter together as a single unit resulting in reduced parameter sensitivity [295]. Space vector modulation is employed in this technique to achieve quick response using current and voltage sensors [294]. The flux is maintained at prescribed levels by using hysteresis control. This results in reduced torque ripple, low harmonic loss and low noise [293]. A similar method was proposed for direct stator flux and electromagnetic torque control [355]. Based on the theory of space vector modulation, a torque angle control for

a current source inverter fed induction motor drive is also studied [20]. The relationship between the developed torque, rotor flux and torque angle is analyzed and the torque control drive is implemented based on this principle [21]. A method for high performance control of rotor flux which is parameter insensitive is proposed using double hysteresis loop to control the flux and stator current [245].

A universal theory of indirect vector control for all ac machines based on the modeling of the salient pole synchronous machines is presented [226]. Scalar decoupled control is another approach which is very similar to indirect vector control in steady state operation [31]. It is obtained by a feedforward transfer function for both voltage and current controlled drives. A synchronous watt torque feed back control is another variation of vector control which provides better torque control [85]. This involves an additional synchronous torque loop.

Another approach proposed for control of induction motors is the sliding mode control which has a good dynamic response, disturbance rejection, low parameter sensitivity [259]. A digital implementation was achieved for which only the bounds of the parameters have to be known [30]. The main disadvantage of this control is the mathematical complexity of this approach which is an impediment for practical realization. Direct self control measures the stator current and flux linkage to control the electromagnetic torque for the entire speed range including field weakening [55]. Speed regulation is achieved using no speed sensors using this control strategy [8].

Vector controlled induction motor drive systems are normally voltage source or current source inverter fed drive systems. A quantitative analysis of the current source and voltage source inverter fed induction motor drive has been presented [147]. The small signal transfer function evaluation has been evaluated for both the strategies using the state variable approach given in [175]. The current source inverter reduces the harmonics, torque ripple and increases the overall efficiency of the drive system [262]. But it presents torque fluctuation, low speed response and power factor [238]. Decoupling control with controlled voltage source exhibits quick rotor response and less sensitivity to rotor resistance variation

[232]. A voltage source inverter to generate current commands with improved power factor is presented in [130].

The PWM technique is widely employed for inverter fed induction motor drives to obtain a fast torque response and flux control [18, 81]. Sinusoidal PWM is commonly applied to analog drives and step PWM is utilized for the digital application. A digital PWM technique using boxes theory was implemented in [280]. Vector control employing trapezoidal PWM technique was attempted for a current source inverter to obtain smooth characteristics [97]. The impact of these strategies on the inverter is presented in [17, 173] and the elimination of harmonics is analyzed in [34]. The current source induction motor under vector control is modeled and the impact of the dead time in the inverter is analyzed [306]. An analysis using a voltage fed PWM control where decoupling is achieved by canceling cross terms between rotor flux and rotor current is performed [298]. A rotor flux linkage control of a current source inverter fed induction motor drive is presented with a linear model [302]. The transient performance with regard to computation time and the PI controller constants is analyzed using this method. A feasibility study of the transistorized PWM inverter for traction applications has been performed highlighting its cost and maintenance advantages [247]. An effort to minimize the overall system losses in this PWM inverter was also attempted [246]. Another optimal study using multi-variable control for efficiency optimization in a speed controlled system is presented in [211]. In this method, the ratio of the torque current to the field current is controlled to minimize the power input.

A speed sensorless scheme was proposed for the constant flux region based on the measurements of voltage and currents [121]. A method which estimates the speed from the instantaneous slip frequency computation is presented in [220]. The slip frequency is estimated by a filter with no time lag from the voltage and current measurements [218]. This scheme is very sensitive to the tuning of the proportional and integral gain constants of the controller. A Model Reference Adaptive System (MRAS) based scheme for rotor speed identifier capable of four quadrant operation is given in [296]. Another scheme using MRAS

using the model of the induction motor in the rotor reference frame estimated the speed from voltage and current measurements [274]. A sensorless scheme using the voltage and current measurements insensitive to stator/rotor resistance variation is presented in [234]. The flux estimator included in this method enables control of the system at standstill. Another scheme achieved speed control without speed sensors and voltage sensors [240]. The change in load torque influences stability and results in flux deviation in this method. Hence a flux compensation circuit is required for good performance characteristics in four quadrant operation.

1.2.6 Implementations

Software packages are essential tools for the analysis of the subsystem interaction. Some efforts were reported for the software package development to analyze the 6 pulse and 12 pulse drive systems [78]. Another study was performed for a flexible multi-axis digital servo [230]. A PC based vector controller which is applicable for dc, induction and synchronous machines is presented in this method.

Vector controlled induction motor drives are implemented either by analog or digital methods. The main advantages of the digital implementation of the vector controller is the elimination of the offset errors and temperature drift. This results in improved controllability and reliability [204]. Also, software control is easier and the reduction of components increases the reliability and the system is extremely noise tolerant [258]. The various methods available in the literature for the digital implementation of vector control and their implications would be discussed in the following paragraphs.

A discrete time model of the vector controller is presented using successive time equations [2]. The system stability of a digital system is discussed from the viewpoints of sampling period, computation time of the microprocessor and feedback parameters by examining the loci of the dominant eigenvalues of the state transition matrix and the transient responses [307]. It concludes that the system has unstable oscillations with high frequency as the feedback gain or the sampling period is increased even if the dead time is zero, for

digital implementations.

The earliest digital implementations employed several eight bit microprocessors to achieve direct vector control [70, 69]. In this method the flux signals are obtained from the sensing coils or with stator voltages and currents and four quadrant operation is demonstrated. Another method employed current tables and different sampling intervals for sensing rotor speed [209]. The dc link voltage is regulated in this scheme to reduce the current and torque ripple. A method using look up tables is presented in [36] and another implementation for constant flux region is given in [342]. A methodology for a single chip microcontroller implementation was presented in [138]. The main advantage of this system is the reduction in the chip count which results in increased reliability of control. A current control scheme based on the space vector modulation technique to achieve quick torque response was implemented using Digital Signal Processors [200].

A multi microprocessor implementation for the voltage and current source model of the vector controller is implemented in [87]. A digitalized speed regulator using multi microprocessors is implemented for the voltage source implementation [149] and another implementation was proposed for high speed response for the speed drive [213]. Multi microprocessor based implementation for robust control of the induction motor has been attempted [311]. In this implementation, vector control is employed for the torque control and model reference complementary control is used for the speed and position loops. This control technique guarantees asymptotic tracking/regulation independent of disturbances and arbitrary perturbations in the drive system parameters. A multi microprocessor based rolling mill is implemented by employing dc and ac current loops to compensate the fundamental output voltage and reduce imbalances of the ac output voltage [263]. The various practical industrial applications of vector controlled induction motor drive systems will be discussed in the following paragraphs.

1.2.7 Applications

The applications of vector controlled systems in various areas such as pinch roll drives, traction drives, robots, etc is reviewed in [159]. A current source inverter fed drive is proposed for starting operation for railway traction [54]. For traction drives, the in-rush current for the induction motor has to be controlled during starting and a method is proposed to achieve this requirement in [38]. An electric car drive is realized using high reliability control of a PWM inverter [116].

Vector control has been extensively employed in steel processing plants and the torque ripple is reduced using PWM techniques [162]. This results in a high quality of steel with few chatter marks. Another extensive application is in rolling mills such as the seamless tube piercing mill where precise speed control over wide voltage range is achieved with rapid acceleration and deceleration characteristics [286]. Vector control also finds applications in the paper and pulp industry to provide a draw control accuracy of more than 0.2% and achieves rated torque production at zero speed range [297, 59]. It is also used for paper machine retrofit applications [252].

Vector control has also been employed in mine hoist drives to provide rapid torque change and precise speed control over a wide speed range [156]. Various applications in the process industry have employed vector control strategy [332, 331]. Another application is for plate mill drives where the cycloconverter fed induction motor drive employing vector control provides superior performance characteristics compared to the other drive systems [107]. The most common application is in the servo industry where the vector controlled induction motor drive is very cost competitive and matches the dc motor performance [174]. Vector control is fast finding a wide range of application in the textile industry [190]. A vector controlled position drive has been successfully employed for a glue dispensing equipment to produce a continuous flow of glue around the periphery of a surface [58].

1.3 SCOPE

The discussion in the previous section provides an insight into the development of the different techniques of vector control and their advantages and limitations for various applications. Based on this survey the following are identified as the key issues to be addressed in this dissertation:

1. The main obstacle for understanding vector control was the familiarity of the inventor with space vector modeling [148]. The advantage of this modeling technique is that the induction motor is treated as two sets of coupled coils resulting in two differential equations. The *d-q* modeling approach is the most popular approach in North America and even though such modeling is available for the indirect vector control technique in the literature, a comprehensive *d-q* modeling, simulation and analysis for the different vector control strategies is yet to be presented. The indirect vector control scheme, which has gained more attention and acceptance has the disadvantage of parameter sensitivity. Various adaptation techniques have been proposed to alleviate this problem. The parameter sensitivity study and the comprehensive study of the merits and demerits of the different schemes for practical applications is of significant importance for the success of indirect vector control induction motor drive systems.

2. The induction motor drive system consists of different sub-systems such as the motor, load, inverter and the controller. With the growing complexity in the development of the ac drive system, there is a need for more than one engineer to interact in a research or product development effort. This necessitates a user friendly, interactive, menu-driven CAE package capable of performing the simulation of the overall drive system including all the sub-system models, while at the same time providing the feature to modify each sub-system independently. This would help in the assessment of the torque ripple, losses, efficiency, torque, speed, and position responses and their bandwidth and evaluate their suitability for a particular application. Such a package would reduce the production cost and decrease the product development cycle time.

3. Most of the industrial applications require variable speed capability which necessitates a speed controller. The design and study of the different parameters in a speed controller would help improve the overall performance of the drive system. The similarity of the vector controlled induction motor drive systems and the separately excited dc motors has been well established in the literature. Using this relationship, a simple scheme for the design of the speed controller has been formulated and the implications studied.

4. Most commercial applications require the elimination of the position sensors from the vector control strategy. This would help in the reduction of the cost of the overall drive system and at the same time decrease its complexity due to reduced signal processing. One such popular example is in automotive applications. The other strong factor for the elimination of a position sensor is for safety reasons [329]. AC drives are currently being used for traction for large coal handling equipment. Due to the coal dust and the hazardous environment, the position sensor has to be explosion proof and should prevent water infiltration. This along with the difficulty in mounting the position transducer necessitates a simple and novel sensorless control scheme using the vector control principle.

5. There is a growing trend towards digital implementation of motor drives due to the recent advances in microprocessor/DSP technology. The implementation of vector controlled induction motor drive systems using digital signal processors with built in peripherals is an added advantage since the reliability of the system increases and the control by software is easier. Also, immunity to noise, ease of diagnostics, and reduced component count makes digital implementation an attractive candidate for modern variable speed drive systems. Hence the experimental verification of the vector control algorithm is performed using a DSP microcontroller which has built in PWM controller, timers and I/O ports.

Organization of the Dissertation

This dissertation is organized as follows. The next chapter presents the principle of vector control for induction machines and classifies the different types of vector control strategy. The modeling, simulation and analysis for these techniques are presented with the results. Experimental results obtained from the digital implementation for one of the vector control algorithms is also provided to verify the simulation results. Chapter 3 describes the systematic derivation of the nonlinear models of the various subsystems involved in an induction motor drive system and the development of a CAE package, VCIM, is presented. The integration of the different subsystems and the interaction between them is discussed and the results obtained from the CAE package are presented to highlight its features and capabilities. Chapter 4 deals with the design and study of the speed controller for a speed/position controlled induction motor drive system. The similarity between the vector controlled induction drive and the dc motor counterpart is utilized to develop the large signal model similar to that of the dc motor. The simulation results are obtained from the CAE package, VCIM and the experimental verification is performed using the DSP based setup. A novel sensorless vector control scheme is formulated and the modeling, simulation and analysis is presented in Chapter 5. The simulation results and the experimental verification using a DSP based vector control system is presented to validate the algorithm. The conclusions are given in Chapter 6. The contribution of this dissertation is presented and the scope for future research in this area identified. The parameters for the drive system under study is given in Appendix A and the voltage sensing algorithm employed in the sensorless technique is presented in Appendix B. The list of symbols used in this dissertation is given in Appendix C.

Chapter 2

VECTOR CONTROL OF INDUCTION MACHINES

2.1 INTRODUCTION

Separately excited dc motors have been employed for high performance speed and servo applications till recently despite the fact that ac motors are less expensive, robust and have low inertia rotors. This was due to the inherent ease of control of a dc motor compared to an ac motor. Vector control transforms the control of an induction motor to that of a separately excited dc motor by creating independent channels for flux and torque control. By reducing the complexity of control of an ac motor, vector control schemes for induction motor drive systems have gained wide acceptance in high performance applications. Crucial to the success of the vector control scheme is the knowledge of the instantaneous position of the rotor flux. Assuming that the rotor flux position is known, the stator current phasor is resolved along and in quadrature to it. The in-phase component is the field current, i_f, and the quadrature component is the torque current, i_t. The resolution of the current requires the rotor flux position known as field angle, θ_f. This field angle can either be measured or estimated. Using measured field angle in the control scheme is known as direct vector control [22] and that using estimated field angle goes by the name of indirect vector control scheme [90].

The decoupling of the torque and field current channels can be accomplished by controlling a set of stator voltage or current vectors. The vector control schemes are classified based on these different control strategies. The modeling, simulation and analysis of these different schemes would help understand the principle of decoupling control. The famil-

iarity of the inventor with space vector modeling led to the development of most of the vector control models using that principle [319]. This technique allows an easier physical understanding of the operation of the system due to the resolution of the induction motor model into two differential equations. Another approach employed for modeling the motors is the *d-q* model which transforms an n-phase machine into two fictitious axes known as the direct or *d*-axis and the quadrature or the *q*-axis. This technique lends itself to easier programming on a computer and is the most widely used technique in North America. The two axis machine requires less numerical computations than the direct three phase machine simulation under balanced sinusoidal excitation. This is due to the constant voltage and constant inductance matrix in the synchronously rotating reference frames. This allows a larger step length in the numerical integration routine of the motor model [93]. The space vector modeling approach remained as the chief obstacle against the vector control technique gaining popularity in USA. This was alleviated to an extent by the development of a *d-q* model for the indirect vector control strategy which is available in the literature [143]. A comprehensive *d-q* modeling, simulation and analysis procedure for the various types of vector control is yet to be presented.

While there has been a tremendous interest on various strategies of vector control, the indirect vector control scheme is being favored over the other schemes in many applications. The increasing popularity of the indirect vector control scheme can be attributed to the following factors:

- Reluctance to install flux-sensing coils or Hall effect transducers in the stator of the induction motor which are necessary for direct vector control.
- Ease of operation of the induction motor drive at and around zero speed. This is due to the difficulty in measurement of the field angle at low speeds, while the field angle estimation method employed by indirect vector control is independent of the operating speed.
- Minimization of the number of transducers in the feedback loop and hence increasing

the reliability of the overall system.

But the major disadvantage of the indirect vector control scheme is that it is machine parameter dependent since the model of the motor is used for flux estimation. The machine parameters are affected by variations in the temperature and the saturation levels of the machine [140, 189]. Any mismatch between the parameters in the motor and that instrumented in the vector controller will result in the deterioration of performance in terms of steady state error and transient oscillations of rotor flux and torque [143]. Consequently, the efficiency of the motor drive decreases [215]. Hitherto parameter sensitivity has been treated as a secondary issue in a vector controlled induction motor drive system. Some of the effects such as the enhanced losses in the motor require a fundamental revision of the research direction. Parameter compensation is important in these motor drives in maintaining/minimizing the losses in the motor resulting in thermal robustness and hence reduced derating of the motor. This has the same importance as the elimination/mitigation of the switching losses in the switching power devices which, in turn, leads to enhanced switching frequencies and output of the static power converters.

Various schemes have been proposed for parameter adaptation in such drives over the past two decades based on one of the following strategies:

1. Direct monitoring of the alignment of the flux and torque producing stator current component axes.

2. Continuous real time measurement of the instantaneous rotor resistance.

3. Measurement of modified reactive power, measurement and estimation of rotor flux, deviation of field angle or a combination of the rotor flux and torque producing components of the stator current. An error in the measured variables corresponds to the parameter variation in the induction motor.

This chapter discusses the principle of vector control and classifies the various types of vector control strategies. The concept of the field angle, θ_f, which is crucial to the

success of any vector control scheme is emphasized with the aid of a phasor diagram in the next section. Section 2.3 describes the modeling, simulation and analysis of the current and voltage source direct vector control followed by the current and voltage source indirect vector control in Section 2.4. The simulation results are validated for the current source indirect vector controller using a DSP based digital implementation of the controller. The description of the setup and the results obtained are presented in Section 2.5 followed by a discussion of the various issues pertaining to vector controlled induction machines.

2.2 PRINCIPLE OF VECTOR CONTROL

The torque is controlled in a dc motor by controlling the armature current while maintaining the field current constant. This is possible due to the fact that the field and armature currents can be controlled independently, since the armature and field windings are physically separate. But in an induction motor, both the rotor flux and the torque are controlled through the stator currents only. Since there are no separate armature or field windings, the control becomes complex. One of the important parameters for the vector control is the rotor flux position, also known as the field angle, θ_f. The field angle is defined as the angle between the stator axis and the rotor field axis.

Assuming that θ_f is available, it is possible to resolve the stator current phasor along the rotor flux and in quadrature to it. The phasor diagram representation of the vector control principle is shown in Fig. 2.1. The in-phase component is the flux producing current, i_f, similar to the field current of a dc motor. The quadrature component is the torque producing current, i_t, similar to the armature current of a dc motor. This process of transformation of the control of an induction motor to that of an equivalent separately excited dc motor is known as vector control. It is also called as decoupling control or field oriented control in the literature. The major effort in vector control is to determine the flux and torque producing components for the given flux and torque commands as shown in Fig. 2.2.

By aligning the field current along the axis of the rotor flux, it can be noted that once

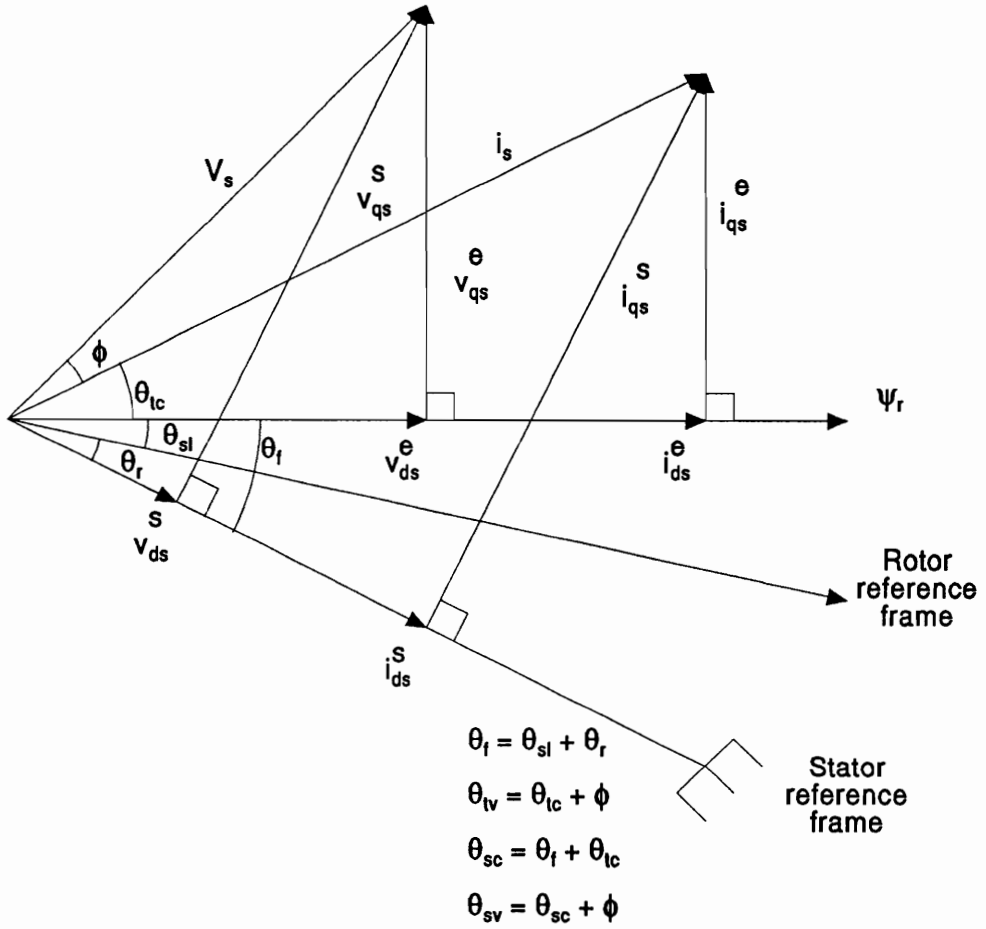

Figure 2.1: Phasor Diagram of the Vector Controller

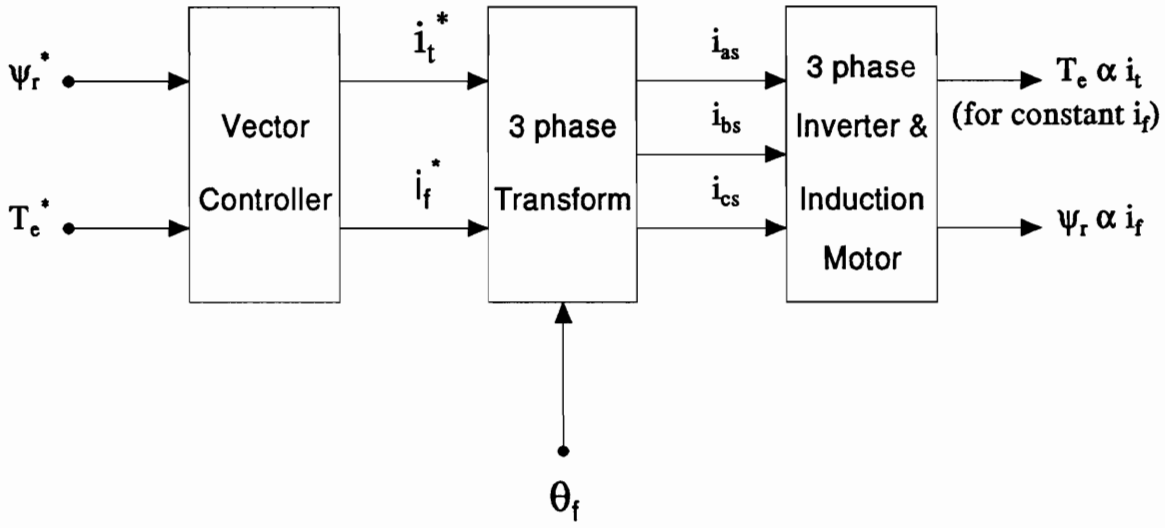

Figure 2.2: Control Block Diagram for the Induction Motor

the value of the rotor flux is obtained, the field angle can be computed. It is also possible to obtain the field angle by computing the slip angle, θ_{sl}, once the rotor position, θ_r, is known. Based on the method by which the field angle is obtained, vector control schemes are classified as shown in Fig. 2.3. In the direct method, the field angle is measured from the outputs of Hall sensors or by integrating the induced emfs from a set of sensing coils placed near the airgap and embedded in stator slots. The Hall sensors are temperature sensitive and the sensing coils produce no voltage or very small voltage at standstill and at very low speeds. This introduces errors and makes the measurement of the field angle difficult. In the indirect method, the field angle is estimated using the dynamic model of the induction motor. It can be calculated either through the output of voltage and current sensors or by measuring the rotor position, θ_r, and computing the slip position, θ_{sl}, from the motor model. The latter method, which needs a position sensor and current sensors, is the most popular method due to its enhanced reliability.

The dynamic model of the induction motor in the d-q reference frame can be represented in any arbitrary reference frames. This facilitates the generalization of the model and hence various models can be derived as particular cases of this model. Three particular cases of the generalized models of the induction motor in the arbitrary reference frames are most commonly used. They are:

- Stator reference frame models.
- Rotor reference frame models.
- Synchronously rotating reference frame models.

In the stator reference frame model, the observer is located on the stator of the machine, while in the rotor reference frame the observer is located on the rotor of the machine. In the synchronous reference frame, the observer is aligned along the axis of the rotor flux of the motor. In this reference frame, the d and q axis stator voltages are simplified to dc quantities and hence their responses will be dc quantities too. From the phasor diagram of the vector controller, it can be noted that the field current is aligned along the axis of the

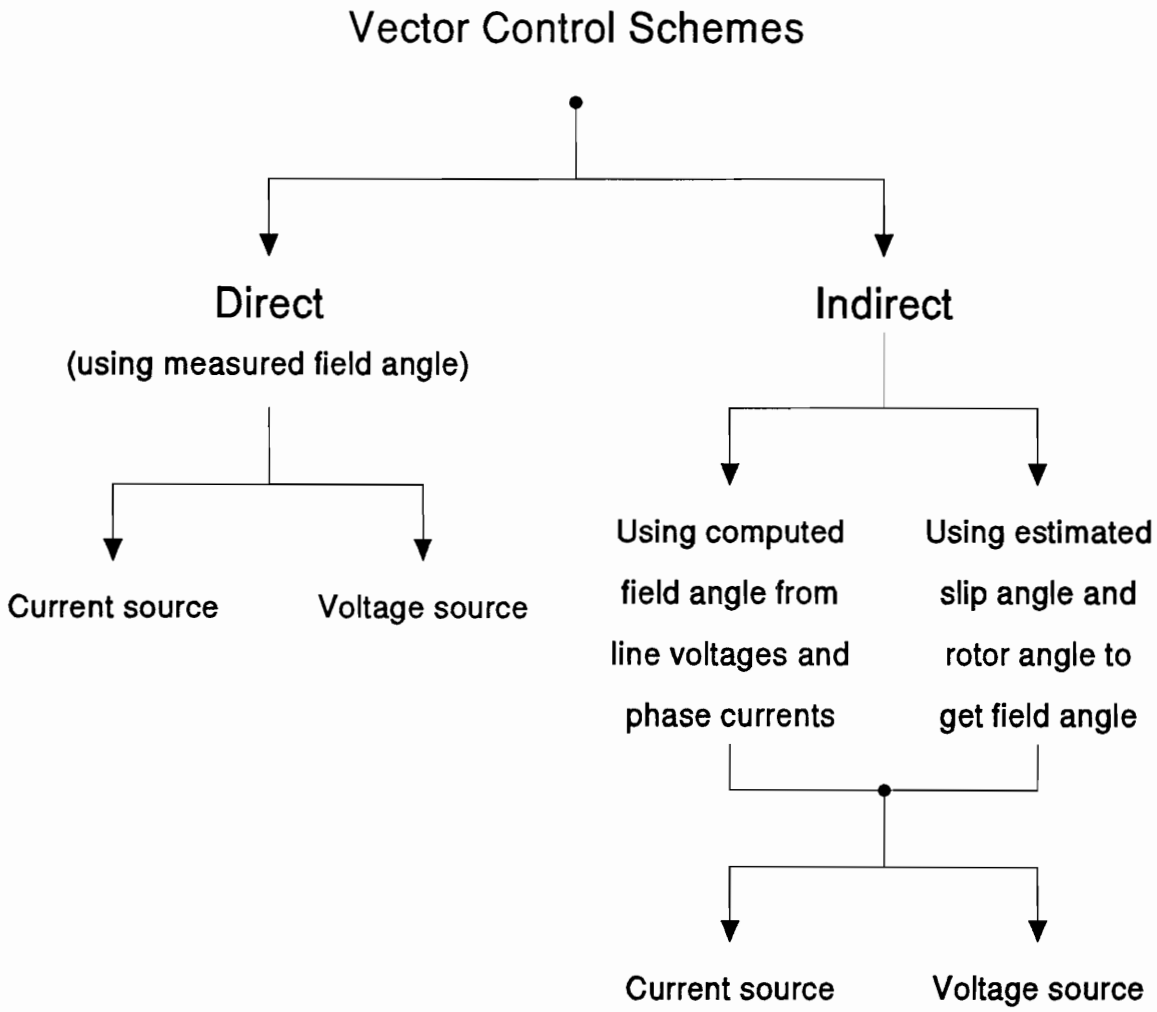

Figure 2.3: Classification of Vector Control Schemes

rotor flux. For ease of analysis, the synchronously rotating reference frames is used for the dynamic model of the induction motor. Once the field angle is known, the control of the electromagnetic torque can be enforced by using the stator voltage phasors or the stator current phasors in the synchronous frame. This leads to the current source and voltage source of vector control schemes.

2.3 DIRECT VECTOR CONTROL

Direct vector control schemes involve the measurement of the rotor flux, and hence the field angle, using Hall sensors or sensing coils. The signals that are available for the control of the induction motor are the field angle and the stator currents obtained from the current transducers. Normally, only two current transducers are used for a balanced three phase system and the third phase current is derived as the negative sum of the other two currents. The torque and flux in the motor can be made to follow their commanded values by controlling the stator currents through a set of current or voltage vectors. The strategy which uses the current vectors is known as current source direct vector control and the technique which uses the voltage vector for the control goes by the name of voltage source direct vector control.

2.3.1 Current Source

The functional block diagram of the current source direct vector control is shown in Fig. 2.4. The input to the vector controller is the commanded values of torque and rotor flux. Using the rotor flux measured by sensors, the commanded value of the stator currents is generated. The error between the actual and the commanded value of the torque and rotor flux is processed through a PI controller to obtain the torque and field currents, respectively. The torque current is directly proportional to the torque in steady state. This dc value of the torque command is added with the error current to produce the required level of torque current command. The torque and field currents thus obtained, are then

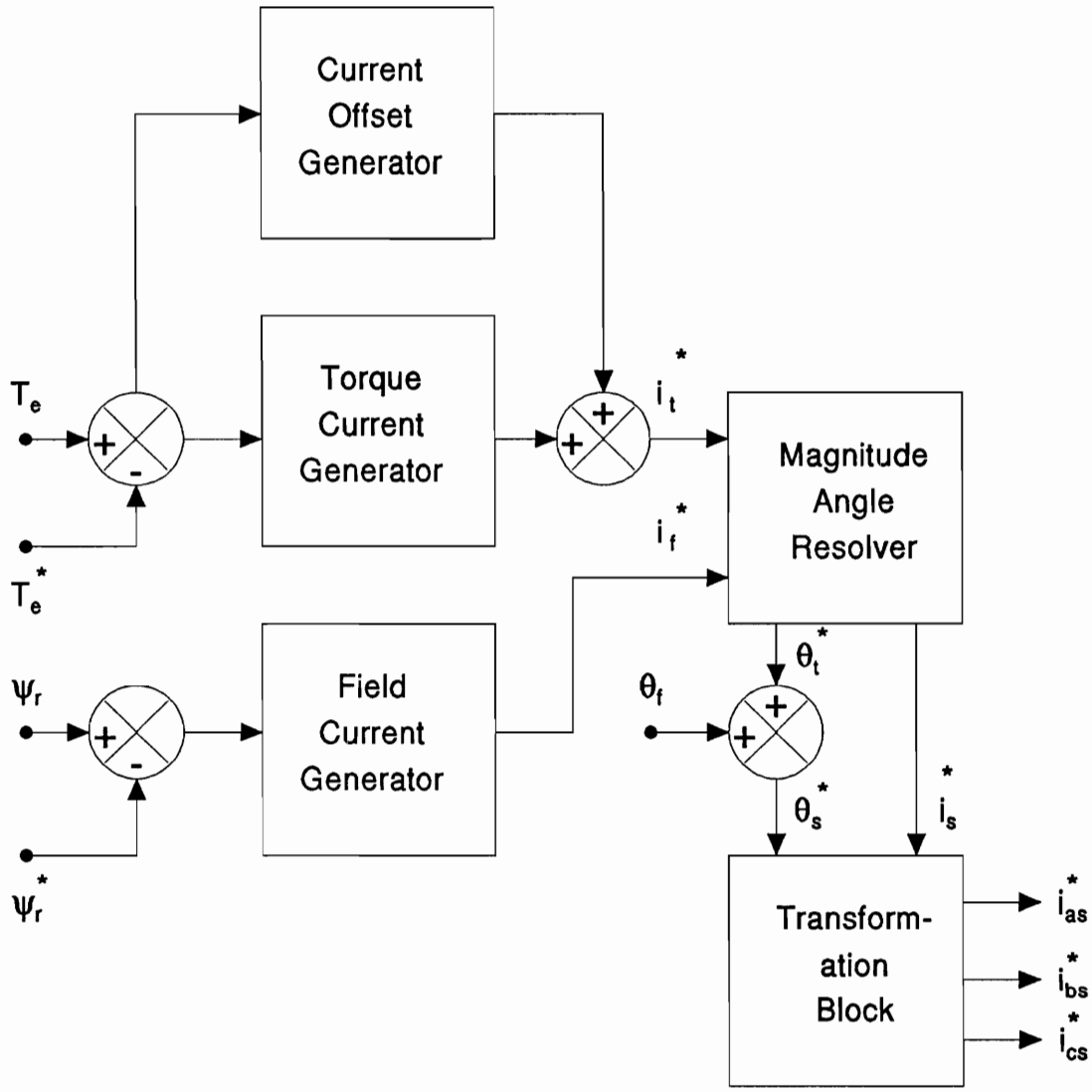

Figure 2.4: Functional Block Diagram of a Current Source Direct Vector Controller

processed through a magnitude and angle resolver to obtain the stator current phasor and the torque angle.

Regardless of the vector control strategy employed, it can be noted that the field current is oriented along the axis of the rotor flux and the torque current is in quadrature to it. By inspection from the phasor diagram shown in Fig. 2.1, it can be noted that,

$$i_t^* = i_{qs}^{e^*} \tag{2.1}$$

$$i_f^* = i_{ds}^{e^*} \tag{2.2}$$

The equations for the torque angle and the stator current phasor can be given as,

$$\theta_{tc}^* = \tan^{-1} \frac{i_t^*}{i_f^*} \tag{2.3}$$

$$i_s^* = \sqrt{i_t^{*2} + i_f^{*2}} \tag{2.4}$$

Since the field angle is available from the Hall sensors, the stator phasor angle for the current source vector control can be obtained as,

$$\theta_{sc}^* = \theta_f + \theta_{tc}^* \tag{2.5}$$

Using the two phase to three phase transformation matrix, the commanded values of the stator currents can be obtained from the following equations:

$$i_{as}^* = i_s^* \sin \theta_{sc}^* \tag{2.6}$$

$$i_{bs}^* = i_s^* \sin(\theta_{sc}^* - \frac{2\pi}{3}) \tag{2.7}$$

$$i_{cs}^* = i_s^* \sin(\theta_{sc}^* + \frac{2\pi}{3}) \tag{2.8}$$

These current commands are then processed through a current controller and compared with the measured values of the actual currents. Using either PWM or hysteresis control

techniques the stator currents are controlled to minimize the error and hence produce the commanded value of torque and flux in the motor.

The model of this vector controller was implemented and the simulation of the overall drive system performed for this strategy. The output characteristics for a torque drive employing a current source direct vector control is illustrated in Fig. 2.5. The inputs to the torque drive are the commanded values of electromagnetic torque and rotor flux. The rotor speed is maintained at a constant value and the rotor flux is equal to the rated value. This condition is achieved by starting the simulation with the value of the field current equal to the rated current. Since the field current is directly proportional to the rotor flux, this condition ensures that the rotor flux reaches the rated value. The normalized values of the commanded/actual speed, commanded flux current and the rotor flux, commanded torque current and the electromagnetic torque, commanded/actual current of phase 'A' are displayed in the figure. It can be noted that the rotor speed is maintained at a constant value of 0.3 p.u. The inner current loop is represented by the commanded and actual values of currents. The actual current follows the commanded value, implemented by a PWM controller at a switching frequency of 1 kHz. A step command of $\pm$ 0.5 p.u. for the torque command and a 1 p.u. command for the rotor flux is applied. The actual value of the electromagnetic torque and rotor flux closely follows the commanded signal. The decoupled field and torque currents are also given in the figure. The dc value of the torque current can be noted once the system reaches steady state. The transient and dynamic response of the current can also be seen in this figure.

2.3.2 Voltage Source

In the voltage source direct vector controller, the torque and flux values are controlled to follow the commanded torque and flux values by controlling the voltage vectors. The functional block diagram of the voltage source direct vector control is shown in Fig. 2.6. The error between the actual and the commanded value of the torque and rotor flux is processed through a PI controller to obtain the torque and field currents, respectively. From the

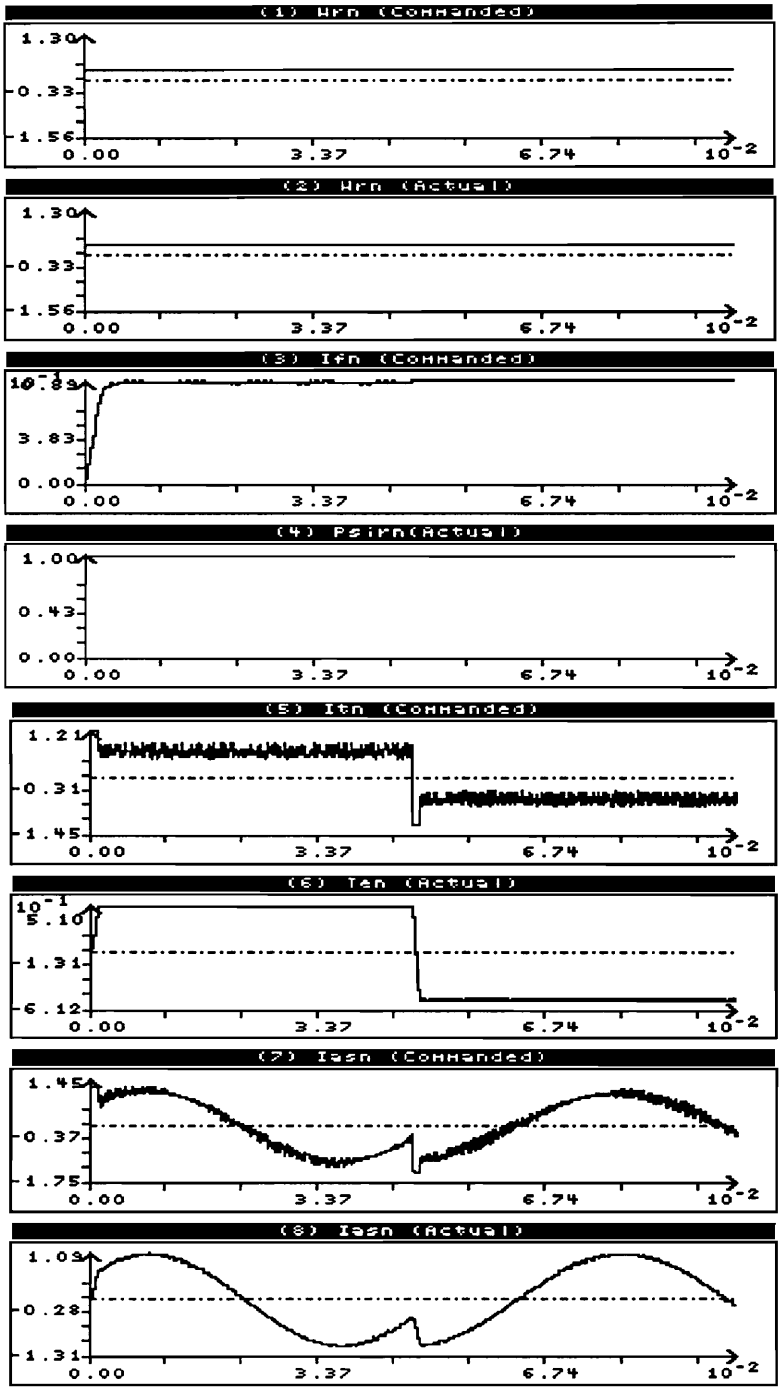

Figure 2.5: Output Characteristics for a Torque Controlled Current Source Direct Vector Control Scheme

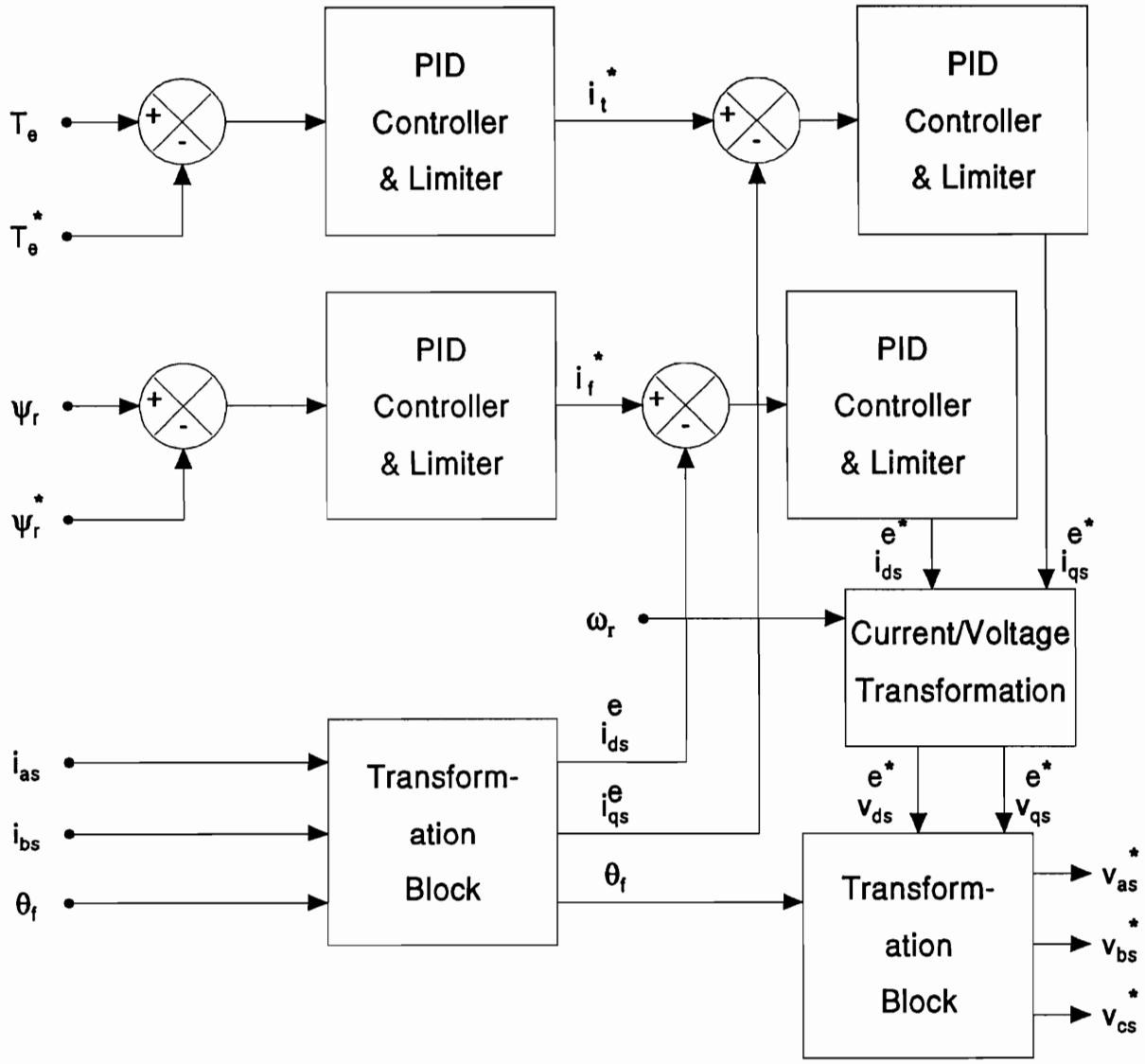

Figure 2.6: Functional Block Diagram of a Voltage Source Direct Vector Controller

measured values of the stator currents the q and d axes stator currents in the synchronously rotating reference frames is calculated using the following transformation:

$$\begin{bmatrix} i^e_{qs} \\ i^e_{ds} \\ i_0 \end{bmatrix} = \frac{2}{3} \begin{bmatrix} \cos\theta_f & \cos\left(\theta_f - \frac{2\pi}{3}\right) & \cos\left(\theta_f + \frac{2\pi}{3}\right) \\ \sin\theta_f & \sin\left(\theta_f - \frac{2\pi}{3}\right) & \sin\left(\theta_f + \frac{2\pi}{3}\right) \\ \frac{1}{2} & \frac{1}{2} & \frac{1}{2} \end{bmatrix} \begin{bmatrix} i_{as} \\ i_{bs} \\ i_{cs} \end{bmatrix} \tag{2.9}$$

As discussed earlier, the torque and field currents are the q and d axes currents in the synchronous reference frame for the vector controller. Hence the error between the torque and q axis current, and the field and d axis current is processed through a PI controller to obtain the current vectors in the q and d axes, respectively. The transformation from the current vector to the voltage vector can be achieved using the following equations. The rotor flux and its derivative are available from the flux sensor and computations. The q and d axis rotor currents are given as,

$$i^e_{qr} = -\frac{L_m}{L_r} i^e_{qs} \tag{2.10}$$

$$i^e_{dr} = \frac{\psi_r}{L_r} - \frac{L_m}{L_r} i^e_{ds} \tag{2.11}$$

Hence the commanded values of q and d axes voltages are given as,

$$v^{e^*}_{qs} = R_s i^e_{qs} + L_a p i^e_{qs} + \omega_e L_a i^e_{ds} + \omega_e \frac{L_m}{L_r} \psi_r \tag{2.12}$$

$$v^{e^*}_{ds} = R_s i^e_{ds} + L_a p i^e_{ds} - \omega_e L_a i^e_{qs} + \frac{L_m}{L_r} p\psi_r \tag{2.13}$$

where,

$$L_a = L_s - \frac{L^2_m}{L_r} \tag{2.14}$$

The q and d axis voltages can then be transformed to the a, b, and c phase voltage vectors by using the following transformation,

$$v_{as}^{*} = v_{s}^{*} \sin \theta_{sv}^{*} \tag{2.15}$$

$$v_{bs}^{*} = v_{s}^{*} \sin(\theta_{sv}^{*} - \frac{2\pi}{3}) \tag{2.16}$$

$$v_{cs}^{*} = v_{s}^{*} \sin(\theta_{sv}^{*} + \frac{2\pi}{3}) \tag{2.17}$$

The three phase voltage vectors thus obtained are then modulated using a PWM controller and the varying duty cycle of the voltage command allows the flux and torque to follow the commanded values of flux and torque, respectively. With this model of vector controller, the simulation of the overall drive system is performed for this strategy.

The output characteristics for a speed drive employing a voltage source direct vector control is illustrated in Fig. 2.7. The input to the speed drive is the commanded value of the rotor speed. This is compared with the actual value of the rotor speed. The error signal is amplified and processed through a speed controller to obtain the torque command. The flux command is obtained from the rotor speed signal with a pre-programmed function generator. The normalized values of the commanded/actual speed, commanded flux current and the rotor flux, commanded torque current and the electromagnetic torque, commanded voltage and actual current of phase 'A' are displayed in Fig. 2.7. The inner loop is represented by the commanded voltage and actual current values. The actual current results from the commanded values of voltages modulated with a carrier waveform using a PWM controller at a switching frequency of 1 kHz. A step command of $\pm$ 0.25 p.u. for the speed command and a 1 p.u. command of the rotor flux is applied. The electromagnetic torque and rotor flux closely follow their commanded signal. The decoupled field and torque currents are also given in the figure. The zero error in the electromagnetic torque indicates steady state for the drive with no load torque. The transient and dynamic response of the current can also be seen.

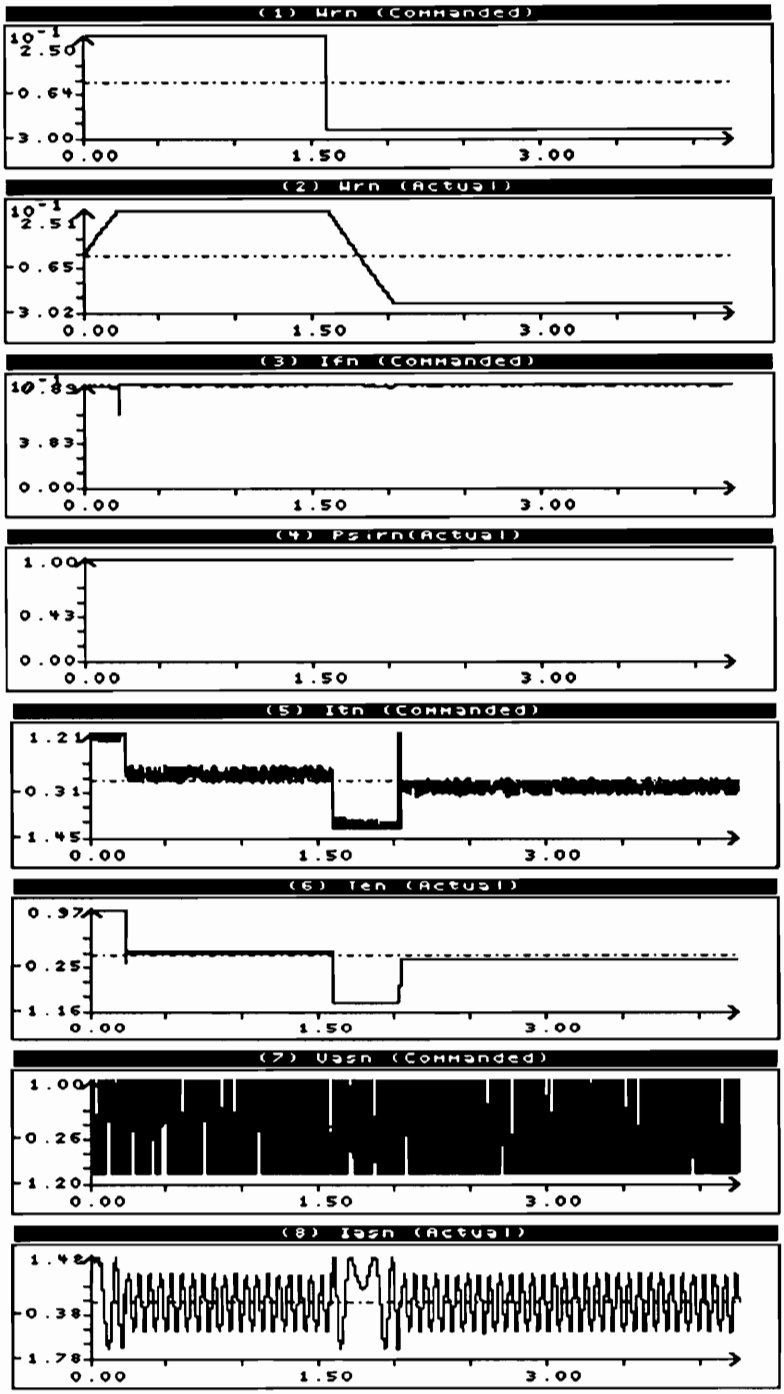

Figure 2.7: Output Characteristics for a Speed Controlled Voltage Source Direct Vector Control Scheme

2.4 INDIRECT VECTOR CONTROL

Unlike the direct vector control technique, the field angle is estimated in the indirect vector control strategy. The field angle is computed using some measurements and motor parameters. The slip angle, the commanded values of the stator current phasor, and the torque angle are estimated using the motor parameters. The rotor position and the stator phase currents are measured using sensors. From the phasor diagram shown in Fig. 2.1, it can be noted that the field angle is the sum of the slip angle and the rotor position. Hence the field angle is estimated using the computed values and control achieved. The torque and flux in the motor can be made to follow their commanded values by controlling the stator currents through a set of current or voltage vectors. The strategy which uses the current vectors is known as current source indirect vector control and the technique which uses the voltage vector for the control goes by the name of voltage source indirect vector control.

2.4.1 Current Source

The functional block diagram of the current source indirect vector control is shown in Fig. 2.8. The indirect vector control algorithm is derived from the dynamic equations of the induction motor in the synchronously rotating reference frames. The rotor equations in terms of the rotor flux linkages are,

$$R_r i_{qr}^e + p\psi_{qr} + (\omega_e - \omega_r)\psi_{dr} = 0 \tag{2.18}$$

$$R_r i_{dr}^e + p\psi_{dr} - (\omega_e - \omega_r)\psi_{qr} = 0 \tag{2.19}$$

The slip speed is given as,

$$\omega_{sl} = \omega_e - \omega_r \tag{2.20}$$

As mentioned earlier, the rotor flux phasor is aligned along the d axis. Hence,

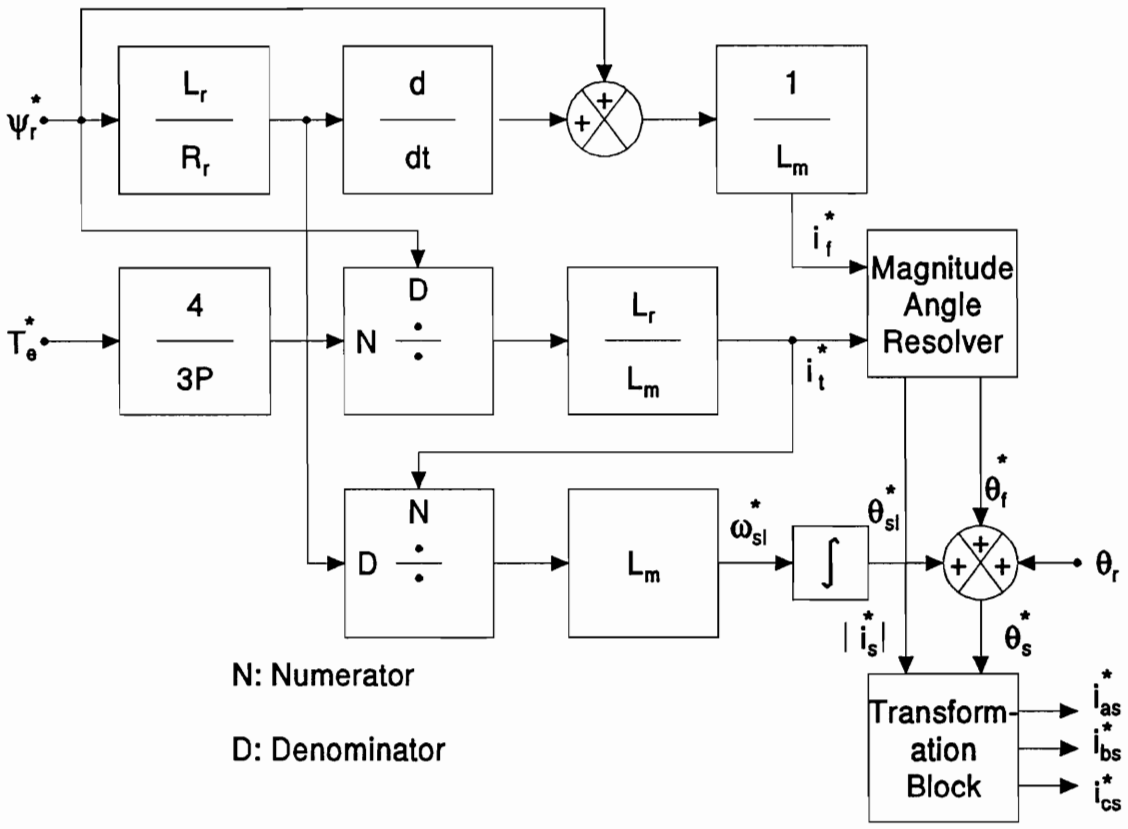

Figure 2.8: Functional Block Diagram of a Current Source Indirect Vector Controller

$$\psi_{dr} = \psi_r \tag{2.21}$$

$$\psi_{qr} = 0 = p\psi_{qr} \tag{2.22}$$

Substituting equations 2.20 - 2.22 into equations 2.18, 2.19, the rotor equations are given as,

$$R_r i^e_{qr} + \omega_{sl}\psi_r = 0 \tag{2.23}$$

$$R_r i^e_{dr} + p\psi_r = 0 \tag{2.24}$$

The rotor flux linkages can be expressed as,

$$\psi_{qr} = L_m i^e_{qs} + L_r i^e_{qr} \tag{2.25}$$

$$\psi_{dr} = L_m i^e_{ds} + L_r i^e_{dr} \tag{2.26}$$

Hence the rotor currents can be derived as,

$$i^e_{qr} = -\frac{L_m}{L_r} i^e_{qs} \tag{2.27}$$

$$i^e_{dr} = \frac{\psi_r}{L_r} - \frac{L_m}{L_r} i^e_{ds} \tag{2.28}$$

The system equations are then given as,

$$\omega_{sl} = \frac{L_m R_r}{L_r} \frac{i^e_{qs}}{\psi_r} \tag{2.29}$$

$$p\psi_r = \frac{R_r}{L_r} [-\psi_r + L_m i^e_{ds}] \tag{2.30}$$

$$T_e = K_t i_{qs}^e \psi_r \tag{2.31}$$

where, K_t is the torque constant given as,

$$K_t = \frac{3}{2}\frac{P}{2}\frac{L_m}{L_r} \tag{2.32}$$

From these, the commanded values of the torque and flux producing components of the stator phase currents, i_t^* and i_f^*, respectively, can be identified and written as,

$$i_t^* = i_{qs}^{e^*} = \frac{2}{3}\frac{2}{P}\frac{L_r}{L_m}\frac{T_e^*}{\psi_r^*} \tag{2.33}$$

$$i_f^* = i_{ds}^{e^*} = \frac{1}{L_m}[1 + \frac{L_r}{R_r}p]\psi_r^* \tag{2.34}$$

The equation for the slip speed is then given as,

$$\omega_{sl}^* = \frac{L_m L_r}{R_r}\frac{i_t^*}{\psi_r^*} \tag{2.35}$$

The torque angle and the stator current phasor are obtained using equations 2.3, 2.4. The stator phasor angle is then given by the following equation:

$$\theta_{sc}^* = \theta_{sl}^* + \theta_{tc}^* + \theta_r \tag{2.36}$$

Using the two phase to three phase transformation given in equations 2.6 - 2.8, the commanded values of the three phase stator currents are obtained. These current commands are then processed through a current controller and compared with the measured values of the actual currents. Using either PWM or hysteresis control techniques, the stator currents are controlled to minimize the error and follow the commanded torque and flux in the motor.

The model of this vector controller was implemented in a PC-based software and the simulation of the overall drive system performed for this strategy. The output characteristics for a position drive employing a current source indirect vector control is illustrated in

Fig. 2.9. The input is the commanded value of the rotor position. This is compared with the actual value of the rotor position obtained from the position encoder. The error signal is amplified and then processed through a position controller to obtain the speed command. The commanded values of the electromagnetic torque and rotor flux are obtained using a speed controller and programmed flux function generator. The normalized values of the commanded/actual speed, commanded/actual torque, commanded/actual current of phase 'A' and the command/actual value of rotor position are displayed in Fig. 2.9. The rotor position command is a ramp signal with a magnitude of $\pm$ 3 radians. It can be noted that the actual value of the rotor position closely follows the commanded value. The motor is at standstill when a constant position command is applied. The torque loop and the inner current loop control enforce the actual value of the electromagnetic torque and stator current to follow their commanded values. The inner current loop is implemented by a PWM current controller at a switching frequency of 1 kHz. and ensures quick response of the drive system.

2.4.2 Voltage Source

The modeling of the voltage source indirect vector control is very similar to that of the current source discussed in the earlier subsection. The functional block diagram of the voltage source indirect vector control is shown in Fig. 2.10. The main difference in this scheme with the current control scheme is that vector control is achieved by controlling the voltage phasors rather than the current phasors. The commanded values of the stator current phasor, torque angle and the field angle are estimated similar to that of the current source indirect vector control. The q and d axes currents in the synchronous reference frames are obtained from the measured stator phase currents and the estimated field angle using the transformation given in equation 2.9. These are compared with the commanded values of torque and field currents, respectively. The error is then processed through a PI controller to obtain the q and d axes current vectors in the synchronous reference frame.

The q and d axis rotor currents, rotor flux and derivative of rotor flux values are calcu-

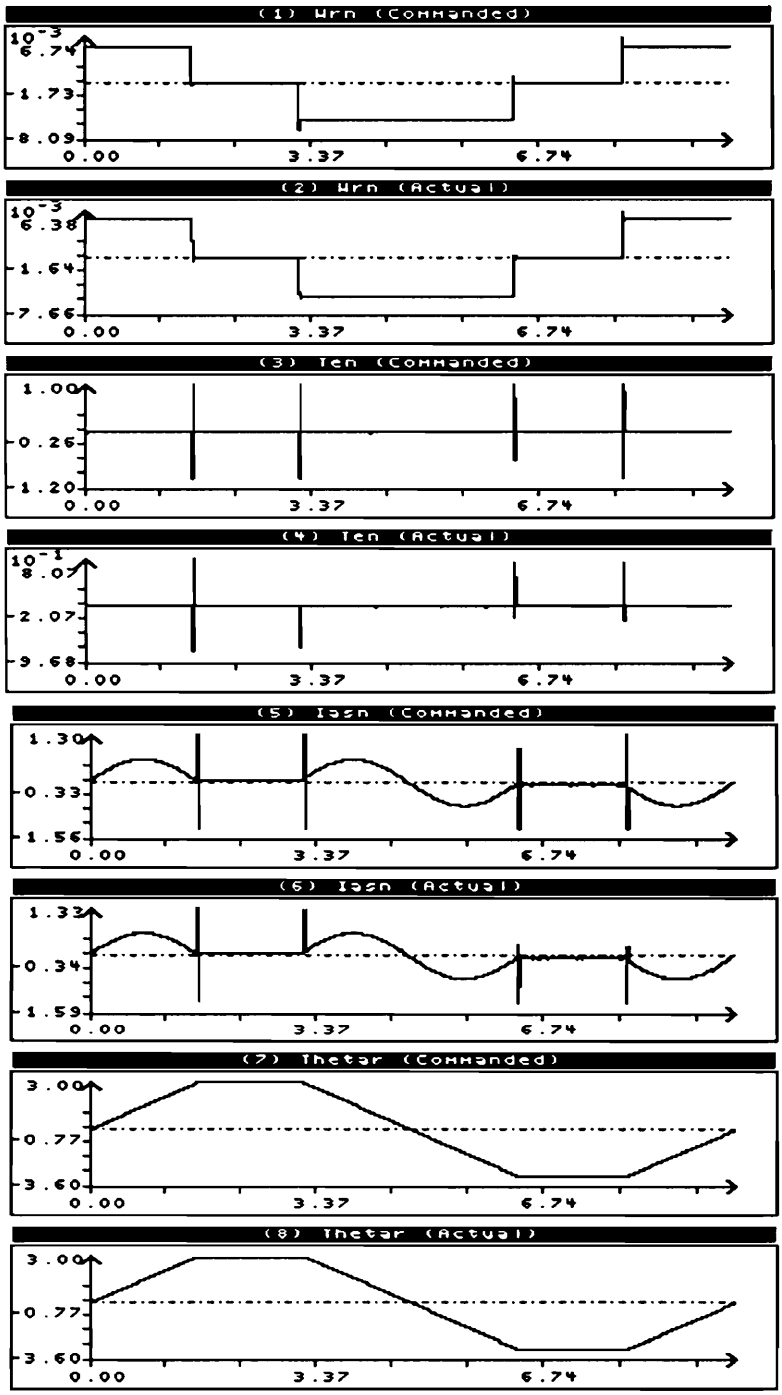

Figure 2.9: Output Characteristics for a Position Controlled Current Source Indirect Vector Control Scheme

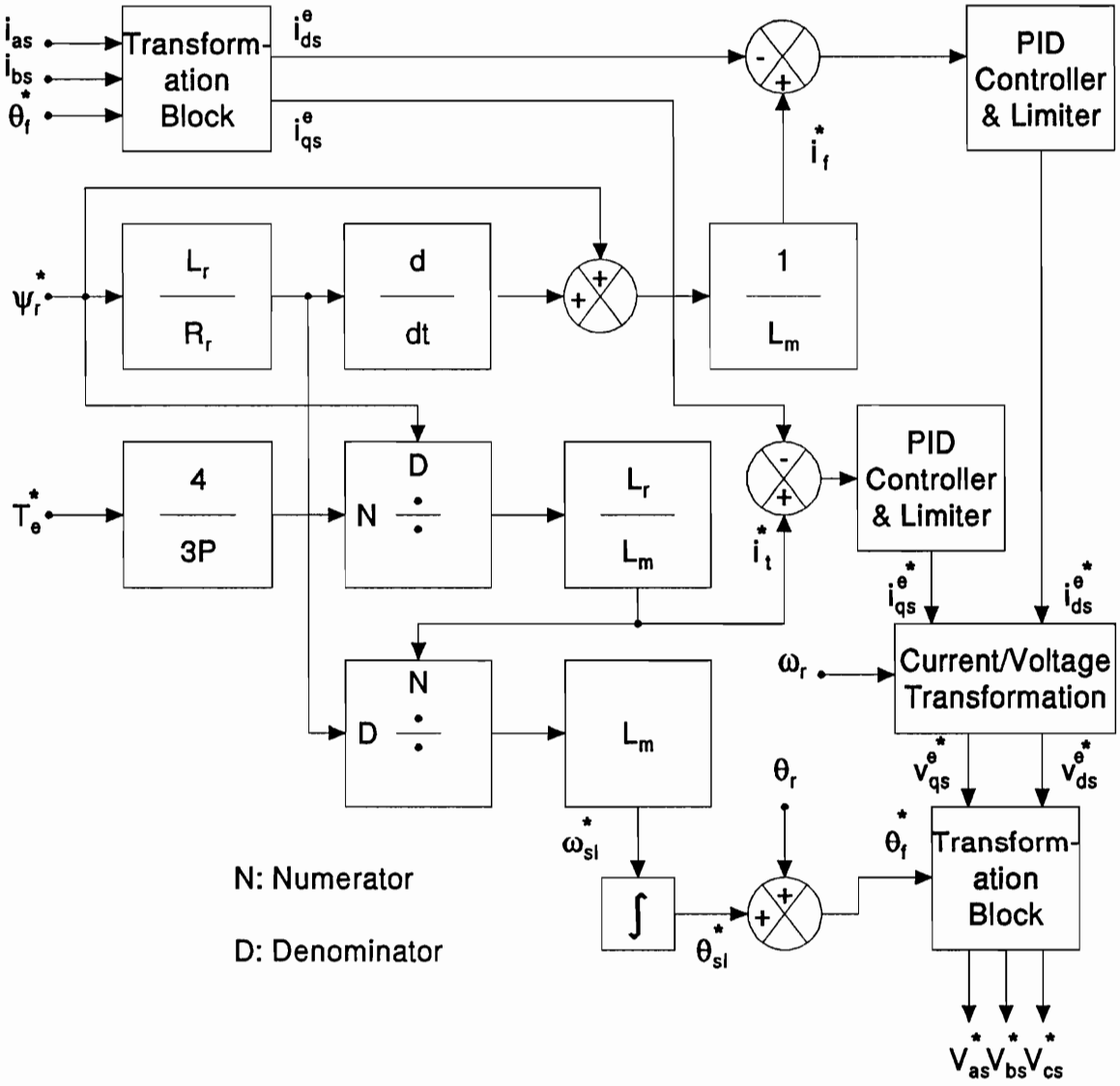

Figure 2.10: Functional Block Diagram of a Voltage Source Indirect Vector Controller

lated using equations 2.27 to 2.30. Hence the commanded values of q and d axes voltages are given as,

$$v_{qs}^{e*} = R_s i_{qs}^e + L_a p i_{qs}^e + \omega_e L_a i_{ds}^e + \omega_e \frac{L_m^2}{L_r^2} \frac{R_r}{\omega_{sl}} i_{qs}^e \tag{2.37}$$

$$v_{ds}^{e*} = R_s i_{ds}^e + L_a p i_{ds}^e - \omega_e L_a i_{qs}^e + \frac{L_m^2}{L_r^2} R_r i_{ds}^e - \frac{L_m^2 R_r^2}{L_r^3 \omega_{sl}} i_{qs}^e \tag{2.38}$$

where,

$$L_a = L_s - \frac{L_m^2}{L_r} \tag{2.39}$$

The commanded values of the voltage phasors are obtained from the transformation given in equations 2.15 - 2.17. It can be noted that the current loop is enforced by the PI controllers for the torque and field currents to ensure a fast response. The three phase voltage reference vectors are then modulated using a PWM controller and the varying duty cycle of the voltage command allows the flux and torque to follow the commanded values of flux and torque, respectively. With the model of this vector controller, the simulation of the overall drive system is performed for this strategy.

The output characteristics of a voltage source direct vector controlled speed drive is illustrated in Fig. 2.11. The input to the speed drive is the commanded value of the rotor speed. The commanded values of the electromagnetic torque and rotor flux are obtained with a speed controller and programmed function generator, respectively. The normalized values of the commanded/actual speed, commanded flux current and the rotor flux, commanded torque current and the electromagnetic torque, commanded voltage and actual current of phase 'A' are displayed in the figure. The inner loop is represented by the commanded voltage and actual current values. The actual current results from the commanded values of voltages modulated with a carrier waveform using a PWM controller. A step command of $\pm$ 0.25 p.u. for the speed command and a 1 p.u. command for the rotor flux is applied. The actual value of the electromagnetic torque and rotor flux closely follows the commanded

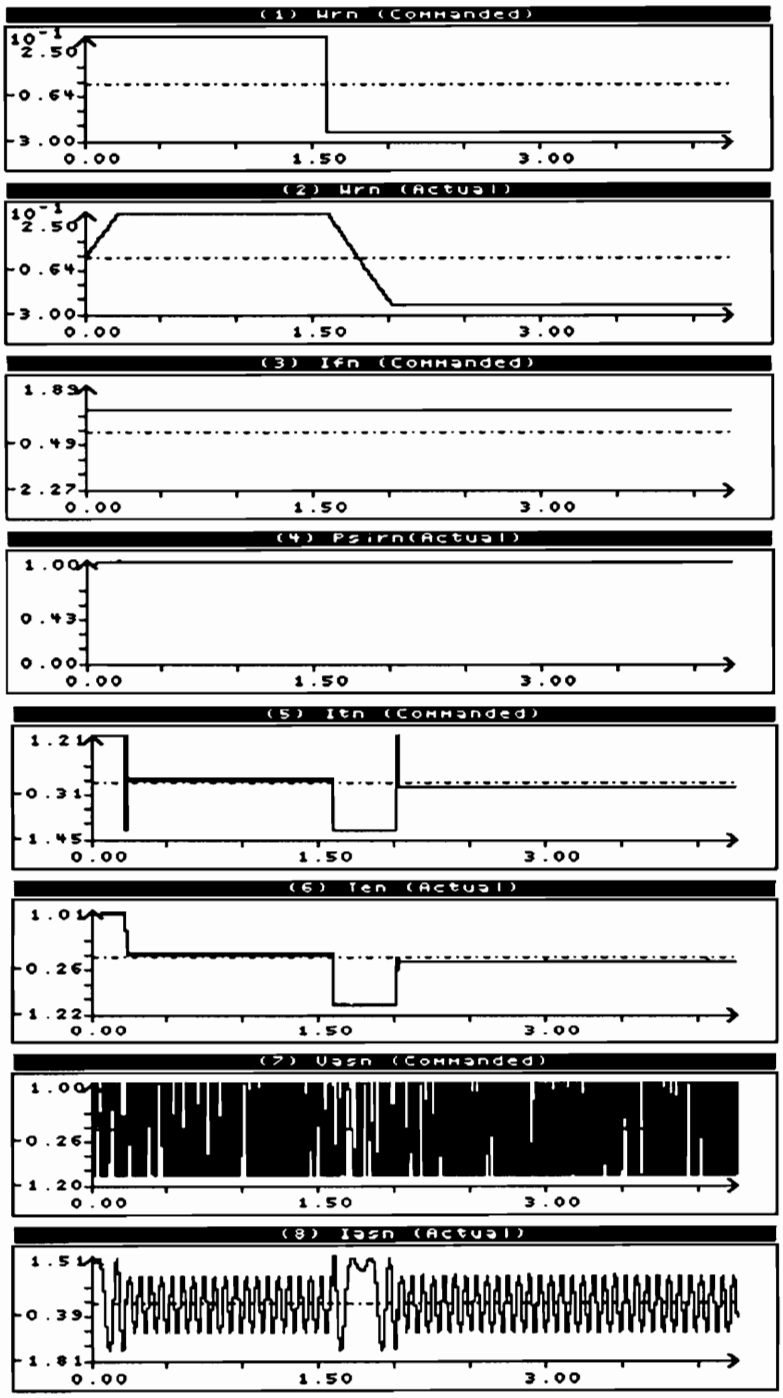

Figure 2.11: Output Characteristics for a Speed Controlled Voltage Source Indirect Vector Control Scheme

signal. The similarity with the direct vector control technique can be noted to verify the validity of the simulation algorithm. The decoupled field and torque currents are also given in the figure. The zero error in the electromagnetic torque indicates steady state for the drive with no load torque.

2.5 EXPERIMENTAL VALIDATION

The modeling, simulation and analysis of the different types of vector control were described in detail in the previous sections and the results presented. It was also seen that due to the reduced number of transducers and better control performance, the current source indirect vector control strategy has found wide applications. In this section, a Digital Signal Processor (DSP) based implementation of such a controller will be described. The results from this setup will be useful in validating the simulation algorithm and also serve as a bench mark for implementation of more complicated algorithms such as sensorless vector control.

The vector controller setup consists of the three different units. They are:

1. Motor and load.
2. Converters.
3. DSP microcontroller.

2.5.1 Motor and Load

A 1HP, 230V, 2 Pole, 60 Hz., 3450 RPM, 3ϕ induction motor is used for this study. The motor parameters and the different constants of the entire drive system are given in detail in Appendix A. The simulation results in the previous sections were obtained for this particular drive configuration. The motor is coupled to a dc motor which also acts as a load. The moment of inertia and the friction coefficient of the induction motor is measured with the dc motor coupled to the induction motor.

An incremental encoder is mounted on the dc motor and generates a pulse stream with a resolution of 1000 pulses per revolution. A counter circuit acts as an interface between the microcontroller and the encoder.

2.5.2 Converters

There are two converters in the drive system. The first one is to convert constant frequency utility ac supply to a dc voltage source with a diode bridge rectifier. The bridge rectifier along with the dc link capacitance performs this conversion. The second converter is a three phase inverter which converters the fixed frequency dc link voltage to a variable frequency ac voltage and serves as the input to the motor.

MOSFET devices are used to build the three phase inverter. The inputs to the inverter are the six gate signals from the DSP microcontroller. These signals are then fed through a gate drive circuit and switches the appropriate devices. The gate drive circuit also performs the additional task of providing isolation between the inverter and the controller. The snubber circuit to protect the devices is made up of a resistor, capacitor, and a diode. The three outputs of the inverter is then fed to the corresponding phase of the motor terminals.

The current transducers to measure the phase currents are mounted in the inverter unit. Only two phase currents are measured since the third current can be reconstructed in a balanced three phase system. The current transducer circuit amplifies and scales the voltage from the current transducer to be within valid limits for the DSP microcontroller.

2.5.3 DSP Microcontroller

A Texas Instrument 320E14 is used to implement the functions of a vector controller. It has a 200 nsec instruction cycle with a 20MHz clock. The main features of this microcontroller is as follows:

1. 32 bit ALU/accumulator

2. 16 by 16 bit multiplier with a 32 bit product

3. 4K word on chip program EPROM

4. Two 16 bit timers

5. Versatile timer event manager with capture and compare outputs

6. Watchdog timer

7. Fifteen external/internal interrupts

8. Seven input and Seven output channels

9. 16 bit bidirectional digital I/O

Power 14, a module designed by Teknic, Inc, has been used for this setup. This module integrates the DSP microcontroller with the additional peripherals such as the Analog to Digital Converter, interface with a personal computer, etc. The functions to be performed by the DSP microcontroller board are as follows:

1. Receive the analog current signals through the ADC and process it for digital calculations.

2. Receive the encoder pulse output from the counter and calculate the rotor position, both in clockwise and anti-clockwise directions. The encoder pulse output can either be received through the capture inputs of the microcontroller or through the digital I/O ports.

3. Generate the PWM cycle for determining the switching frequency. A 1 kHz switching frequency is implemented in this controller.

4. Receive the torque/speed commands from an ASCII file and generate the commanded currents for the three phases using the indirect vector control algorithm.

5. Implement the PWM algorithm by comparing the actual and commanded values of current.

6. Generate the gating signals for the six devices of the inverter using the compare outputs of the microcontroller.

7. Implement the speed controller which can be a Proportional, Proportional and Integral, or a Proportional and Integral and Derivative controller, for a speed drive system.

The software for performing the above functions is based on the structure developed earlier using a single chip microcontroller [138]. The program is modular in structure which makes the addition of new functions easy. Each task described above are implemented in the form of subroutines to enhance the modular structure. The PWM cycle generation is implemented with the aid of the timer interrupts of the processor. The current signals which are analog in nature, are processed through an analog to digital converter fed into the processor. The position signal is input to the processor in digital format and only the incremental position value is computed in the DSP. All the other computations for the vector control algorithm are performed in the main program using the powerful instruction set of the DSP/microcontroller.

2.5.4 Results

The simulation and experimental results of the step response of a current source indirect vector controller is shown in Fig. 2.12. For the speed drive system the actual speed, the commanded speed and the commanded value of torque is shown in the figure for experimental verification. The commanded value of torque and the actual speed is included from the simulation results. The step signal is useful to evaluate the dynamic response of the drive system for the worst case possibility. A step command of $\pm$ 1000 RPM for the rotor speed is applied. The speed response closely follows the command value of speed. From the figure, it can be noted that there is a close correlation between the simulation and the experimental results.

The simulation and experimental results of the sinusoidal response of a current source

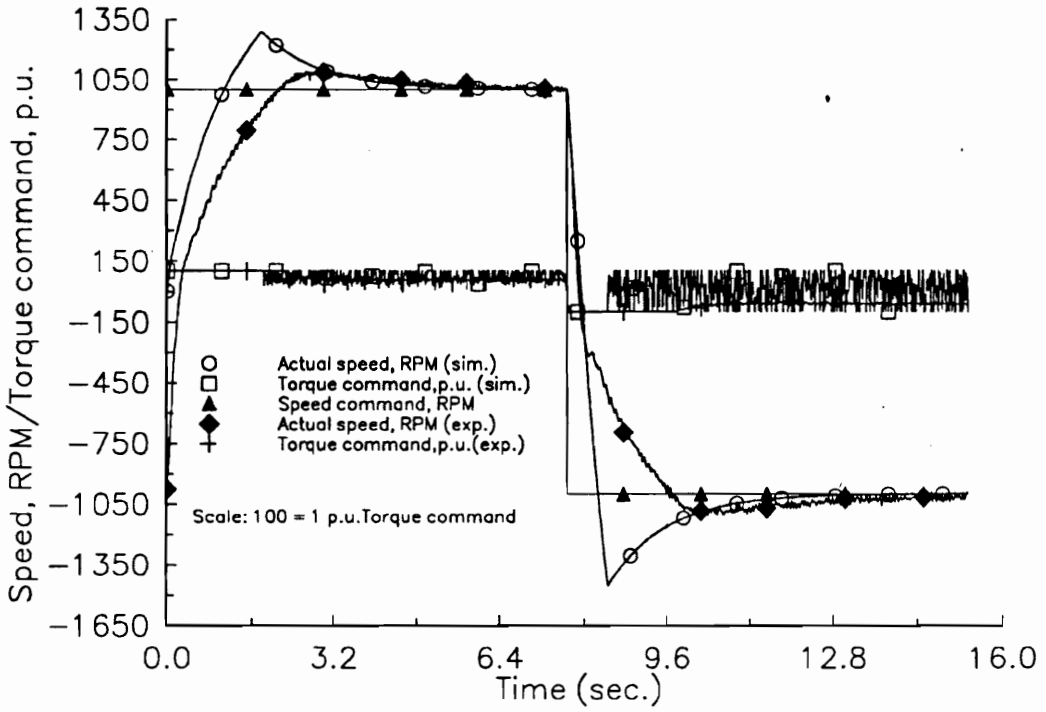

Figure 2.12: Simulation/Experimental Results of Step Speed Response of a Current Source Indirect Vector Controlled Induction Motor Drive

indirect vector controller is shown in Fig. 2.13. The actual speed, commanded speed and the commanded value of torque is shown in the figure for experimental verification and the simulation results illustrates the behavior of of the drive system. The sinusoidal signal is useful in determining the bandwidth of the overall drive system. A sinusoidal command of $\pm$ 1000 RPM for the rotor speed is applied. The actual value of speed closely follows the commanded speed and hence the frequency of the commanded signal is within the bandwidth of the drive system. A close correlation for the experimental and the simulation results can be observed from the figures.

2.6 DISCUSSION

The various vector control strategies have been classified and the principle of vector control has been presented in detail. The modeling, simulation and analysis of the current/voltage source direct/indirect vector control has been discussed in detail and the results for the various drive configurations are given to verify the validity of the schemes. The indirect vector control strategy is gaining more acceptance due to the absence of Halls sensors and better performance characteristics over a wide speed range. The main disadvantage of the indirect vector control scheme is the dependency on motor parameters. These parameters change with temperature and saturation which leads to errors in the calculation of the field angle. Such errors result in poor performance of the motor drives as seen from the results presented. The parameter sensitivity and compensation study is important from the point of view of optimum motor and converter use.

To obtain a detailed analysis of the vector control scheme on the induction motors for any practical application, it is imperative that the entire motor drive system is considered. The induction motor drive system typically consists of the motor, load, converter and the controller. Hence it can be noted that in the product development cycle, engineers involved in various fields have to interact with each other to better understand the overall drive system for a particular application. This necessitates a Computer Aided Engineering

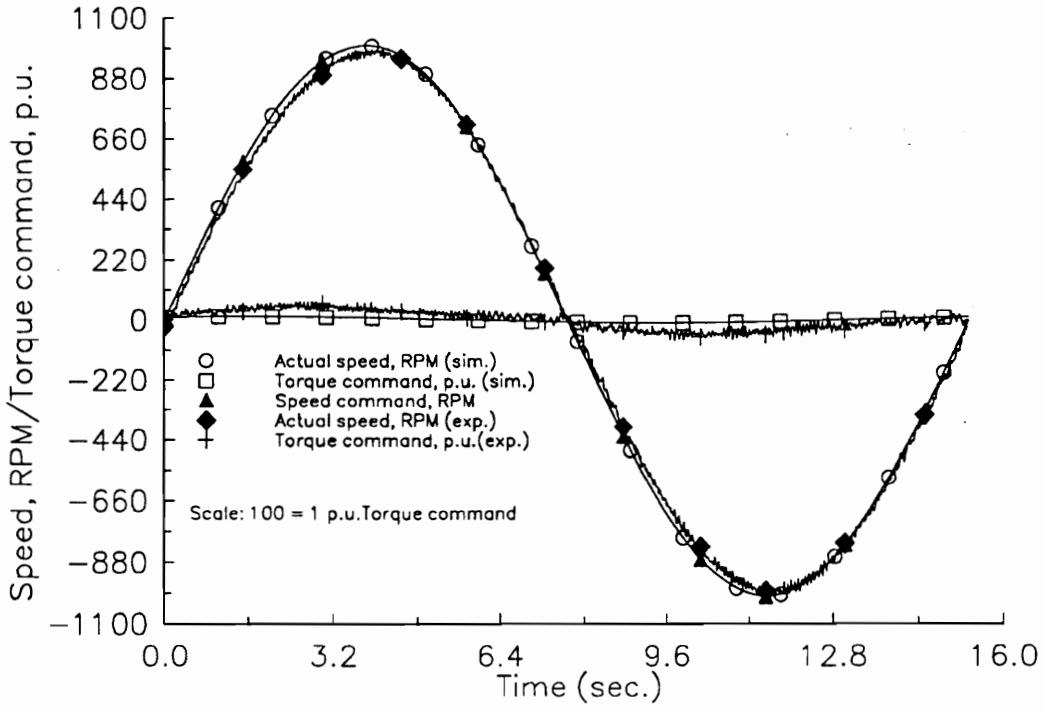

Figure 2.13: Simulation/Experimental Results of Sinusoidal Speed Response of a Current Source Indirect Vector Controlled Induction Motor Drive

(CAE) package which should be capable of simulating the interaction between the various subsystems involved in a drive system and provide the input/output in an user friendly environment. The added advantage of such a package is the resulting standardization of the terminology which would help in reducing the communication gap. The overall drive system can also be evaluated by incorporating the different vector control strategies along with the parameter sensitivity and other modules in such an environment. Such a CAE package would minimize the product development time and the prototype cost. An effort has been made in this direction and the development and features of such a CAE package, VCIM, would be discussed in detail in the next chapter.

Chapter 3

CAE ANALYSIS OF THE INDUCTION MOTOR DRIVE SYSTEM

3.1 INTRODUCTION

With the advent of vector control there has been a growing demand in the industry for the use of ac machines instead of the dc machines. This, along with the development in the semiconductor devices and control electronics, has accelerated the growth of vector controlled ac motor drive systems for variable torque and variable speed applications. The advantages of the ac drive systems are that they are robust, less expensive, have a higher power density and require minimum maintenance since there are no brushes or commutators as in the case of the dc drive systems. AC drive systems are multi-input multi-output systems. A set of stator currents and their frequencies have to be controlled to maintain the electromagnetic torque and the field flux constant. This increases the order of complexity of the system and each one of the control variables have a direct influence on the field flux and electromagnetic torque.

Variable speed drive systems consist of an electric motor, electronic converter, controller and load. The design of the electronic converter and controller are closely intertwined with the characteristics of the electric motor and load. The ac machines such as induction, permanent magnet synchronous and brushless dc motors, and switched reluctance motors are nonlinear in nature. Their nonlinearity is further compounded when they are connected to the power electronic converters which are discrete in nature due to the switching. The integration of the motor, converter, controller and load to achieve a certain performance index requires a knowledge of the individual subsystems and their interactions. The development

of new electronically controlled variable speed drive systems is a slow process in the industry due to a considerable time being spent on their analysis and design. The dynamic simulation is one of the key steps in the validation of the design process of the motor drive system, eliminating possible mistakes in the prototype construction and testing. While there has been a considerable amount of research towards the modeling, simulation and analysis of the drive system, very little attention has been devoted towards the development of a user-friendly, interactive CAE simulation package. The modeling tools available for these drive systems are limited since there are no custom-tailored software packages available for this purpose. Moreover the mathematical models for some of these drives are still evolving in the research laboratories. With the growing complexity in the development process of an ac drive system there is a need for more than one engineer to interact in a research or product development effort. This enhances the need for a CAE package capable of performing the simulation of the drive system including the motor, load, inverter, and the controllers while at the same time providing the feature to modify each subsystem independently. The ability to simulate the interaction of the subsystems would reduce the production cost and development time. An effort has been made to fill the need for an interactive simulation to assess the torque ripple, losses, efficiency, torque, speed and position responses and their bandwidth and the suitability of the drive system for a particular application.

The models for the vector controlled induction motor drive has been presented in the earlier chapter. The modeling of permanent magnet synchronous [133, 249] and brushless dc motor drive [133, 250] and switched reluctance motor drive [133] have been attempted. A number of factors have not been incorporated earlier. They are:

1. Modeling of the power devices in the converters.
2. Modeling of the various industrial loads in variable speed motor drive dynamics.
3. Modeling of the various speed, torque, and position controllers with limiters.
4. Modeling of the field weakening in the permanent magnet brushless dc and synchronous motor drives.

5. Overall efficiency model of the drive systems in steady state.

6. Ripple torque analysis in the variable speed drive systems and Fourier spectrum of the various currents and voltages in the converters.

7. Frequency response analysis of the entire drive system to obtain the transfer function and the bode plots.

8. A menu-driven user-friendly steady state and dynamic analysis, design and application software of these drive systems for use in the research and development environments both in the industry and academia.

This chapter describes the systematic derivation of the nonlinear models for the vector controlled induction motor drive systems including their loads and development of a CAE package, known as VCIM. Based on this principle a set of CAE packages for the brushless drive systems such as the permanent magnet synchronous, permanent magnet brushless dc and switched reluctance motor drive systems were also developed. These software packages are intended for analysis, design and application of these motor drives both in the research and industrial environment. The chapter is organized as follows. The next section identifies the requirements of the CAE package for the analysis of any brushless motor drive system. Section 3.3 describes the induction motor drive system and details the various subsystem models involved in the entire drive system. This is followed by a description of the CAE features which are incorporated in the package, VCIM in Section 3.4 and the various issues relating to its implementation in Section 3.5. The results obtained from VCIM are presented to highlight the package features in Section 3.6 followed by a discussion on the various issues relating to the development of CAE packages for such a task.

3.2 CAE SYSTEM REQUIREMENTS

The requirements of a CAE package to perform the dynamic analysis of any brushless drive system are shown in Fig. 3.1 and include the following: to operate in a PC based

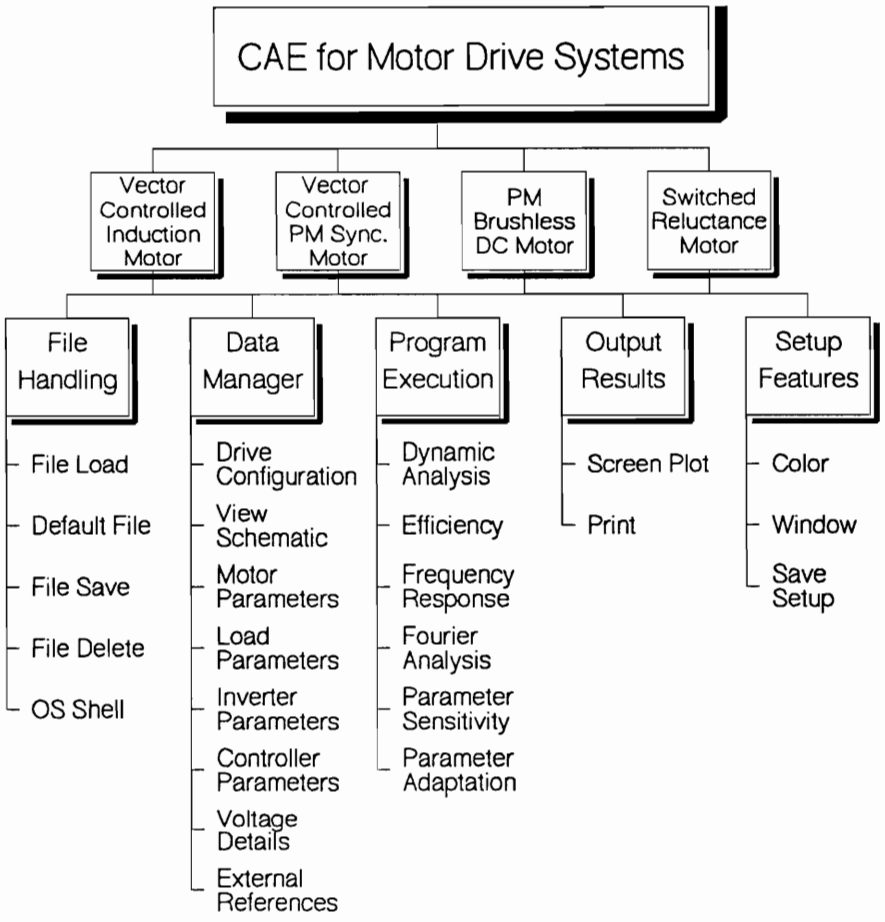

Figure 3.1: CAE System Requirements

environment with file handling, data management, numeric calculation, graphic/tabulated output and on-line help capabilities.

3.2.1 File Handling

The package should be able to interact with the operating system to enable the user to save, retrieve and delete files containing the drive system parameters. The ability to work with several drive system configurations is accomplished by this feature. In an environment where engineers design subsystems independently, multiple files allow users to vary subsystem parameters without affecting the other drive system modules. In addition, a default file should be included as a tutorial for new users. Another useful feature in the CAE package is the ability to exit to the Operating System shell from the program. This would enable the user to perform DOS operations and return back to package without losing any data in the computation.

3.2.2 Data Management

A drive system consists of several modules such as motor, inverter, controller, load, etc. Each subsystem is described by various model dependent parameters. The user of the CAE package should be able to modify the parameters of each module independently and at the same time integrate it with the overall drive system. For example, a torque drive application would not contain the speed controller parameters in the controller module.

3.2.3 Numeric Calculation

For the drive system described by the parameters, the following calculations should be performed by the CAE package:

1. Dynamic analysis of the drive system.

2. Steady state efficiency characteristics.

3. Frequency response and transfer function calculations to determine the stability of the overall drive system.

4. Fourier transform analysis of the current, torque, voltage and speed response of the drive system.

5. Parameter sensitivity studies.

3.2.4 Output

The simulation of the drive system should produce data that can be examined either graphically or in tabular form stored in an output file. The user should be able to produce a hardcopy of the graphic windows. A full screen display containing various output characteristics (in the time or frequency domain) should be provided for the performance analysis of the entire drive system. A full screen display of each characteristic would allow the user to study in more detail the drive system behavior. The ability to further zoom into a subset of the time axis would enable the user to examine the transients.

3.2.5 On-line Help

With many software packages, a detailed users manual is required. With improvements in software design, on-line help should be made available with all software packages. The following three features would increase the user friendliness of the package and reduce the importance of the users manual. A brief description of the selected parameter should appear on the screen as the user edits the various sub-module parameters. At every stage of the package a help screen should be available to the user upon a single keystroke to provide information about the selected function and the various options available. An interactive graphic schema of the drive system would aid the user in understanding the drive system configuration.

3.3 DRIVE SYSTEM DESCRIPTION

The basic functional diagram of the induction motor drive system is given in Fig. 3.2. It should be noted that there are three modes of operation, viz., (i) Torque drive (with the speed and position loops open), (ii) Speed drive (with the outer position loop open), and (iii) Position drive. To enable the analysis of the entire drive system the modeling of the following subsystems is required:

1. Modeling of the motor.
2. Modeling of the converters.
3. Modeling of the vector or decoupling controllers.
4. Modeling of the position, speed and current controllers.
5. Modeling of the various loads.
6. Modeling of the various input commands.
7. Steady state efficiency module for the entire drive system including motor, converters and load.
8. Steady state parameter sensitivity effects.

3.3.1 Induction Motor model

The dynamic model of the induction motor in the synchronously rotating reference frames is given by the following transformation:

$$\begin{bmatrix} v_{qs}^e \\ v_{ds}^e \\ v_{qr}^e \\ v_{dr}^e \end{bmatrix} = \begin{bmatrix} R_s + L_s p & \omega_s L_s & L_m p & \omega_s L_m \\ -\omega_s L_s & R_s + L_s p & -\omega_s L_m & L_m p \\ L_m p & \omega_{sl} L_m & R_r + L_r p & \omega_{sl} L_r \\ -\omega_{sl} L_m & L_m p & -\omega_{sl} L_r & R_r + L_r p \end{bmatrix} \begin{bmatrix} i_{qs}^e \\ i_{ds}^e \\ i_{qr}^e \\ i_{dr}^e \end{bmatrix} \tag{3.1}$$

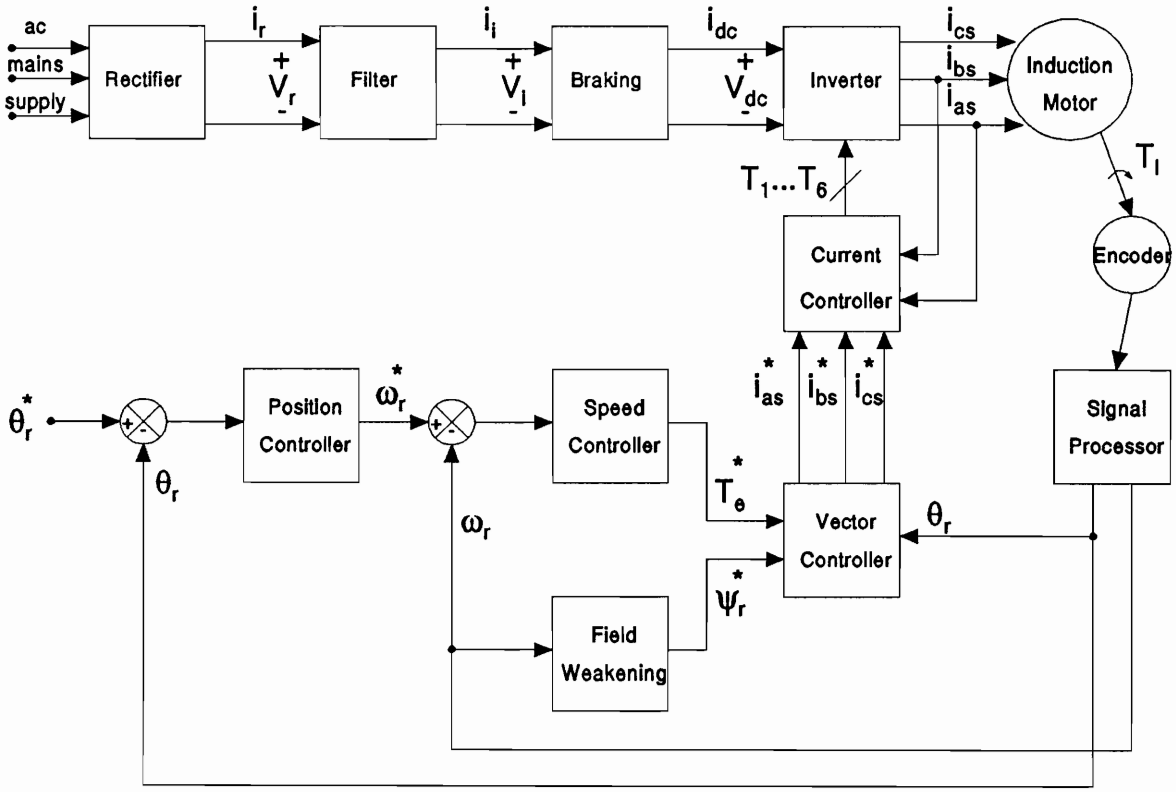

Figure 3.2: Vector Controlled Induction Motor Drive System

from which the electromagnetic torque, T_e, is calculated using:

$$T_e = \frac{3}{2}\frac{P}{2} L_m(i^e_{qs} i^e_{dr} - i^e_{ds} i^e_{qr}) \tag{3.2}$$

where, R_s, R_r, L_s, L_r are the stator and rotor resistances and self inductances, respectively. ω_s,ω_r are the stator and rotor electric frequency in radians/sec. v^e_{qs}, v^e_{ds}, v^e_{qr}, v^e_{dr}, i^e_{qs}, i^e_{ds}, i^e_{qr}, i^e_{dr} are the stator and rotor, d and q axes, voltages and currents in synchronous frames, respectively. ω_{sl} is the slip speed and the operator $\frac{d}{dt}$ is represented by p. The speed is computed from the acceleration torque equation using the load torque, T_l, Moment of Inertia, J, and the viscous friction coefficient, B:

$$J\frac{d\omega_r}{dt} + B\omega_r = \frac{P}{2}(T_e - T_l) \tag{3.3}$$

and the rotor position is given as $\theta_r = \omega_r t$.

3.3.2 Modeling of converters

There are two converters in the motor drive system. The first one is to convert the constant frequency utility ac supply to a dc voltage or current source with a diode bridge rectifier or a phase controlled rectifier. The bridge rectifier along with the dc link filter is modeled using circuit level simulation. The commutating inductance at the source of the rectifier is also taken into account in the model to provide accurate characteristics of source current and dc link voltage and currents. The second converter is a three phase inverter in the ac drive systems and a dc to dc converter in the case of a switched reluctance motor drive. The devices that could be used in the second converter can be SCRs, power transistors, MOSFETs, IGBTs, GTOs or MCTs. Each of these devices can be generally characterized by turn on, storage and turn off times for use in the modeling. Hitherto, the inverter and front end converter were modeled as a blackbox with a gain and a time constant. That does not go far to evaluate the actual dynamic situation in a drive system. A discrete modeling based on its turn on, storage and turn off time is built in the package to include the effects of the converter switching in the drive system dynamics. The turn on

and turn off stresses are relieved by the snubber circuits and are modeled as they are in the simulation to obtain the true switching picture and hence to get the switching stresses on the devices in the converters. This will enable the sizing of the required converter power devices and the filters.

3.3.3 Modeling of the vector controllers

AC motor drives such as the induction and permanent magnet synchronous and brushless motor drive systems are multi-input multi-output systems. To control the electromagnetic torque and field flux, a set of stator currents and their frequencies have to be controlled. The number of control variables become too many and each one of these has a direct influence on the field flux and electromagnetic torque. Independent control of the field flux and torque is required for high performance applications. That is made possible by a decoupling controller. This decoupling controller will transform the torque and field flux commands into equivalent current commands to influence these variables independently. This is similar to the dc motor drive where field flux is controlled by the field current and torque by the armature current, if the field current is maintained constant. Hence the decoupling controller transforms the control of the ac motor into that of an equivalent dc motor drive. This will enable the independent control of field flux and electromagnetic torque, thus simplifying the control task of an ac motor drive which is a multi-input multi-output system. A class of decoupling controllers, known as vector controllers, has been widely accepted in the industry.

If the rotor field flux is available for feedback control then it is known as direct vector controller and if the field flux is computed then it is known as indirect vector controller. Many high performance systems fall under the latter category. The disadvantage of the indirect vector controller is that it is dependent on the motor parameters such as the mutual inductance, rotor self inductance and rotor resistance. All these motor parameters are sensitive to variation in saturation levels and temperature. This will result in the coupling of the flux and torque channels, contrary to the intended objectives of their decoupling.

Hence it becomes necessary to know the effects of the parameter sensitivity on the drive system performance both in steady state and dynamic situations. A systematic derivation of the various algorithms is given in Chapter 2.

3.3.4 Modeling of the current, speed and position controllers

Current controllers

The current controllers determine the speed of response of the current loop and hence the torque generation in the machine. Apart from the speed of response of the current loop, it is desirable to minimize the current harmonics and hence the torque ripple. Various current controllers have come into existence with different performance indexes for use in the vector controlled induction, permanent magnet synchronous and brushless dc motor drives. The most widely used current controllers are viz., (i) Pulse Width Modulated (PWM) current controllers, and (ii) Hysteresis current controllers.

It is important to assess the impact of the power device characteristics, motor parameters, and load parameters on the performance of the current controllers and hence the total drive system, for a given application to identify the most suitable current control strategy and current controller. These controllers are modeled and integrated in the CAE package to study the research implications of the various current control strategies.

Speed and Position controllers

The speed and position controllers determine the dynamics of the drive system with reference to the rise time and overshoot and also offset the mechanical resonances in the load. It is usual to use a proportional or proportional and integral or a proportional-integral-derivative controller in the industry. But the tuning of this controller to achieve a certain performance with the nonlinear motor drive is a time consuming process if trial and error approach is resorted to. From the frequency response, the controller parameters can be chosen to closely approximate the control specifications. Then the tuning can be done

within a few iterations taking fully into account the nonlinearity of the motor drive system.

3.3.5 Load modeling

Until now in the literature, the load is modeled as an inertia and a frictional constant. It is unusual to encounter such a simplistic load in practice and this fact calls for the simulation of realistic loads such as fan, pump, compressor and nonlinear loads driven by the ac drive systems. The load modeling and the study of its effect on the drive system performance has manifold advantages of precisely sizing the converter, motor and determining in advance any of the mechanical resonance and oscillation problems when driven from the ac drive systems. These oscillation problems if confirmed in the simulation could be overcome by the judicious selection of the parameters in the speed and current controllers.

3.3.6 Modeling of the reference inputs and disturbances

The reference inputs and disturbances required for application to evaluate the dynamic drive system performance are identified to be any one of the following:

1. Step signal input.
2. Trapezoidal signal input.
3. Sinusoidal signal input.

The step signal for input or disturbance is chosen with a view to evaluate the dynamic responses of the drive system in the worst case. The trapezoidal signal is intended for testing the drive system under realistic industrial conditions. The sinusoids with flexibility for biasing them positive or negative are intended for finding the bandwidth under all the nonlinearities and to study the effects of excitation under resonance. A great amount of programmability and flexibility is built into these test signals so that they can satisfy most of the realistic needs of the user.

3.3.7 Steady state efficiency module

The computation of the steady state efficiency is required to optimize the control strategy and to reduce the operating energy costs of the drive system. Also this module is intended to compare the various drive systems and this is one of the authentic criterion for comparison in many of the appliance drives such as refrigerator, freezer, washer, dryer and hvac compressor motor drives. Such an efficiency calculation should include not only the motor but also the inverter and controlled or uncontrolled rectifier used for ac to dc power conversion. The algorithm proposed considers all the losses in the electronic converter switches, diodes, and motor. The motor losses will include all the copper losses and core losses which are available either as a constant or a function of operating frequency. The friction and windage losses are given as a constant for a particular speed or entered as a function of speed through graphical means. The overall efficiency is evaluated as the ratio of the rotor output to the input of the electronic converter from the ac mains supply. An instantaneous calculation of efficiency will be difficult to interpret as there is an interchange of energy from the source to motor and vice versa. The input and output are averaged over the period of 360 mechanical degrees and then the efficiency is calculated from these average values.

3.3.8 Steady state parameter sensitivity module

The indirect vector control strategy is dependent on the rotor resistance, R_r, the mutual inductance, L_m, and the self inductance of the rotor, L_r. The inductances change with the saturation of the magnetic material while the rotor resistance is affected by the variation in the temperature [132]. The increase in temperature increases the rotor resistance. In case of the current source inverters used in high performance drive systems, if the stator current is maintained constant this has the effect of increasing the magnetizing current and hence saturating the machine. Core losses in the motor increases with the saturation of the magnetic path and in the end necessitates a considerable derating of the machine.

In a torque controlled induction motor drive, i.e., with the outer speed loop open, the

rotor flux linkages and the electromagnetic torque are the external command signals while the actual slip speed is maintained equal to the command value. The mismatch between the controller and the motor parameters introduces deviations in the flux and torque producing components of the stator current and hence the torque angle. Once the outer speed loop is closed, the electromagnetic torque, T_e^*, will be modified until the actual output torque equals the load torque in steady state. Thus, the effect of parameter variations on steady state performance is reduced. The temperature and saturation effects are studied for the torque, flux, slip speed and the peak stator current phasor.

3.3.9 Drive systems

The features discussed in the earlier sections for the vector controlled induction motor drive systems can also be used in the development of CAE packages for the following brushless drive systems:

1. Permanent magnet synchronous motor drive system.
2. Permanent magnet brushless dc motor drive system [137].
3. Switched reluctance motor drive system [13, 284].

All the features discussed in the earlier sections are incorporated for all these drive systems listed above. For the case of a switched reluctance motor drive system, in addition to the development of the dynamic simulation package, SRMDYN, the task included the integration of other software packages into a single powerful tool. The author had earlier been involved in the development of a CAD package for the design and analysis of a switched reluctance motor and a steady state analysis package of the converter for the switched reluctance motor [284]. These packages are currently integrated into a single CAE tool, known as SRMCAD, which combines the features and functions of all the three packages. These CAE systems constitute the development of modern drive systems for which no such analysis software packages are currently available. Still quite a number of industrial houses

are in the process of developing these advanced drive systems and these CAE packages will be of help in their efforts.

3.4 CAE SYSTEM FEATURES

The major features required by the CAE package to perform the above task are identified as follows:

1. File management.
2. Data development.
3. Run commands.
4. Plot commands.
5. Setup choices.
6. Help features.
7. Quit command.

Each of the above features has a set of options and they will be individually described in the following subsections.

3.4.1 File management

Four options are available for this feature and they are:

1. Default drive system for loading.
2. User-defined system for loading.
3. Save the current drive system.
4. Exit to Operating System.

The default drive system is for tutorial purposes to help the beginner. The user-defined system stores all the drive systems that the user may have worked on and any one of them can be loaded for future simulations. The save option stores the current drive system that the user maybe working on into the disk space for future use. The option to exit from the CAE package to the operating system enables the user to perform some basic operation outside the CAE shell without losing the current data environment.

3.4.2 Data development

The data development section has the following features:

1. Drive configuration.
2. Schematic of the drive system.
3. Motor parameters.
4. Load parameters.
5. Inverter parameters.
6. Controller parameters.
7. External references.

These features are explained in the following paragraphs.

Drive configuration

This capability facilitates the selection of different types of drive configuration. The possible choices are the torque, speed or position drive. The torque drive has the speed and position loop open, while the speed drive has the outer position loop open.

Drive schematic

The drive schematic has the capability to provide a graphical representation of the torque, speed, and position drive systems. A sample output of a position drive schematic is given in Fig. 3.3. The individual subsystems are displayed in detail upon the user's request made possible by moving a lens/cursor on each one of them. The torque, speed, and position controlled drive schematics are given in this module. This feature would help a new engineer to become familiar with the entire drive system. Also, if more than one individual is working on a development effort, the schematic would enable them to communicate with each other due to the standardization of the symbols and notations.

Motor parameters

The motor parameters such as inductances, resistances, emf constant, power, voltage, frequency, friction coefficient, and moment of inertia, etc., are defined and included in this module. A brief definition of the parameter selected is described in the window box placed at the bottom of the screen with its standard units to help the user.

3.4.3 Inverter parameters

The inverter switches are characterized by the turn on, storage and turn off times, conduction voltage drop and the voltage drop across the free-wheeling diode which is anti-parallel to the switch. Apart from these, the snubber resistor and capacitor values are obtained to model the turn-off process completely.

The input rectifier which converts the ac source to a constant dc link voltage is modeled either a controlled or an uncontrolled rectifier. The dc link voltage is characterized by:

$$V_{dc} = 1.35 V_{ll} \cos \alpha \tag{3.4}$$

where V_{ll} is the line-line voltage and α is the triggering angle. For uncontrolled rectifiers, the triggering angle is 0 degrees.

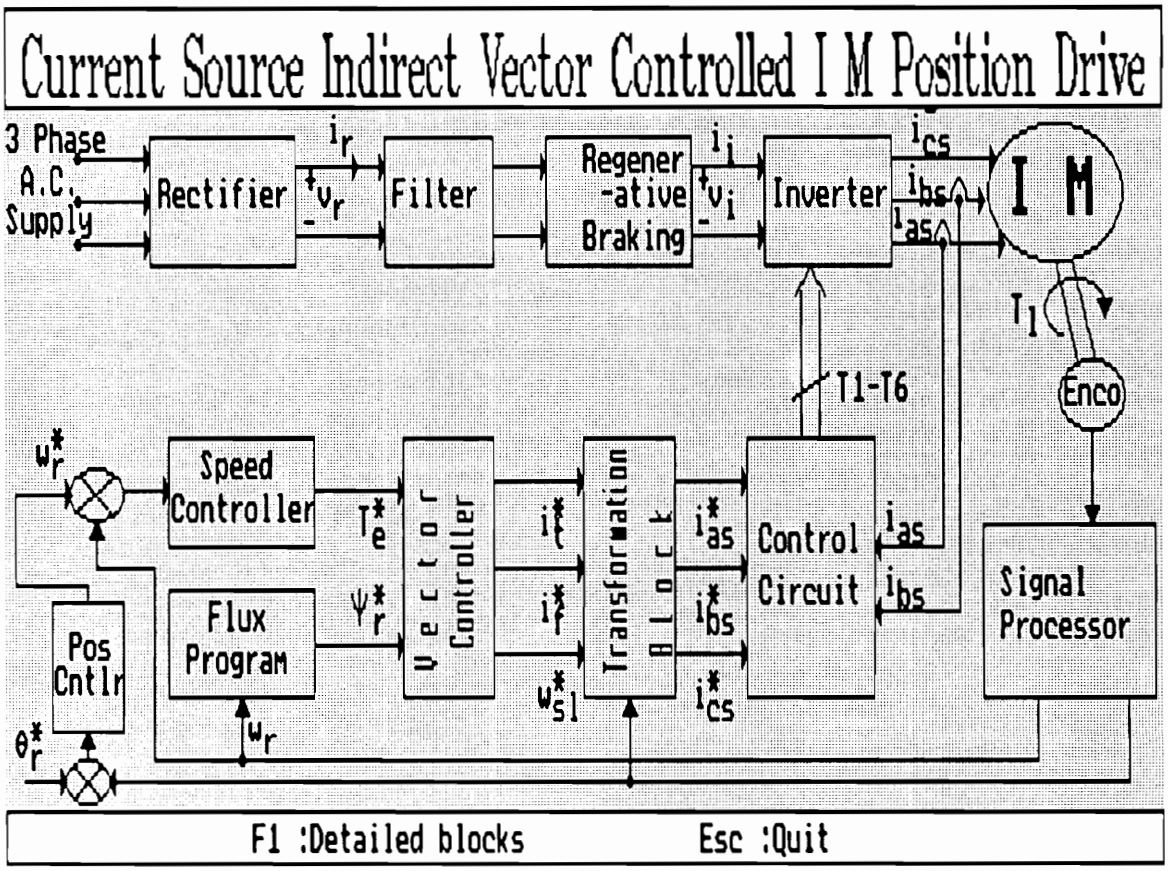

Figure 3.3: Sample Output of the Position Drive Schematic

3.4.4 Controller parameters

The controller parameters consists of the following independent modules:

1. Current controller.
2. Speed/position controller.
3. Current limiter.
4. Torque/speed limiter.
5. Field weakening.

A brief explanation of each module listed above is given in the following paragraphs.

Current controller

There are two options for current control, viz., hysteresis and pulse-width modulated (PWM) current controllers. The hysteresis current controller is characterized by the current window, i.e., the current deviation allowed for the actual current from the value of the reference current. The PWM current controller is characterized by the carrier frequency, and the current controller gain.

The PWM current controller equation is given as follows for phase 'A'. A similar relationship holds for 'B' and 'C' phases.

$$V_{as} = \begin{cases} \frac{V_{dc}}{2} - \text{ device drops} & \text{if } i_{as} - i_{as}^{*} > \text{ carrier amp.} \\ -\frac{V_{dc}}{2} + \text{ device drops} & \text{if } i_{as} - i_{as}^{*} \leq \text{ carrier amp.} \end{cases} \tag{3.5}$$

where i_{as} and V_{as} are the phase 'A' current and voltage, respectively. V_{dc} is the dc link voltage. The hysteresis current controller for one phase, say 'A', satisfies the following conditions:

$$V_{as} = \begin{cases} -\frac{V_{dc}}{2} + \text{ device drops} & \text{if } i_{as} - i_{as}^* \geq \Delta_i \\ \frac{V_{dc}}{2} - \text{ device drops} & \text{if } i_{as} - i_{as}^* \leq \Delta_i \end{cases} \tag{3.6}$$

Speed/position controllers

Three type of speed/position controllers are implemented for the drive systems and they are proportional (P) type, proportional integral (PI) type or proportional integral and derivative (PID) type. These would require the proportional, integral and derivative gains depending upon which speed/position controller is chosen.

The position controller to calculate the speed command for any position error signal is:

$$\omega_r^* = K_p(\theta_r^* - \theta_r) + K_i \int (\theta_r^* - \theta_r)\, dt + K_d \frac{d(\theta_r^* - \theta_r)}{dt} \tag{3.7}$$

The speed controller to calculate the torque command for any speed error signal is:

$$T_e^* = K_p(\omega_r^* - \omega_r) + K_i \int (\omega_r^* - \omega_r)\, dt + K_d \frac{d(\omega_r^* - \omega_r)}{dt} \tag{3.8}$$

where, K_p, K_i and K_d are the proportional, integral and derivative gain constants respectively.

Current limiter

The current limiter is required for the purpose of primarily protecting the converter and the process from thermal breakdown and catastrophe, respectively. This current limiter is dependent upon the converter capability, motor ratings and load restrictions. They are usually in the range of 1 to 6 p.u. in practice. Therefore, a flexible current limiter is built into this software package.

Torque/speed limiter

The torque/speed limiter serves a similar purpose by limiting the torque/speed command signal. A variable limiter is built into the software package.

Flux programming

Field weakening for operation beyond the rated speed is usually achieved by flux programming. It is usual to have a rated flux up to the base speed and then to vary it as a function of speed so that the power output of the drive system is constant. This is already programmed but requires only the maximum speed input for the flux programming. This feature is common for both the indirect vector controlled induction and permanent magnet synchronous motor drive systems.

The flux program is performed to satisfy the following conditions:

$$\psi_r^* = \begin{cases} 1 \text{ p.u.} & \text{if } |\omega_r| \leq 1 \text{ p.u.} \\ \frac{1}{\omega_r} \text{ p.u.} & \text{if } |\omega_r| > 1 \text{ p.u.} \end{cases} \tag{3.9}$$

where, ψ_r^* is the commanded value of normalized rotor flux.

Flux programming is effected in the permanent magnet brushless dc motor drive systems by phase advancing the stator current in relation to the flux. Hence an input is required as to the magnitude of the phase advance angle in electrical degrees. This has to be a variable. The impact of the phase advance on the torque, power output and the dynamic behavior of the system is of value in application considerations. The phase advance feature is already built into the system.

Load parameters

The load parameters contribute to a definition of a friction, fan or pump loads, a mixed load which is a combination of a constant, friction and pump loads and a compressor load. In addition to these type of loads the CAE package also has the ability to model a user defined load. For this type of load, the user is given the option of programming the load torque of the drive system as a function of speed or time. On selecting this option, the user is requested to define the load torque for various values of either speed or time. Once the data values are entered, the user is given an option of viewing the load characteristics on

the screen to verify its validity. While these do not exhaust all the loads encountered in practice, they are certainly the most prevalent loads for variable speed drive systems.

The step load is characterized by the following equation:

$$T_l(t) = Au(t - t_1) - Au(t - t_2) + Bu(t - t_3) - Bu(t - t_4), \text{ Nm} \tag{3.10}$$

where, $u(t)$ is defined as the unit step function.

For frictional loads:

$$T_l(t) = A\omega_r, \text{ Nm/rad/s} \tag{3.11}$$

For fan/pump loads:

$$T_l(t) = A\omega_r^2, \text{ Nm/(rad/s)}^2 \tag{3.12}$$

For mixed loads:

$$T_l(t) = A + B\omega_r + C\omega_r^2, \text{ Nm} \tag{3.13}$$

where A, B and C are constants. Compressor load is characterized by Fig. 3.4.

External references

The external references are for the torque, speed, and position command inputs. They are made available in the following three forms:

1. Positive and negative step inputs with programmable "on times" and "off times" for each.

2. Trapezoidal references with both positive and negative programmable magnitudes and time durations.

3. Sinusoidal references with programmable magnitudes and frequencies.

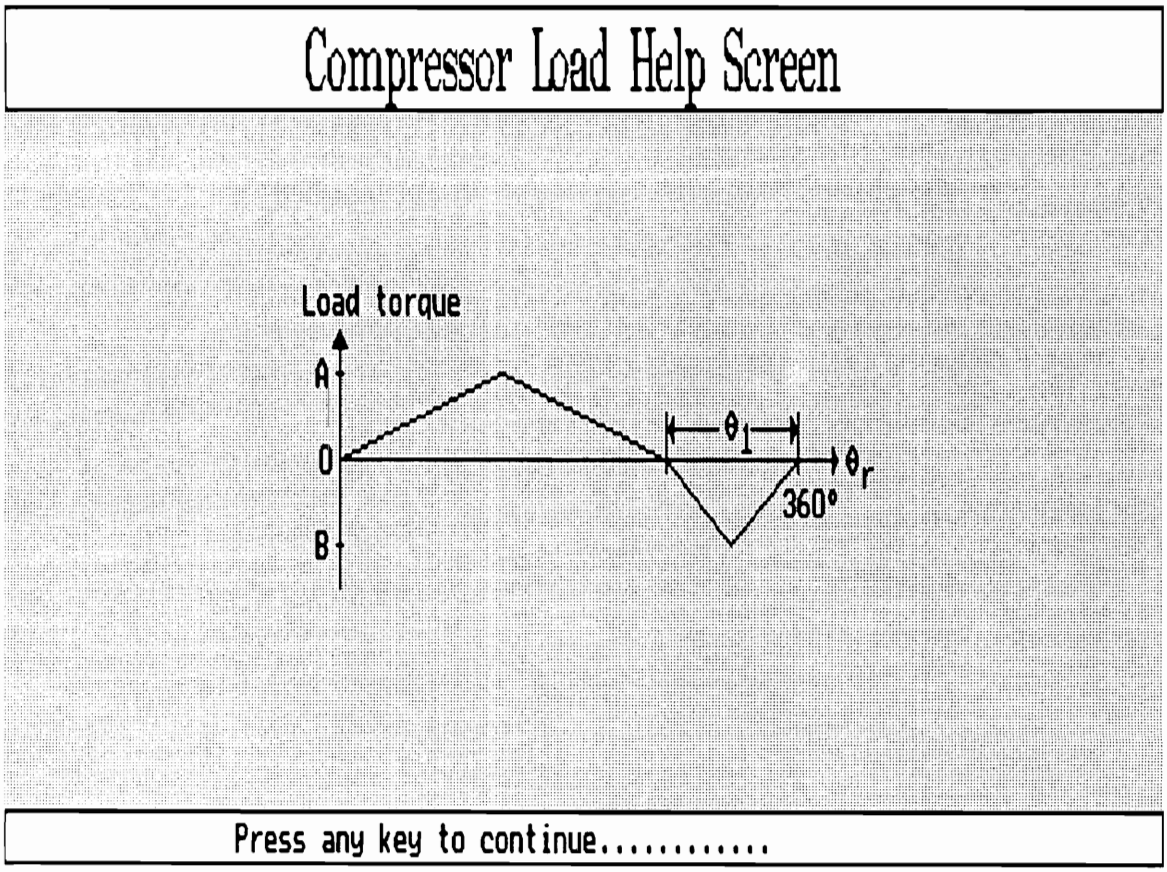

Figure 3.4: Typical Compressor Load Characteristics

The step reference is for the purpose of evaluating the time domain performance of the drive system for torque, speed, and position inputs and disturbances. The trapezoidal references closely resemble the references encountered in practice and hence will be useful in evaluating an actual application. The sinusoidal references can be used to evaluate the bandwidth of the position, speed, or torque loop by observing the attenuation for increasing input frequencies. It should be noted that this type of evaluation involves no approximations in the converter or linearization of the motor and controller equations. This is the only way the speed or current loop bandwidth can be estimated in the motor drive systems. Step responses are also important to characterize a system such as a fast response robotic drive. These reference signals have been incorporated into the software packages with the input parameters defined in Fig. 3.5.

3.4.5 Run options

The requirements of the run option include:

1. Dynamic simulation of the entire drive system.
2. Steady state efficiency calculation.
3. Fast Fourier Transform of current, voltage, torque and speed.
4. Parameter Sensitivity study.

A full screen display describing all the drive parameters prior to these run commands helps to verify the parameters. A hard copy of the screen can also be used for documentation purposes. During execution of the commands, the progress of the calculation is also reported. These features enhance the usefulness of the software package.

3.4.6 Plot features

The capability to plot on a screen or printer is required for a graphical analysis of the simulations. Additional features such as the selection of variables for plotting and zooming

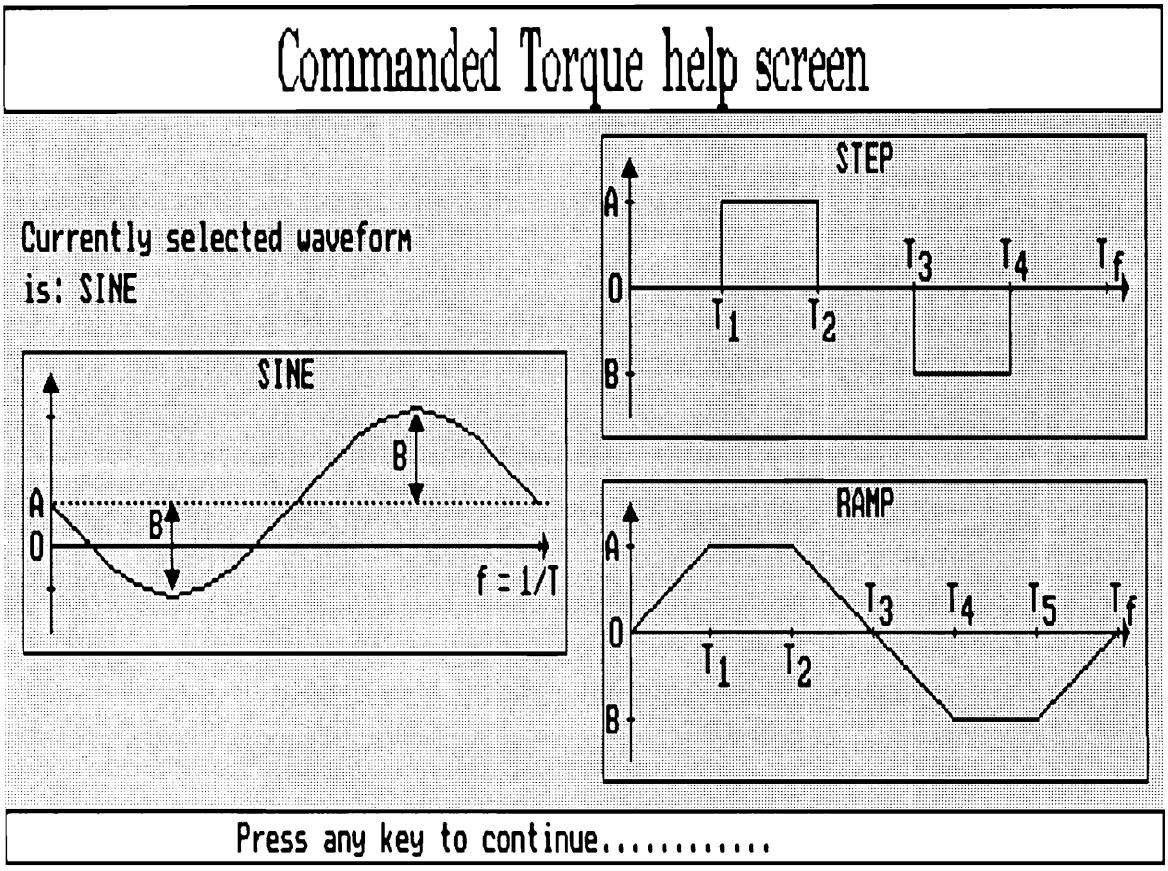

Figure 3.5: Sample Full Screen Help Menu of External Reference Signals

to examine in detail the torque and current waveforms for ripples, etc., is incorporated for enhancing the analysis capability. An added feature is the option to micro zoom into any plot which helps in the detailed study of the drive system characteristics.

3.4.7 Setup features

The setup of the colors for various levels of the menu screen is required for increasing the comfort zone of an individual user. Output files should be set for different variables of interest in the drive system.

3.4.8 Help features and users manual

Context-sensitive help in the form of pull-down screens is required whenever the user needs it. Interactive help screens available upon a single keystroke eliminates the need for detailed user manuals. This can be made much more sectionalized and indexed to make it into a manual for beginners using these CAE packages. These manuals can be either in script or readme type of files. The CAE packages have been developed for the modern drive systems satisfying the criteria listed in the previous sections. The main features of the CAE packages are summarized below:

- The CAE system, developed in PASCAL and FORTRAN, is highly interactive with powerful graphics capability. A context-sensitive, detailed on-line help is available on a single keystroke.
- The I/O structure utilizes easy-to-use window-based pull-down menus.
- A default drive system is provided in a file and may be used as a tutorial for the new users.
- The CAE packages are capable of simulating a torque, speed, and a position drive.
- An on-line schema for a torque, speed or a position drive is available with a built-in option to magnify any block in the drive.

- All the parameters can be changed individually or loaded from an existing file. The current values can also be stored in a new file.
- A switch-by-switch model of the inverter including the on-time, off-time and storage time of the devices is built-in.
- Option is provided for using either a PWM or a Hysteresis current controller. In the case of a speed/position drive, the speed/position controller can be either a Proportional (P), Proportional and Integral (PI) or a Proportional, Integral and Differential (PID) controller.
- A step, ramp or a sinusoidal response of the torque/speed/position is performed with provision for the user to vary the amplitude/frequency of the input commanded value and the results determine the bandwidth of the corresponding loop.
- A full screen display of all the values of a particular drive system is provided before initiating the simulation, to help the user verify all the input values.
- A screen plot consisting of eight characteristics with an option to zoom any one of the graphs for full screen viewing is provided. Further macro zooming into any selected graph in the time domain is also built into the CAE packages.
- A high resolution hard copy capability is also provided for obtaining high quality printouts.

3.5 IMPLEMENTATION DETAILS

Three software environments are needed to implement the features of the desired CAE packages: a user friendly input interface and editing environment, an intensive computation section to perform the actual simulation and a graphic environment to present the results. The hardware required to perform this task will also be described in the following subsections.

3.5.1 Input Environment

The requirements of this module include pop-up windows, multiple help screens, the ability to input and output data files and the overall control of the program. Pascal was chosen as the programming language for this task for reasons given below.

Turbo Pascal, with built-in windowing functions, allows the separation of drive system parameters into several windows and hence a modular structure. This aids the user to modify specific subsystem parameters. The use of well organized windows and strategically placed operation information makes the program more user friendly. The last line of the screen has been reserved in this package for program operation information. This information includes a brief description of how to accomplish several tasks such as opening and closing windows, editing, etc. The user friendly requirement of the CAE package is accomplished with full screens of help information, in text or graphic format, available upon request at almost every stage of the program.

The next requirement is the use of data files to store the parameters of a drive system. ASCII data files were used so that a user can edit the files with only a text editor. The user can choose a file to load from a list of available files found in the current sub-directory. Also, as the specifications are changed, they can be saved to a disk. If the user-specified file name is being used by another file, the user should be warned and allowed to specify another file name.

The last requirement is the ability to run other programs from within the current environment. Choosing the run option creates a temporary file containing the current drive system parameters. Once the simulation program is executed, control is returned to the main environment. Advantages of this structure are the ability to continue unaffected after a simulation program crash, to determine whether the simulation program terminated normally and to indicate the type of error encountered.

3.5.2 Numeric Calculations

This environment performs the calculation of various output characteristics of the drive system such as speed, torque, currents and voltages. Since several of the algorithms for simulation have previously been implemented in Fortran, it was selected for this task. The data is read in from the temporary data file created by the input environment. The calculations are made for each instant of time by solving a system of nonlinear differential equations using the fourth order Runge-Kutta algorithm. Due to the iterative nature of this algorithm, the execution speed is of prime importance. Microsoft FORTRAN 5.0 was used to compile this program because it produced faster codes than several other versions of Fortran.

The data produced during simulation is available in tabular form for use in the graphic environment. Due to the resolution limitations of the monitor to display the graphs, and the memory constraints for the data file, the number of data points output to the data file is regulated. A limit of 1500 data points has been implemented by writing to the data file only after a calculated number of iterations have been completed. Thus, the output is effectively sampled at up to 1500 equal intervals during the simulation.

3.5.3 Graphic Environment

The requirements of this environment include graphic representation of the simulation results and the ability to read and store those values. A program was developed that could read the data file created by the simulation package and display the data in eight graphs on the same screen. By selecting one of the graphs, a full screen display could be produced. Further magnification along the time axis is also available. This features aids in the examination of the transients in the simulation results. In addition, a hard copy of the graphs can be obtained. The user is prompted at the bottom of the screen with all of the available features.

3.5.4 Hardware

The software was developed on an IBM PS/2 model 50 with a 30 Mb hard drive and an EGA monitor. The software will run on an IBM PC, XT, AT, PS/2, or any true compatible that has an EGA or VGA monitor. The hard drive is not a requirement, but due to the size of the output files and the slow access speed of floppy drives, a hard drive is highly recommended.

The size of the executable code for all the programs needed for each CAE package that has been developed is about 1 Mb. A sample data file produced by the simulation module is about 200 Kb. Therefore, the space recommended to run the software is at least 2 Mb. This would provide space for several default drive system specification files and more than one simulation result file.

3.6 RESULTS

The results obtained using the CAE packages are presented and discussed in this section. The various user-friendly features described in the previous sections are implemented in these packages. A sample screen containing the interactive windows is illustrated in Fig. 3.6. It can be noted that each item can be selected by moving the arrow keys and a brief definition of the item selected is displayed in the WATCH box on the bottom of the screen. A sample full screen help menu of external reference signals is illustrated earlier in Fig. 3.5. This feature provides detailed help on a single keystroke and guides through the various options in the software. This would help a new user to adapt to the package very quickly.

A full screen display of the various parameters of the drive system is displayed before the actual simulation is performed. This helps the user to check the validity of the drive system specified and provides an option to modify any of the erroneous values thus saving simulation time. One such display for a speed drive system is illustrated in Fig. 3.7. The input to the drive system is the speed command which is maintained at the commanded value by controlling the set of stator currents. The data screen contains seven groups of

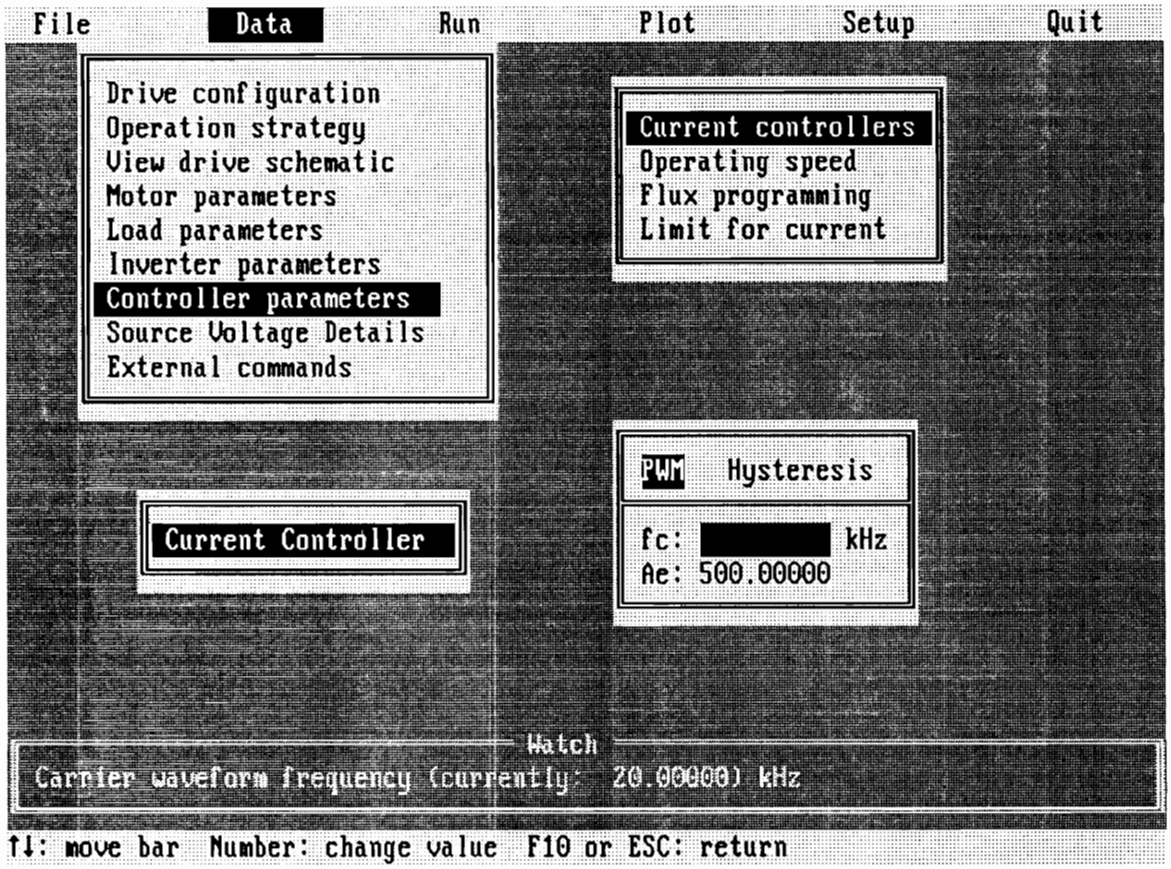

Figure 3.6: Full Screen Display of an Interactive Session

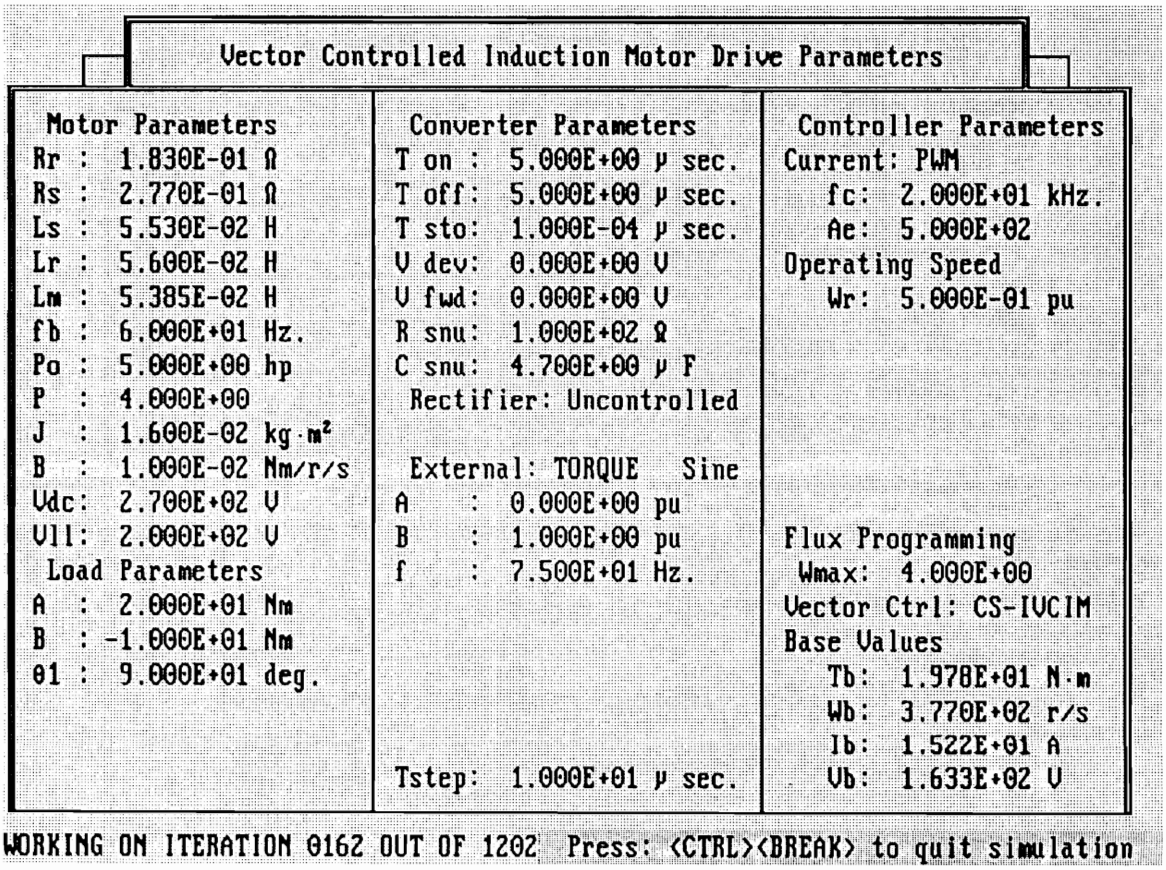

Figure 3.7: Parameter Screen Defining the Drive System

data, viz., motor parameters, load parameters, converter parameters, external commands, time step, controller parameters, flux programming and the base values. Once the user selects to run the simulation, the iteration steps are displayed on the bottom of the screen.

The graphical output obtained using the speed drive system is shown in Fig. 3.8. For the torque drive system the normalized values of the actual speed, commanded flux current and the rotor flux, load torque commanded torque current and the electromagnetic torque, commanded and actual current of phase 'A' are displayed. A sinusoidal command of ± 1 p.u. for the electromagnetic torque signal is applied. This is useful in determining the bandwidth of the overall drive system. The torque response closely follows the commanded signal. A compressor load is applied and the load profile can be noted from the characteristics. The decoupled field and torque currents from the vector controller are given with the actual rotor flux and electromagnetic torque obtained from the drive system. The inner current loop is represented by the commanded and actual values. The actual current follows the commanded value of the current, implemented by a PWM controller. The transient and steady state response of the current can also be seen in this figure.

Fig. 3.9 illustrates the flux trajectory for drive system described here. The q and d axes rotor flux values are plotted and it can be noted that the orthogonality is maintained by the circular trajectory. This is an effective tool to verify the decoupling nature of the vector control strategy.

The temperature and saturation effects of the torque and flux characteristics of a torque drive are shown in Fig. 3.10. The torque command versus actual torque/flux characteristics, assuming a constant saturation factor for various slip speeds, is presented in the top two plots of Fig. 3.10. The parameter α is the temperature factor and is defined as the ratio of the rotor time constant of the motor and its instrumented value in the vector controller. The parameter β is the saturation factor and is defined as the ratio of the actual mutual inductance and the instrumented value in the vector controller. For $\alpha < 1$ which signifies an increase in the rotor temperature, the electromagnetic torque and the rotor flux linkage is greater than the commanded value. Though the rotor flux is shown to increase beyond

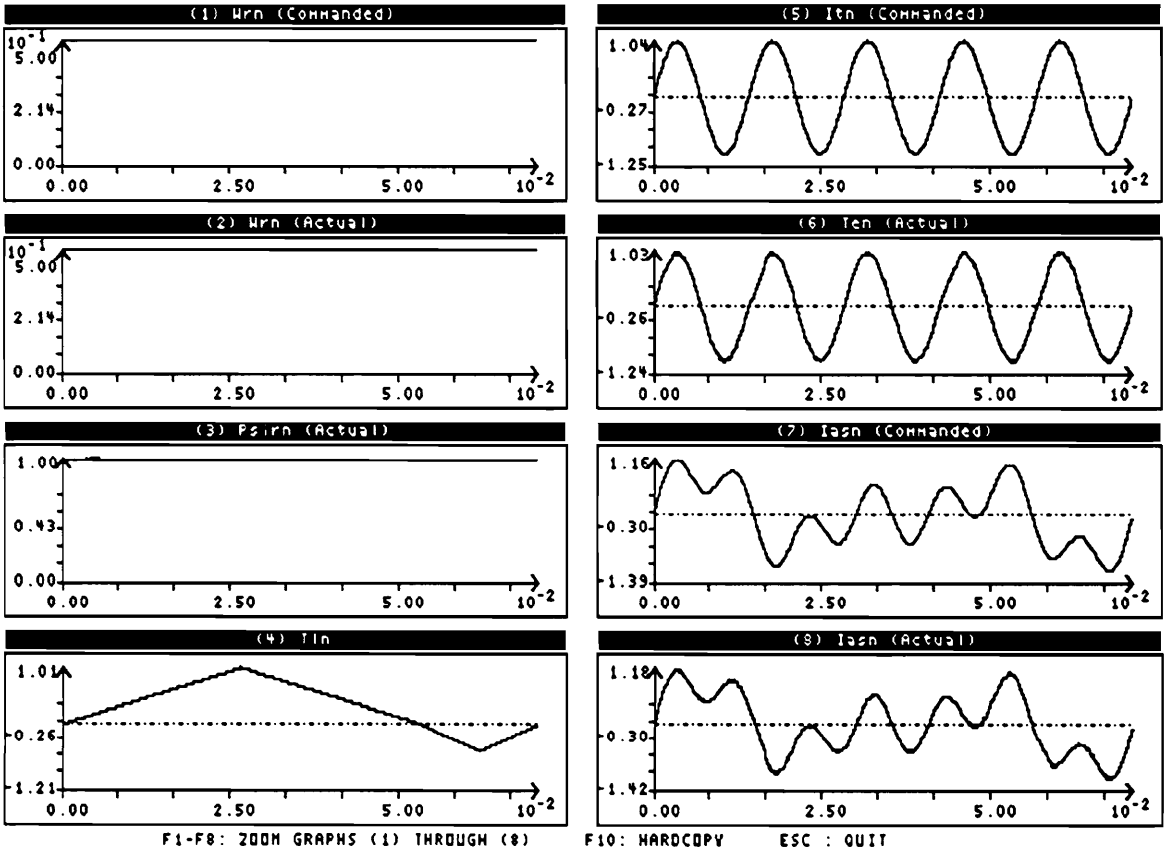

Figure 3.8: Eight Graph Full Screen Display of the Output Characteristics

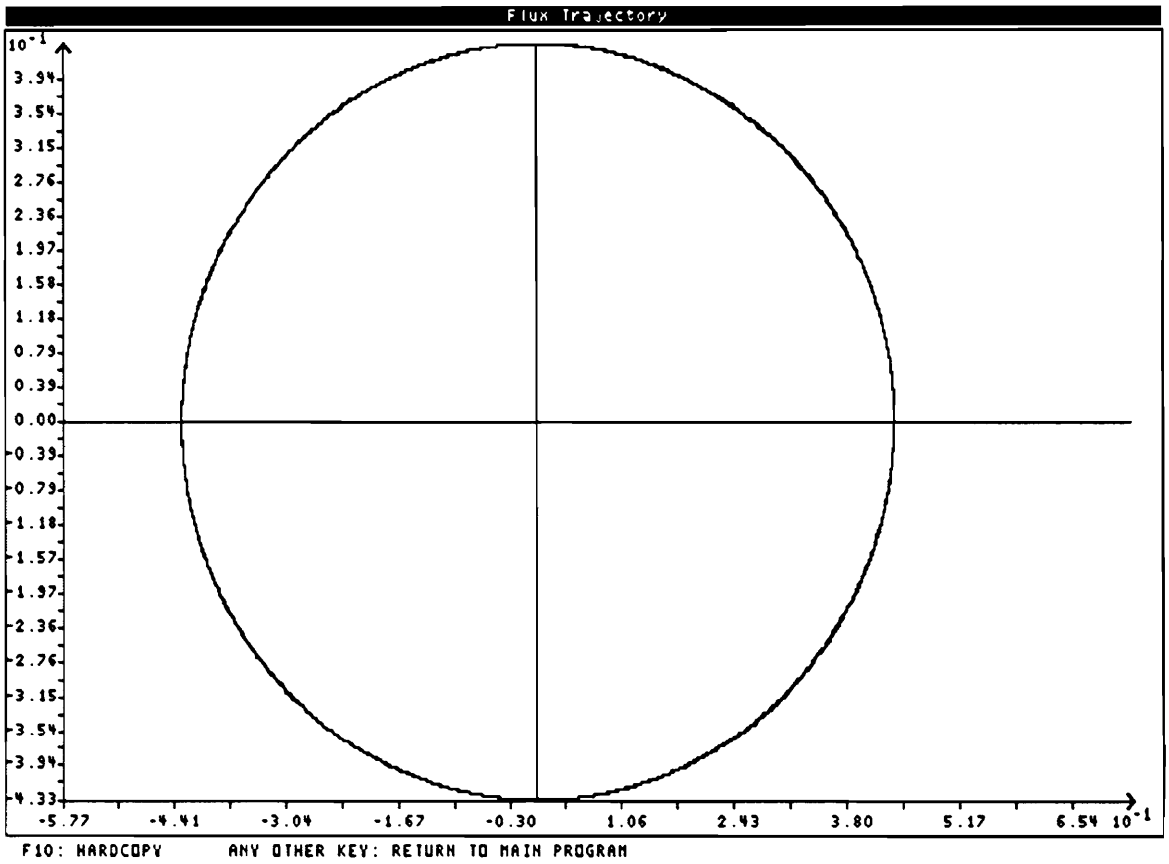

Figure 3.9: Flux Trajectory

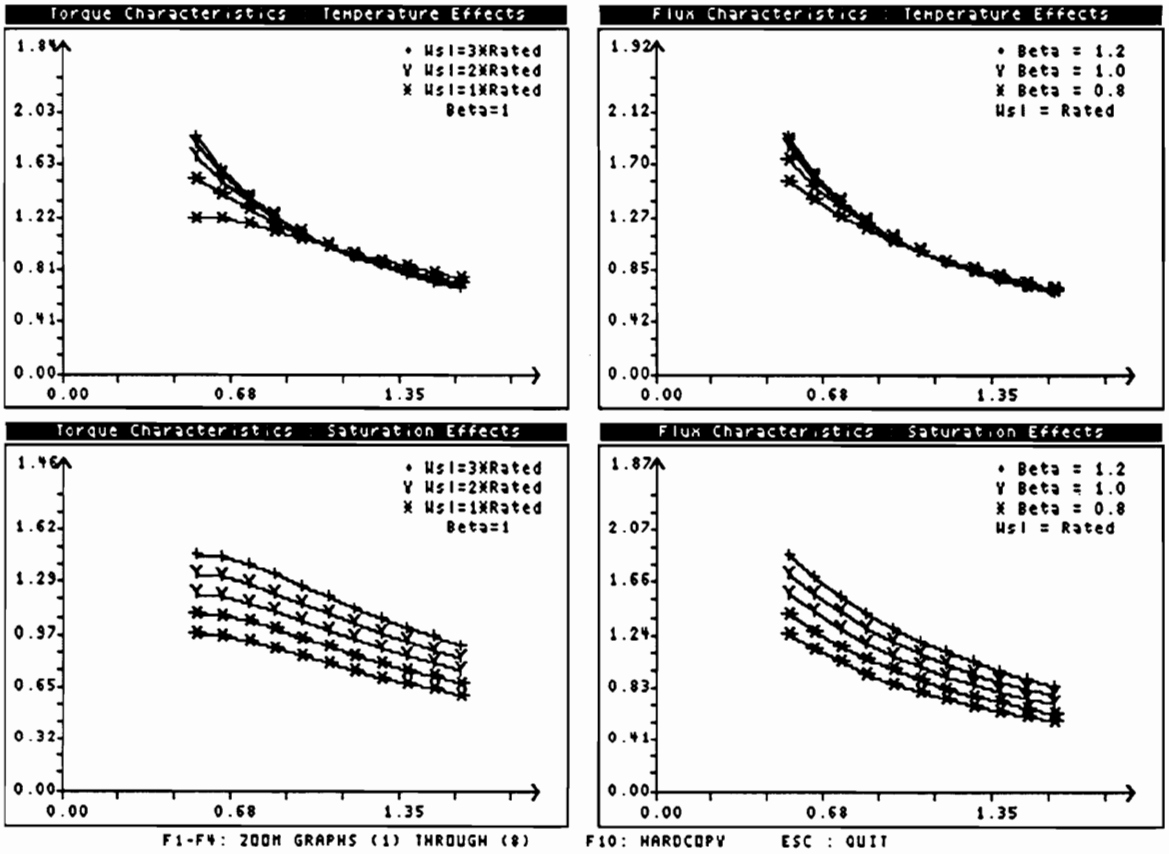

Figure 3.10: Temperature/Saturation Effects of the Torque/Flux Characteristics of a Torque Controlled Indirect Vector Controlled Induction Motor Drive

1.2 p.u., it is difficult to maintain this high value due to saturation. An increase in α indicates an increase in motor saturation at ambient temperature and for such operating conditions the torque is less than the commanded value. The bottom two plots of Fig. 3.10 illustrate the saturation effects of the torque and flux characteristics. It can be noted that both the torque and flux values increase when α is less than one and decrease when α is greater than one. Hence it can be noted that linearity of the input-output torque relationship has degraded and the induction motor drive is unsuitable for use in torque control applications. Either an outer speed loop or a torque loop/parameter compensator becomes essential to achieve a linear torque amplifier.

The temperature/saturation effects for the torque, flux, slip speed and peak stator current for a speed drive are illustrated in Fig. 3.11. It can be noted that the torque and flux follow the commanded values for $\alpha = 1$, at any rotor speed. With decreasing α the torque is less than its commanded value up to 0.75 p.u. load torque, beyond which the actual torque is greater than the commanded value. When α is greater than one the behavior is just the opposite. The rotor flux decreases for values of α greater than one up to 0.7 p.u. load torque and then remains constant. At α equals 0.5, the actual value of flux increases monotonically with the load torque. Due to the saturation of the motor, only a modest increase in magnitude results.

The slip speed is linear for $\alpha = 1$, but exhibits other trends for various values of α. For α less than one, the slip speed is higher than the nominal value up to a reasonable fraction of full load, beyond which it becomes slightly less than the nominal value. The peak stator current has a close resemblance to the slip speed characteristics. This trend signifies that the rotor losses increase for values of load torque less than 0.8 p.u.

The bottom four plots of Fig. 3.11 illustrates the saturation effects for the torque, flux, slip speed and the peak stator current. As expected, saturation decreases the flux level by 20 percent, while the value of torque is lower than that of the command value. From the slip speed characteristics, it can be noted that $\alpha = 0.5$ and around 1 p.u. load torque, the drive will have lower losses than its nominal value and designed peak capacity, even when

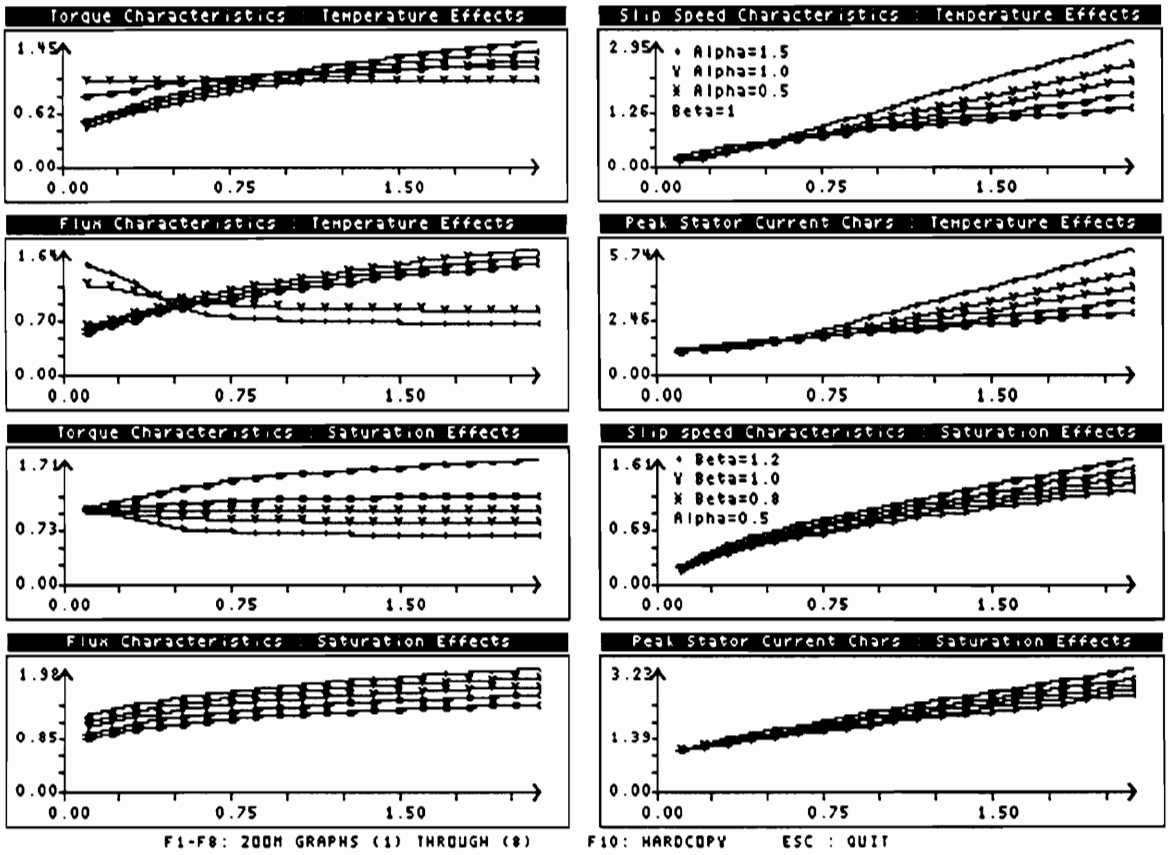

Figure 3.11: Temperature/Saturation Effects of the Steady State Characteristics of a Speed Controlled Indirect Vector Controlled Induction Motor Drive

the saturation effects is included. This is due to the fact that saturation has increased the peak stator current. The drive operation is usually confined to values of torque 1 p.u. and lower, and in this region, it can be noted that the stator losses are higher. This is highly undesirable from the point of view of thermal rating of the motor and the overall system efficiency. Various other modules such as steady state efficiency, and Fourier spectral analysis are built into the system and their results help to better understand the overall drive system.

3.7 DISCUSSION

The methodology for the development of a CAE package for the dynamic analysis of vector controlled induction motor drive systems is presented. This package would aid in the assessment of the torque ripple, losses, efficiency, torque, speed, and position responses and their bandwidth and the suitability of the drive system for a particular application. Based on this principle, four such packages, VCIM, PMBD, PMSM, and SRMCAD were developed for the computer simulation of variable speed motor drive systems. This chapter describes in detail the various subsystems involved in the drive system. The usefulness of the CAE packages has been emphasized by going through the features incorporated and the discussion of the results obtained. The development of such CAE packages for ac drive systems would benefit the drives industry by helping to reduce the development time and product cost. Even though quite a number of features have been discussed and implemented in these packages, the author believes that this is just the beginning of research and development in this area. Future research can be addressed to developing time optimal algorithms for control, detailed subsystem modeling for increased accuracy, object oriented coding for multi motor drive systems, and an effort can be made towards the development of Expert Systems for such tasks.

A number of drive systems for various industrial applications are variable speed drives. This would lead to the fact that many vector control induction motor drives require the

speed controller to maintain a low speed error signal. Hence, care should be taken in the design of the parameters for the speed controller. The similarity of the vector controlled induction motor drives and the separately excited dc motor has been stressed earlier. The large signal model for the design and study of the speed controller parameters has been presented in [133]. A similar method for the vector controlled induction motor drives would help reduce the complexity of the design process. This would also lead to enhanced performance characteristics of the overall drive system. An effort has been made to develop such an algorithm and would be described in the next chapter. A method to reduce the overshoot of the rotor speed within allowable limits using this study is also presented.

Chapter 4

DESIGN AND STUDY OF THE SPEED CONTROLLER

4.1 INTRODUCTION

A number of modern manufacturing processes, such as the machine tools require variable speed drives. The most commonly found applications for the speed controlled motor drive systems are in steel, textile, paper and pulp, and mining industry. As discussed in the earlier chapters, vector controlled induction motor drive systems are extensively employed for such applications. The successful operation of these drives is dependent on the performance of the speed controller. The proportional plus integral (PI) controller is normally employed to maintain the error between the commanded and actual values of the rotor speed minimum. The design of the gain and time constants of the speed controller is of paramount importance in meeting the dynamic specifications of the motor. The large signal model for the speed controlled dc motor has been developed earlier and a systematic approach was presented for the design and study of the speed controller [133]. Such a study would help in improving the overall response of the drive system. The similarity between the separately excited dc motor and the vector controlled induction motor drive has been established in the earlier chapters. By utilizing this similarity, an identical approach for developing the large signal model would simplify the design of the speed controller and hence improve the overall response.

This chapter deals with the design and study of the speed controller for an indirect vector controlled induction motor drive system. The large signal model is formulated for the indirect vector controlled induction motor drive in the next section. This is followed by

a step by step derivation of the transfer function of the overall drive system. A method to reduce the overshoot of the speed response based on the model developed is also presented in Section 4.3. The simulation results for the design of a speed controller for a given drive system using this method is presented in Section 4.4. Section 4.5 presents the experimental verification obtained using the DSP based setup described earlier, followed by a discussion of the various issues on this topic.

4.2 MODELING OF THE SPEED CONTROLLED DRIVE

Speed controlled drives, operating only in the constant torque region, are employed in many applications due to the simplicity of control. In a dc motor drive, this is achieved by armature control which has the advantage of a faster response compared to that of a field control which is sluggish. It can also be noted that since the operating speed is always less than the base speed of the motor, field weakening is not necessary. In other words, the field current is maintained constant for all operating conditions.

The induction motor has a tachogenerator whose output is utilized for closing the speed loop. The motor will drive a load which will be assumed to be frictional for the purpose of this study. The output of the tachogenerator is filtered to remove the ripples to provide the rotor speed signal, ω_r. The speed command, ω_r^*, is compared with the actual speed, ω_r, to produce a speed error signal. This signal is processed through a speed controller to determine the torque command. The torque command is limited so as to keep it within safe allowable limits and the current command is obtained by proper scaling. Since the field current is maintained constant, the control of the stator phase currents is equivalent to controlling the torque current in the vector controller. The torque current is obtained from the electromagnetic torque and the torque constant. The commanded value of the torque current is compared with the actual torque current so as to have a zero current error. The current error signal is processed through a current controller to obtain the q axis voltage or the torque voltage. From the equations of the vector controller, the induction motor

drive has been modeled with an inner induced emf loop, similar to that of a dc motor. The interaction of the emf loop and the inner current loop increases the complexity in the development of the model.

The inner current loop assures a fast current response and the limiter also maintains the current to a safe preset level. This inner current loop makes the converter a linear current amplifier. The outer speed loop ensures that the actual speed is always equal to the commanded speed and any transient is overcome within the shortest time without exceeding the motor and converter capabilities. The transfer functions of the various subsystems will be described in detail in the following subsections.

4.2.1 Induction Motor

The q and d axes stator voltages of the induction motor in the synchronously rotating reference frames are given as,

$$v_{qs}^e = (R_s + L_s p) i_{qs}^e + \omega_e L_s i_{ds}^e + L_m p i_{qr}^e + \omega_e L_m i_{dr}^e \tag{4.1}$$

$$v_{ds}^e = -\omega_e L_s i_{qs}^e + (R_s + L_s p) i_{ds}^e - \omega_e L_m i_{qr}^e + L_m p i_{dr}^e \tag{4.2}$$

But, from the derivation of the vector controller discussed earlier, the following relationships are known,

$$\begin{aligned} i_{qs}^e &= i_t \\ i_{ds}^e &= i_f \\ \psi_{qr} &= 0 \\ \psi_{dr} &= \psi_r \end{aligned} \tag{4.3}$$

For this study, since the motor operates in the constant torque region, there is no field weakening and the field current is constant. Hence,

$$pi_f = 0$$
$$p\psi_r = 0 \tag{4.4}$$

The rotor flux and synchronous stator frequency are given as,

$$\psi_r = L_m i_f \tag{4.5}$$

$$\omega_e = \omega_{sl} + \omega_r \tag{4.6}$$

Also, the q and d axes rotor currents are given as,

$$i^e_{qr} = -\frac{L_m}{L_r} i_t \tag{4.7}$$

$$\begin{aligned} i^e_{dr} &= \frac{\psi_r}{L_r} - \frac{L_m}{L_r} i_f \\ &= \frac{L_m}{L_r} i_f - \frac{L_m}{L_r} i_f \\ &= 0 = p i^e_{dr} \end{aligned} \tag{4.8}$$

Rewriting the q axis voltage or the torque voltage using the above relationships,

$$\begin{aligned} v^e_{qs} &= (R_s + L_s p) i_t + \omega_e L_s i_f - \frac{L_m^2}{L_r} p i_t \\ &= R_s i_t + (\frac{L_s L_r - L_m^2}{L_r}) p i_t + \omega_e L_s i_f \\ &= (R_s + L_a p) i_t + \omega_e L_s i_f \end{aligned} \tag{4.9}$$

where,

$$L_a = \frac{L_s L_r - L_m^2}{L_r} \tag{4.10}$$

Hence,

$$i_t = \frac{v_{qs}^e - \omega_e L_s i_f}{(R_s + L_a p)} = \frac{v_{qs}^e - (\omega_r + \omega_{sl}) L_s i_f}{(R_s + L_a p)} \tag{4.11}$$

From the dynamic model of the induction motor, the equations for the slip frequency and the electromagnetic torque are given as,

$$\begin{aligned} \omega_{sl} &= \frac{L_m R_r}{L_r} \frac{i_t}{\psi_r} \\ &= \frac{R_r}{L_r} \frac{i_t}{i_f} \end{aligned} \tag{4.12}$$

$$\begin{aligned} T_e &= \frac{3}{2} \frac{P}{2} \frac{L_m}{L_r} i_t \psi_r \\ &= (\frac{3}{2} \frac{P}{2} \frac{L_m^2}{L_r} i_f) i_t \\ &= K_t i_t \end{aligned} \tag{4.13}$$

where K_t is the torque constant, defined as,

$$K_t = \frac{3}{2} \frac{P}{2} \frac{L_m^2}{L_r} i_f \tag{4.14}$$

The transfer function for the induction motor torque channel is given as,

$$G_a(s) = \frac{i_t(s)}{V_e(s)} = \frac{K_a}{1 + sT_a} \tag{4.15}$$

where, from equation 4.11,

$$V_e(s) = v_{qs}^e - \omega_e L_s i_f(s) \tag{4.16}$$

and the gain and time constants are given as,

$$K_a = \frac{1}{R_s} \tag{4.17}$$

$$T_a = \frac{L_a}{R_s} \tag{4.18}$$

4.2.2 Load

The load is modeled as a function of moment of inertia, J, with a viscous friction coefficient of B. Then the acceleration torque drives the load and is given by,

$$J\frac{d\omega_r}{dt} + B\omega_r = \frac{P}{2}(T_e - T_l) \tag{4.19}$$

where, T_l is the load torque. The load torque is assumed to be frictional for the purpose of this study. Hence, the load is proportional to speed and given as,

$$T_l = B_l\omega_m \tag{4.20}$$

The transfer function for the frictional load is given as,

$$G_m(s) = \frac{\omega_r}{T_e(s)} = \frac{K_m}{1 + sT_m} \tag{4.21}$$

where the gain and time constants are given as,

$$K_m = \left(\frac{P}{2}\right)\frac{1}{B + B_l} = \left(\frac{P}{2}\right)\frac{1}{B_t} \tag{4.22}$$

$$T_m = \frac{J}{B_t} \tag{4.23}$$

4.2.3 Current Controller

The most commonly used techniques for current control are the hysteresis and PWM. In the case of a hysteresis controller, the response is instantaneous and hence the controller is modeled as a simple gain of unity. For this study, a standard PWM controller is employed to reduce the current error. The PWM controller has a delay of half the time period of

the carrier waveform with a frequency of f_c. It can be noted from the block diagram that the input of the PWM controller is the error torque current, i_{te}, in volts, and the output is the q axis stator voltage in the synchronously rotating reference frames. The maximum rms voltage of the q-axis voltage under steady state conditions cannot exceed $0.45 \times V_{dc}$. The inverter gain can then be represented as a function of the peak voltage capability corresponding to the available control voltage. Hence its transfer function is given as,

$$G_c(s) = \frac{v_{qs}^e}{i_{te}(s)} = \frac{K_c}{1 + sT_c} \tag{4.24}$$

where

$$i_{te}(s) = i_{tm}^*(s) - i_{tm}(s) \tag{4.25}$$

and the gain and time constants are given as,

$$K_c = \sqrt{2} \times 0.45 \times \frac{V_{dc}}{V_c} \tag{4.26}$$

$$T_c = \frac{1}{2f_c} \tag{4.27}$$

where V_c is the control voltage and, f_c is the switching frequency of the PWM controller.

4.2.4 Speed Controller

The proportional plus integral (PI) controller is the most commonly used technique for the speed controller. It consists of proportional and integral gain constants. The speed controller to calculate the torque command for any speed error signal is:

$$T_e^* = K_p(\omega_r^* - \omega_r) + K_i \int (\omega_r^* - \omega_r)\, dt \tag{4.28}$$

where, K_p and K_i are the proportional, and integral gain constants, respectively. The transfer function of the speed controller is given as,

$$G_s(s) = \frac{K_s(1 + sT_s)}{sT_s} \tag{4.29}$$

where the gain and time constants are given as,

$$K_s = K_p \tag{4.30}$$

$$T_s = \frac{K_p}{K_i} \tag{4.31}$$

4.2.5 Speed Feedback

Most of the high performance drives use a dc tachogenerator and the filter required is a low pass with a time constant of 2 msec. or less. The transfer function of the feedback filter is given as,

$$H(s) = \frac{\omega_{rm}(s)}{\omega_r(s)} = \frac{K_\omega}{1 + sT_\omega} \tag{4.32}$$

where K_ω is the gain and T_ω is the time constant of the dc tachogenerator and filter.

4.3 OVERALL TRANSFER FUNCTION EVALUATION

The step by step derivation of the overall transfer function of the drive system is given in Fig. 4.1. The equations for the motor are incorporated in the induction motor, EMF calculator, and slip speed calculator blocks in the figure. By including the slip speed calculator into the motor model and simplifying the loop, the new transfer function is given as,

$$G_b(s) = \frac{i_t(s)}{v_{qs}^e - \omega_r L_s i_f} = \frac{K_b}{1 + sT_b} \tag{4.33}$$

where the gain and time constants are given as,

$$K_b = K_a \,/\, \left(1 + \frac{R_r L_s}{R_s L_r}\right) = K_a \,/ K_j \tag{4.34}$$

$$T_b = \frac{T_a}{K_j} \tag{4.35}$$

The following are the transfer functions defined in the step (iv) of the block diagram reduction, given in Fig. 4.1:

$$G_1(s) = \frac{T_e(s)}{\omega_r^*(s) - \omega_{rm}(s)} = \frac{K_s(1 + sTs)}{sT_s} \tag{4.36}$$

$$G_2(s) = \frac{v_{qs}^e}{i_{tm}^*(s) - i_{tm}(s)} = \frac{K_c}{1 + sT_c} \tag{4.37}$$

$$G_3(s) = \frac{i_t(s)}{v_{qs}^e - \omega_r L_s i_f} = \frac{K_b}{1 + sT_b} \tag{4.38}$$

$$G_4(s) = \frac{\omega_r(s)}{T_e(s)} = \frac{K_m}{1 + sT_m} \tag{4.39}$$

$$H(s) = \frac{\omega_{rm}(s)}{\omega_r(s)} = \frac{H_\omega}{1 + sT_\omega} \tag{4.40}$$

By further reduction and arriving at step (vi) as shown in the figure,

$$G_5(s) = \frac{G_2(s)G_3(s)}{1 + G_3(s)G_4(s)K_t L_s i_f} \tag{4.41}$$

Similar to the derivation of the transfer function of the dc motor, the second order model of the current loop is replaced with an approximate first order model to design the speed loop. This helps to reduce the order of the overall speed loop gain function. This leads to the approximation of the following transfer function,

$$G_2(s)G_3(s) = \frac{K_c K_b}{(1 + sT_c)(1 + sT_b)} \approx \frac{K_r}{1 + sT_r} \tag{4.42}$$

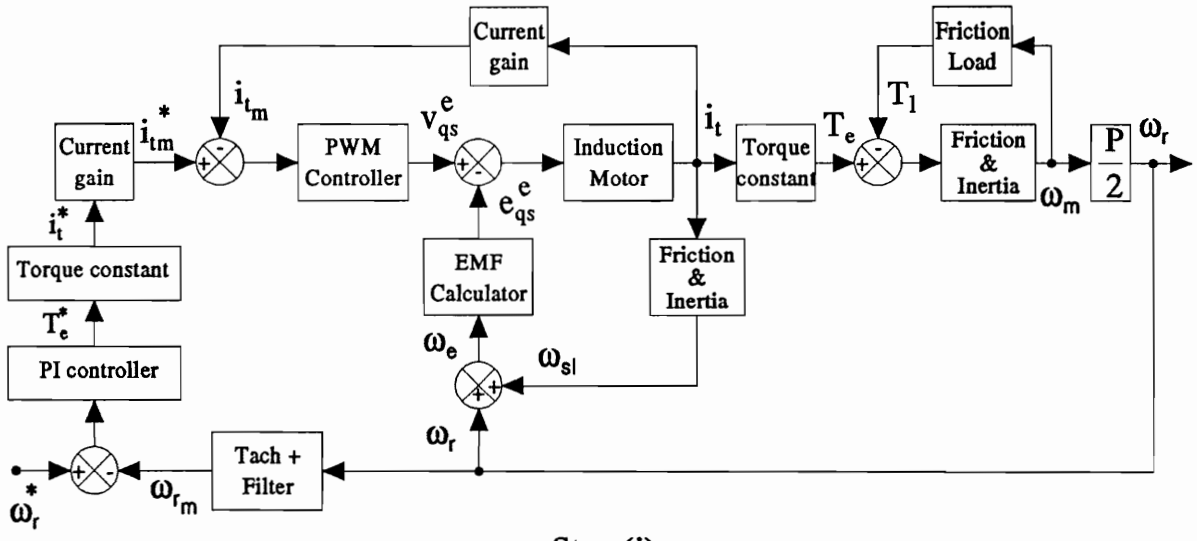

Step (i)

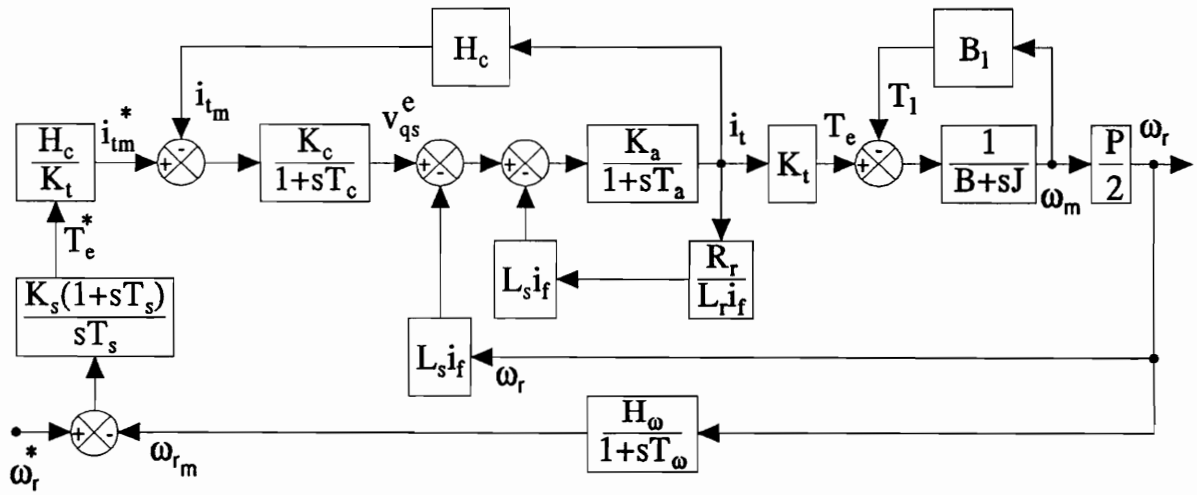

Step (ii)

Figure 4.1: Step by Step Derivation of a Speed Controlled Indirect Vector Controlled Induction Motor Drive System

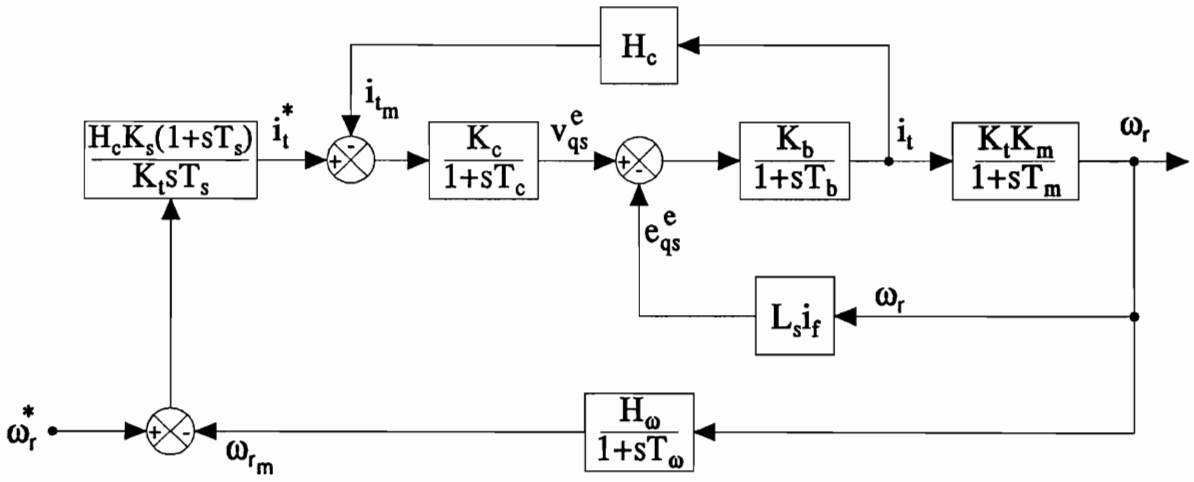

Step (iii)

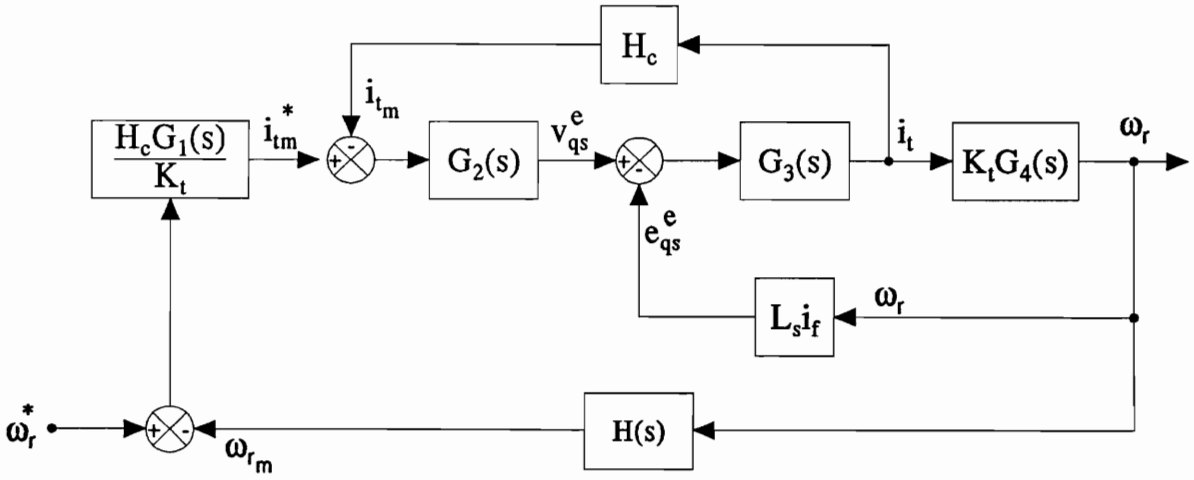

Step (iv)

Figure 4.1: Step by Step Derivation of a Speed Controlled Indirect Vector Controlled Induction Motor Drive System

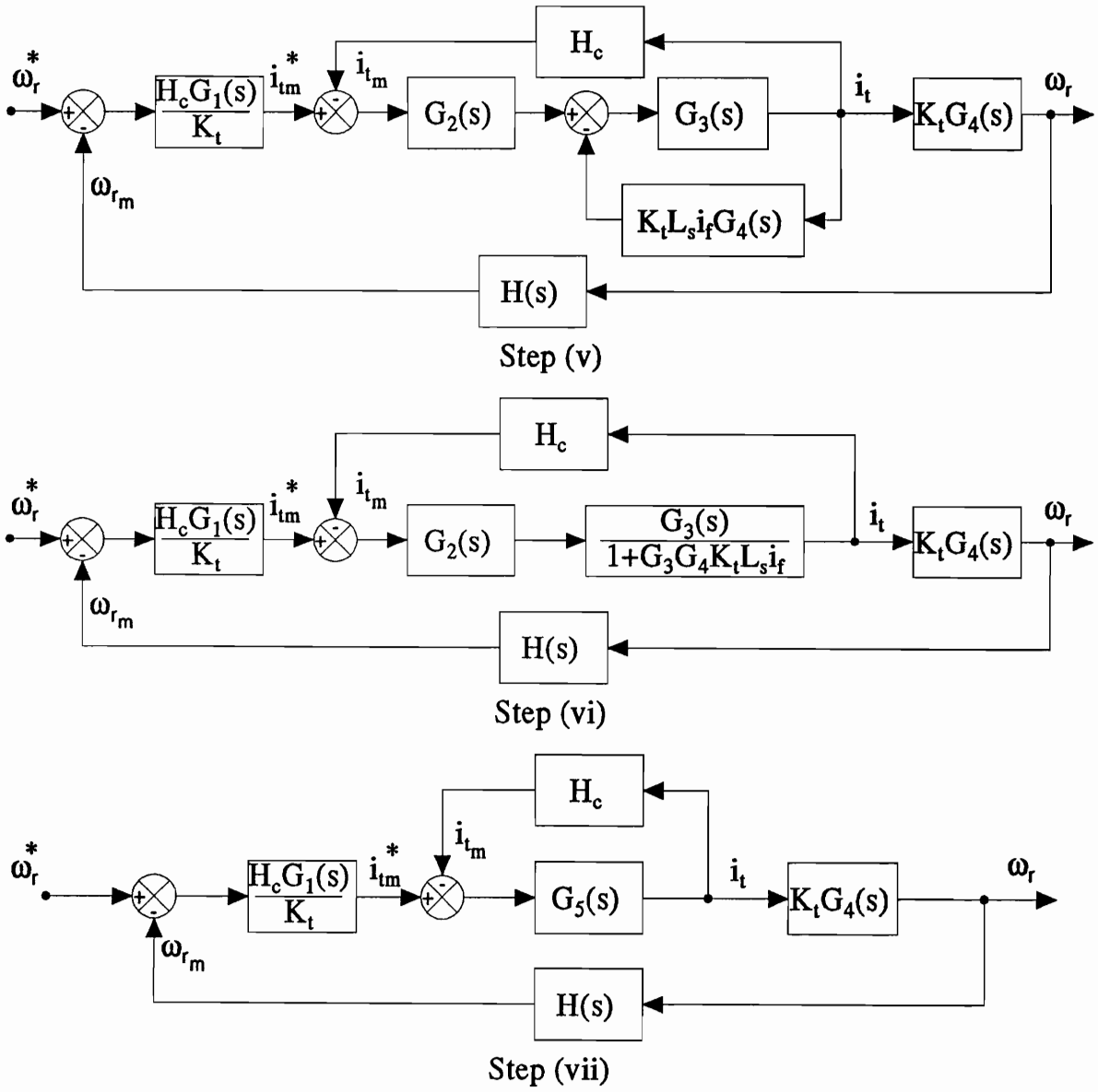

Figure 4.1: Step by Step Derivation of a Speed Controlled Indirect Vector Controlled Induction Motor Drive System

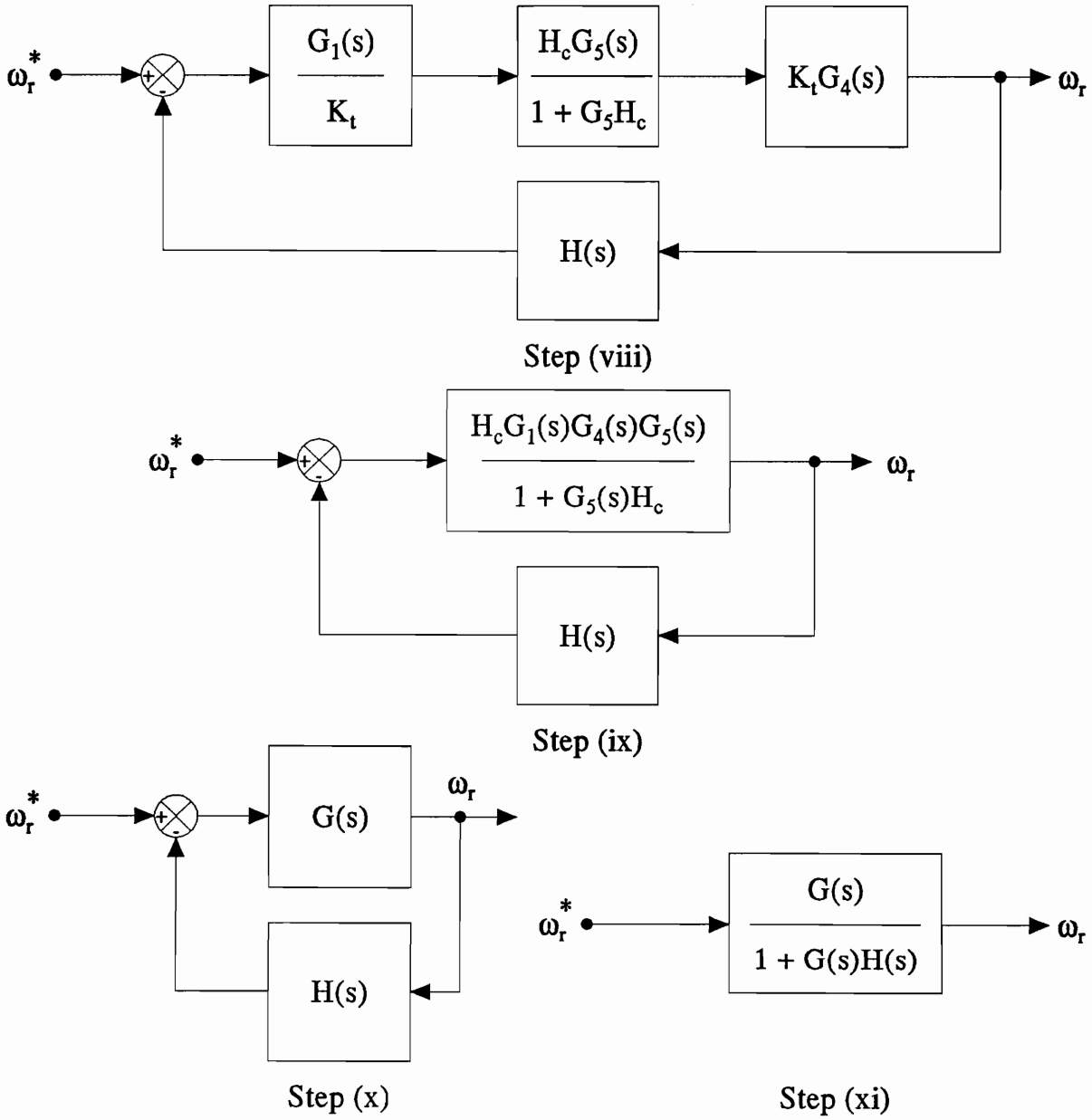

Figure 4.1: Step by Step Derivation of a Speed Controlled Indirect Vector Controlled Induction Motor Drive System

where, T_r is the equivalent time constant given as,

$$T_r \approx T_b + T_c \tag{4.43}$$

and,

$$K_r = K_b\, K_c \tag{4.44}$$

The transfer function G_5 is defined as,

$$G_5(s) = \frac{i_t(s)}{i_{tm}^*(s) - i_{tm}(s)} = \frac{K_r(1 + sT_m)}{(1 + sT_c)[(1 + sT_b)(1 + sT_m) + K_d]} \tag{4.45}$$

where,

$$K_d = K_b\, K_m\, K_t\, L_s\, i_f \tag{4.46}$$

Some more simplification is necessary to synthesize a controller without resorting to a computer. Noting that T_m is in the order of 1 sec, in the vicinity of the gain crossover frequency, the following approximation is valid:

$$(1 + sT_m) \approx sT_m \tag{4.47}$$

The current loop transfer function can then be written as,

$$\begin{aligned} G_6(s) &= \frac{i_t(s)}{i_t^*(s)} \\ &= H_c K_r s T_m \times \left[\frac{1}{s^2(T_r T_m) + s(T_m + H_c K_r T_m + K_d T_c) + K_d}\right] \\ &= \frac{H_c K_r s T_m}{K_1} \left[\frac{1}{(1 + sT_1)(1 + sT_2)}\right] \end{aligned} \tag{4.48}$$

where,

$$K_1 = K_d \tag{4.49}$$

$$T_1 = \frac{-2T_rT_m}{-b - \sqrt{b^2 - 4K_dT_rT_m}} \tag{4.50}$$

$$T_2 = \frac{-2T_rT_m}{-b + \sqrt{b^2 - 4K_dT_rT_m}} \tag{4.51}$$

and

$$b = T_m + H_cK_rT_m + T_cK_d \tag{4.52}$$

Since the value of T_1 is much greater than that of T_2, and in the order of 1 sec, the following approximation in the vicinity of the gain crossover frequency is valid:

$$(1 + sT_2) \approx sT_2 \tag{4.53}$$

The current loop transfer function taking into account this approximation can then be written as,

$$\begin{aligned} G_6(s) &= \frac{i_t(s)}{i_t^*(s)} \\ &= \frac{H_cK_rT_m}{K_dT_2}\left[\frac{1}{(1 + sT_1)}\right] \end{aligned} \tag{4.54}$$

Hence, the overall open loop transfer function is given as,

$$G(s) = \frac{H_cK_mK_sK_r}{K_d\,T_2}\left[\frac{(1 + sT_s)}{s^2T_s\,(1 + sT_1)}\right] \tag{4.55}$$

The loop gain function is given as,

$$\begin{aligned} GH(s) &= \frac{K_mK_rH_cH_\omega}{K_dT_2}\,\frac{K_s(1 + sT_s)}{s^2T_s}\left[\frac{1}{(1 + sT_1)(1 + sT_\omega)}\right] \\ &\approx K_2\frac{K_s}{T_s}\left[\frac{(1 + sT_s)}{s^2(1 + sT_1\omega)}\right] \end{aligned} \tag{4.56}$$

The above approximation involves the equivalent time delay of the speed feedback filter and current loop. Their sum is very much less than the integration time constant, T_s, and hence the equivalent time delay, $T_{1\omega}$, can be considered as the sum of the two delays, T_ω and T_1, which is the smaller value of the two roots. This step is very much similar to the equivalent time delay introduced in the simplification of the current loop transfer function. Hence the equivalent time constant is given as,

$$T_{1\omega} \approx T_1 + T_\omega \tag{4.57}$$

and the gain constant is given as,

$$K_2 = \frac{H_c H_\omega K_m K_i}{K_d T_2} \tag{4.58}$$

The overall closed loop transfer function of the speed loop can then be written as,

$$\frac{\omega_r(s)}{\omega_r^*(s)} = \frac{1}{H_\omega}(1 + sT_s)\left[\frac{1 + sT_\omega}{s^3T_x + s^2T_y + sT_s + 1}\right] \tag{4.59}$$

where,

$$T_x = \frac{T_{1\omega}T_s}{K_2K_s} \tag{4.60}$$

$$T_y = \frac{T_s}{K_2K_s} \tag{4.61}$$

In many high performance systems, the speed filter time constant is very small compared to other time constants. Hence the zero of the transfer function involving the filter time constant can be approximated by,

$$1 + sT_\omega \approx 1 \tag{4.62}$$

Then the closed loop transfer function of the speed to its command is given as,

$$\begin{aligned}\frac{\omega_r}{\omega_r^*} &= \frac{1}{H_\omega}(1+sT_s)\left[\frac{1}{s^3T_x+s^2T_y+sT_s+1}\right] \\ &= \frac{1}{H_\omega}\left[\frac{a_0+a_1s}{a_0+a_1s+a_2s^2+a_3s^3}\right] \end{aligned} \tag{4.63}$$

where,

$$a_0 = 1 \tag{4.64}$$

$$a_1 = T_s \tag{4.65}$$

$$a_2 = \frac{T_s}{K_2K_s} \tag{4.66}$$

$$a_3 = \frac{T_{1\omega}T_s}{K_2K_s} \tag{4.67}$$

For optimal response, the magnitude of the frequency response is to be as close as possible to a value of one over a wide frequency range which guarantees a high bandwidth and hence faster response. The magnitude of the function in the j-domain is given as,

$$f|(j\omega)| = \sqrt{\frac{a_0^2+\omega^2a_1^2}{a_0^2+\omega^2(a_1^2-2a_0a_2)+\omega^4(a_2^2-2a_1a_3)+\omega^6a_3^2}} \tag{4.68}$$

This is optimized by making the coefficients of ω^2 and ω^4 zero which yields the following conditions:

$$a_1^2 = 2a_0a_2 \tag{4.69}$$

$$a_2^2 = 2a_1a_3 \tag{4.70}$$

Substituting these conditions in terms of the motor and controller parameters given in 4.64 - 4.67,

$$T_s^2 = \frac{2T_s}{K_sK_2} \tag{4.71}$$

resulting in

$$T_s K_s = \frac{2}{K_2} \tag{4.72}$$

Similarly,

$$\frac{T_s^2}{K_s^2 K_2^2} = \frac{2T_s^2 T_{1\omega}}{K_s K_2} \tag{4.73}$$

which after simplification gives the speed controller gain as,

$$K_s = \frac{1}{2K_2 T_{1\omega}} \tag{4.74}$$

Substituting equation 4.74 into 4.72 gives the time constant of the speed controller as,

$$T_s = 4T_{1\omega} \tag{4.75}$$

Substituting for K_s and T_s in 4.63 gives the closed loop transfer function of the speed to its command as,

$$\frac{\omega_r(s)}{\omega_r^*(s)} = \frac{1}{H_\omega}\left[\frac{1+4Ts}{1+4Ts+8T^2s^2+8T^3s^3}\right] \tag{4.76}$$

where,

$$T = T_{1\omega} \tag{4.77}$$

This function described in equation 4.76 is known as symmetric optimum. For the open loop gain function, the corner points are $\frac{1}{4T}$ and $\frac{1}{T}$ with the gain crossover frequency of $\frac{1}{2T}$. In the vicinity of the gain crossover frequency the slope of the magnitude response is -20 db/decade which is the most desirable characteristic for good dynamic behavior. Because of its symmetry at the gain crossover frequency, this transfer function is known as a symmetric optimum function. Further this transfer function has the following features:

1. Approximate time constant of the system is $4T$.

2. The step response is given by,

$$f_{opt}(t) = \frac{1}{H_\omega}\left[1 + e^{-t/2T} - 2e^{-t/4T}cos(\frac{\sqrt{3}t}{4T})\right] \tag{4.78}$$

with a rise time of $3.1T$, maximum overshoot of 43.4% and a settling time of $16.5T$.

3. Since the overshoot is high, it can be reduced by compensating for its cause, the zero by a pole in the speed command path as shown in the Fig. 4.2. The resulting transfer function of the speed to its command is,

$$\frac{\omega_r(s)}{\omega_r^*(s)} = \frac{1}{H_\omega}\left[\frac{1}{1 + 4Ts + 8T^2s^2 + 8T^3s^3}\right] \tag{4.79}$$

The step response for this modified transfer function is given as,

$$f_{opt_m}(t) = \frac{1}{H_\omega}\left[1 - e^{-t/2T} - \frac{2}{\sqrt{3}}e^{-t/2T}sin(\frac{\sqrt{3}t}{4T})\right] \tag{4.80}$$

with a rise time of $7.6T$, maximum overshoot of 8.1% and a settling time of $13.3T$. Even though the rise time has increased, the overshoot has been reduced to approximately 20% of its previous value and the settling time has come down by 19%.

4. The poles of the transfer function are,

$$s = \frac{-1}{2T}; \frac{-1}{4T} \pm \frac{j\sqrt{3}}{4T} \tag{4.81}$$

As the real part of the poles are negative and since there are no repeated poles at the origin, the system is asymptotically stable. Hence in the symmetric optimum design, the system stability is guaranteed and there is no need to check for it in the design process.

5. Symmetric optimum eliminates the effects due to the disturbance very rapidly compared to other optimum techniques employed in practical systems such as linear and

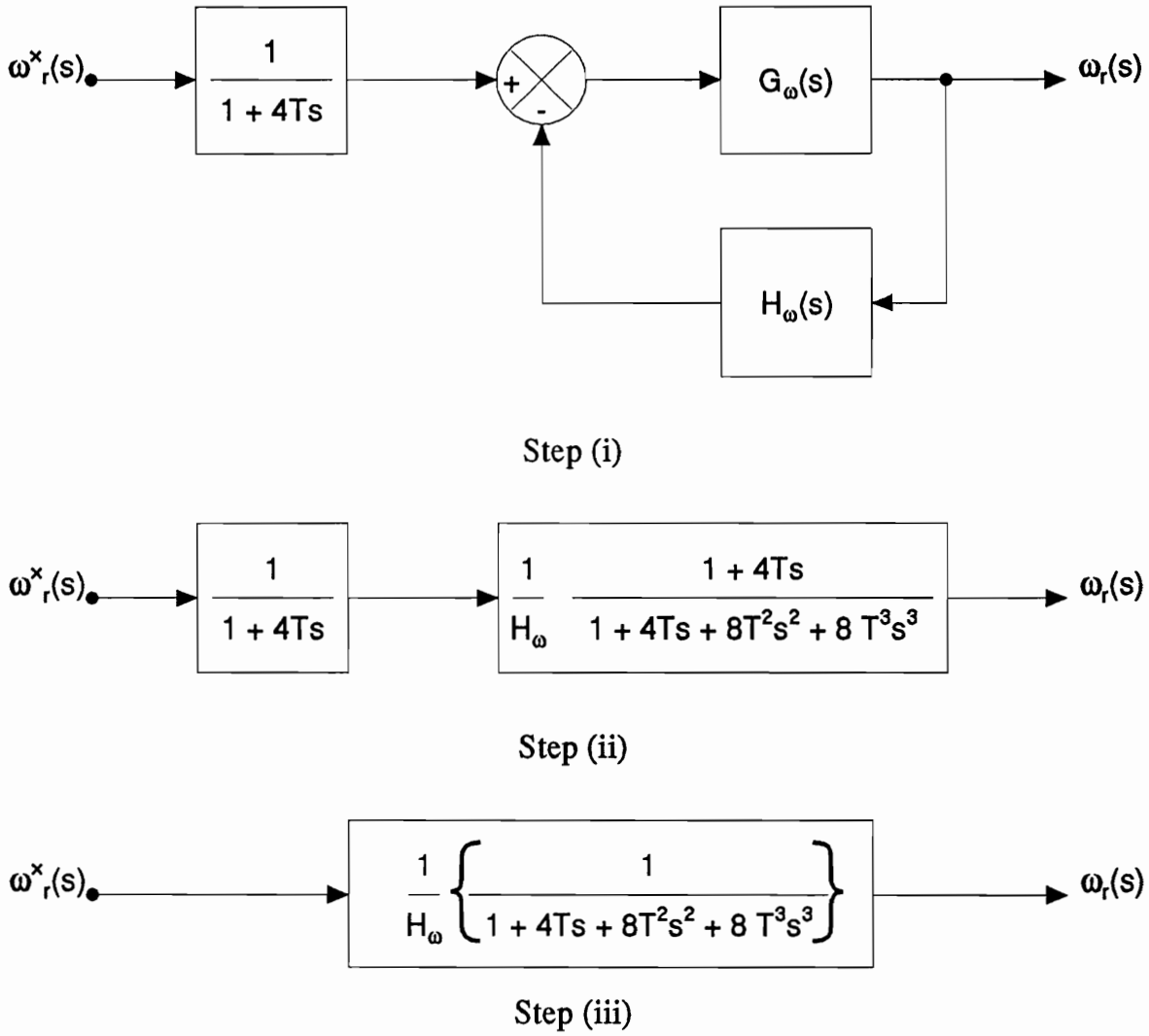

Figure 4.2: Compensator for Overshoot Reduction

modulus optimum etc. This approach indicates one of the possible methods to synthesize the speed controller. The judicious choice of approximations is based on the physical constants of the motor, converter and transducer gains and delays is to be emphasized here.

4.4 SIMULATION RESULTS

The results which are presented in this section are obtained for the motor drive system described by the following parameters. The induction motor operates in the constant flux region and its ratings are 1HP, 220V, 2 pole, 60 Hz., 3450RPM, Y-connected motor. The motor parameters are given in appendix A. A dc motor coupled to the induction motor provides a constant load of 0.4707 Nm. The rated flux of the motor, ψ_r, is 0.363 Wb.Trns and the rated torque, T_e, is calculated to be 1.744 Nm. For the purpose of this study, the PWM converter is supplied from a dc supply with a dc link voltage of 100 V. The maximum control input voltage is $\pm$ 5V. The tachogenerator has a transfer function $G_\omega(s) = \frac{0.01166}{(1+0.002s)}$. The speed reference voltage has a maximum of 5V. The current limit in the system is set to 8A.

The dc link voltage, V_{dc} is given as,

$$V_{dc} = 100V$$

The rated voltage required by the motor is 230V. Hence the maximum safe control voltage is 5V and this has to correspond to the maximum current error, i.e. i_{max}

$$\begin{aligned} i \text{ max} &= 8A \\ H_c &= \frac{V_c}{i_{max}} \\ &= \frac{5}{8} \\ &= 0.625V/A \end{aligned}$$

The gain and time constant of the PWM inverter are given as,

$$\begin{aligned} K_c &= \sqrt{2} \times 0.45 \times \frac{V_{dc}}{V_c} \\ &= \frac{0.6364 \times 100}{5} \\ &= 12.728 \end{aligned}$$

$$\begin{aligned} T_c &= \frac{1}{2 \times f_c} \\ &= \frac{1}{2 \times 1000} \\ &= 0.5 \text{ msec} \end{aligned}$$

The transfer function of the converter is given as,

$$G_c(s) = \frac{12.73}{(1 + 0.0005s)}$$

The equivalent inductance of the motor is given as,

$$\begin{aligned} L_a &= \frac{L_s L_r - L_m^2}{L_r} \\ &= 0.06524H \end{aligned}$$

The gain and time constant of the induction motor are given as,

$$\begin{aligned} K_a &= \frac{1}{R_s} \\ &= 0.4615 \end{aligned}$$

$$\begin{aligned} T_a &= \frac{L_a}{R_s} \\ &= \frac{0.06524}{2.1667} \\ &= 0.03634 \text{ sec} \end{aligned}$$

The transfer function of the induction motor is given as,

$$G_a(s) = \frac{0.4615}{(1 + 0.03634s)}$$

The torque constant of the motor is calculated as,

$$\begin{aligned} K_t &= \frac{3}{2}\frac{P}{2}\frac{L_m}{L_r}\psi_r \\ &= 0.451 \end{aligned}$$

The field current is given as,

$$i_f = \frac{\psi_r}{L_m} = 1.724A$$

The gain and time constant of the load for no load conditions, i.e., $B_l = 0$, are given as,

$$\begin{aligned} K_m &= \frac{P}{2}\frac{1}{B + B_l} \\ &= 648.09 \end{aligned}$$

$$\begin{aligned} T_m &= \frac{J}{B + B_l} \\ &= 2.676 \text{ sec} \end{aligned}$$

The transfer function of the load is given as,

$$G_m(s) = \frac{648.09}{(1 + 2.676s)}$$

Proceeding further with the block diagram simplification, the following values are calculated.

$$\begin{aligned} T_1 &= 6.48 \text{ msec} \\ T_{1\omega} &= T_1 + T_\omega = 6.48 + 2 = 8.48 \text{ msec} \\ T_2 &= 0.2759 \text{ sec} \\ K_2 &= \frac{H_c K_m K_r H_\omega}{K_d T_2} = \frac{0.625 \times 648.09 \times 3.31 \times 0.01166}{31.414 \times 0.2759} = 1.803 \\ T &= T_{1\omega} = 8.48 \text{ msec} \\ T_s &= 4T = 4 \times 0.008484 = 0.0339 \text{ sec} \\ K_p &= \frac{2}{K_2 T_s} = \frac{2}{1.803 \times 0.0339} = 32.681 \\ K_i &= \frac{K_s}{T_s} = \frac{32.681}{0.0339} = 963.032 \end{aligned}$$

Hence, the symmetric optimum function is given as,

$$G(s) = \left(\frac{1}{0.01166}\right)\left[\frac{1 + 0.0339s}{1 + 0.0339s + 5.76 \times 10^{-4}s^2 + 4.885 \times 10^{-6}s^3}\right]$$

The frequency and time domain responses of the speed to its command without the compensator is shown in Fig. 4.3. It can be noted that the function closely follows the characteristics of the symmetric optimum function. The maximum overshoot can be reduced by adding a compensator for the speed command as discussed earlier. The smoothing of the overshoot with the cancellation of the zero with a pole at $\frac{1}{4T}$ is shown in Fig. 4.4. It should be noted that such a close correlation of the time domain response is achieved if there is no limit on the torque produced in the motor, since a linear relationship between the speed error and the torque is assumed. But in practical drive systems, the torque capability of the motor limits the maximum allowable torque and the small and large signal response of such a system is considered for the study.

The proportional and integral constants designed using the symmetric optimum technique is incorporated into the CAE package, VCIM, and the drive system is defined by the corresponding parameters. The small signal response of the drive system is studied by applying a 0.02 p.u. speed command from standstill. This condition is equivalent to that of a 2% perturbation of the input signal. The time domain characteristics is presented in Fig. 4.5. It can be noted that there is a close correlation of the response obtained with the linear model. There is an increase in the settling time of the speed due to the fact that the maximum torque allowed is limited to 1 p.u. The limiter function can be observed from the behavior of the actual torque response in the characteristic.

The performance of the controller for wide load torque variations is illustrated in Fig. 4.6. The motor drive system is allowed to reach steady state and then a load torque disturbance of ± 0.5 p.u. is applied. It can be noted from the figure that there is only a minor variation in the actual speed value for such a wide range of load torque variation. This response is helpful in determining the integrity of the controller.

The overshoot of the response can be smoothed by the cancellation of the zero in the

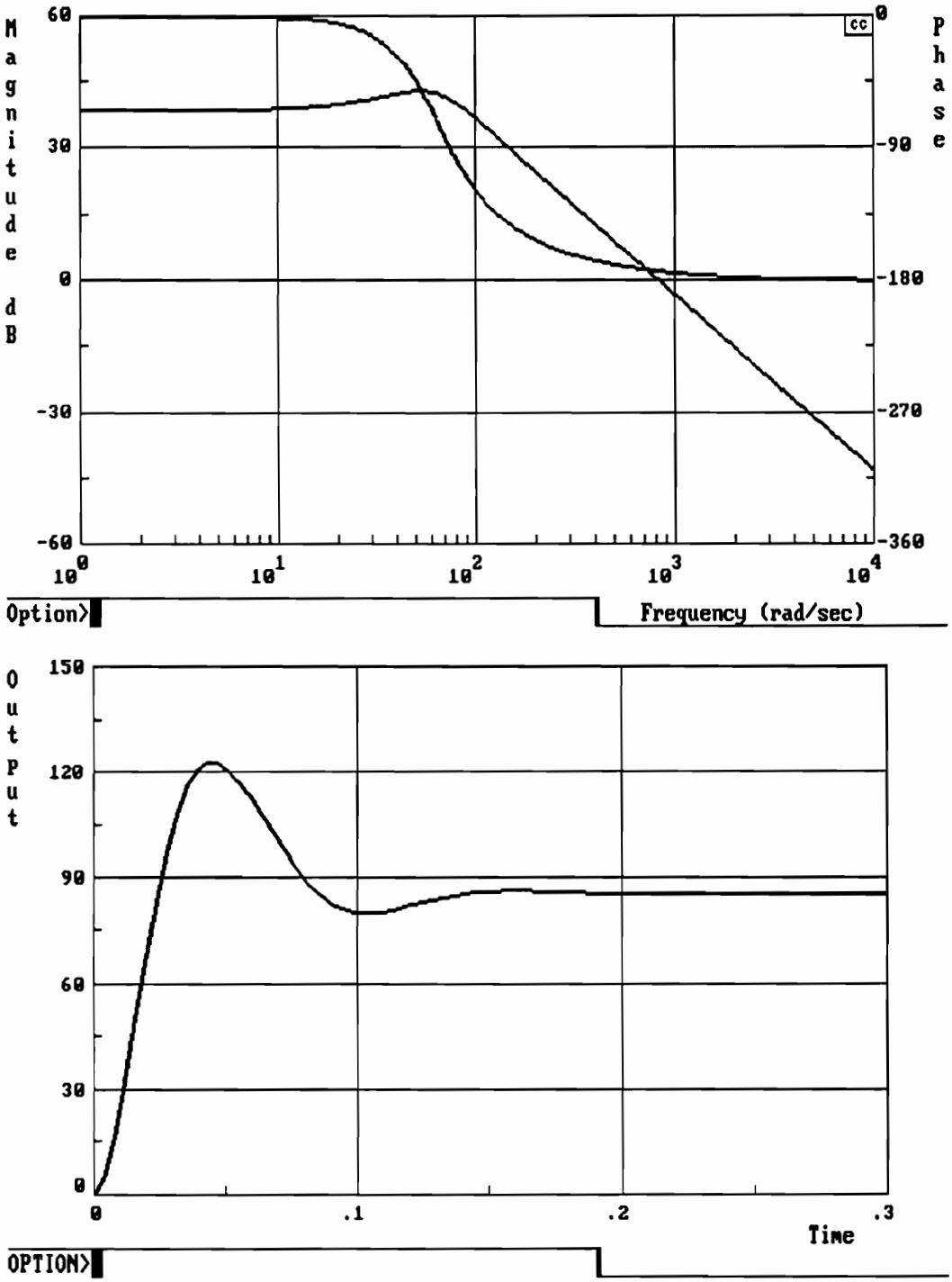

Figure 4.3: Frequency/Time Domain Response without Compensator

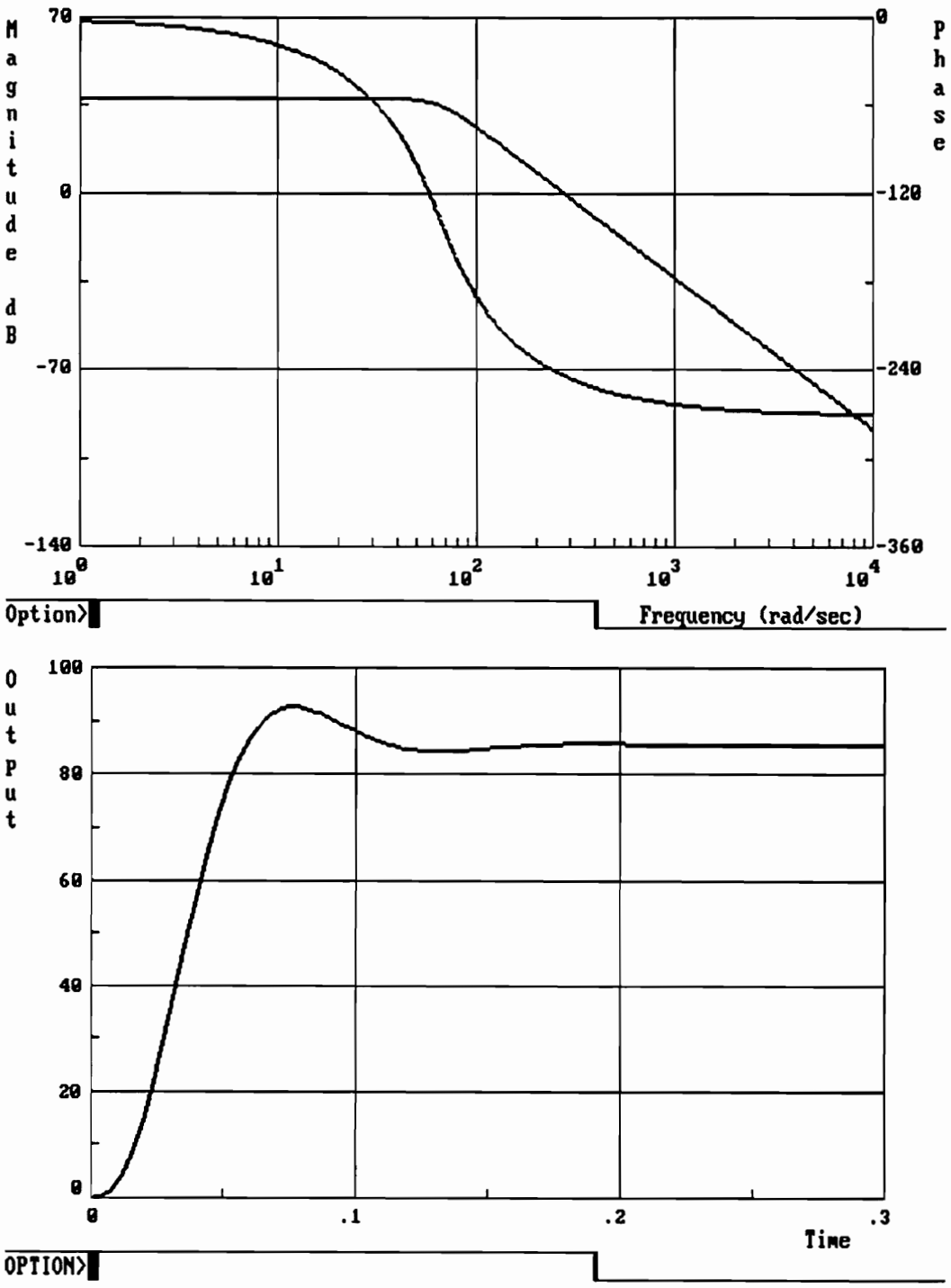

Figure 4.4: Frequency/Time Domain Response with Compensator

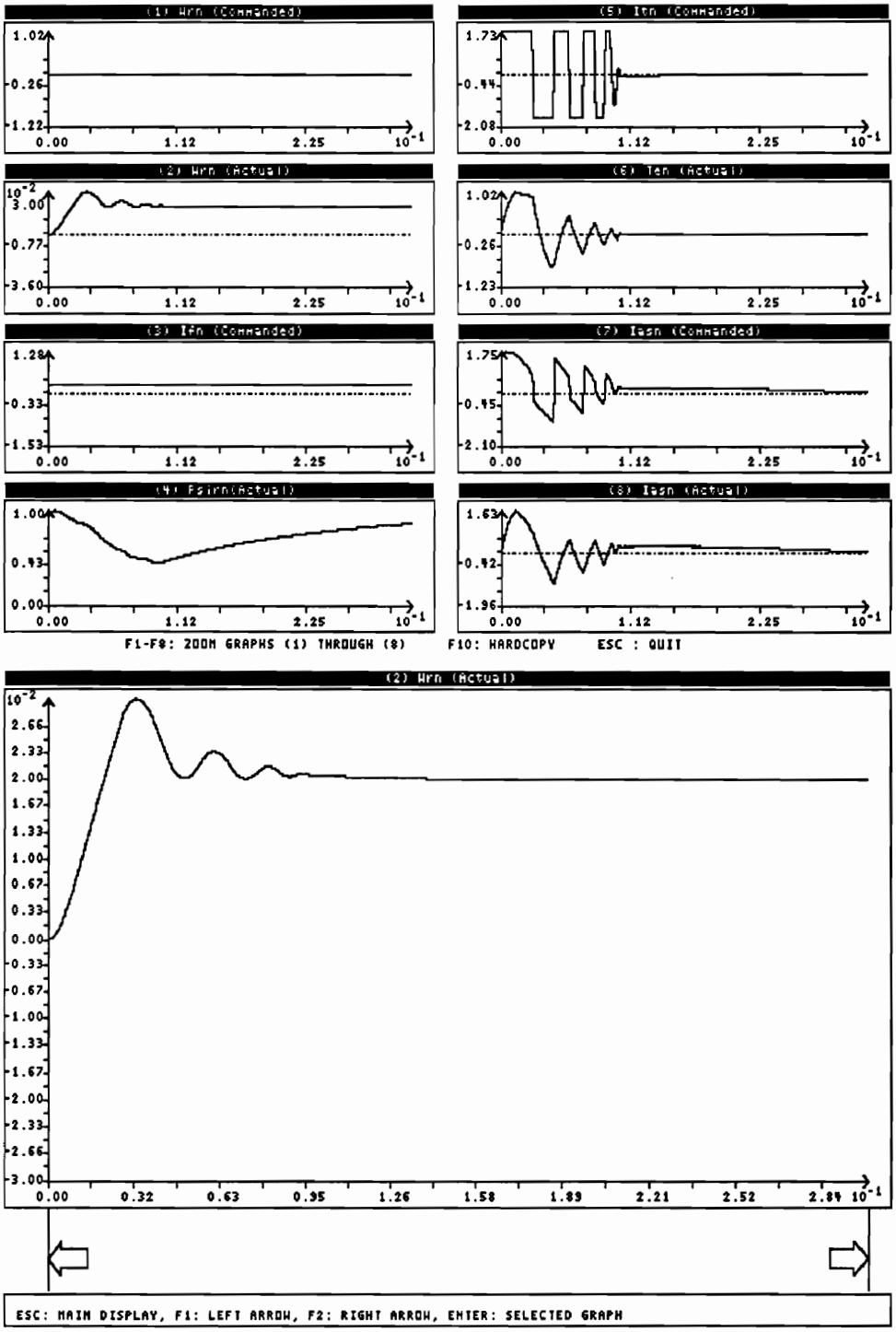

Figure 4.5: Small Signal Response without Compensator

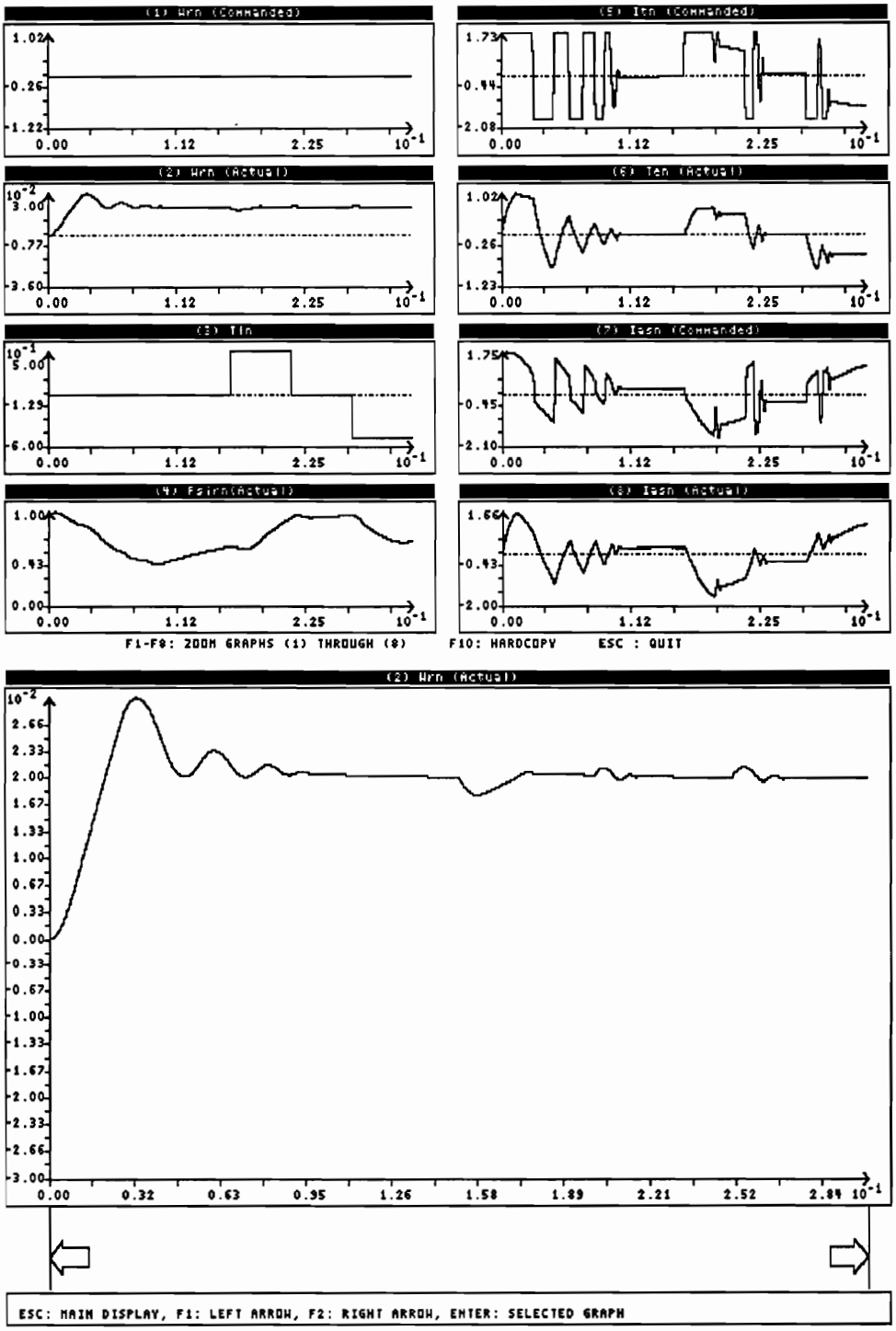

Figure 4.6: Load Torque Disturbance without Compensator

symmetric optimum function. This is equivalent to that of a soft start of the drive system. The small signal response of the drive system is studied by applying a 0.02 p.u. speed command from standstill with the soft start feature. The time domain characteristics is presented in Fig. 4.7. The close correlation of the response to that of the linear model can be observed. There is a considerable decrease in the peak overshoot and the settling time of the system compared to that without a compensator, as expected.

The performance of the controller for wide load torque variations with the compensator is illustrated in Fig. 4.8. Similar to the study performed without the compensator, the motor drive system is allowed to reach steady state and then a load torque disturbance of ± 0.5 p.u. is applied. It can be noted from the figure that there is minimal variation in the actual speed value for such a wide range of load torque variation.

The sensitivity of the drive system to parameter variations is studied for the speed controller using the symmetric optimum technique. As discussed in the earlier chapters, the indirect vector control strategy is sensitive to variations in the rotor resistance, R_r, and the mutual inductance, L_m. Fig. 4.9 illustrates the large signal drive response for a 100% variation in the value of rotor resistance. The simulation results presented are for a damping factor of 0.5 without the compensator. It can be noted that there is only a minor difference in the peak overshoot value when compared to Fig. 4.12. The rise time and the settling time for both the cases are equal.

Fig. 4.10 illustrates the response of the drive system for a 80% variation of the mutual inductance value. It can be noted that there is a considerable decrease in the peak overshoot of the speed response and consequently an increase in the rise time and the settling time when compared to Fig. 4.12. On the contrary, when the mutual inductance is increased to 120% of its original value, there is an increase in the overshoot and decrease in the rise time and settling time, as shown in Fig. 4.11.

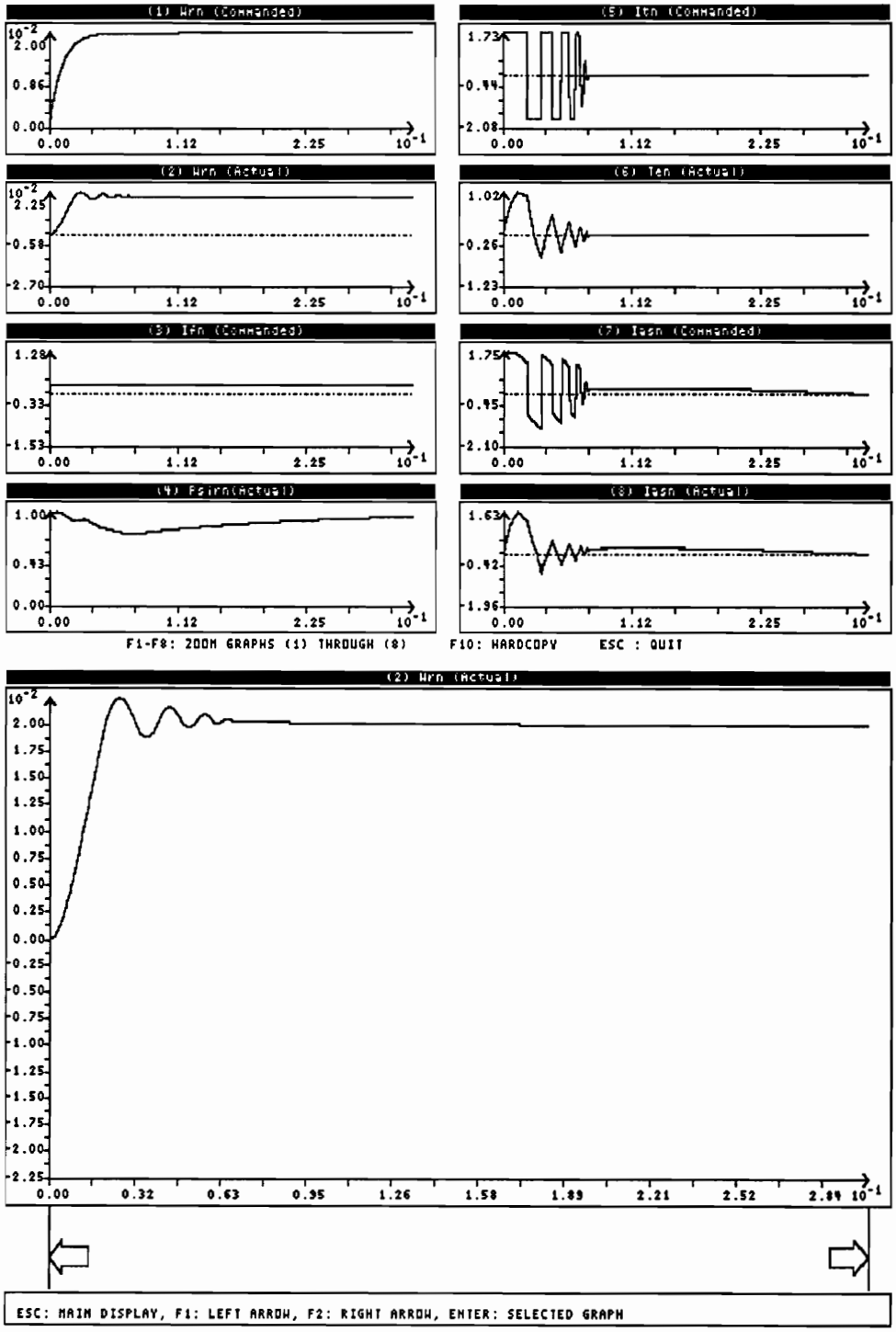

Figure 4.7: Small Signal Response with Compensator

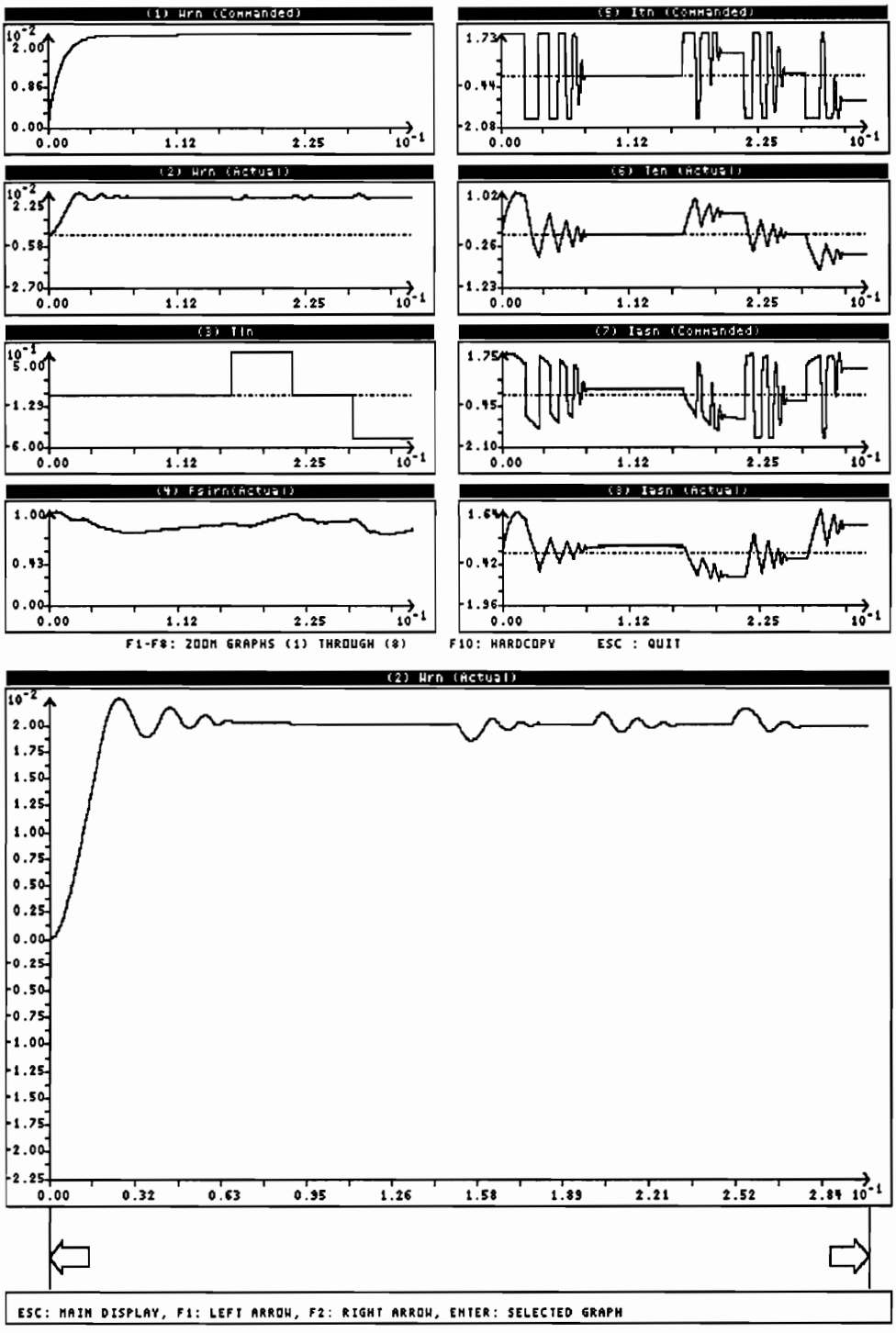

Figure 4.8: Load Torque Disturbance with Compensator

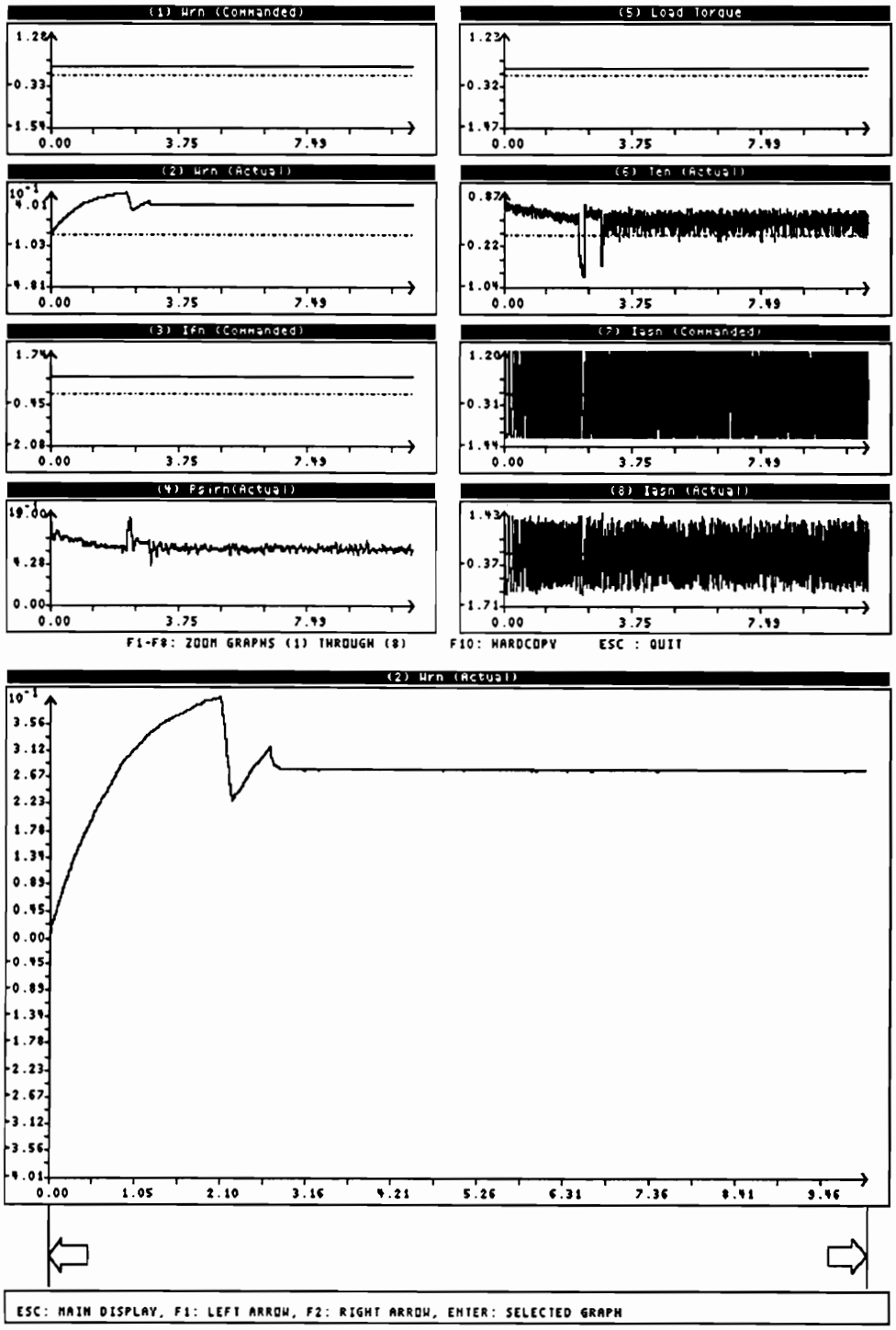

Figure 4.9: Parameter Sensitivity Study: 100% Rotor Resistance Variation

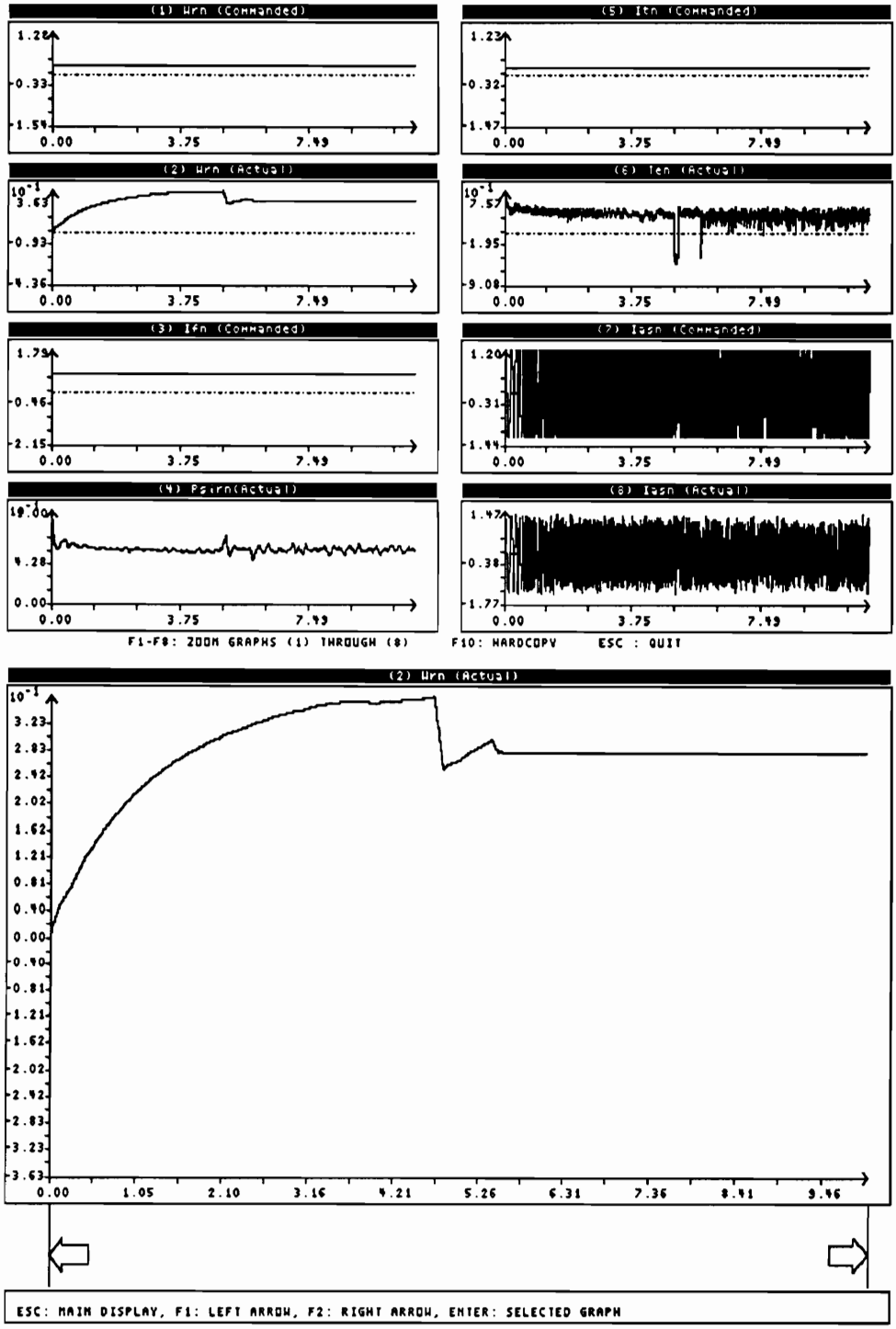

Figure 4.10: Parameter Sensitivity Study: 80% Mutual Inductance Variation

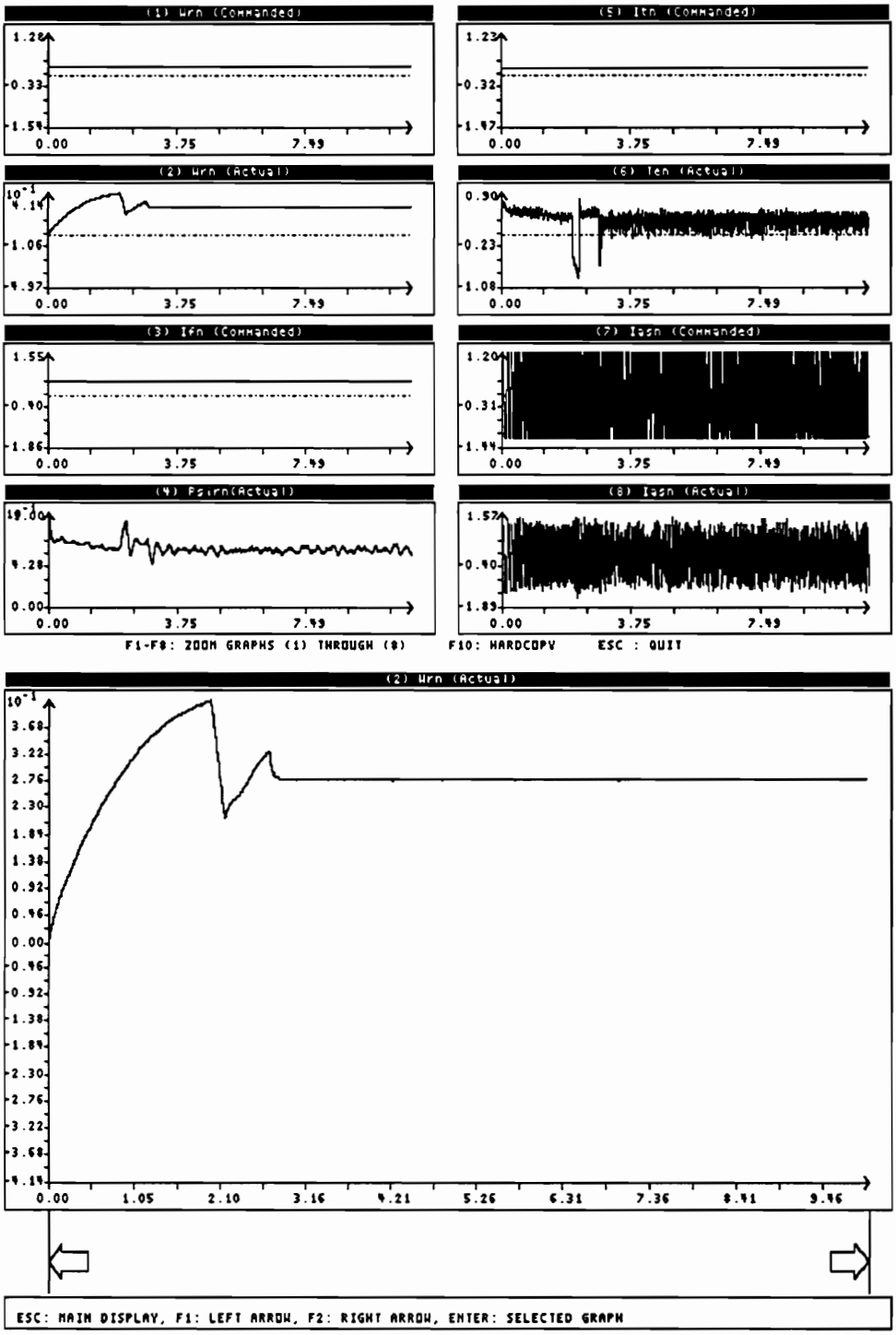

Figure 4.11: Parameter Sensitivity Study: 120% Mutual Inductance Variation

4.5 EXPERIMENTAL VERIFICATION

The drive system simulated in the previous section is implemented using a DSP based vector controller. The experimental setup has been described in detail in Chapter 2. The designed values of the speed and proportional constants are incorporated for the simulation and experimental verification.

The simulation and experimental results for the large signal response of the drive system without compensation is presented in Fig. 4.12. A commanded speed value of 0.28 p.u. which corresponds to 1000 RPM, is applied from standstill to the motor drive system. As can be noted from both the cases, the drive system reaches steady state after a maximum overshoot value corresponding to that of the linear symmetric optimum function. The rise time of the waveform in the simulation results is 2.5 seconds compared to 2.676 seconds predicted in the derivations. Also, the peak overshoot of the speed profile is 44.3% compared to 43% in the symmetric optimum function. The commanded and actual values of the rotor speed and the electromagnetic torque command is shown in the experimental results. It can be noted that there is a very close correlation between the profiles of the experimental and the theoretical predictions. The rise time of the waveform is 2.8 seconds compared to 2.676 seconds predicted in the derivations. The peak overshoot of the speed profile is 48% compared to 43% of the symmetric optimum function. The simulation results has not captured the higher overshoot of the speed response due to the idealized modeling of the inverter and other subsystems. The oscillations in the speed response till the steady state is reached can be attributed to the bang-bang nature of the torque limiter. This can be observed from the torque response in this figure.

It can be noted that the symmetric optimum function is designed for a damping factor of 0.5. The oscillations in the large signal response can be reduced by increasing the damping factor. Two such cases are studied and the simulation and experimental results for a damping factor of 0.707 and 1 is presented in Fig. 4.13 and 4.14, respectively.

The following parameters for these two cases are given below. For a damping factor of

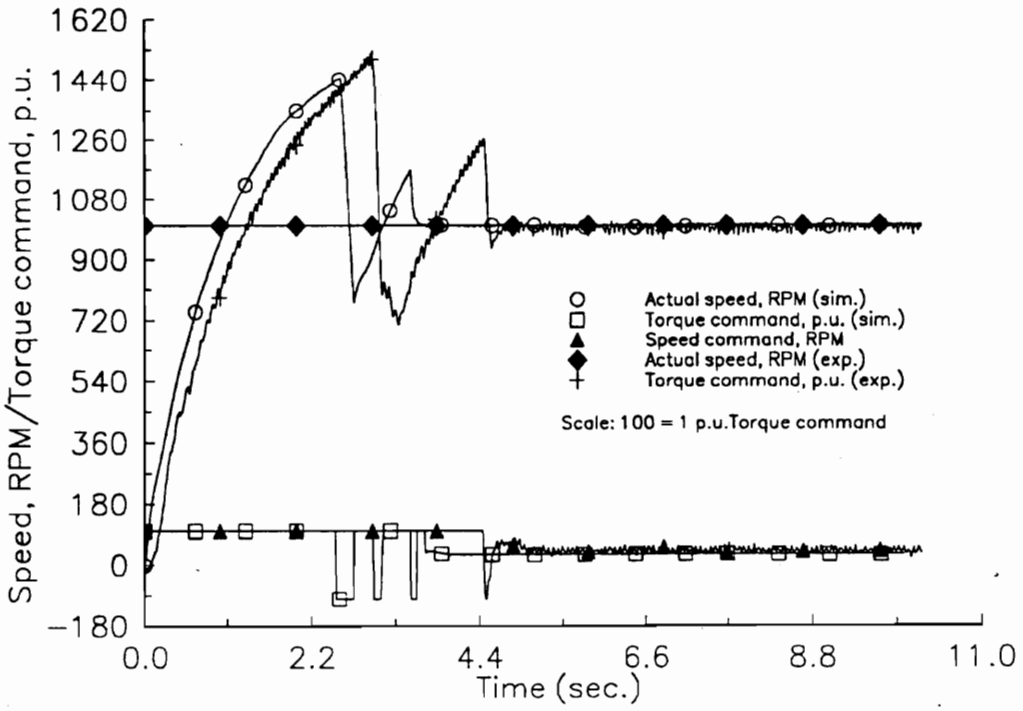

Figure 4.12: Simulation/Experimental Results of Large Signal Response without Compensator: Damping factor = 0.5

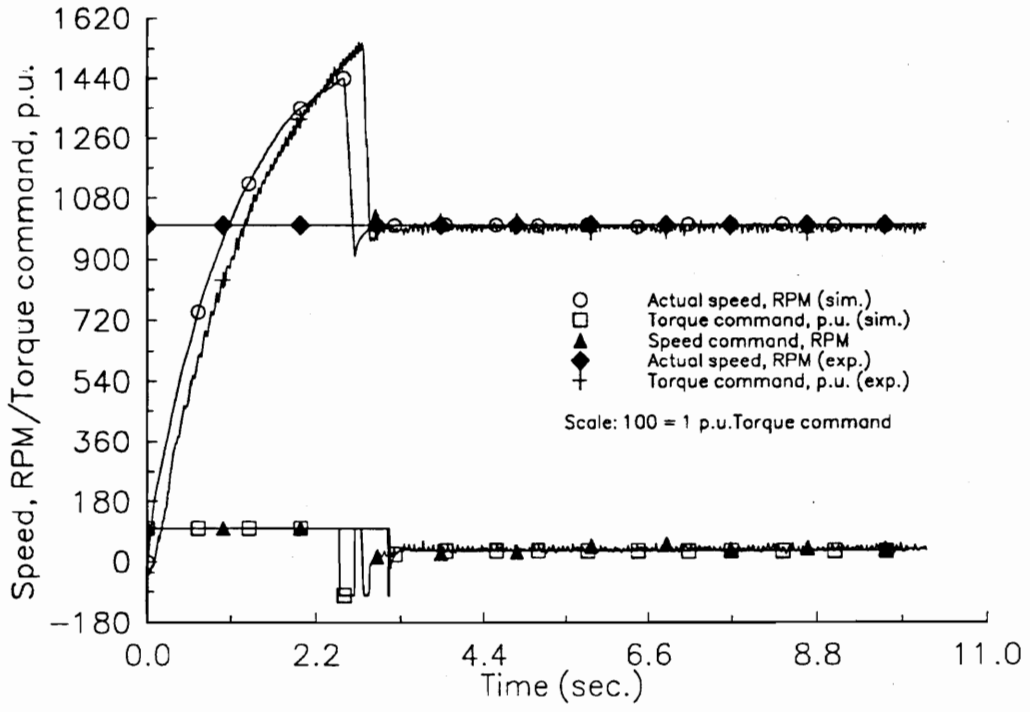

Figure 4.13: Simulation/Experimental Results of Large Signal Response without Compensator: Damping factor = 0.707

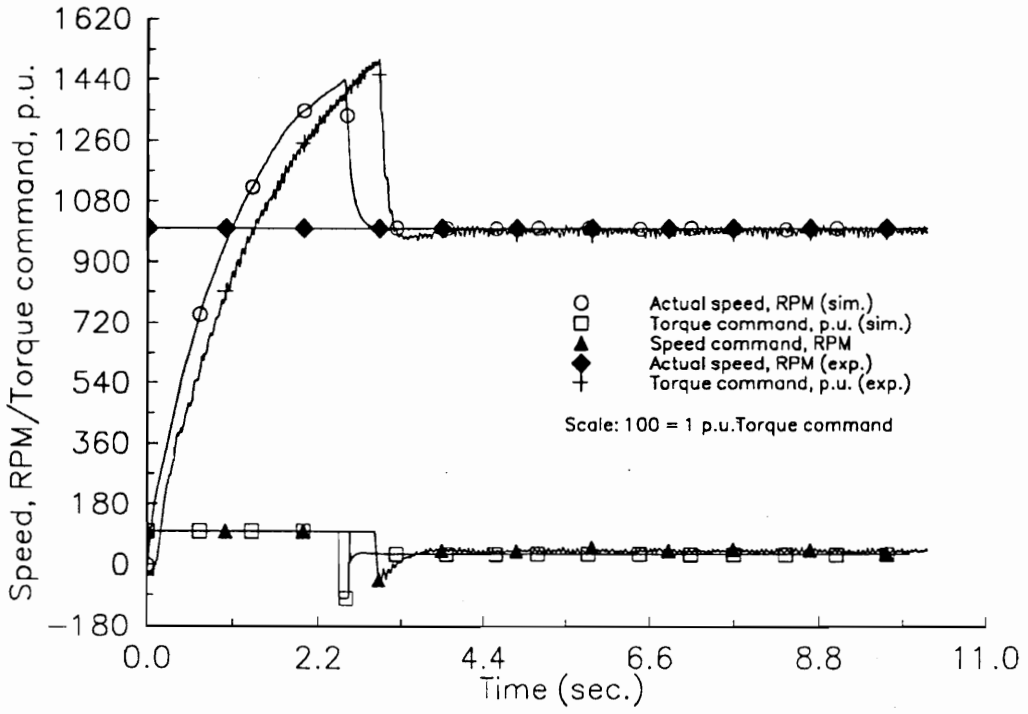

Figure 4.14: Simulation/Experimental Results of Large Signal Response without Compensator: Damping factor = 1

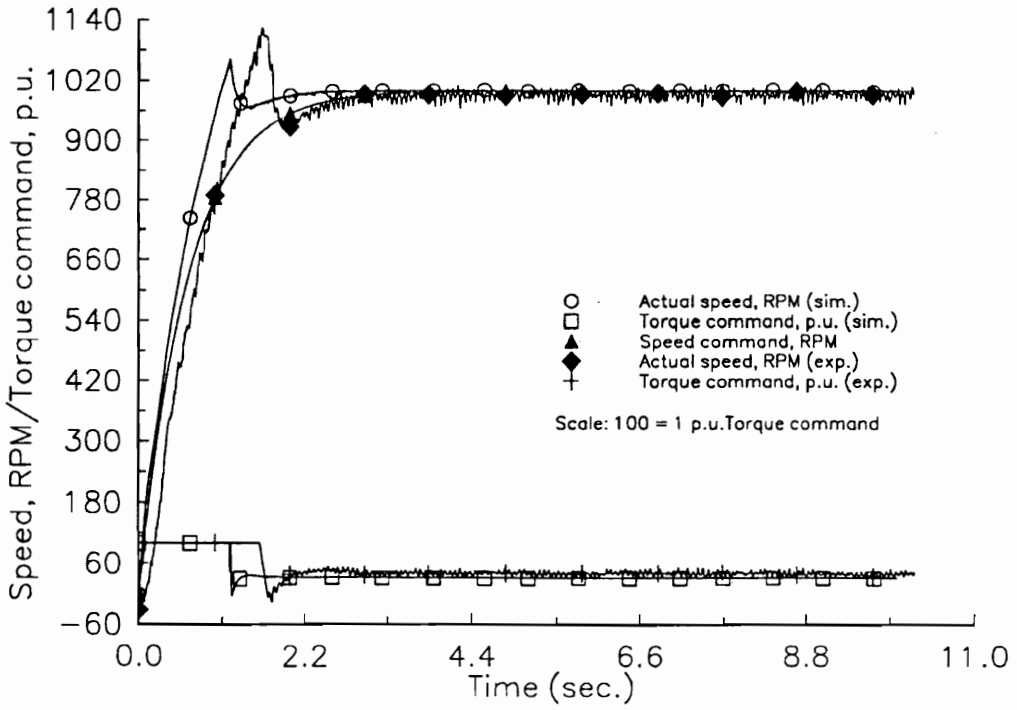

Figure 4.17: Simulation/Experimental Results of Large Signal Response with Compensator: Damping factor = 1

4.6 DISCUSSION

A simple methodology has been presented in the chapter which facilitates the design of a speed controller of the indirect vector controller controlled induction motor drive without resorting to a computer. The algorithm has been formulated by exploiting the similarity between the vector controlled induction motor drive and the separately excited dc motor.

The speed loop transfer function expressed in terms of T, is significant in that it clearly links the dynamic performance to the speed feedback and current loop time constants. It can be observed that a faster current loop with a smaller speed filter time constant accelerates the speed response. Expressing T in terms of the motor, converter and transducer gains and delays using earlier expressions,

$$\begin{aligned} T &= T_{1\omega} \\ &= T_1 + T_\omega \\ &= \frac{-2(T_b + T_c)T_m}{-b - \sqrt{b^2 - 4K_d(T_b + T_c)T_m}} + T_\omega \end{aligned} \tag{4.88}$$

where the value of b, is given by equation 4.52. This clearly shows the influence of the subsystem parameters on the system dynamics. A clear understanding of this would help in the proper selection of the subsystems to obtain the required dynamic performance of the speed controlled motor drive system. Further this derivation demonstrates that the system behavior to a large degree depends on the subsystem parameters rather than on the current and speed controller parameters or on the sophistication of their design.

Chapter 5

NOVEL SENSORLESS VECTOR CONTROL SCHEME

5.1 INTRODUCTION

High performance inverter-fed induction motor drive systems are realized using vector control schemes. The vector controller requires the position of the rotor flux for successful control of the induction motor. Schemes using the measured and estimated positions of the rotor flux are known as direct and indirect vector control schemes, respectively. The majority of induction motor servo systems are based on the indirect vector control strategy, which uses the machine parameters to estimate the position of the rotor flux. The modeling of this controller and the parameter sensitivity effects are discussed in the earlier chapters. Crucial to the success of indirect vector control is the knowledge of the rotor position which is obtained by using position transducers.

The inclusion of a position sensor increases the cost and the mechanical complexity of the drive system. Many applications require the minimization of the transducers in the control strategy for reduction of cost and increased reliability of the system. Hence a novel scheme has been proposed to eliminate the position sensor from the indirect vector control strategy. This is achieved by modeling the induction motor in the stator reference frame and using the airgap power. The line voltages and stator phase currents are required for the calculation of the airgap power. While the measurement of line voltages is possible with isolation amplifiers, it may not be a cost effective solution to low power motor drives. Hence, the line voltages are reconstructed from the base drive signals applied to the inverter using an algorithm proposed earlier [141]. The only input to the scheme are the two stator

phase currents measured by current transducers. Since the neutral of the motor is isolated, the third phase current is obtained as the negative sum of the other two measured currents. The base drive signals are obtained by comparing the measured and commanded values of stator currents. The commanded values of the three phase stator currents are obtained by the current source indirect vector control strategy.

This chapter describes the formulation and systematic derivation of the novel sensorless vector controller scheme for induction motor drive systems. The computer simulation is performed with the aid of the CAE package, VCIM, discussed in Chapter 3. The experimental verification is performed using a DSP based vector controller, discussed in Chapter 2. The chapter is organized as follows. The next section gives the derivation of the novel sensorless scheme for indirect vector control induction motor drive systems. Section 5.3 presents the simulation results obtained from the CAE package and the experimental verification is given in Section 5.4. The various issues pertaining to this scheme and sensorless vector control are discussed in Section 5.5.

5.2 MODELING OF THE PROPOSED SCHEME

The basic functional diagram of the proposed position sensorless vector control scheme is presented in Fig. 5.1. Since the calculation of the airgap power is crucial to this scheme, the modeling of the motor is performed in the stator reference frames. It can be seen that the system consists of three modules. They are, the voltage sensing module, position calculator module and the vector control module. The following subsections provide a detailed description of the modeling of each of these modules.

5.2.1 Voltage Sensing Module

The voltage sensing algorithm reconstructs the line voltages from the base drive control signals. The base drive control signals are obtained by comparing the measured stator phase currents and the command values of the stator currents which is calculated by the

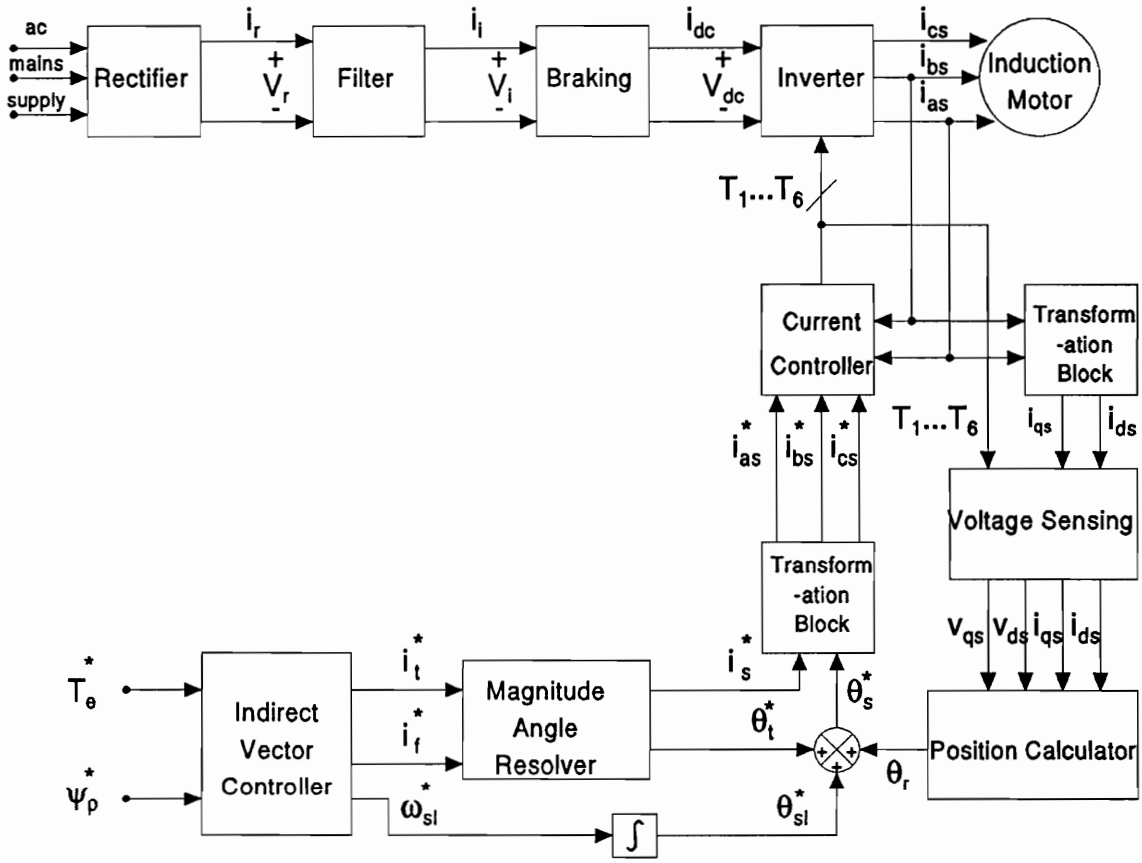

Figure 5.1: Novel Position Sensorless Indirect Vector Control Scheme

vector control module. The inverter power circuit of the induction motor drive is shown in Fig. 5.2. Even though transistor switches are considered, the algorithms can be suitably modified for both thyristor and GTO switches. The following assumptions are made in the derivation of the algorithm.

- The power transistors and freewheeling diodes are ideal switches.
- The carrier switching frequency of the inverter is limited to 2.5 kHz.
- A current source inverter is feeding the induction motor.
- The base drive signals are isolated.
- A constant dc bus voltage is maintained.

A detailed description of the algorithm and the relevant equations are given in Appendix B.

5.2.2 Position Calculator Module

The position calculator module estimates the value of the rotor position from the given set of phase voltages and currents. For a balanced three phase system, the phase voltages obtained from the voltage sensing module can be transformed into the two axis voltages in the stationary reference frame by,

$$v_{qs} = V_{as} \tag{5.1}$$

$$v_{ds} = \frac{1}{\sqrt{3}}(V_{as} + 2V_{cs}) \tag{5.2}$$

The stator currents can also be similarly transformed using the following equations,

$$i_{qs} = i_{as} \tag{5.3}$$

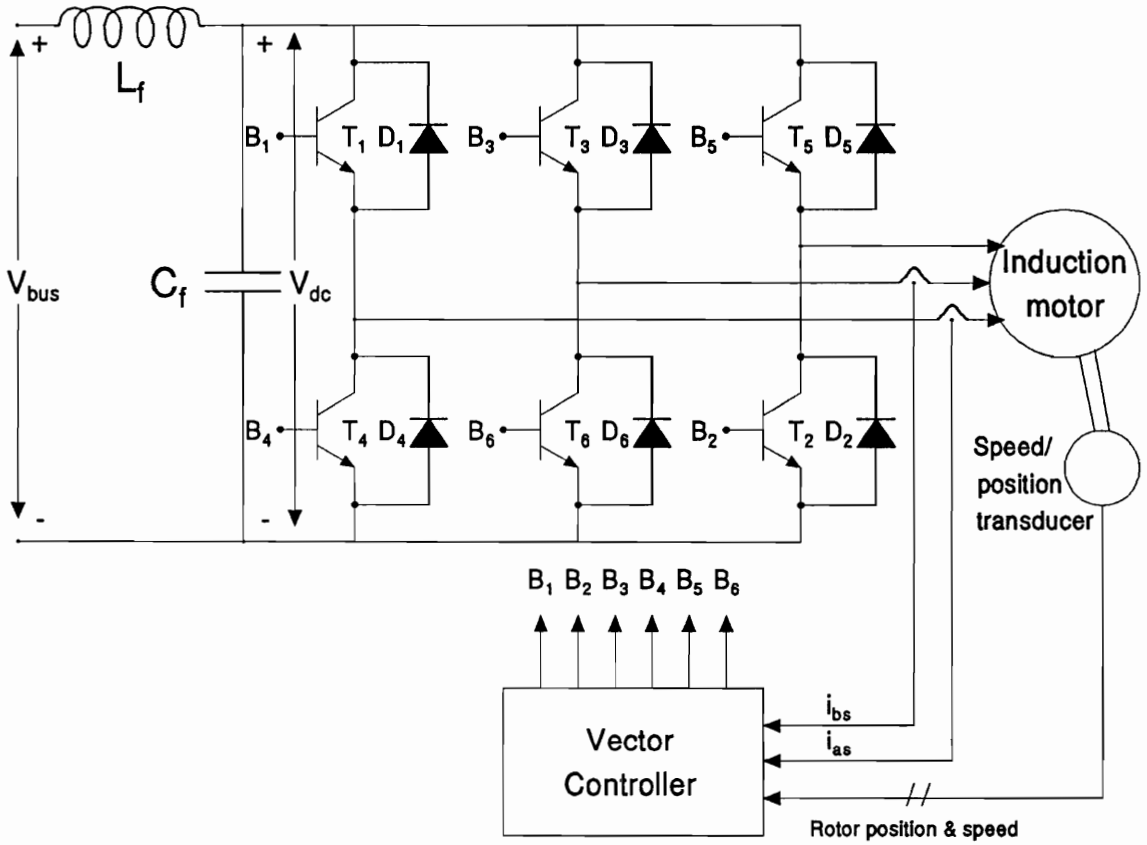

Figure 5.2: Current Source Inverter Fed Indirect Vector Controlled Induction Motor Drive

$$i_{ds} = \frac{1}{\sqrt{3}}(i_{as} + 2i_{cs}) \tag{5.4}$$

From the phasor diagram representation of the vector controller given in Fig. 2.1, the following relationship can be deduced.

$$\begin{aligned} \theta_{sc} &= \theta_{tc} + \theta_{sl} + \theta_r \\ &= \theta_{tc} + \theta_f \end{aligned} \tag{5.5}$$

where, θ_{sc} is the stator electric angle, θ_{tc} is the torque angle, θ_{sl} is the slip frequency angle, θ_r is the rotor position and θ_f is the field angle for a current source vector controller. The dynamic equations of the induction machine in the stator reference frame is given below.

$$\begin{bmatrix} v_{qs} \\ v_{ds} \\ v_{qr} \\ v_{dr} \end{bmatrix} = \begin{bmatrix} R_s + L_s p & 0 & L_m p & 0 \\ 0 & R_s + L_s p & 0 & L_m p \\ L_m p & -\omega_r L_m & R_r + L_r p & -\omega_r L_r \\ \omega_r L_m & L_m p & \omega_r L_r & R_r + L_r p \end{bmatrix} \begin{bmatrix} i_{qs} \\ i_{ds} \\ i_{qr} \\ i_{dr} \end{bmatrix} \tag{5.6}$$

from which the electromagnetic torque, T_e, is calculated using:

$$T_e = \frac{3}{2}\frac{P}{2} L_m(i_{qs}i_{dr} - i_{ds}i_{qr}) \tag{5.7}$$

where, R_s, R_r, L_s, L_r are the stator and rotor resistances and self inductances, respectively. ω_s, ω_r are the stator and rotor electric frequency in radians/sec. v_{qs}, v_{ds}, v_{qr}, v_{dr}, i_{qs}, i_{ds}, i_{qr}, i_{dr} are the stator and rotor, d and q axes, voltages and currents in synchronous frames, respectively. ω_r is the rotor speed and the operator $\frac{d}{dt}$ is represented by p. The speed is computed from the acceleration torque equation using the load torque, T_l, Moment of Inertia, J, and the viscous friction coefficient, B,

$$J\frac{d\omega_r}{dt} + B\omega_r = \frac{P}{2}(T_e - T_l) \tag{5.8}$$

and the rotor position is given as $\theta_r = \omega_r t$.

For the proposed scheme, only the stator phase currents and voltages are available for computing the field angle for vector control. Since the electromagnetic torque equation given above is dependent on the rotor currents, it cannot be used for the computation of T_e in the proposed scheme. The stator current phasor, i_s, and the stator electric angle, θ_{sc} are obtained from the q and d axes currents as follows,

$$i_s = \sqrt{i_{qs}^2 + i_{ds}^2} \tag{5.9}$$

$$\theta_{sc} = /tan^{-1}(\frac{i_{qs}}{i_{ds}}) \tag{5.10}$$

From the dynamic model of the motor in the stator reference frame, it can be noted that,

$$v_{qs} = (R_s + L_s p)i_{qs} + L_m p i_{qr} \tag{5.11}$$

$$v_{ds} = (R_s + L_s p)i_{ds} + L_m p i_{dr} \tag{5.12}$$

Alternately, using the flux linkage model of the induction motor, the above equations can be written as,

$$v_{qs} = R_s i_{qs} + p\psi_{qs} \tag{5.13}$$

$$v_{ds} = R_s i_{ds} + p\psi_{ds} \tag{5.14}$$

where, ψ_{qs} and ψ_{ds} are the q and d axes stator flux linkages in the stator reference frames. Hence the q and d axes stator flux linkages can be computed using the following equations:

$$\psi_{qs} = \int (v_{qs} - R_s i_{qs})dt \tag{5.15}$$

$$\psi_{ds} = \int (v_{ds} - R_s i_{ds}) dt \tag{5.16}$$

But, the stator d and q axes flux linkages can also be written as,

$$\psi_{qs} = L_m i_{qr} + L_s i_{qs} \tag{5.17}$$

$$\psi_{ds} = L_m i_{dr} + L_s i_{ds} \tag{5.18}$$

The rotor current equations are given as,

$$i_{qr} = \frac{\psi_{qs} - L_s i_{qs}}{L_m} \tag{5.19}$$

$$i_{dr} = \frac{\psi_{ds} - L_s i_{ds}}{L_m} \tag{5.20}$$

Hence, the rotor flux linkages are given as,

$$\psi_{qr} = L_m i_{qs} + L_s i_{qr} \tag{5.21}$$

$$\psi_{dr} = L_m i_{ds} + L_s i_{dr} \tag{5.22}$$

The magnitude of the rotor flux and the field angle are then calculated using the equations,

$$\psi_r = \sqrt{\psi_{qr}^2 + \psi_{dr}^2} \tag{5.23}$$

$$\theta_f = \tan^{-1}(\frac{\psi_{qr}}{\psi_{dr}}) \tag{5.24}$$

Substituting the values of the q and d axes rotor currents in equations for the expression for electromagnetic torque,

$$T_e = \frac{3}{2}\frac{P}{2}\left(i_{qs}\psi_{ds} - i_{ds}\psi_{qs}\right) \tag{5.25}$$

The slip frequency and the slip frequency angles are defined by the following equations,

$$\omega_{sl} = \frac{2}{3}\frac{P}{2}\frac{R_r T_e}{\psi_r^2} \tag{5.26}$$

$$\theta_{sl} = \int \omega_{sl} \tag{5.27}$$

From the phasor diagram representation of the vector controller given in Fig. 2.1, the rotor position can be determined as,

$$\theta_r = \theta_f - \theta_{sl} \tag{5.28}$$

Since the q and d axes stator voltages and currents, and the stator current phasors are known, the airgap power is deduced from the following relationship,

$$P_a = \frac{3}{2}\left(v_{qs}i_{qs} + v_{ds}i_{ds} - R_s i_s^2\right) \tag{5.29}$$

The stator frequency, ω_s, can be calculated from the airgap power and the electromagnetic torque as,

$$\omega_s = \frac{P_a}{T_e}\frac{P}{2} \tag{5.30}$$

The rotor speed, ω_r, for closing the speed loop can then be obtained from the following relationship,

$$\omega_r = \omega_s - \omega_{sl} \tag{5.31}$$

5.2.3 Vector Controller Module

The input to the vector controller module are the commanded values of electromagnetic torque and rotor flux. Using the current source indirect vector control algorithm, the commanded values of the three phase currents are calculated. The relevant theory and equations are already presented in Chapter 2.

The commanded values of the torque angle, θ_t^*, and slip angle, θ_{sl}^*, are combined with the value of the rotor position estimated in the previous section to obtain the commanded value of the stator electrical angle as,

$$\theta_s^* = \theta_t^* + \theta_{sl}^* + \theta_r \tag{5.32}$$

The commanded values of the stator current can then be obtained as follows,

$$\begin{aligned} i_{as}^* &= i_s^* \sin\theta_s^* \\ i_{bs}^* &= i_s^* \sin(\theta_s^* - \frac{2\pi}{3}) \\ i_{cs}^* &= i_s^* \sin(\theta_s^* + \frac{2\pi}{3}) \end{aligned} \tag{5.33}$$

5.3 SIMULATION RESULTS

The simulation results for the proposed sensorless vector control scheme are presented in this section. The scheme is integrated into the CAE package, VCIM, as a separate module. The output characteristics for a torque drive system employing the proposed sensorless algorithm is illustrated in Fig. 5.3. The inputs to the torque drive are the commanded values of electromagnetic torque and rotor flux. The rotor speed is maintained at a constant value and the rotor flux is equal to the rated value. This condition is achieved by starting the simulation with the value of the field current equal to the rated current. Since the field current is directly proportional to the rotor flux, this condition ensures that the rotor flux reaches the rated value. In this simulation experiment, the rotor speed is maintained at

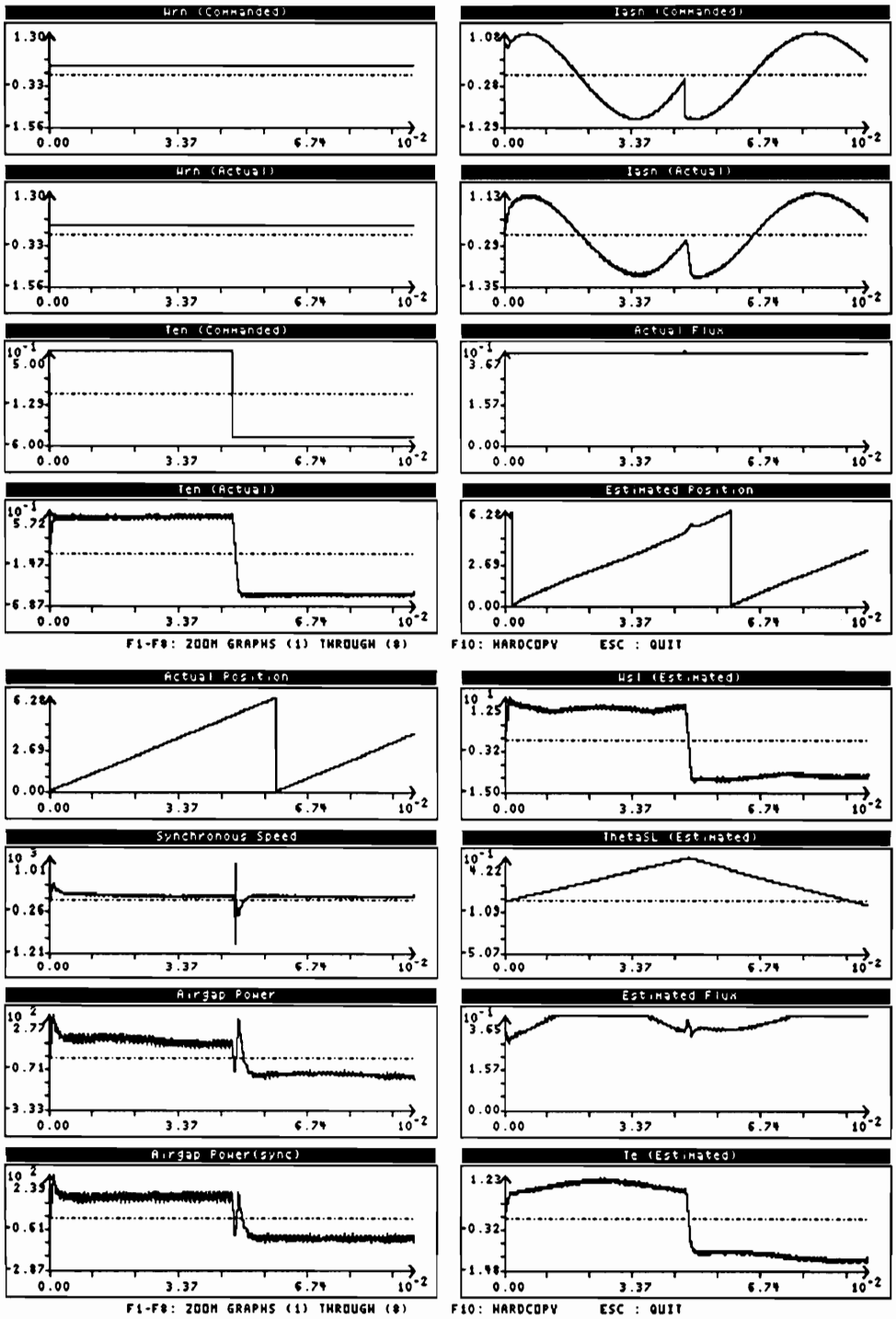

Figure 5.3: Output Characteristics for a Torque Controlled Drive System using Sensorless Algorithm

0.3 p.u. which corresponds to a mechanical speed of 1080 RPM. The normalized values of the commanded/actual speed, commanded/actual torque, commanded/actual current of phase 'A', actual rotor flux and the estimated rotor position are displayed in the figure. The inner current loop is represented by the commanded and actual values of currents. The actual current follows the commanded value, implemented by a PWM controller with a carrier frequency of 1 kHz. A step command of ± 0.5 p.u. for the torque command and a 1 p.u. command for the rotor flux is applied. The actual value of the electromagnetic torque and rotor flux closely follows the commanded signal, as seen from the figure. The estimated value of the rotor position using the algorithm is also shown in the figure and closely follows the actual rotor position in the system.

The output characteristics for a torque drive system for low speed operation employing the proposed sensorless algorithm is illustrated in Fig. 5.4. In this simulation experiment, the rotor speed is maintained at 0.03 p.u. which corresponds to a mechanical speed of 108 RPM. The normalized values of the commanded/actual speed, commanded/actual torque, commanded/actual current of phase 'A', actual rotor flux and the estimated rotor position are displayed in the figure. The inner current loop is represented by the commanded and actual values of currents. The actual current follows the commanded value, implemented by a PWM controller with a carrier frequency of 1 kHz. A step command of ± 0.5 p.u. for the torque command and a 1 p.u. command for the rotor flux is applied. It can be noted that even at this low speed the electromagnetic torque closely follows the commanded value The rotor flux is maintained at 1 p.u. value as seen from the figure. The estimated value of the rotor position using the algorithm is also shown in the figure and closely follows the actual rotor position in the system.

The output characteristics for a speed drive system employing the proposed sensorless algorithm is illustrated in Fig. 5.5. The input to the speed drive is the commanded value of the rotor speed. This is compared with the actual value of the rotor speed. The error signal is amplified and processed through a speed controller to get the torque command. The flux command is obtained from the rotor speed signal by flux programming. The normalized

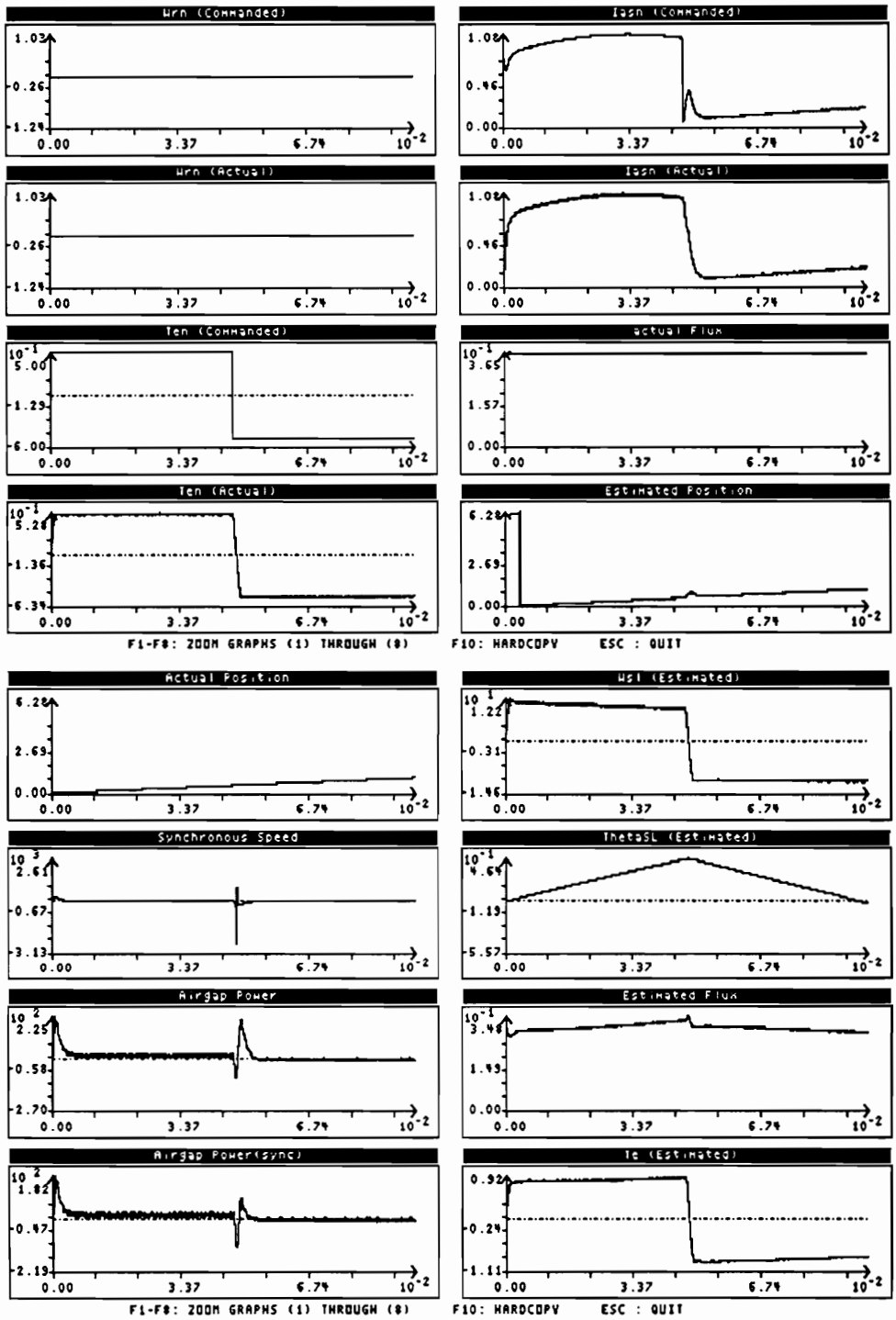

Figure 5.4: Output Characteristics for a Low Speed Torque Controlled Drive System using Sensorless Algorithm

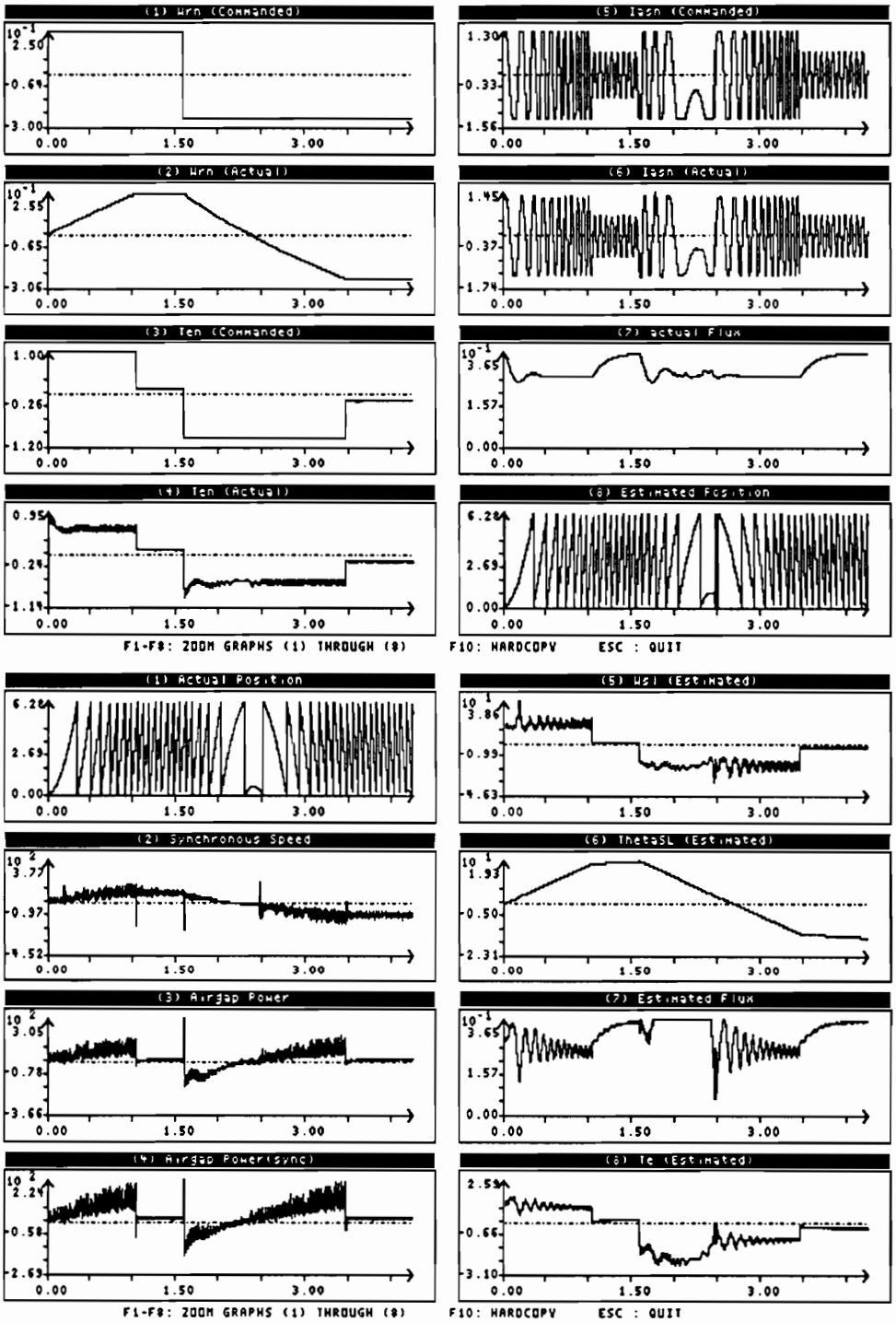

Figure 5.5: Output Characteristics for a Speed Controlled Drive System using Sensorless Algorithm

values of the commanded/actual speed, commanded/actual torque, commanded/actual current of phase 'A', actual rotor flux and the estimated rotor position are displayed in the figure. The inner current loop is represented by the commanded and actual values of currents. The actual current follows the commanded value, implemented by a PWM controller with a carrier frequency of 1 kHz. A step command of $\pm$ 0.5 p.u. for the speed command and a 1 p.u. command for the rotor flux is applied. The actual value of the electromagnetic torque and rotor flux closely follows the commanded signal. The zero error in the electromagnetic torque indicates steady state for the drive with no load torque. The transient and dynamic response of the current can also be seen. It can be noted that even at this low speed the electromagnetic torque closely follows the commanded value The rotor flux is maintained at 1 p.u. value as seen from the figure. The estimated value of the rotor position using the algorithm is also shown in the figure and closely follows the actual rotor position in the system.

5.4 EXPERIMENTAL VERIFICATION

The simulation results presented for the drive system in the previous section is implemented using the DSP based controller described in the earlier chapters. The experimental results obtained from this setup is presented in this section to verify the validity of the proposed algorithm.

The experimental setup is implemented as follows: The voltage sensing module is implemented external to the DSP. The inputs to this module are the currents measured by the transducers and the gate drive signals generated by the DSP. The logic equations of the algorithm are implemented by a Programming Logic Device (PLD). The line voltages obtained from the PLD are then processed to obtain the phase voltages corresponding to the dc link voltage. The integrator function to estimate the d and q axes stator flux is also implemented by external hardware. The stator flux values are then fed to the DSP through the two channels of the analog to digital converter.

Once the stator flux values are available in the DSP, the position estimator module computes the rotor position using the algebraic expressions described earlier. The inverse tangent function to compute the field angle is stored as tables and retrieved in the assembly program. The integration function to obtain the slip angle from slip speed is implemented by trapezoidal algorithm.

The estimated value of the rotor position is input into the vector controller algorithm described earlier and the three phase commanded values of currents are generated. The actual values of the current are controlled to follow the commanded values with the PWM timers built-in the processor. The simulation results for the step torque characteristics of a torque drive system employing the proposed sensorless algorithm is illustrated in Fig. 5.6. The motor is allowed to accelerate to a certain speed value from standstill. The normalized values of the commanded/actual speed, commanded/actual torque, commanded/actual current of phase 'A', actual rotor flux and the estimated rotor position are displayed in this figure. The inner current loop is represented by the commanded and actual values of currents. The actual current follows the commanded value, implemented by a PWM controller with a carrier frequency of 1 kHz. A step command of torque and a 1 p.u. command for the rotor flux is applied. It can be noted that the electromagnetic torque closely follows the commanded value The rotor flux is maintained at 1 p.u. value as seen from the figure. The estimated value of the rotor position using the algorithm is also shown in the figure and closely follows the actual rotor position in the system.

The experimental validation for this condition is presented in Fig. 5.7. The commanded value of torque and the rotor speed value in RPM is presented in this figure. Similar to the simulation, a step command of torque is applied and the motor is started from standstill. The position sensor is removed from the experimental setup and the estimated position is applied to the algorithm in place of the sensor position. The response of the speed for this condition shown in this figure closely follows the simulation results presented earlier in Fig. 5.6. The output characteristics for the speed drive can then be obtained by closing the outer speed loop similar to that of the sensor based vector control.

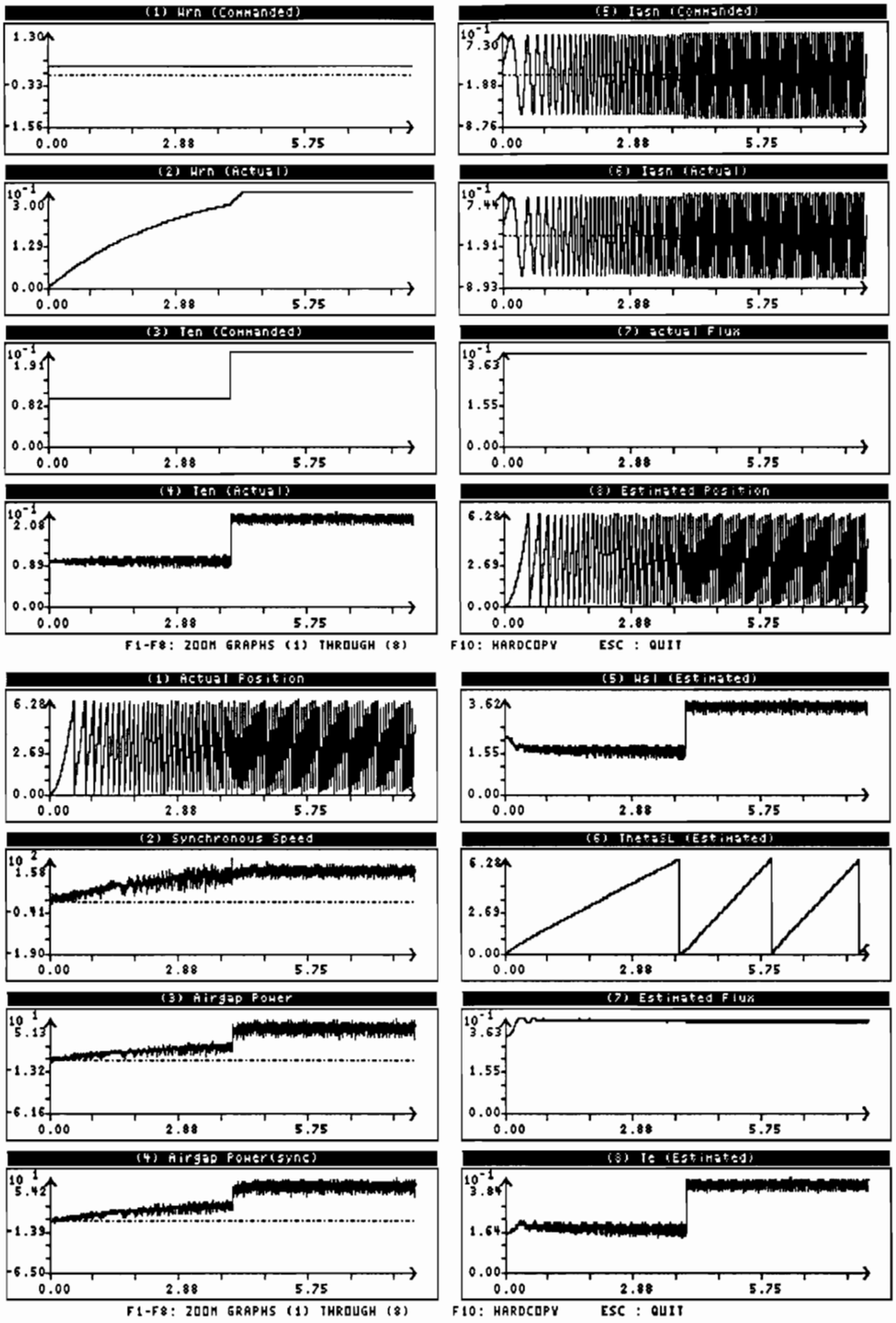

Figure 5.6: Simulation Results of Step Torque Response using Sensorless Algorithm

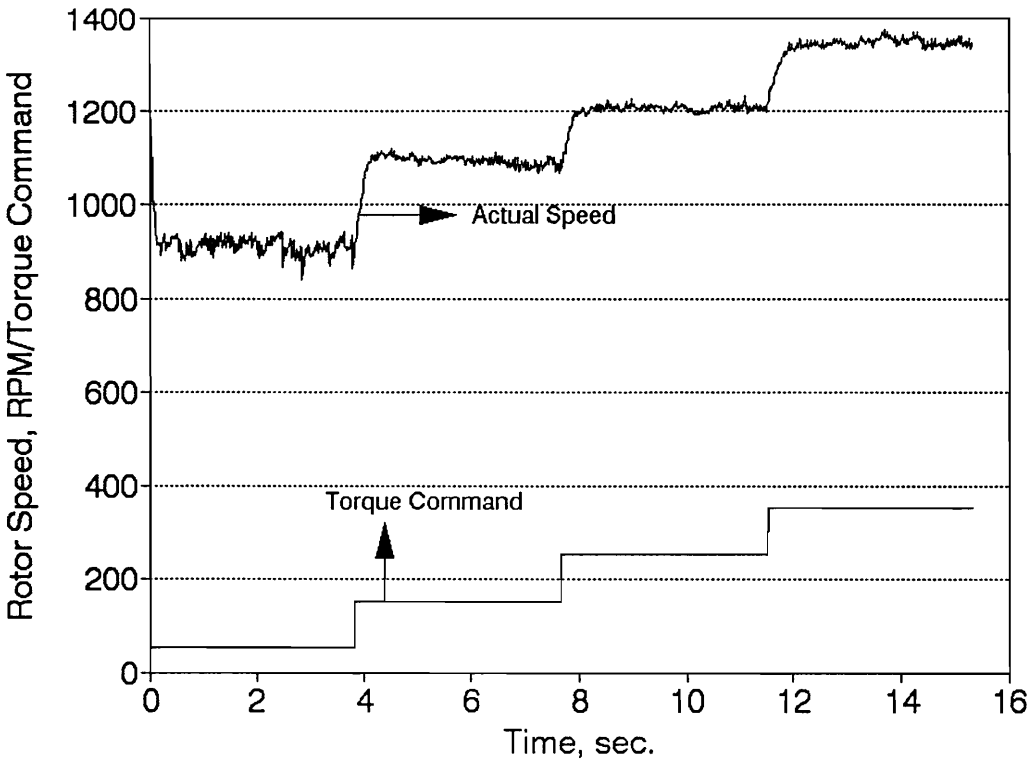

Figure 5.7: Experimental Results of Step Torque Response using Sensorless Algorithm

5.5 DISCUSSION

A novel sensorless vector control scheme which requires only two current transducers for the measurement of phase currents is formulated in this chapter. The phase voltages are estimated from the gate drive signals and the phase current measurement from which the rotor position is obtained. The simulation results of a torque drive for different values of rotor speed is presented to verify the algorithm. A speed drive simulation is also presented using the sensorless algorithm to illustrate the four quadrant operation of the drive system without position sensors.

The experimental verification has been performed by employing the DSP based vector controller discussed in the earlier chapters. An experimental run for the torque drive system using this setup is presented to validate the algorithm. It was noted that the switching frequency of the PWM controller was limited to 1 kHz. due to the software limitation of the processor. This introduced large ripples in the current which introduced errors in the position estimator routine. Also the leakage inductance of the motor used in the experimental setup was significant enough to introduce deviations in the estimation of the rotor flux. These two factors has limited the implementation of the speed drive system using the current experimental setup.

This disadvantage can be overcome by implementing the algorithm by analog circuitry or by using a faster Digital Signal Processor to perform only the mathematical calculations. The PWM algorithm can be made to function externally, thus enabling the user to control the current ripple. With such a setup, the speed drive can be implemented and critical issues such as parameter sensitivity of this algorithm and adaptation schemes can be evaluated.

Chapter 6

CONCLUSIONS

6.1 INTRODUCTION

With the advent of vector control and the recent advances in the semiconductor technology, ac machines are replacing the conventional dc machines in many industrial applications. In spite of the numerous advantages of the vector controlled induction motor drive systems, there are certain key issues which needed to be addressed in detail. The first issue pertaining to the classification and the modeling, simulation and analysis of the different types of vector control schemes in the popular d-q reference frames, and the parameter sensitivity and adaptation schemes for the indirect vector controlled induction motor drive systems is given in detail. The next issue relating to the formulation and development of a Computer Aided Engineering package for vector controlled induction motor drive systems which includes all the subsystem modeling in an user friendly environment is presented. The development of an algorithm similar to the dc motor for the study and design of a speed controller is dealt with in the next section. Finally the modeling, analysis simulation and experimental verification of a novel sensorless vector control scheme is also presented in this dissertation.

The next section discusses the various tasks which have been accomplished and the contributions of this research work. The final section of this chapter identifies scope for further research in this direction.

6.2 CONTRIBUTIONS

A comprehensive literature survey was performed and the tasks to be performed in this dissertation were identified. The author believes that the following are the contributions of

this work:

1. A comprehensive literature survey has been performed on vector control issues and key issues of research identified. The modeling, simulation and analysis of the various vector control schemes, all in the *d-q* reference frames, have been performed and the results presented. To confirm the validity of the simulation results, the indirect vector controlled induction motor drive system is implemented experimentally with a DSP based controller.

2. The methodology for the development of a CAE package for the dynamic analysis of the different vector control strategies which includes all the models of the various subsystems is developed. This package would help in the assessment of the torque ripple, losses, efficiency, torque, speed, and position responses and their bandwidth evaluation and determine the suitability for a particular application. The various results are presented to highlight the capability and features of the CAE package. Based on the principle of development of this package, CAE packages for other brushless drive systems such as the permanent magnet synchronous motor, permanent magnet brushless dc motor and the switched reluctance motor drives are also developed.

3. By utilizing the similarity between the vector controlled induction motor drive systems and the separately excited dc motor drive systems, a method for designing the parameters for the speed controlled in a speed/position drive system is formulated and analyzed. The results obtained from the analytical derivations are incorporated into the CAE package and the simulation results presented and discussed. The experimental verification of the results is also performed with the DSP based vector controller.

4. A novel sensorless vector control scheme with only current transducers is proposed and the modeling and analysis are presented. The simulation results from the CAE package for different conditions of the torque drive and the speed drive system are presented to validate the proposed algorithm.

6.3 FUTURE RECOMMENDATIONS

Based on the work accomplished in this dissertation, the author believes that the following tasks are recommended for possible future work:

1. **Subsystem modeling:** Even though, the various subsystems in the motor drive system has been incorporated into the CAE package, VCIM, the author believes more detailed modeling of all the subsystems for different conditions can be accomplished to make the package an even more efficient tool.

2. **Parameter sensitivity:** The various issues relating to parameter sensitivity were discussed in the earlier chapters. The sensorless vector control scheme presented is based on the indirect vector technique, which is itself parameter sensitive. Hence, a detailed parameter sensitive study on this algorithm and adaptation technique to alleviate this problem can be performed. Since the airgap power is already available in this method, an earlier adaptation method based on airgap power calculation can be an ideal candidate [41, 42].

REFERENCES

[1] Abbondanti, A., "Method of Flux Control in Induction Motors Driven By Variable Frequency, Variable Voltage Supplies," *Conf. Record of IEEE Industrial Applications Society International Semiconductor Power Converter Conference*, pp. 177–184, 1977.

[2] Akagi, H., Nabae, A., "High Performance Control Strategy of Cycloconverter-Fed Induction Motor Drive System Based on Digital Control Theory," *Trans. on IEEE-Industrial Electronics*, vol. IE-33, no. 2, pp. 126–131, May 1986.

[3] Akagi, H., Masaki, R., Takahashi, I., Nabae, A., "Decoupled Optimum Current Control of Cycloconverter Induction Machine System," *Electrical Engineering in Japan*, vol 103, no 2, pp. 115–121, Mar/Apr 1983.

[4] Andria, G., Dell'Aquila, A., Salvatore, L., "Signal Processing For Determining Flux and Torque of Induction Motors," *Conf. Record of Third International Conference on Power Electronics and Variable Speed Drives*, Conf Publ. no 291, pp. 296–301, July 1988.

[5] Andria, G., Dell'Aquila, A., Salvatore, L., "On-Line Identification of Induction Motor Parameters," *Proc. Symposium on Electrical Drive*, pp. 201–214, Sep 1987.

[6] Ansuj, S., Shokooh, F., Schinzinger, R., "Parameter Estimation for Induction Machines Based on Sensitivity Analysis," *Trans. on IEEE-Industry Applications Society*, vol IA–25, no 6, pp. 1035–1040, Nov/Dec 1989.

[7] Artime, J., Diez, A., Sanz, J., "A New Method for On-Line Estimation of Induction Motor Parameters," *Proc. Third International Conference on Electrical Machines and Drives*, pp. 226–228, Nov 1987.

[8] Baader, U., Depenbrock, M., Gierse Georg., "Direct Self-Control of Inverter-Fed Induction Machine Basis for Speed Control without Speed-Measurement," *Conf. Record of IEEE-Industry Applications Society Annual Meeting*, vol 1, pp. 486–492, Oct 1989.

[9] Bassi, E., Benzi, F., Bolognani, S., Buja, G.S., "A Field Orientation for Current Fed Induction Motor (CSIM) Drive Based on the Torque-Angle Closed Loop Control," *Conf. Record of IEEE-Industry Applications Society Annual Meeting*, vol 1, pp. 384–389, Oct 1989.

[10] Bassi, E., Benzi, F., "Vector Control for Induction Machine Drives : Theoretical Aspects and Applications Examples (Italian)," *Energia Elettrica*, vol 63, no. 7-8, pp. 291–306, Jul-Aug 1986.

[11] Bausch, H., Hontheim, H., Kolletschke, H. -D., "The Influence of Decoupling Methods on the Dynamic Behaviour of a Field-Oriented Controlled Induction Machine," *Proc. ICEM '86 Munchen. International Conference on Electrical Machines*, vol 2, pp. 648–651, Sep 1986.

[12] Bayer, K.H., Blaschke, F., "Stability Problems with the Control of Induction Motors using the Method of Field Orientation," *Conf. Record of IFAC Symposium on Power Electronics*, pp. 483–492, 1977.

[13] Bedingfield, R.A., "Development of CAE System for Switched Reluctance Motor Drive Systems," *M.S. Thesis*, The Bradley Department of Electrical Engineering, Virginia Polytechnic Institute & State University, Blacksburg, VA, Jul 1991.

[14] Bellini, A., Gifalli, G., Ulivi, G., "A Microcomputer Based Direct Field Oriented Control of Induction Motors," *Proc. ICEM '86 Munchen. International Conference on Electrical Machines*, vol 2, pp. 652–655, Sep 1986.

[15] Ben-Brahim, L., Kawamura, A., "Digital Current Regulation of Field Oriented Controlled Induction Motor Based on Predictive Flux Observer," *Conf. Record of IEEE-Industry Applications Society Annual Meeting*, vol 1, pp. 601–612, Oct 1990.

[16] Benvenuto, F., Burdese, G., De Luca, S., Moroni, R., "Torque Regulation of a Controlled Current Induction Motor Drive using Field Orientation Technique," *Conf. Record of Colloque International Sur la Commande et la Regulation Numeriques des Machines Electriques Lyon*, pp. IV/58–67, Apr 1980.

[17] Bishop, K.W.J., McLoughlin, P.D., "The Impact of Technology on Inverter Drives," *Conf. Record of Second International Conference on Power Electronics and Variable-Speed Drives*, Conf. Publ. no 264, pp. 106–111, Nov 1986.

[18] Bishop, K.W.J., Critchley, D.R., "Future of Inverter Fed Induction Drives," *Proc. Conference on Drives/Motors/Controls*, pp. 40–47, Oct 1983.

[19] Biswas, S.K., Sendaula, H., Caro, T., "Self Tuning Vector Control for Induction Motors," *Proc. IEEE Industrial Electronics Conference*, pp. 276–280, Nov 1989.

[20] Biswas, S.K., Sathiakumar, S., Vithayathil,J., "A Direct Torque Angle Controlled CSI Fed Induction Motor Drive with Constant Slip Frequency Operation ". *Conf. Record of IEEE-Industry Applications Society Annual Meeting*, pp. 210–215, Sep 1986.

[21] Biswas, S.K., Sathiakumar, S., Vithayathil, J., "High Efficiency Direct Torque Control Scheme for a CSI Fed Induction Motor Drive," *Conf. Record of IEEE-Industry Applications Society Annual Meeting*, pp. 216–221, Sep 1986.

[22] Blaschke, F., "Das Verfahren der Feldorientierung zur Regelung der Drehfelmachine (German)," ("The Method of Field Orientation for Control of Three Phase Machines,") *Ph.D. Dissertation*, TU Braunschweig, 1973.

[23] Blaschke, F., "The Principle of Field Orientation as Applied to the New Transvektor Closed-Loop Control System for Rotating-Field Machines," *Siemens Review*, vol 34, pp. 217–220, May 1972.

[24] Blaschke, F., "A New Method For the Structural Decoupling of AC Induction Machines," *Proc. IFAC Symposium, Dusseldorf*, pp. 1–15(6.3.1), Oct 1971.

[25] Blaschke, V.F., Ripperger, H., Steinkonig, H., "Regelung umrichtergespeister Asynchronmaschinen mit eingepragtem Standerstrom (German)," *Siemens-Zeitschrift*, no. 42, pp. 773–777, 1968.

[26] Blasko, V., Moreira, J.C., Lipo, T.A., "A New Field Oriented Controller Utilizing Spatial Position Measurement of Rotor End Ring Current," *Conf. Record of IEEE Power Electronics Specialists' Conference*, pp. 295–300, Jun 1989.

[27] Boldea, I., Pfeiffer, I., Trica, A., "Modified Sliding Mode (MSM) Versus PI Speed Control of a Current- Controlled Field-Oriented Induction Motor Drive," *Electric Machines and Power Systems*, vol 16, no. 3, pp. 209–223, 1989.

[28] Boldea, I., Nasar, S.A., "Torque Vector Control (TVC) - A Class of Fast and Robust Torque - Speed and Position Digital Controllers for Electric Drives," *Electric Machines and Power Systems*, vol 15, no. 3, pp. 135–147, 1988.

[29] Brostov, Y.A., Pashkov, N.N., Junger, I.B., "Induction Zero Overshoot Response Nonlinear Model Control," *Electric Technology U.S.S.R.*, no 2, pp. 35–41, 1987.

[30] Bose, B.K., "Sliding Model Control of Induction Motor," *Conf. Record of IEEE-Industry Applications Society Annual Meeting*, pp. 479–486, Oct 1985.

[31] Bose, B.K., "Scalar Decoupled Control Induction Motor," *Trans. on IEEE-Industry Applications Society*, vol IA–20, no 1, pp. 216–225, Jan/Feb 1984.

[32] Brickwedde, A., "Cycloconverter Fed High Performance Induction Motors for Rolling Steel Mill Industrial Drives," *Proc. Second European Conference on Power Electronics and Applications*, vol 2, pp. 1181–1189, Sep 1987.

[33] Cahill, T.M., "Microprocessor Based Vector Controlled Induction Spindle Drive - Application Considerations," *Proc. Sixth Annual Control Engineering Conference*, pp. 50–54, May 1987.

[34] Cardwell, B.J., "Torque Control of AC Induction Motor Traction Drives," *Conf. Record of International Conference on 'Electric Railway Systems for a New Century'*, (Conf. Publ. no 279), pp. 73–77, Sep 1987.

[35] Chan, C.C., Wang, H., "An Effective Method for Rotor Resistance Identification for High- Performance Induction Motor Vector Control," *IEEE Transactions on Industrial Electronics*, vol 37, no. 6, pp. 477–482, Dec 1990.

[36] Cheng-lin, Gu., Xing-shi, T., "A Microprocessor Based PWM Variable-Speed System with Modified Field Oriented Control," *Proc. ICEM '86 Munchen. International Conference on Electrical Machines*, vol 2, pp. 660–663, Sep 1986.

[37] Chura, V., "Squirrel-Cage Motor Controlled Stator Leakage Flux," *Acta Tech. CSAV (Czechoslovakia)*, vol 30, no 4, pp. 117–125, 1985.

[38] Colleran, P.J., Rogers, W.E., "Controlled Starting of AC Induction Motors," *Trans. on IEEE Industry Applications Society*, vol IA-19, no. 6, pp. 1014–1018, Nov/Dec 1983.

[39] Critchley, D.R., Jones, R., "High Performance AC Controller," *IEE Colloquium on 'Control of Induction Motors'*, (Digest no 60), pp. 5/1–3, Apr 1989.

[40] Daboussi, Z., Mohan, N., "Digital Simulation of Field-Oriented Control of Induction Motor Drives Using EMTP," *Trans. on IEEE Energy Conversion*, vol 3, no 3, pp. 667–673, Sep 1988.

[41] Dalal, D., Krishnan, R., "Parameter Compensation for Indirect Vector Controlled Induction Motor Drive using Estimated airgap power," *Conf. Record of IEEE-Industry Applications Society Annual Meeting*, pp. 170–176, Oct 1987.

[42] Dalal, D., "Novel Parameter Compensation Scheme for Indirect Vector Controlled Induction Motor Drives," *M.S. Thesis*, The Bradley Department of Electrical Engineering, Virginia Polytechnic Institute & State University, Blacksburg, VA, Jul 1987.

[43] Debowski, A., "Indirect Control Based on Dual Observer for Current-Fed Induction Motor by Field Weakening," *Proc. Symposium on Electrical Drive*, pp. 201–214, Sep 1987.

[44] Debowski, A., "Indirect Field Oriented Control for Current-Fed Induction Motor Based on Dual Observer," *Proc. ICEM '86 Munchen. International Conference on Electrical Machines*, vol 2, pp. 860–863, Sep 1986.

[45] De Doncker, R.W., Profumo, F., Pastorelli, M., "Self Tuning of Induction Motor Servo Drives using the Universal Field Oriented Controller," *Proc. IEEE Power Electronics Specialists' Conference*, pp. 649–655, Jun 1990.

[46] De Doncker, R., Profumo, F., "The Universal Field Oriented Controller Applied to Tapped Stator Windings Induction Motors," *Conf. Record of IEEE Power Electronics Specialists' Conference*, pp. 1031–1036, Jun 1989.

[47] De Doncker, R.W., Novotny, D.W., "Universal Field Oriented Controller," *Conf. Record of IEEE Industry Applications Society Annual Meeting*, pp. 450–456, Oct 1988.

[48] De Doncker, R., "Field Oriented Controllers with Rotor Deep Bar Compensation Circuits," *Conf. Record of IEEE Industry Applications Society Annual Meeting*, pp. 142–149, Oct 1987.

[49] De Doncker, R., Vandenput, A., Geysen, W., "Thermal Models of Inverter Fed Asynchronous Machines Suited for Adaptive Temperature Compensation of Field Oriented Controllers," *Conf. Record of IEEE Industry Applications Society Annual Meeting*, pp. 132–139, Sep 1986.

[50] De Doncker, R.W., Vandenput, A., Geysen, W., "A Digital Field Oriented Controller Using the Double Cage Induction Motor Model," *Conf. Record of IEEE Power Electronics Specialists' Conference*, pp. 502–509, Jun 1986.

[51] Delfiore, S., Franceschini, G., Tassoni, C., "Spice Aided Analysis of UPS Vector Control," *Proc. Eleventh International Telecommunications Energy Conference - Intelec '89. Part 2 (of 2)*, Oct 1989.

[52] Del Pizzo, A., Pagano, E., Perfetto, A., "Comparative Analysis and Parameter Sensitivity of Field Oriented Speed Controlled Asynchronous Motors," *Proc. Fourth International Conference on Electrical Machines and Drives*, pp. 322–327, Sep 1989.

[53] Denoncin, A.L., Charleroi, B., "Experience ACEC/MIVA," *Proc. Power Electronics and Applications*, vol 2, pp. 5/89–93, Oct 1985.

[54] Denoncin, L., Detemmerman, B., Lataire, P., "Control of a Current Inverter-Fed Asynchronous Machine for Railway Traction and Alternative Motors in General," *Conf. Record of Control in Power Electronics and Electrical Drives*, pp. 643–650, Sep 1984.

[55] Depenbrock, M., "Direct Self-Control (DSC) of Inverter-Fed Induction Machine," *Trans. on IEEE-Power Electronics*, vol 3, no 4, pp. 420–429, Oct 1988.

[56] Diana, G., Harley, R.G., "Aid for Teaching Field Oriented Control Applied to Induction Machines," *IEEE Transactions on Power Systems*, vol 4, no. 3, pp. 1258–1262, Aug 1989.

[57] Diez, A., Garcia, D.F., Cancelas, J.A., Lopez, H., "Adaptive Control of an Asynchronous Eolic Generator using the Field-Oriented Technique," *Mediterranean Electrotechnical Conference (MELECON '89)*, pp. 99–104, Apr 1989.

[58] Dimitri, D.S., Olson, W., Berg, D., "A.C. Induction Motor - Vector Control Cubic Motion Generator Dispenses Glue in Smooth, Continuous flow over Irregular Shapes," *IEEE Conf. Record of Fortieth Annual Conference of Electrical Engineering Problems in Rubber and Plastic Industries*, pp. 52–59, April 1988.

[59] Eisenbrown, R., Kerkkanen, Y., "High Performance AC Drives for Pulp and Paper Mill Application," *Conf. Record of IEEE-Annual Pulp and Paper Industry Technical Conference*, pp. 177–187, Jun 1984.

[60] Erdman, W.L., Hoft, R.G., "A Trajectory Sensitivity Approach to Parameter Disturbance Problems in Indirect Field Oriented Drive Systems," *Conf. Record of IEEE-Industry Applications Society Annual Meeting*, pp. 617–631, Oct 1989.

[61] Finch, J.W., Acarnley, P.P., Atkinson, D.J., "Practical Implementation and Test Facility for Field Oriented Induction Motor Drives," *Proc. Fourth International Conference on Electrical Machines and Drives*, pp. 288–292, Sep 1989.

[62] Floter, W., Ripperger, H., "Field-Oriented Closed-Loop Control of an Induction Machine with Transvektor Control System," *Siemens Review*, vol 39, no 6, pp. 248–252, Jun 1972.

[63] Floter, W., Ripperger, H., "Field Oriented Closed-Loop Control of an Induction Machine with the New TRANSVECTOR Control System," *Siemens-Z.45*, pp. 761–764, 1971.

[64] Fratta, A., Vagati, A., Villata, F., "Vector Control of Induction Motors without Shaft Transducers," *Conf. Record of IEEE-Power Electronics Specialists' Conference*, vol 2, pp. 839–846, Apr 1988.

[65] Fujisawa, T., Akita, K., "Sampling Time Effects on the Slip-Frequency-Type Vector Control of an Induction Motor," *Electrical Engineering in Japan (English translation of Denki Gakkkai Ronbunshi)*, vol 109, no. 5, pp. 85–92, Sep-Oct 1989.

[66] Fulton, D.E., "Characteristics of Induction Servos," *Proc. Ninth International Motor-Con Conference*, pp. 109–115, Oct 1986.

[67] Fulton, D.E., "Poor man's Vector Control or a User's Guide to Introduction Motor Servos," *Proceedings of the Fifth Annual Control Engineering Conference*, pp. 391–397, May 1986.

[68] Gabriel, R., Leonhard, W., "Microprocessor Control of Induction Motor," *Proc. International Semiconductor Power Converter Conference*, pp. 385–396, May 1982.

[69] Gabriel, R., Leonhard, W., Nordby, C., "Field Oriented Control of a Standard AC-Motor Using Microprocessor," *Trans. on IEEE-Industry Applications Society*, vol IA-16, no 2, pp. 186–192, Mar/Apr 1980.

[70] Gabriel, R., Leonhard, W., Nordby, C., "Microprocessor Control of Induction Motors Using Field Coordinates," *Proc. IEEE International Conference on Electrical Variable-Speed Drives*, pp. 146–150, Sep 1979.

[71] Galler, D., "Energy Efficient Control of AC Induction Motor Driven Vehicles," *Conf. Record of IEEE Industry Applications Society Annual Meeting*, pp. 301–308, Oct 1980.

[72] Garces, L.J., "Parameter Adaptation for Speed Controlled Static AC Drive with Squirrel Cage Induction Motor," *Conf. Record of IEEE-Industry Applications Society Annual Meeting*, pp. 843–850, Oct 1979.

[73] Garcia-Cerrada, A., Taufiq, J.A., "Convergence of Rotor Flux Estimation in Field Oriented Control," *Conf. Record of Third International Conference Power Electronics and Variable Speed Drives*, (Conf. Publ. no 291), pp. 291–295, July 1988.

[74] George, N.R., "Speed Control of DL Motor Using Triac Electronic Regulator for Supply and Winder Drives in Cable Industry," *Electric India (India)*, vol 26, no 16, pp. 5–10, Aug 1986.

[75] Gerasimyak, R.P., "Frequency Characteristics of an Induction Motor with Parametric Control of the Stator and Rotor Circuits," *Elektrotekhnika (USSR)*, vol 56, no 11, pp. 31–34, 1985.

[76] Gol, O., "Modelling of Inverter/Induction-Machine Drives," *Conf. Record of International Conference on Electrical Machines*, vol 2, pp. 670–677, Sep 1980.

[77] Gratzfeld, P., Weinhardt, M., "Improvement of the Dynamic Behavior of a Bogie Drive with Two Induction Motors Fed by a Common Inverter ," *Conf. Record of International Power Electronics Conference*, vol 2, pp. 1556–1566, Mar 1983.

[78] Grieve, D.W., Cross, D.M., "Recent Developments in the Design and Applications of Large, High Performance Cycloconverter Drive Systems," *Conf. Record of Third International Conference on Power Electronics and Variable-Speed Drives*, (Conf. Publ. no 291), pp. 309–314, July 1988.

[79] Gross, D.M., Taylor, D.M., "Squirrel cage Induction Motor Cyclo-converter drive at the British Coal Wearmouth Colliery," *GEC Review*, vol 4, no 3, pp. 154–163, 1988.

[80] Habtler, T.G., Divan, D.M., "Control Strategies for Direct Torque Control Using Discrete Pulse Modulation," *Conf. Record of IEEE-Industry Applications Society Annual Meeting*, vol 1, pp. 514–522, Oct 1989.

[81] Hajdu, E., Jardan, R.K., "Voltage Source Inverter Drive with Direct Torque Control," *Conf. Record of Second International Conference on Power Electronics and Variable-Speed Drives*, (Conf. Publ. no 264) pp. 80–84, Nov 1986.

[82] Hakata, H., Yamakoshi, H., Tatara, S., "Recent Developments and Applications of AC Variable-Speed Drives for Rolling Mill Main Stands," *Toshiba Review (International Edition)*, no 160, pp. 7–12, Summer 1987.

[83] Halasz, S., El-Sayed, M.M., "A.C. Inverter Drive with Field Oriented Control and Optimum PWM Strategy," *Lectures presented at the International Seminar on Microprocessors*, vol 32, no. 1, pp. 67–75, Oct 1986.

[84] Halasz, S., Schmidt, I., Horvath, M., "Transistorized PWM Inverter Asynchronous Motor Drive," *Conf. Record of International Conference on Electrical Machines*, vol 2, pp. 688–694, Sep 1980.

[85] Harashima, F., Kondo, S., Hachiken, E., Onno, Y., Ohnishi, K., "Synchronous Watt Torque Feedback Control of Induction Motor Drives," *Conf. Record of IEEE-Industry Applications Society Annual Meeting*, pp. 156–162, Oct 1987.

[86] Harashima, F., Arihara, E., Ohnishi, K., Kondo, S., "Microcomputer-Controlled Induction Motor Considering the Effects of Secondary Resistance Variation," *Conf. Record of IEEE-Industry Applications Society Annual Meeting*, pp. 548–553, Oct 1985.

[87] Harashima, F., Kondo, S., Ohnishi, K., Kajita, M., "Multimicroprocessor-Based Control System for Quick Response Induction Motor Drive," *Trans. on IEEE Industry Applications Society*, vol IA-21, no 3, pp. 602–609, May/Jun 1985.

[88] Hasegawa, T., Kurosawa, R., Hosoda, H., Abe, K., "Microcomputer-Based Motor Drive System with Simulator Following Control," *Proc. IEEE Industrial Electronics Conference*, pp. 41-46, Sep 1986.

[89] Hashimoto, H., Ohno, Y., Kondo, S., Harashima, F., "Torque Control of Induction Motor Using Predictive Observer," *Conf. Record of IEEE Power Electronics Specialists' Conference*, pp. 271–278, Jun 1989.

[90] Hasse, K., "Zur Dynamik Drehzahlgeregelter Antriebe mit Stomrichtergespeisten Asynchron-Kurzchlusslaufermachinen (German),"("On the Dynamics of Speed Control of Static Ac Drives with Squirrel-Cage Induction Machines,") *Ph.D. Dissertation*, TH Darmstadt, 1969.

[91] Hirose, K., Kawamura, A., Hoft, R., "Comparison of Field Oriented and Field Acceleration Methods of Induction Motor Control," *Conf. Record of IEEE-Power Electronics Specialists' Conference*, pp. 170–180, Jun 1984.

[92] Ho. E., Sen, P.C., "High Performance Parameter Insensitive Drive using a Series-Connected Wound Rotor Induction Motor," *Conf. Record of 1988 IEEE Industry Applications Society Annual Meeting*, pp. 239–245, Oct 1988.

[93] Ho, E.Y., Sen, P.C., "Digital Simulation of PWM Induction Motor Drives for Transient and Steady State Performance," *Trans. on IEEE-Industrial Electronics*, vol IE-33, no 1, pp. 66–77, Feb 1986.

[94] Holtz, J., Khambadkone, A., "Vector Controlled Induction Drive with a Self-Commissioning Scheme," *Proc. IEEE Industrial Electronics Conference*, vol II, pp. 927-932, Nov 1990.

[95] Holtz, J., Thimm, T., "Identification of the Machine Parameters in a Vector Controlled Induction Motor Drive System," *Conf. Record of IEEE-Industry Applications Society Annual Meeting*, vol 1, pp. 601–606, Oct 1989.

[96] Holtz, J., Bube, E., "Field-Oriented Asynchronous Pulsewidth Modulation for High Performance AC Machine Drives Operating at Low Switching Frequency," *Conf. Record of IEEE Industry Applications Society Annual Meeting*, pp. 412–417, Oct 1988.

[97] Hombu, M., Ueda, A., Nakazato, M., "Current Source Inverters with Sinusoidal Inputs and Outputs," *Hitachi Review*, vol 36, no 1, pp. 29–34, Feb 1987.

[98] Hori, Y., Cotter, V., Kaya, Y., "A Novel Induction Machine Flux Observer and its Application to a High Performance AC Drive System," *Proc. Automatic Control - World Congress, Selected Papers from the 10th Triennial World Congress of the International Federation of Automatic Control*, vol 3, pp. 363-368, Jul 1987.

[99] Horstmann, D., Stanke, G., "Field Oriented Control with Suboriented Pulse Pattern Generation of PWM Converter Fed Induction Machines," *5th IFAC/IFIP Symposium of Software for Computer Control 1988 (SOCOCO '88)*, pp. 91–98, Apr 1988.

[100] Hosoda, H., Tatara, S., Kurosawa, R., Hakata, H., Katsuhiko Doi., "New Concept High-Performance Large-Scale AC Drive System - Cross Current type Cycloconverter Fed Induction Motor with High-Performance Digital Vector Control," *Conf. Record of IEEE-Industry Applications Society Annual Meeting*, pp. 229–234, Sep 1986.

[101] Hung, K.T., Lorenz, R.D., "A Stator Flux Error-Based, Adaptive Tuning Approach for Feedforward Field Oriented Induction Machine Drives," *Conf. Record of IEEE-Industry Applications Society Annual Meeting*, vol 1, pp. 589–594, Oct 1990.

[102] Hunter, G.P., Ramsden, V.S., "New Improved Modulation Method for a Cycloconverter Driving an Induction Motor," *Proc. B IEE Electric Power Applications*, vol 135, no 6, pp. 324–333, Nov 1988.

[103] Irisa, T., Takata, S., Ueda, R., Sonoda, T., "Effect of Machine Structure on Identification of Spatial Position and its Magnitude of Rotor Flux in Induction Motor Vector Control," *IEE International Conference on Power Electronics and Variable-Speed Drives*, no 234, pp. 352–356, May 1984.

[104] Irisa, T., Takata, S., Ueda, R., Sonoda, T., Mochizuki, T., "A Novel Approach on Parameter Self Tuning Method in Ac Servo Systems," *Proc. Third IFAC Symposium in Power Electronics and Drives*, pp. 41–48, 1983.

[105] Ishida, M., Iwata, K., "Steady-State Characteristics of a Torque and Speed Control System of an Induction Motor Utilizing Rotor Slot Harmonics for Slip Frequency Sensing," *Trans. on IEEE Power Electronics*, vol PE-2, no 3, pp. 257–263, July 1987.

[106] Ishida, M., Iwata, K., "Steady-State Characteristics of a Torque and Speed Control System of an Induction Motor Utilizing Rotor Slot Harmonics for Slip Frequency Sensing," *Conf. Record of IEEE Power Electronics Specialists' Conference*, pp. 653–660, Jun 1985.

[107] Ishihara, K., Katayama, S., Kokubu, T., Yasaka, M., Kurosawa, R., "Application of a New Drive Systems for Plate Mill Drives," *Trans. on IEEE-Industry Applications Society*, vol IA-22, no 2, pp. 345–351, Mar/Apr 1986.

[108] Islam, S.M., Somuah, C.B., "Efficient High Performance Voltage Decoupled Induction Motor Drive with Excitation Control," *IEEE transactions on Energy Conversion*, vol 4, no. 1, pp. 109–117, Mar 1989.

[109] Iwasaki, M., Oyama, K., Tsunehiro, Y., "Current-Fed Inverter with Static Var Generator for Induction Motor Drive," *Electrical Engineering in Japan*, vol 103, no 3, pp. 100–108, May/Jun 1983.

[110] Jardan, R.K., Horvath, M., "Low Frequency Operation of Current-Fed Induction Motors," *Proc. International Conference on Electrical Machines*, vol 3, pp. 843–846, Sep 1984.

[111] Jardan, R.K., Horvath, M., "Current-Source Inverter Induction Motor Drive with Field-Oriented Control," *Proc. Second Annual International Motor-Con Conference*, pp. 72–85, Mar 1982.

[112] Jardan, R.K., Horvath, M., "Flux Control in Current Source Inverter Drives," *Conf. Record of International Conference on Electrical Machines*, vol 2, pp. 785–792, Sep 1980.

[113] Joetten, R., Maeder, G., "Control Methods for Good Dynamic Performance Induction Motor Drives Based on Current and Voltages as Measured Quantities," *Trans. on IEEE Industry Applications Society*, vol IA-19, no 3, pp. 356-363, May/Jun 1983.

[114] Kanekal, R., "Modeling, Simulation and Analysis of an Indirect Vector Controlled Induction Motor Drive," *M.S. Thesis*, The Bradley Department of Electrical Engineering, Virginia Polytechnic Institute & State University, Blacksburg, VA, Nov 1987.

[115] Karybakas, C.A., "Generalized Torque Performance of Two-Phase Induction Motors Controlled By Triac-An Approximate Analysis," *Trans. on IEEE Industrial Electronics and Control Instrumentation*, vol IECI-28, no 1, pp. 40–45, Feb 1981.

[116] Katta, T., Ibamoto, M., Narita, H., Kiwaki, H., Onoda, Y., Okamatsu, S., Tsuboi, T., Schimuzu, Y., "High Reliability Control Circuit of PWM Inverter for Electric Car Drive," *Conf. Record of IEEE Power Electronics Specialists' Conference*, pp. 311–317, Jun 1979.

[117] Kawamura, A., Hoft, R., "An Analysis of Induction Motor Field Oriented or Vector Control," *Conf. Record of IEEE-Power Electronics Specialists' Conference*, pp. 91–101, Jun 1983.

[118] Kazmierkowski, M.P., Sulkowski, W., "A Novel Vector Control Scheme for Transistor PWM Inverter-Fed Induction Motor Drive," *Trans. on IEEE-Industrial Electronics*, vol. IE-38, no. 1, pp. 41–48, May 1991.

[119] Kazmierkowski, M.P., Sulkowski, W., "Transistor Inverter-Fed Induction Motor Drive with Vector Control System," *Conf. Record of IEEE-Industry Applications Society Annual Meeting*, pp. 162–168, Sep 1986.

[120] Kazmierkowski, M.P., Kopcke, H.-J., "Current Source Inverter-Fed Induction Motor Drive System Controlled without a Speed Sensor," *Proc. Power Electronics and Applications*, vol 2, pp. 3/345–350, Oct 1985.

[121] Kazmierkowski, M.P., Kopcke, H.-J., "A Simple Control System for Current Source Inverter-Fed Induction Motor Drives," *Trans. on IEEE Industry Applications Society*, vol IA-21, no 3, pp. 617–623, May/Jun 1985.

[122] Kazmierkowski, M.P., Kopcke, H.-J., "Comparison of Dynamic Behavior of Frequency Converter Fed Induction Machine Drives," *Conf. Record of Control in Power Electronics and Electrical Drives*, pp. 313–320, Sep 1984.

[123] Kerkman, R.J., Rowan, T.M., Leggate, D., "Indirect Field Oriented Control of an Induction Motor in the Field Weakening Region," *Conf. Record of IEEE-Industry Applications Society Annual Meeting*, vol 1, pp. 375–383, Oct 1989.

[124] Khater, F., Lorenz, R.D., Novotny, D.W., Tang, K., "The Selection of Flux Level in Field Oriented Induction Machine Controllers with Consideration of Magnetic Saturation Effects," *IEEE transactions on Industry Applications*, vol IA-23, no. 2, pp. 276–282, Mar/Apr 1987.

[125] Kilicaslan, B., Ersak, A., "Analysis of a PWM Inverter Driven Induction Machine," *Conf. Record of International Conference on Electrical Machines*, vol 2, pp. 678–687, Sep 1980.

[126] Kimoto, K., Kameko, Y., Hashimoto, K., Ohnishi, "Decoupling Control of an Induction Motor Operated with a PAM Inverter," *Conf. Record of IEEE Power Electronics Specialists' Conference*, pp. 1091–1098, Apr 1988.

[127] Kirschen, D.S., Novotny, D.W., Lipo, T.A., "Optimal Efficiency Control of an Induction Motor Drive," *Trans. on IEEE-Energy Conversion*, vol EC-2, no 1, pp. 70–76, Mar 1987.

[128] Kobayashi, T., Sahashi, M., Inomata, K., Domon, T., Suzuki, I., "Development of an Amorphous Torque Sensor for Induction Motors," *IEEE Translation Journal on Magnetics in Japan*, Vol TMJ-2, no 12, pp 1162–1163, Nov 1985.

[129] Kohata, M., Hayashi, H., "Quick Response Control of Induction Motor using Voltage Source Inverter," *Conf. Record of International Power Electronics Conference*, vol 1, pp. 708–719, Mar 1983.

[130] Kohlmeier, H., Niermeyer, O., Schroder, D., "High Dynamic Four-Quadrant AC-Motor Drive with Improved Power Factor and on-line Optimized Pulse Pattern with PROMC (Precalculation of Reference for Optimal Model Control)," *Proc. of Power Electronics and Applications*, vol 2, pp. 3/173–178, Oct 1985.

[131] Koyama, M., Yano, M., Kamiyama, I., Yano, S., "Microprocessor-Based Vector Control System for Induction Motor Drives with Rotor Time Constant Identification Function," *Trans. on IEEE-Industry Applications Society*, vol IE-33, no 2, pp. 453–459, May/Jun 1986.

[132] Koyama, M., Sugimoto, H., Mimura, M., Kawasaki, K., "Effects of Parameter Change on Coordinate Control System of Induction Motor," *Conf. Record of International Power Electronics Conference*, pp. 684-695, Mar 1983.

[133] Krishnan, R. "Electronic Control of Machines," *Prentice Hall*, Englewood Cliffs, NJ, 1992.

[134] Krishnan, R., Bharadwaj, A.S., "Computer Simulation of Modern Variable Speed Motor Drive Systems," *Project Report*, Submitted to Center of Innovative Technology, VA, Jan 1992.

[135] Krishnan, R., Bharadwaj, A.S., "A Review of Parameter Sensitivity and Adaptation in Indirect Vector Controlled Induction Motor Drive Systems," *IEEE Trans. on Power Electronics*, vol 6, no 4, pp. 695–703, Oct 1991.

[136] Krishnan, R., Bharadwaj, A.S., Bedingfield, R.A., "Computer Aided Simulation for the Dynamic Analysis of the Indirect Vector Controlled Induction Motor Drive Systems," *Proc. Fifth IFAC/IMACS Symposium on Computer Aided Design in Control Systems*, pp. 583–588, University of Wales, Swansea, UK, Jul 1991.

[137] Krishnan, R., Bedingfield, R.A., Bharadwaj, A.S., Ramakrishna P., "Design and Development of a User-Friendly PC-Based CAE Software for the Analysis of

Torque/Speed/Position Controlled PM Brushless DC Motor Drive System Dynamics," *Conf. Record of IEEE-Industry Applications Society Annual Meeting*, pp. 1388–1394, Oct 1991.

[138] Krishnan, R., Bharadwaj, A.S., "Single Chip Microcontroller Implementation of an Indirect Vector Controlled Induction Motor Drive System," *Conf. Record of IEEE Power Electronics Specialists' Conference*, pp. 265–270, Jun 1989.

[139] Krishnan, R. "Accuracy Response and Reliability of the Ac and Dc Motor Drive," *Proc. Workshop on Electrical Machines and Drive*, National Science Foundation Large-Scale Nonlinear Systems Program, pp. 32–52, Oct 1988.

[140] Krishnan, R., Pillay, P., "Parameter Sensitivity in Vector Controlled AC Motor Drives," *Proc. IEEE-Industrial Electronics Conference*, vol 1, pp. 212–218, Nov 1987.

[141] Krishnan, R., Doran, F.C., "A Method of Sensing Line Voltages for Parameter Adaptation of Inverter Fed Induction Motor Servo Drives," *Trans. on IEEE-Industry Applications Society*, vol IA-23, no 4, pp. 617–622, Jul/Aug 1987.

[142] Krishnan, R., Doran, F.C., Lotas, T.S., "Identification of Thermally Safe Load Cycles for an Induction Position Servo," *Trans. on IEEE Industry Applications Society*, vol IA-23, no 4, pp. 636–643, Jul/Aug 1987.

[143] Krishnan, R., Doran, F.C., "Study of Parameter Sensitivity in High Performance Inverter-Fed Induction Motor Drive Systems," *Trans. on IEEE Industry Applications Society*, vol IA-23, no 4, pp. 623–635, Jul/Aug 1987.

[144] Krishnan, R., Pillay, P., "Sensitivity Analysis and Comparison of Parameter Compensation Schemes in Vector Controlled Induction Motor Drives," *Conf. Record of IEEE-Industry Applications Society Annual Meeting*, pp. 155–161, Sep 1986.

[145] Krishnan, R., Lindsay, J.F., Stefanovic, V.R., "Comparison of Control Schemes for Inverter Fed Induction Motor Drives," *Conf. Record of IEE Conference on Power Electronics and Variable Speed Drives*, (Conf. Publ. no 234), pp. 312–316, May 1984.

[146] Krishnan, R., "Control and Dynamics of Inverter-Fed Induction Motor," *Ph.D. Dissertation, Concordia University, Montreal, Quebec, Canada*, Mar 1982.

[147] Krishnan, R., Stefanovic, V.R., Lindsay, J.F., "Control Characteristics of Inverter-Fed Induction Motor," *Conf. Record of IEEE-Industry Applications Society Annual Meeting*, pp. 548–561, Oct 1981.

[148] Krishnan, R., Maslowski, W.A., Stefanovic, V.R., "Control Principles in Current Source Induction Motor Drives," *Conf. Record of IEEE-Industry Applications Society Annual Meeting*, pp. 605–617, Oct 1980.

[149] Kubo, K., Watanabe, M., Ohmae, T., Kamiyama, K., "Fully Digitialized Speed Regulator using Multiprocessor System for Induction Motor Drives," *Trans. on IEEE-Industry Applications Society*, vol IA-21, no 4, pp. 1001–1008, Jul/Aug 1985.

[150] Kubota, H., Matsuse, K., Nakano, T., "New Adaptive Flux Observer of Induction Motor for Wide Speed Range Motor Drives," *Proc. IEEE Industrial Electronics Conference*, vol II, pp. 921-926, Nov 1990.

[151] Kubota, H., Matsuse, K., Fukao, T., "Indirect Field Oriented Control of CSI-Fed Induction motor with State Observer," *Conf. Record of IEEE Industry Applications Society Annual Meeting*, pp. 138–141, Oct 1987.

[152] Kubota, H., Matsuse, K., Fukao, T., "New Control Method of Inverter-Fed Induction Motor Drive by using State Observer with Rotor Resistance Identification," *Conf. Record of IEEE-Industry Applications Society Annual Meeting*, pp. 601–606, Oct 1985.

[153] Kubota, H., Matsuse, K., Fukao, T., "A Control Method of Induction Motor Driven by Current-Source Type Inverter using a State Observer," *Electrical Engineering in Japan*, vol 105, no 5, pp. 119–127, Sep/Oct 1985.

[154] Kubota, H., Matsuse, K., Amano, M., Fukao, T., "New Inverter-Fed Induction Motor Drive with Microprocessor-Based State Observer for Estimating Torque," *Proc. IEEE-Industrial Electronics Conference*, pp. 857–862, Oct 1984.

[155] Kuga, T., Kawabata, Y., "World's First Cycloconverter Application to Induction Motor-Powered Mine Hoist Drive Systems," *Toshiba Review (International Edition)*, no 151, pp. 17–20, Spring 1985.

[156] Kuga, T., Sugi, K., "Sinusoidal Cycloconverter for Mine Hoist Drive," *Proc. IEEE-Industrial Electronics Conference*, pp. 572–574, Oct 1984.

[157] Kumamoto, A., Hirane, Y., "An Experimental Implementation of a Variable-Speed Induction Motor System Based on Modern Adaptive Control Theory," *Proc. Second European Conference on Power Electronics and Applications*, vol 2, pp. 889–894, Sep 1987.

[158] Kume, T., Sawa, T., Yoshida, T., Sawamura, M., Sakamoto, M., "High Speed Vector Control Without Encoder for a High Speed Spindle Motor," *Conf. Record of IEEE-Industry Applications Society Annual Meeting*, vol 1, pp. 390–394, Oct 1990.

[159] Kume, T., Iwakane, T., Sawa, T., Yoshida, T., Naga Ikuo., "Wide Constant Power Range Vector Controlled AC Motor Drive using Winding Change over Technique," *Conf. Record of IEEE-Industry Applications Society*, vol 1, pp. 470–475, Oct 1988.

[160] Kume, T., Iwakane, T., "High Performance Vector-Controlled AC Motor Drives: Applications and New Technologies," *Trans. on IEEE Industry Applications Society*, vol IA-23, no 5, pp. 872–880, Sep/Oct 1987.

[161] Kumamoto, A., Tada, S., Hirane, Y., "Speed Regulation of an Induction Motor using Model Reference Adaptive Control," *IEEE Control Systems Magazine* vol 6, no. 5, pp. 25–29, Oct 1986.

[162] Kurosawa, R., Shimamura, T., Uchino, H., Sugi, K., "Micro-Computer Based High Power Cycloconverter-Fed Induction Motor Drive," *Conf. Record of IEEE-Industry Applications Society Annual Meeting*, pp. 462–467, Oct 1982.

[163] Kyranastassis, G.J., Galanos, G.D., "Dynamic Simulation of A Cycloconverter Driven Three Phase Squirrel Cage Induction Motor," *Conf. Record of International Conference on Electrical Machines*, vol 2, pp. 712–719, Sep 1980.

[164] Leander, P., "Thyristor Locomotives with Three Phase Drives-Development for the Future," *ElectroTechnology (GB)*, vol 12, no 4, pp. 160–163, Oct 1984.

[165] Le Doeuff, R., Lung, C., Gudefin, E.J., "Study by Digital Simulation of an Induction Machine by a Three Phased Cycloconverter," *Conf. Record of International Conference on Electrical Machines*, vol 2, pp. 704–711, Sep 1980.

[166] Leonhard, W., "Field Orientation for Controlling AC Machines - Principle and Applications," *Conf. Record of Third International Conference on Power Electronics and Variable Speed Drives*, (Conf. Publ. no 291), pp. 277–282, July 1988.

[167] Leonhard, W., "Control of Electric Drives," *Springer Verlag*, New York, 1985.

[168] Leonhard, W., "Control of AC-Machines with the Help of Micro-Electronics," *Conf. Record of Control in Power Electronics and Electrical Drives*, pp. 769–792, Sep 1984.

[169] Leonhard, W., "Introduction to AC Motor Control Using Field Coordinates," *Conf. Record of Simposia Sulla Evoluziona Nella Diamica Della Machine Elettriche Rotanti, Tirrania*, pp. 370–376, 1975.

[170] Levi, E., Vuckovic, V., Vukosavic, S., "Study of main flux saturation effects in field-oriented induction motor drives," *Proc. IEEE Industrial Electronics Conference* pp. 219–224, Nov 1989.

[171] Levi, E., Vuckovic, V., "Field-Oriented Control of Induction Machines in the Presence of Magnetic Saturation," *Electric Machines and Power Systems* vol 16, no. 2, pp. 133–147, 1989.

[172] Levi, E., "Matematicki modeli vektroski upravljanih zasicenih asinhronih masina / Mathematical models of saturated induction machines with field-oriented control, (Serbo-croatian)" *Elektrotehnika* vol 31, no. 5-6, pp. 181–188, Sep-Dec 1988.

[173] Li, Y.D., Defornel, B., Pietrzak-David, M., "New Approach for Flux Control of PWM-Fed Induction Drive," *Conf. Record of Third International Conference on*

Power Electronics and Variable-Speed Drives, (Conf. Publ. no 291), pp. 301–304, July 1988.

[174] Li, Y., He, G., Cheng, H., Jin, Z., "Microcomputer Based Vector Control System with Current Source Inverter," *Conf. Record of IEEE-Industry Applications Society Annual Meeting*, pp. 549–554, Sep 1986.

[175] Lipo, T.A., Plunkett, A.B., "A Novel Approach to Induction Motor Transfer Functions," *Trans. on IEEE Power Apparatus and Systems*, vol PAS-93, no 5, pp. 1410–1418, Sep/Oct 1974.

[176] Liu, C.H., Chen,C., Feng, Y.F., "Modeling and Implementation of a Microprocessor-Based CSI-Fed Induction Motor Drive using Field-Oriented Control," *IEEE Transactions on Industry Applications* vol 25, no. 4, pp. 588–597, Jul-Aug 1989.

[177] Liu, C,H., Chen, C,C.,Chou, L.C., "Microprocessor-Based Field-Oriented Control of Current Source Inverter Fed Induction Motor Drives," *Chung-kuo Kung Ch'eng Hsueh K'an / Journal of the Chinese Institute of Engineers* vol 10, no.1, pp. 53–66, Jan 1987.

[178] Lobo, I., Lorenzo, S., Amigo, J., Ruiz, J.M., "AC Motor Dynamic Performance Study Using Field Orientation," *Proc. IEEE Industrial Electronics Conference*, vol I, pp. 193-197, Nov 1990.

[179] Lorenz, R.D., Novotny, D.W., "Optimal Utilization of Induction Machines in Field Oriented Drives," *Journal of Electrical and Electronics Engineering* vol 10, no. 2, pp. 95–101, Jun 1990.

[180] Lorenz, R.D., Lawson, D.B., "Simplified Approach to Continuous On-Line Tuning of Field-Oriented Induction Machine Drives," *IEEE Transactions on Industry Applications* vol 26, no. 3, pp. 420–424, May/Jun 1990.

[181] Lorenz, R.D., Novotny, D.W., "Saturation Effects in Field Oriented Induction Machines," *Trans. on IEEE Industry Applications Society*, vol IA-26, no 2, pp. 283–289, Mar/Apr 1990.

[182] Lorenz, R.D., Lawson, D.B., "Flux and Torque Decoupling Control for Field-Weakened Operation of Field-Oriented Induction Machines," *IEEE Transactions on Industry Applications* vol 26, no. 2, pp. 290–295, Mar/Apr 1990.

[183] Lorenz, R.D., Divan, D.M., "Dynamic Analysis and Experimental Evaluation of Delta Modulators for Field Oriented AC Machine Current Regulators," *IEEE Transactions on Industry Applications* vol 26, no. 2, pp. 296–301, Mar/Apr 1990.

[184] Lorenz, R.D., Yang, S.M., "AC Induction Servo Sizing for Motion Control Applications via Loss Minimizing Real-Time Flux Control," *Conf. Record of IEEE-Industry Applications Society Annual Meeting*, vol 1, pp. 612–616, Oct 1989.

[185] Lorenz, R.D., Lawson, D.B., "Simplified Approach to Continuous, On-Line Tuning of Field Oriented Induction Machine Drives," *Conf. Record of IEEE Industry Applications Society Annual Meeting*, pp. 444–449, Oct 1988.

[186] Lorenz, R.D., Yang, S.M., "Efficiency-Optimized Flux Trajectories for Closed Cycle Operation of Field Oriented Induction Machine Drives," *Conf. Record of IEEE Industry Applications Society Annual Meeting*, pp. 457–462, Oct 1988.

[187] Lorenz, R.D., Lawson, D.B., "Performance of Feedforward Current Regulators for Field-Oriented Induction Machine Controllers," *Trans. on IEEE Industry Applications Society*, vol IA-23, no 4, pp. 597–602, Jul/Aug 1987.

[188] Lorenz, R.D., Lucas, M.O., Lawson, D.B., "Synthesis of a State Variable Motion Controller for High Performance Field Oriented Induction Machine Drives," *Conf. Record of IEEE Industry Applications Society Annual Meeting*, pp. 607–612, Oct 1985.

[189] Lorenz, R.D., "Tuning of Field Oriented Induction Motor Controllers for High Performance Applications," *Conf. Record of IEEE Industry Applications Society Annual Meeting*, pp. 607–612, Oct 1985.

[190] Lukitsch, W.J., "Microcomputer Controls Torque for Textile Industry," *Conf. Record of IEEE-Annual Textile Industry Conference*, pp. 2/1–3, May 1987.

[191] Magureanu, R., Kreindler, L., Floricau, D., Solacolu, C., "Current versus Voltage Control of the Induction Motor Operating at Constant Rotor Flux," *Proc. Third International Conference on Electrical Machines and Drives*, pp. 221–225, Nov 1987.

[192] Mahmoud, S.A., Lashin, A.E., Hassan, S.A., "Torque/Speed Control of Wound Rotor Induction Motors Using a DC Chopper Circuit," *Electric Machines and Power Systems*, vol 11, no 1, pp. 25–39, 1986.

[193] Matsui, T., Okuyama, T., Takahashi, J., Sukegawa, T., Kamiyama, K., "A High Accuracy Current Component Detection Method for Fully Digital Vector-Controlled PWM VSI-Fed AC Drives," *Conf. Record of IEEE-Power Electronics Specialists' Conference*, pp. 877–884, Apr 1988.

[194] Matsugae, H., Hatchisu, Y., Nagao, Y., Fujita, K., "DSP-Based all Digital, Vector Control Induction Motor Drives for Spindle System," *Proc. IEEE Power Electronics Specialists' Conference* vol 2, pp. 636–640, Jun 1990.

[195] Matsumoto, H., Takami, H., Takase, R., "Vector Control Scheme for an Induction Motor Controlled by a Voltage Model Operation with Current Control Loop," *Conf. Record of IEEE-Industry Applications Society Annual Meeting*, vol 1, pp. 368–374, Oct 1989.

[196] Matsuo, T., Blasko, V., Moreira, J.C., Lipo, T.A., "A New Direct Field Oriented Controller Employing Rotor End Ring Current Detection," *IEEE Power Electronics Specialists' Conference* pp. 599–605, Jun 1990.

[197] Matsuo, T., Lipo, T.A., "Rotor Parameter Identification Scheme for Vector-Controlled Induction Motor Drives," *Trans. on IEEE Industry Applications Society*, vol IA-21, no 3, pp. 624–632, May/Jun 1985.

[198] Matsuo, T., "Rotor Resistance Identification in the Field Oriented Control of Squirrel-Cage Induction Motor Driven by Static Converter," *M.S. Thesis*, University of Wisconsin, Madison, 1983.

[199] Meshkat, S., "Field-Oriented Control Produces Precision AC Induction Servo," *Power Conversion and Intelligent motion* vol 15, no. 2, pp. 46–48, Feb 1989.

[200] Miki, I., Nakao, O., Nishiyama, S., "A New Simplified Current Control Method for Field Oriented Induction Motor Drives," *Conf. Record of IEEE-Industry Applications Society Annual Meeting*, vol 1, pp. 390–395, Oct 1989.

[201] Minami, K., "Model Based Speed and Parameter Estimation for Induction Machines," *M.S. Thesis*, Massachussetts Institute of Technology, Cambridge, 1988.

[202] Min-Ho, P., Woong, J.S., "Optimal Starting Torque Control of Wound Rotor Induction Motor by Microprocessor," *Trans. on Korean Institute of Electrical Engineering*, vol 33, no 8, pp. 316–324, 1984.

[203] Miura, S., Todo, Y., "Vector Control Drive System 'V**2 (square) Motor/Controller," *Hitachi Review* vol 38, no. 6, pp. 299–302, Dec 1989.

[204] Miyazaki, M., Kuroiwa, A., Kudor, T., "High Performance Vector Control Drive System by Microprocessor-based Current Source Inverter," *Proc. IEEE-Industrial Electronics Conference*, pp. 821–826, Oct 1984.

[205] Mochizuki, T., Ueda, R., Takata, S., Yoshida, Y., "A New Synthesizing Method of a Current Controlled Inverter Induction Motor System," *Conf. Record of International Conference on Electrical Machines*, vol 2, pp. 752–759, Sep 1980.

[206] Moreira, J.C., Lipo, T.A., "A New Method for Rotor Time Constant Tuning in Indirect Field Oriented Control," *IEEE Power Electronics Specialists' Conference* pp. 573–580, Jun 1990.

[207] Morimoto, S., Takeda, Y., Hirasa, T., Taniguchi, K., "Expansion of Operating Limits for Permanent Magnet Motor by Current Vector Control Considering Inverter Capacity," *IEEE Transactions on Industry Applications* vol 26, pp. 866–871, Sep-Oct 1990.

[208] Morimoto, M., Sato, S., Sumito, K., Oshitani, K., "Voltage Modulation Factor of the Magnetic Flux Control PWM Method for Inverter," *Trans. on IEEE-Industrial Electronics*, vol. IE-38, no. 1, pp. 57–61, Feb 1991.

[209] Morishita, T., Yoshida, K., Awata, H., "Transvector Control of Induction Motor with Current Table," *IEE International Conference on Power Electronics and Variable-Speed Drives*, no 234, pp. 292–295, May 1984.

[210] Murata, T., Tsuchiya, T., Takeda, I., "Vector Control for Induction Machine on the Application of Optimal Control Theory," *IEEE Transactions on Industrial Electronics* vol 37, no. 4, pp. 283–290, Aug 1990.

[211] Murata, T., Tsuchiya, T., Takeda, I., "A New Synthesis Method for Efficiency Optimized Speed Control System of Vector Controlled Induction Machine," *Conf. Record of IEEE-Power Electronics Specialists' Conference*, pp. 862–869, Apr 1988.

[212] Mutoh, N., Ueda, A., Nando, K., Ibori, S., "Tripless Control Methods for General Purpose Inverters," *Conf. Record of IEEE-Power Electronics Specialists' Conference*, pp. 1292–1299, Apr 1988.

[213] Mutoh, N., Nagase, H., Sakai, K., Ninomiya, H., "High Response Digital Speed-Control System for Induction Motors," *Trans. on IEEE-Industrial Electronics*, vol IE-33, no 1, pp. 52–58, Feb 1986.

[214] Myrcik, C., "Improved Control Structure for Field Orientation Controlled Induction Motor Drive," *Archiwum Electrotechiki (Warsaw)*, vol 34, no 1–2, pp. 319–333, 1985.

[215] Nabae, A., Otsuka, K., Uchino, H., Kurosowa, R., "An Approach to Flux Control of Induction Motors Operated with Variable Frequency Power Supply," *Conf. Record of IEEE-Industry Applications Society Annual Meeting*, pp. 890–896, Oct 1978.

[216] Nakagawa, T., Hirata, A., Saito, S., Miyazaki, M., "New Application of Current-Type Inverters," *Conf. Record of IEEE-Industry Applications Society Annual Meeting*, pp. 891–896, Oct 1980.

[217] Nakamura, K., Kimura, A., Iwataki, M., "Inverter Drive System for AC Rolling Stocks," *Hitachi Review (Japan)*, vol 37, no 6, pp. 371–376, Dec 1988.

[218] Nakano, H., Takahashi, I., "Sensor less Field Oriented Control of an Induction Motor Using an Instantaneous Slip Frequency Estimation Method," *Conf. Record of IEEE-Power Electronics Specialists' Conference*, pp. 847–854, Apr 1988.

[219] Nakano, M., Mukai, Y., Yoshida, Y., "Torque Sensors for Induction Motors Using Amorphous Microcore Field Sensors," *IEEE Translation Journal on Magnetics in Japan*, vol TJMJ-2, no 12, Dec 1987.

[220] Nakano, H., Horie, S., Matsuo, T., Iwata, K., "Vector Control System for Induction Motor using a Speed Estimation Based on Instantaneous Slip Frequency Principles," *Electrical Engineering in Japan*, vol 107, no 4, pp. 95–103, Jul/Aug 1987.

[221] Naunin, D., "The Calculation of the Dynamic Behavior of Electric Machines by Space-Phasors," *Electric Machines and Electromechanics*, pp. 33–45, Jul 1979.

[222] Niermeyer, O., Schroder, D., "Induction Motor Drive with Parameter Identification Using a New Predictive Current Control Strategy," *Conf. Record of IEEE Power Electronics Specialists' Conference*, pp. 287–294, Jun 1989.

[223] Nomura, M., Ashikaga, T., Terashima, M., Nakamura, T., "High Response Induction Motor Control System with Compensation for Secondary Resistance Variation," *Conf. Record of IEEE Power Electronics Specialists' Conference*, pp. 46–51, Jun 1987.

[224] Nordin, K.B., Novotny, D.W., Zinger, D.S., "The Influence of Motor Parameter Deviations in Feedforward Field Orientation Systems," *IEEE Transactions on Industry Applications*, vol IA-21, no 4, pp. 1009–1015, July/Aug 1985.

[225] Ogasawara, S., Akagi, H., Nabae, A., "Generalized Theory of Indirect Vector Control of AC Machines," *IEEE Transactions on Industry Applications*, vol IA-24, no 3, pp. 470–478, May/Jun 1988.

[226] Ogasawara, S., Akagi, H., Nabae, A., "Universal Theory for the Flux Feedforward Type Vector Control," *Electrical Engineering in Japan*, vol 106, no 3, pp. 59–66, May/Jun 1986.

[227] Ohm, D.Y., "Principles of Vector Control. Part II," *Powerconversion & Intelligent Motion* vol 16, no. 9, Sep 1990.

[228] Ohm, D.Y., Khersonsky, Y., Kimzey, J.R., "Rotor Time Constant Adaptation Method for Induction Motors Using DC Link Power Measurements," *Conf. Record of IEEE-Industry Applications Society Annual Meeting*, vol 1, pp. 588–593, Oct 1989.

[229] Ohm, D.Y., Khersonsky, Y., Kimzey, J.R., "Operating Characteristics of Indirect Field Oriented Induction Motor," *Fourth Annual IEEE Applied Power Electronics Conference and Exposition - APEC 89*, pp. 91–100, Mar 1989.

[230] Ohmae, T., Obaro, S., Watanabe, M., Matsuda, T., "Flexible Multi-Axis Digital Servo System," *Proc IEEE-Industrial Electronics Conference*, pp. 23–27, Sep 1986.

[231] Ohnishi, K., Ueda, Y., Miyachi, K., "Model Reference Adaptive System against Rotor Resistance Variation in Induction Motor Drive," *Trans. on IEEE-Industrial Electronics*, vol IA-22, no 3, pp. 217–223, Aug 1986.

[232] Ohnishi, K., Suzuki, H., Miyachi, K., Terashima, M., "Decoupling Control of Secondary Flux and Secondary Current in Induction Motor Drive with Controlled Voltage Source and its Comparison with Volts/Hertz Control," *Trans. on IEEE Industry Applications Society*, vol IA-21, no 1, pp. 241–247, Jan/Feb 1985.

[233] Ohta, M., Maruto, M., Kaga, A., Obi, H., Nakamoto, N., "Advanced AC Propulsion with High Power GTO and Digital Control for Electric Rolling Stock," *Conf. Record of IEEE Industry Applications Society Annual Meeting*, pp. 307–314, Oct 1983.

[234] Ohtani, T., Takada, N., Tanaka, K., "Vector Control of Induction Motors Without Shaft Encoders," *Conf. Record of IEEE-Industry Applications Society Annual Meeting*, vol 1, pp. 500–507, Oct 1989.

[235] Ohtani, T., "New Method of Torque Control Free from Motor Parameter Variation in Induction Motor Drives," *Conf. Record of IEEE-Industry Applications Society Annual Meeting*, pp. 203–209, Sep 1986.

[236] Ohtani, T., *et al.* "Parameter Adaptation for Vector Controlled Induction Motor Drive Systems," *Yasakawa Denki*, vol 181, pp. 232–238, 1983.

[237] Ohtani, T., "Torque Control Using the Flux Derived from Magnetic Energy in Induction Motors Driven by Static Converter," *Conf. Record of International Power Electronics Conference*, pp. 696–707, Mar 1983.

[238] Ohyama, K., Daijou, M., Yoshida, T., Tsunehiro, Y., "A PWM Control Method of Current Source Inverter for Induction Motor Drive," *Electrical Engineering in Japan*, vol 105, no 6, pp. 117–126, Nov/Dec 1985.

[239] Ojo, O., Vipin, M., "Steady State Performance Evaluation of Saturated Field Oriented Induction Motors," *Conf. Record of IEEE-Industry Applications Society Annual Meeting*, vol 1, pp. 51–60, Oct 1990.

[240] Okuyama, T., Fujimoto, N., Matsui, T., Kubota, Y., "High Performance Speed Control Scheme of Induction Motor without Speed and Voltage Sensors," *Conf. Record of IEEE-Industry Applications Society Annual Meeting*, pp. 106–111, Sep 1986.

[241] Oszlanyi, G., Faigel, G., Pekker, S., Jannossy, A., "Orientation Distribution of Magnetic Field Oriented Yba//2Cu//30//6 Powders," *Physica C: Superconductivity* vol 167, no. 1-2, pp. 157–161, Apr 1990.

[242] Oyama, J., Higuchi, T., Abe, N., Toba, S., Yamada, E., "Characteristics of AC-Excited Brushless Synchronous Motor under Vector Control," *Conf. Record IEEE Power Electronics Specialists' Conference*, pp. 423–430, Apr 1988.

[243] Pacas, J.M., "Field-Oriented Control of the Cycloconverter Fed Doubly Fed Induction Machine," *Proc. Power Electronics & Application* pp. 3.333–3.337, Oct 1985.

[244] Park, M., Lee, H., "Sensorless Vector Control of Permanent Magnet Synchronous Motor using Adaptive Identification," *Proc. IEEE Industrial Electronics Conference* pp. 209–214, Nov 1989.

[245] Park, S-S., Cho, G-H., "A Direct Rotor Flux Controlled Induction Motor Drive for High Performance Applications," *Conf. Record of IEEE Power Electronics Specialists' Conference*, pp. 279–286, Jun 1989.

[246] Peak, S.C., Oldenkamp, J.L., "A Study of System Losses in a Transistorized Inverter-Induction Motor Drive System," *Trans. on IEEE Industry Applications Society*, vol IA-21, no 1, pp. 248–258, Jan/Feb 1985.

[247] Peak, S.C., Plunkett, A.B., "Transistorized PWM Inverter-Induction Motor Drive System," *Trans. on IEEE Industry Applications Society*, vol IA-19, no 3, pp. 379–387, May/Jun 1983.

[248] Pillay, P., "Vector control of AC permanent Magnet Machines," *Proc. Fourth International Conference on Electrical Machines and Drives*, pp. 293–297, Sep 1989.

[249] P. Pillay and R. Krishnan, "Modeling, Simulation, and Analysis of Permanent-Magnet Motor Drives, Part I : The Permanent-Magnet Synchronous Motor Drive," *Trans. on IEEE Industry Applications Society*, vol IA-25, no 2, pp. 265–273, Mar/Apr 1989.

[250] P. Pillay and R. Krishnan, "Modeling, Simulation, and Analysis of Permanent-Magnet Motor Drives, Part II : The Brushless DC Motor Drive," *Trans. on IEEE Industry Applications Society*, vol IA-25, no 2, pp. 274–279, Mar/Apr 1989.

[251] Plunkett, A.B., "Direct Flux and Torque Regulation in a PWM Inverter-Induction Motor Drive," *Trans. on IEEE Industry Applications Society*, vol IA-13, no 2, pp. 139–146, Mar/Apr 1977.

[252] Rector, H., Wasko, C.R., "Paper Machine Retro-fit Using AC Vector Control Drives," *Conf. Record of Annual Pulp and Paper Industry Technical Conference*, pp. 91–94, April 1985.

[253] Rekioua, T., Meibody T.F., Le D.R., "New approach for the Field-Oriented Control of Brushless, Synchronous, Permanent Magnet Machines," *Fourth International Conference on Power Electronics and Variable-Speed Drives*, pp. 46–50, Jul 1990.

[254] Rettig, C.E., "U.S. Patent No. 3,962,614", Jun 1976.

[255] Roos, J.G., Enslin, J.H.R., "Analysis, Simulation and Practical Evaluation of Torque Vector Control Strategies for Medium Power Highly Responsive PMSM Drives," *Fourth International Conference on Power Electronics and Variable-Speed Drives* pp. 34–39, Jul 1990.

[256] Rowan, T.M., Kerkman, R.J., Leggate, D., "A Simple On-Line Adaptation for Indirect Field Orientation of An Induction Machine," *Conf. Record of IEEE-Industry Applications Society Annual Meeting*, vol 1, pp. 579–587, Oct 1989.

[257] Rubin, N.P., Harley, R.G., Diana, G., "Evaluation of Various Slip Estimation Techniques for an Induction Machine Operating under Field Oriented Control Conditions," *Conf. Record of IEEE-Industry Applications Society Annual Meeting*, vol 1, pp. 595–600, Oct 1990.

[258] Ruohonen, I., "A Vector Controlled Cage Induction Motor Drive for Demanding Industrial Applications," *Proc. IEE Second International Conference on Power Electronics Variable Speed Drives*, (Conf. Publ No.264), pp. 191–195, Nov 1986.

[259] Sabanovic, A., Izosimov, D.B., "Application of Sliding Modes to Induction Motor Control," *Trans. on IEEE Industry Applications Society*, vol IA-17, no 1, pp. 41–49, Jan/Feb 1981.

[260] Sabanovic, A., Bilalovic, F., Music, O., "Control of Angular Position, Speed, Acceleration and Shaft Torque of Induction Motor," *Proc. Second Annual International Motor-Con Conference*, pp. 1–9, Mar 1982.

[261] Sahu, R., "Two Squirrel Cage Induction Motor Drive for Belt Conveyors of Large Capacity," *Conf. Record of IEEE Industry Applications Society Annual Meeting*, pp. 1082–1084, Oct 1977.

[262] Saito, S., Nakagawa, T., Hirata, A., Miyazaki, M., "New Application of Current-Type Inverter," *Trans. on IEEE-Industry Applications Society*, vol IA-20, no 1, pp. 226–235, Jan/Feb 1984.

[263] Saito, K., Kamiyama, K., Sukegawa, T., Matsui, T., "Multimicroprocessor-based Fully Digital AC Drive System for Rolling Mills," *Trans. on IEEE Industry Applications Society*, vol IA-23, no 3, pp. 538–544, May/June 1987.

[264] Saitoh, T., Okuyama, T., Matsui, T., "An Automated Secondary Resistance Identification Scheme in Vector Controlled Induction Motor Drives," *Conf. Record of IEEE-Industry Applications Society Annual Meeting*, vol 1, pp. 594–600, Oct 1989.

[265] Sangwongwanich, S., Ishida, M., Okuma, S., Uchikawa, Y., Iwata, K., "Time-Optimal Single-Step Velocity Response Control Scheme for Field-Oriented Induction Machines Considering Saturation Level," *IEEE Transactions on Power Electronics* vol 6, no. 1, pp. 108–117, Jan 1991.

[266] Sangwongwanich, S., Doki, S., Yonemoto, T., Okuma, S., "Adaptive Sliding Observers for Direct Field-Oriented Control of Induction Motor," *Proc. IEEE Industrial Electronics Conference*, vol II, pp. 915-920, Nov 1990.

[267] Sangwongwanich, S., Okuma, S., Uchikawa, Y., Ishida, M., Iwata, K., "Realization of Time-Optimal Single-Step Velocity Response Control of Field Oriented Induction Machines Under the Condition of Nonsaturation of Flux," *Conf. Record of IEEE Industry Applications Society Annual Meeting*, pp. 344–351, Oct 1988.

[268] Sangwongwanich, S., Ishida, M., Okuma, S., Iwata, K., "Manipulation of Rotor Flux for Time-Optimal Single-Step Velocity Response of Field-Oriented Induction Machines," *IEEE Transactions on Industry Applications* vol 24, no. 2, pp. 262–270, Mar/Apr 1988.

[269] Sathiakumar, S., Betz, R.E., Evans, R.J., "Adaptive Field-Oriented Control of an IM using Predictive Control," *IEEE Transactions on Aerospace and Electronic Systems* vol 26, no. 2, pp. 218–224, Mar 1990.

[270] Sathiakumar, S., Betz, R.E., Evans, R.J., "Adaptive Field Oriented Control of an Induction Machine using a One-Step Ahead Controller," *Proc. of IEEE Conference on decision and control* pp. 1979–1983, Dec 1987.

[271] Satoh, T., Yamamoto, T., Kataoka, K., Miyazaki, M., Matsuda, T., "An Application of AC Driving System for Processing Line, " *Conf. Record of International Power Electronics Conference*, vol 1, pp. 756–765, Mar 1983.

[272] Sattler, K., Sachaefer, U., Gheysens, R., "Field Oriented Control of an Induction Motor with Field Weakening under Consideration of Saturation and Rotor Heating," *Fourth International Conference on Power Electronics and Variable - Speed Drives*, pp. 286–291, Jul 1990.

[273] Savary, P., Nakaoka, M., Maruhashi, T., "High-Frequency Resonant Inverter using Current-Vector Control Scheme and its Performance Evaluations," *IEEE Transactions on Industrial Electronics* vol IE-34, no. 2, pp. 247–256, May 1987.

[274] Schauder, C.D., "Adaptive Speed Identification for Vector Control of Induction Motors Without Rotational Transducers," *Conf. Record of IEEE-Industry Applications Society Annual Meeting*, vol 1, pp. 493–499, Oct 1989.

[275] Schauder, C.D., Choo, F.H., Roberts, M.T., "High Performance Torque-Controlled Induction Motor Drives," *Trans. on IEEE Industry Applications Society*, vol IA-19, no 3, pp. 349–355, May/Jun 1983.

[276] Schauder, C.D., Caddy, R., "Current Control of Voltage Source Inverters for Fast-Quadrant Drive Performance," *Trans. on IEEE Industry Applications Society*, vol IA-18, no 2, pp. 163–171, May/Jun 1982.

[277] Schierling, H., "Self-Commissioning - A Novel Feature of Modern Inverter-Fed Induction Motor Drives," *Conf. Record of Third International Conference on Power Electronics and Variable Speed Drives*, Conf Publ. no 291, pp. 287–290, July 1988.

[278] Schmidt, R., "On-Line Identification on the Secondary Resistance of an Induction Motor in the Low Frequency Range using a Test Vector," *Proc. International Conference on Electrical Machines*, pp. 221–225, 1988.

[279] Schumacher, W., Leonhard, W., "Transistor-Fed AC-Servo with Microprocessor Control," *Conf. Record of International Power Electronics Conference*, pp. 1465–1476, Mar 1983.

[280] Shaker, M., Lorenzo, S., Ruiz, J.M., Martin, A., "Microprocessor Control for Induction Motor Using Boxes Theory," *Conf. Record of IEEE-Industry Applications Society Annual Meeting*, pp. 773–779, Oct 1987.

[281] Shubenko, V.A., Shreiner, R.T., Gil'derbrand, D.A., "Control of the Rotor Linkage of the Frequency-Controlled Induction Motors (Russian)," *Elektrichestvo*, no 10, pp. 13–18, Oct 1971.

[282] Singh, B.P., Gupta, J.R.P., "Simplified Analysis of Current Source Inverter Fed Induction Motor," *Proc. Second Annual International Motor-Con Conference*, pp. 181–189, Mar 1982.

[283] Sivakumar, S., Sharaf, A.M., Natarajan, K., "Improving The Performance of Indirect Field Oriented Schemes for Induction Motor Drives," *Conf. Record of IEEE Industry Applications Society Annual Meeting*, pp. 147–154, Sep 1986.

[284] Sourirajan, A., "Computer Aided Design of a Switched Reluctance Motor," *M.S. Thesis*, The Bradley Department of Electrical Engineering, Virginia Polytechnic Institute & State University, Blacksburg, VA, Jul 1987.

[285] Stanciu, D., Gavat, St., Tudor, V., "Wide Speed Range Induction Motor Drive with Vector Control Transistor Converter," *Proc. Power Electronics and Applications*, vol 2, pp. 103–106, Oct 1985.

[286] Sugi, K., Naito, Y., Kurosawa, R., Kano, Y., Katayama, S.I., Yoshida, T., "A Microcomputer-Based High Capacity Cycloconverter Drive for Main Rolling Mill," *Conf. Record of International Power Electronics Conference*, vol 1, pp. 744-755, Mar 1983.

[287] Sugimoto, H., Tamai, S., "Secondary Resistance Identification of an Induction-Motor Applied Model Reference Adaptive System and its Characteristics," *Trans. on IEEE Industry Applications Society*, vol IA-23, no 2, pp. 296–303, Mar/Apr 1987.

[288] Sugimoto, H., Tamai, S., Yano, M., "High Performance Induction Motor Drive System," *Proc. IEEE-Industrial Electronics Conference*, pp. 833–838, Oct 1984.

[289] Sul, S.K., Lipo, T.A., "Field Oriented Control of an Induction Machine in a High Frequency Link Power System," *Proc. IEEE Power Electronics Specialists' Conference* pp. 1084–1090, Apr 1988.

[290] Sul, S.K., "A Novel Technique of Rotor Resistance Estimation Considering Variation of Mutual Inductance," *Conf. Record of IEEE Industry Applications Annual Meeting*, pp. 184–188, Oct 1987.

[291] Surek, D., "Design of Adjustable-Speed Drives for Compressors (German)," *Maschinenbautechnik*, vol 36, no 8, pp. 364–370, Aug 1987.

[292] Tadakuma, S., Tanaka, S., Miura, K., Naito, H., "Vector-Controlled Induction Motors under Feedforward and Feedback Controls," *Electrical Engineering in Japan (English transalation of Denki Gakkai Ronbunshi* vol 110, no. 5, pp. 100–110, 1990.

[293] Takahashi, I., Ohmori, Y., "High Performance Direct Torque Control of an Induction Motor," *Trans. on IEEE-Industry Applications Society*, vol 25, no 2, pp. 257–264, Mar/Apr 1989.

[294] Takahashi, I., Noguchi, T., "A New Quick-Response and High Efficiency Control Strategy of an Induction Motor," *Trans. on IEEE Industry Applications Society*, vol IA-22, no 5, pp. 820–827, Sep/Oct 1986.

[295] Takahashi, I., Noguchi, T., "Quick Control of an Induction Motor by means of Instantaneous Slip Frequency Control," *Electrical Engineering in Japan*, vol 106, no 2, pp. 46–53, Mar/Apr 1986.

[296] Tamai, S., Sugimoto, H., Yano, M., "Speed Sensor-less Vector Control of Induction Motor with Model Reference Adaptive System," *Conf. Record of IEEE-Industry Applications Society Annual Meeting*, pp. 189–195, Oct 1987.

[297] Tanaka, H., Nagatani, Y., Ehara, M., "Driving System Incorporating Vector Control Inverter for Large-Scale Paper Machine," *Trans. on IEEE-Industry Applications Society*, vol IA-19, no 3, pp. 450–455, May/Jun 1983.

[298] Terashima, M., Nomura, M., Ashikaga, T., Nakamura, T., "Fully Digital Controlled Decoupled Control System in Induction Motor Drive," *Proc. IEEE-Industrial Electronics Conference*, pp. 845–850, Oct 1984.

[299] Tsuboi, T., Nakamura, K., "Control System for Traction Drives," *Hitachi Review*, vol 25, no 6, pp. 311–316, Dec 1986.

[300] Tsuji, M., Yamada, E., Izumi, K., Oyama, J., "Stability Analysis of a CSI-Fed Induction Motor with Digital Vector Controller," *Conf. Record of IEEE Power Electronics Specialists' Conference*, pp. 885–892, April 1988.

[301] Tsuji, M., Yamada, E., Izumi, K., Oyama, J., "A Sampled-Data Model of CSI-IM Vector Control System Using a Microcomputer," *Proc. Symposium on Electrical Drive*, pp. 279–284, Sep 1987.

[302] Tsuji, M., Yamada, E., Izumi, K., Oyama, J., "Rotor Flux Linkage Control of CSI-IM Vector Control System," *Proc. ICEM '86 Munchen. International Conference on Electrical Machines*, vol 3, pp. 896–899, Sep 1986.

[303] Tsuji, M., Yamada, E., Izumi, K., Oyama, J., "Comparison Between Computed and Test Results of a Vector Controlled Induction Motor Using Microprocessor," *Proc. ICEM '86 Munchen. International Conference on Electrical Machines*, vol 2, pp. 685–688, Sep 1986.

[304] Tsuji, T., "Measurement of Squirrel Cage Rotor Current by Twin Stator Induction Motors," *Proc. ICEM '86 Munchen. International Conference on Electrical Machines*, vol 2, pp. 404–407, Sep 1986.

[305] Tsuji, M., Yamada, E., Izumi, K., Oyama, J., "Transient Characteristics of CSI-IM Vector Control System for Special Operating Condition (Inverter Fed Induction Motor)," *Proc. Symposium on Electromechanics and Industrial Electronics Applied to Manufacturing Processes*, pp. 37–43, Sep 1985.

[306] Tsuji, M., Yamada, E., Izumi, K., Oyama, J., "Modeling of Current Source Inverter-Fed Induction Motor under Vector Control," *Proc. IEEE-Industrial Electronics Conference*, pp. 827–832, Oct 1984.

[307] Tsuji, M., Yamada, E., Izumi, K., Oyama, J., "Stability Analysis of a Current Source Inverter-Fed Induction Motor Under Vector Control," *Proc. International Conference on Electrical Machines*, vol 3, pp. 867–870, Sep 1984.

[308] Tsukahara, T., Nagao, Y., Kato, M., Hirotsu, K., Sasaki, H., "High Performance Inverter Driving System FRENIC 5000VG for Industrial Use," *Fuji Electric Review (Japan)*, vol 33, no 2, pp. 71–76, 1987.

[309] Tuijp, W.F.J., Honderd, G., Deleroi, W., Jonglind, W., "The Application of an Induction Motor as a Servo Drive," *System Analysis Modeling and Simulation (East Germany)*, vol 6, no 3, pp. 197–215, 1989.

[310] Tuttas, C., "Feldorientierte Reglerstrukturen der Asynchronmaschine Field- oriented control algorithms of the asynchronous machine," *ETZ Archiv* vol 10, no. 10, pp. 331–333, Oct 1988. (German)

[311] Tzou, Y-Y., W, H-J., "Multimicroprocessor-Based Robust Control of an AC Induction Servo Motor," *Conf. Record of IEEE Industry Applications Society*, vol 1, pp. 337–343, Oct 1988.

[312] Ueda, R., Sonoda, T., Fujitani, K., Yuzo Yoshida, Toshiyuki Irisa., "Investigations of Induction Motor Characteristics by Means of Vector Control," *Conf. Record of IEEE Industry Applications Society Annual Meeting*, pp. 578–585, Oct 1985.

[313] Ueda, Y., Suzuki, K., Ohnishi, K., Harashima, F., Miyachi, K., "A New Microcomputer Based Adaptive Compensation for Rotor Resistance Variation in Quick Response Induction Motor Drive," *Proc. IEEE-Industrial Electronics Conference*, pp. 863–868, Oct 1984.

[314] Ueda, Y., *et al.* "A Digital Compensation Method for Rotor Resistance Variation in High Performance Slip Frequency Control of Induction Motor," *Report of IEE of Japan*, RM-84-34.

[315] Valouch, V., "Current Control Systems of the Field-Oriented Controlled IM Drive," *Acta Techinca CSAV (Ceskoslovensk Akademie Ved* vol 35, no. 2, pp. 175–186, 1990.

[316] Valouch, V., "New High Quality Field Oriented Control of Induction Motor drives," *Acta Techica CSAV (Ceskoslovensk Akademie Ved)* vol 34, no. 3, pp. 331–347, 1989.

[317] Valouch, V., "Direct Control of Torque for Drives with Current Supplied Induction Motor and Voltage Inverter," *Elektrotech Obz. (Czechoslovakia)*, vol 73, no 5-6, pp. 317–325, May/Jun 1984.

[318] Varnovitsky, M., "Closed-Loop Torque Control System with an AC Induction Motor," *Proc. Fourth Annual International Motor-Con Conference*, pp. 8–14, Apr 1983.

[319] Vas, P., "Vector Control of AC Machines," *Oxford University Press* New York, 1990.

[320] Vas, P., Alakula, M., "Field-Oriented Control of Saturated Induction Machines," *IEEE Transactions on Energy Conversion* vol 5, no. 1, pp. 218–224, Mar 1990.

[321] Velez-Reyes, M., Minami, K., Verghese, G.C., "Recursive Speed and Parameter Estimation of Induction Machines," *Conf. Record of IEEE-Industry Applications Society Annual Meeting*, vol 1, pp. 607–611, Oct 1989.

[322] Velez-Reyes, M., "Speed and Parameter Estimation for Induction Machines," *M.S. Thesis*, Massachussetts Institute of Technology, Cambridge, 1988.

[323] Walczyna, A.M., "Static and Dynamic Properties of a Current Controlled Doubly-Fed Induction Machine," *Automatic Control - World Congress, Selected Papers from the 10th Triennial World Congress of the International Federation of Automatic Control*, vol 3, pp. 387–392, July 1987.

[324] Walter, P.J., Klein, F.N., "Vector Control gives AC Drive the Edge over DC," *Power Conversion & Intelligent Motion* vol 15, no. 6, pp. 60–62, 64, Jun 1989.

[325] Walton, S.J., "Progress in the Controllability of AC Motors," *Trans. on the Institution of Professional Engineers New Zealand*, vol 15, no 2, pp. 91–96, July 1988.

[326] Wang, C., Novotny, D.W., Lipo, T.A., "Automated Rotor Time Constant Measurement System for Indirect Field Oriented Drives," *IEEE Transactions on Industry Applications*, vol 24, no. 1, pp. 151–159, Sep 1986.

[327] Warwick, J.D., Ascherl, J.L., "Variable Frequency Drive for Existing Medium Voltage Induction Motors," *Proc. American Power Conference*, vol 47, pp. 473–479, Apr 1985.

[328] Wasko, C.R., "Universal AC Dynamomotor for Testing Motor Drive Systems," *Conf. Record of IEEE-Industry Applications Society Annual Meeting*, pp. 409–412, Oct 1987.

[329] Wasko, C.R., "AC Drives in Traction Applications," *Trans. on IEEE Industry Applications Society*, vol IA-22, no 5, pp. 842–846, Sep/Oct 1986.

[330] Wasko, C.R., "500 HP, 120 Hz Current-Fed Field-Oriented Control Inverter for Fuel Pump Test Stands," *Conf. Record of IEEE Industry Applications Society Annual Meeting* pp. 314–320, Sep 1986.

[331] Wasko, C.R., "AC Vector Control Drives for Process Applications," *Conf. Record of IEEE-Industry Applications Society Annual Meeting*, pp. 134-137, Oct 1985.

[332] Wasko, C.R., "AC Vector Control Drives for Process Applications," *Conf. Record of IEEE-1985 Thirty-Seventh Annual Conference of Electrical Engineering Problems in the Rubber and Plastics Industries*, pp. 6–9, April 1985.

[333] Washsh, S., " Harmonic Analysis by Park-Vectors for Pulsating Torques and DC Current of Induction Motor Drives with PWM Inverter," *Conf. Record of International Conference on Electrical Machines*, vol 2, pp. 695–703, Sep 1980.

[334] Webster, M.R., Diana, G., Levy, D.C., Harley, R.G., "A High Performance Interactive, Real Time Controller for a Field Oriented Controlled AC Servo Drive," *Conf. Record of IEEE-Industry Applications Society Annual Meeting*, vol 1, pp. 613–618, Oct 1990.

[335] Webster, M., Levy, D., Diana, G., Harley, R., "Space Vector Modulation and Field Oriented Control : Using Transputers and Signal Processing for Speed Control of Induction Motors," *COMSIG 1989: Proceedings of Southern African Conference on Communications and Signal Processing*, pp. 119–124, 1989.

[336] Wu, Z.K., Strangas, E.G., "Feed forward Field Orientation Control of an Induction Motor using a PWM Voltage Source Inverter and Standardized Single-Board Computers," *IEEE Transactions on Industrial Electronics*, vol. 35, no. 1, pp. 75–79, Feb 1988.

[337] Xu, X., Novotny, D.W., "Implementation of Direct Stator Flux Orientation Control on a Versatile DSP Based System," *Conf. Record of IEEE-Industry Applications Society Annual Meeting*, vol 1, pp. 404–409, Oct 1990.

[338] Xu, X., Novotny, D.W., "A Low Cost Stator Flux Oriented Voltage Source Variable Speed Drive," *Conf. Record of IEEE-Industry Applications Society Annual Meeting*, vol 1, pp. 410–415, Oct 1990.

[339] Xu, X., Novotny, D.W., "Bus Utilization of Discrete CRPWM Inverters for Field Oriented Drives," *Conf. Record of IEEE Industry Applications Society Annual Meeting*, pp. 362–367, Oct 1989.

[340] Xu, X., De Donker, R., Novotny, D.W., "A Stator Flux Oriented Induction Machine Drive," *Conference Record of IEEE-Power Electronics Specialists' Conference*, pp. 870–876, Apr 1988.

[341] Xu, Y., Cui, G., "Multiprocessor Control of a AC Motor Slip-Frequency Vector Control System," *Conf. Record of IEEE-Industry Applications Society Annual Meeting*, vol 1, pp. 672–675, Oct 1990.

[342] Yamada, E., Izumi, K., Tsuji, M., Oyama, J., "Comparison Between Computed and Test Results of a Vector Controlled Induction Motor Using Microprocessor," *Proc. ICEM '86 Munchen. International Conference on Electrical Machines*, vol 2, pp. 685–688, Sep 1986.

[343] Yamamura, S., "Modern Theory of AC Motor Drive - Analysis and Control of AC Traction Motor Drive," *Proc. International Conference on Maglev and Linear Drives*, pp. 31–37, May 1987.

[344] Yamamura, S., "Theory of Analysis of Transient Phenomena of AC Machines via Phase Separation Method and Decaying Vector Symmetrical Component Method," *Electrical Engineering in Japan*, vol 105, no 4, pp. 117–125, Jul/Aug 1985.

[345] Yamamura, S., Nakagawa, S., Kawamura, A., "Voltage Type Control of Induction Motor by Means of Field Acceleration Method," *Electrical Engineering in Japan*, vol 104, no 4, pp. 89–94, Jul/Aug 1984.

[346] Yamamura, S., Zhong, X-H., Nakagawa, S., Kawamura, A., "Analysis of Transient Phenomena and Field Acceleration Control of Induction Motors as AC Servomotor of Quick Response," *Electrical Engineering in Japan*, vol 103, no 4, pp. 67–73, Jul/Aug 1983.

[347] Yamamura, S., Nakagawa, T., Kawamura, A., "Equivalent Circuit of Induction Motor as Servo Motor of Quick Response," *Conf. Record of International Power Electronics Conference*, vol 1, pp. 732–743, Mar 1983.

[348] Yoshida, Y., Mohri, K., Kasai, K., Kondo, T., Iwabuchi, N., "Novel Rotor Current Detection Using Amorphous-Core Magnetometer," *Proc. IEEE-Industrial Electronics Conference*, pp. 147–152, Nov 1983.

[349] Yoshioka, T., Miyazaki, K., Okuyama, T., "Quick Response of AC Motor Drive System," *Hitachi Review*, vol 31, no 4, pp. 179–184, Aug 1982.

[350] Yu, L.Y.M., "Constant Starting Torque Control of Wound Rotor Induction Motors," *Trans. on IEEE Power Apparatus System*, vol PAS-89, no 4, pp. 646–651, Apr 1970.

[351] Zai, L.C., Lipo, T.A., "Extended Kalman Filter Approach to Rotor Time Constant Measurement in PWM Induction Motor Drives," *Conf. Record of 1987 IEEE Industry Applications Society Annual Meeting*, pp. 177–183, Oct 1987.

[352] Zanevskii, E.S., Legotkina, T.S., Litsyn, N.M., "Modeling of Transients in an Automated System for Programmed Hardening of Long Conical Products," *Elektrtekhnika (USSR)*, vol 55, no 11, pp. 36–38, 1985.

[353] Zhang, J., Barton, T.H., "Microprocessor-Based Primary Current Control for a Cage Induction Motor Drive," *Trans. on IEEE Power Electronics*, vol 4, no 1, pp. 73–82, Jan 1989.

[354] Zhang, J., Thiagarajan, V., Grant, T., Barton, T.H., "New approach to Field Orientation Control of a CSI Induction Motor Drive," *IEE Proceedings, Part B: Electric Power Applications* vol 135, no. 1, pp. 1–7, Jan 1988.

[355] Zhong, H.Y., Messinger, H.P., Rashid, M., "A New Microcomputer Based Torque Control System for Three Phase Induction Motors," *Conf. Record of IEEE-Industry Applications Society Annual Meeting*, vol 2, pp. 2322-2326, Oct 1989.

[356] Zimmermann, W., "Inverter Drive with Sinusoidal Machine Voltages and Vector Control (German)," *ETZ Archiv*, vol 10, no 8, pp. 259–266, Aug 1988.

[357] Zinger, D., Profumo, F., Lipo, T.A., Novotny, D.W., "A Direct Field Oriented Controller for Induction Motor Drives Using Tapped Stator Windings," *Conf. Record of IEEE-Power Electronics Specialists' Conference*, pp. 855–861, Apr 1988.

[358] Zuckerberger, A., Alexandrovitz, A., "Controller Design Method for CSIM Drives Operating Under Different Control Strategies," *Conf. Record of IEEE-Industry Applications Society Annual Meeting*, vol 1, pp. 352–362, Oct 1988.

Appendix A

MOTOR DRIVE SYSTEM PARAMETERS

Stator resistance	R_s	= 2.167 Ω
Rotor resistance	R_r	= 1.78 Ω
Stator inductance	L_s	= 0.2397 H
Rotor inductance	L_r	= 0.2541 H
Mutual inductance	L_m	= 0.2105 H
Coefficient of viscous friction	B	= 0.00154 Nm/(rad/sec)
Moment of inertia	J	= 0.00413 Kg. m^2
Number of poles	P	= 2
Rated output power	P_o	= 1 HP
Rated speed	N_s	= 3450 RPM
Rated voltage	V_r	= 230 V
Base value of current	I_b	= 2.647 A
Base value of torque	T_b	= 2.064 Nm
Base value of voltage	V_b	= 187.8 V
Maximum current limit	I_{max}	= 8 A
Maximum torque limit	T_{max}	= 2.064 Nm
PWM switching frequency	f_c	= 1 kHz

Appendix B

VOLTAGE SENSING ALGORITHM

The voltage sensing algorithm proposed in [141] reconstructs the line voltages from the base drive control signals and the measured stator currents. It is reproduced in this Appendix.

B.1 Current Segment Identification

The three stator phase currents are divided into 60 degree segments with each interval distinctly identifying a mode of operation of the inverter bridge. This is accomplished by generating six functions, A, B, C, D, E, and F as shown in Fig. B.1 for a phase sequence of abc. BA1, BA3, and BA5 are the positive half cycles of the a, b, and c stator phase currents. The other relationships are expressed as follows:

$$\begin{aligned} BA4 &= \overline{BA1} \\ BA6 &= \overline{BA3} \\ BA2 &= \overline{BA5} \end{aligned} \tag{B.1}$$

and,

$$\begin{aligned} A &= BA1.BA5 \\ B &= BA2.BA6 \\ C &= BA3.BA1 \\ D &= BA4.BA2 \end{aligned} \tag{B.2}$$

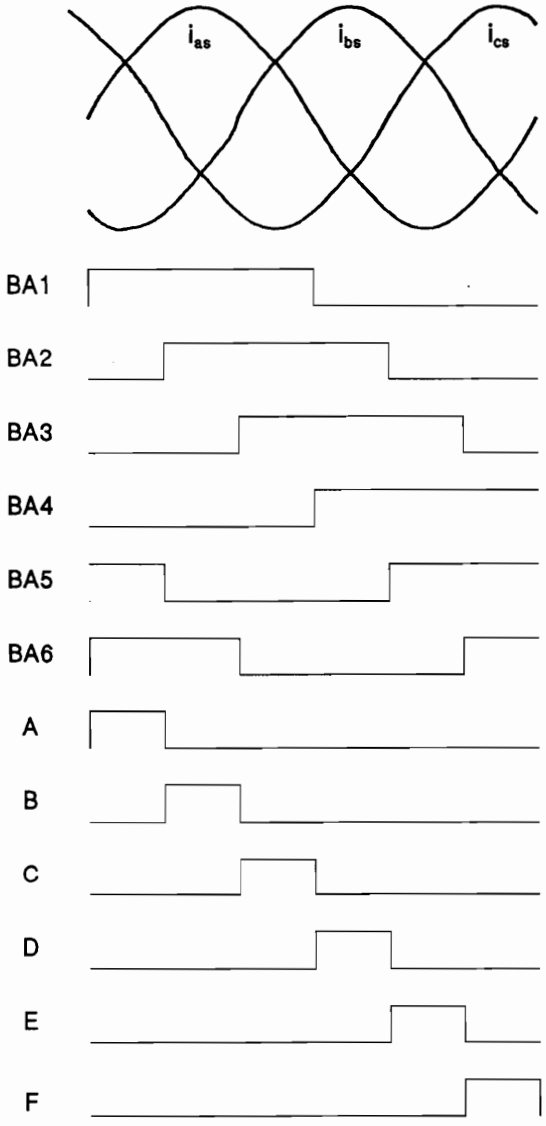

Figure B.1: Current Segment Identification

$$E = BA5.BA3$$

$$F = BA6.BA4$$

Also, it can be noted from Fig. 5.2 that B1 through B6 are the base drive signals for the switches T1 through T6.

B.2 Switching Function for Voltage Sensing

For each current segment identified in the previous subsection, the input line voltage is characterized by a circuit configuration. A step by step derivation of the switching function for the line voltage V_{ab} with all the different circuit configurations is given in detail in the following paragraphs. The circuit configurations for the current segments, A through F are given in Fig. B.2. It can be noted that regardless of the current segment, the line voltage V_{ab} would be equal to the positive dc bus voltage if the switches T_1 and T_6 are ON. The switching function for this condition is given as,

$$(A + B + C + D + E + F).B1.B6 \tag{B.3}$$

Similarly, V_{ab} would be equal to the negative dc bus voltage if the switches T_3 and T_4 are ON. This can be characterized by the following switching function,

$$(A + B + C + D + E + F).B3.B4 \tag{B.4}$$

Fig. B.2(a) corresponds to the circuit configuration for the current segment A. There are five valid conditions which are given here along with their switching function. If all the four switches are OFF and the diodes D_3 and D_4 are freewheeling, V_{ab} is equal to the negative dc bus voltage. The switching function for this condition is given as,

$$A.\overline{B1}.\overline{B3}.\overline{B4}.\overline{B6} \tag{B.5}$$

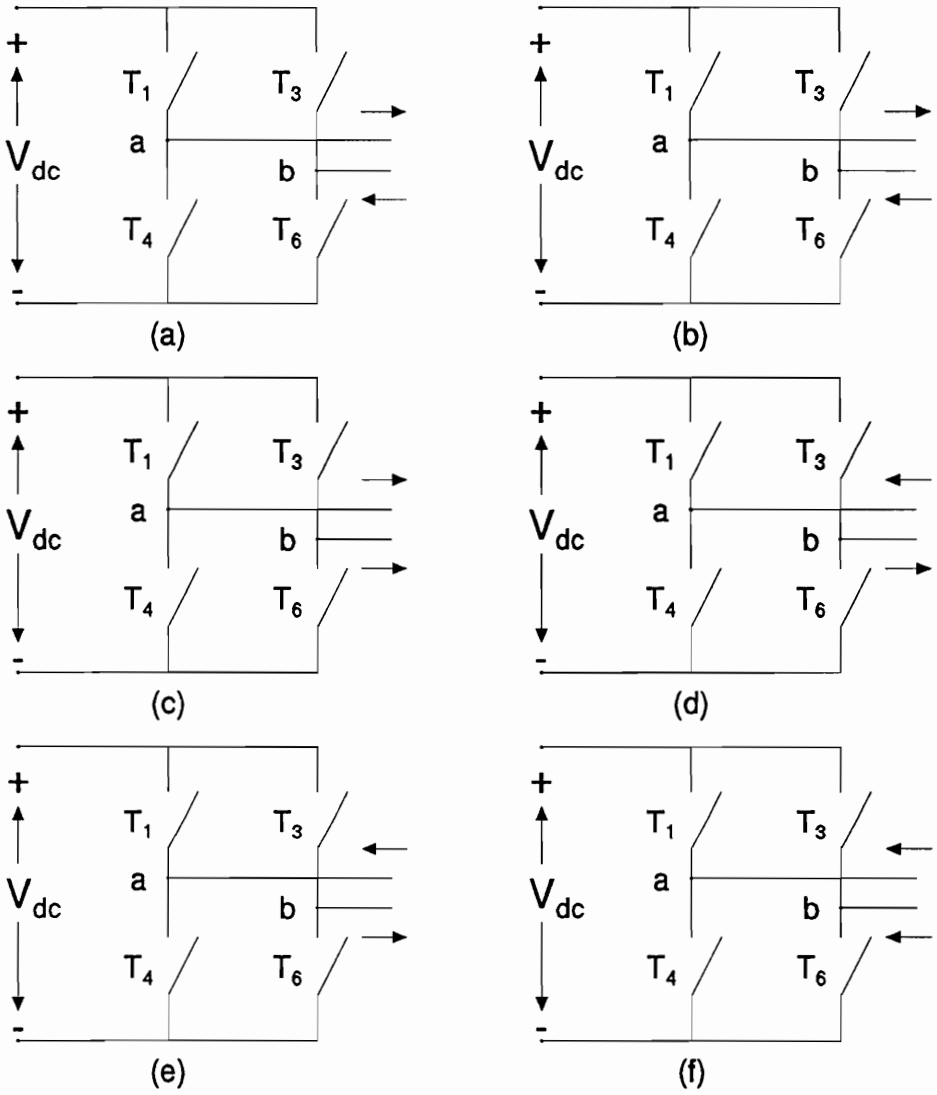

Figure B.2: Circuit Configuration of Various Modes

The next valid condition is if T_3 is ON and both the diodes D_3 and D_4 are freewheeling, in which case V_{ab} is equal to the negative dc bus voltage. The switching function is given as,

$$A.\overline{B1}.B3.\overline{B4}.\overline{B6} \tag{B.6}$$

The third condition is if T_4 is ON and both the diodes D_3 and D_4 are freewheeling, and again V_{ab} is equal to the negative dc bus voltage. The switching function is given as,

$$A.\overline{B1}.\overline{B3}.B4.\overline{B6} \tag{B.7}$$

The fourth condition is if the transistor T_6 is ON and the return path is provided through the freewheeling diode, D_4, in which case V_{ab} is equal to zero. The switching function for this condition is given as,

$$A.\overline{B1}.\overline{B3}.\overline{B4}.B6 \tag{B.8}$$

The last is if the transistor T_1 is ON and the return path is provided through the freewheeling diode, D_3, in which case V_{ab} is equal to zero. The switching function for this condition is given as,

$$A.B1.\overline{B3}.\overline{B4}.\overline{B6} \tag{B.9}$$

In a similar fashion, for the current segment B, the valid conditions and the switching functions are given from Fig. B.2(b) as,

$$\begin{aligned}
All\ OFF:\ D_3, D_4 &\Rightarrow B.\overline{B1}.\overline{B3}.\overline{B4}.\overline{B6} \Rightarrow V_{ab} = -V_{dc} \\
T_3\ ON:\ D_3, D_4 &\Rightarrow B.\overline{B1}.B3.\overline{B4}.\overline{B6} \Rightarrow V_{ab} = -V_{dc} \\
T_4\ ON:\ D_3, D_4 &\Rightarrow B.\overline{B1}.\overline{B3}.B4.\overline{B6} \Rightarrow V_{ab} = -V_{dc} \\
T_6\ ON:\ B_6, D_4 &\Rightarrow B.\overline{B1}.\overline{B3}.\overline{B4}.B6 \Rightarrow V_{ab} = 0
\end{aligned} \tag{B.10}$$

$$T_1\ ON:\ B_1, D_3 \ \Rightarrow B.B1.\overline{B3}.\overline{B4}.\overline{B6} \ \Rightarrow V_{ab} = 0$$

The circuit configuration for current segment C, is given in Fig. B.2(c). The valid conditions and switching functions are given as,

$$\begin{aligned}
All\ OFF:\ D_4, D_6 &\Rightarrow B.\overline{B1}.\overline{B3}.\overline{B4}.\overline{B6} \ \Rightarrow V_{ab} = 0 \\
T_3\ ON:\ B_3, D_4 &\Rightarrow B.\overline{B1}.B3.\overline{B4}.\overline{B6} \ \Rightarrow V_{ab} = -V_{dc} \\
T_4\ ON:\ D_4, D_6 &\Rightarrow B.\overline{B1}.\overline{B3}.B4.\overline{B6} \ \Rightarrow V_{ab} = 0 \\
T_6\ ON:\ D_4, D_6 &\Rightarrow B.\overline{B1}.\overline{B3}.\overline{B4}.B6 \ \Rightarrow V_{ab} = 0 \\
T_1\ ON:\ B_1, D_6 &\Rightarrow B.B1.\overline{B3}.\overline{B4}.\overline{B6} \ \Rightarrow V_{ab} = +V_{dc}
\end{aligned} \tag{B.11}$$

The circuit configurations for the current segments D, E, and F are given in Fig. B.2 (d), (e), and (f), respectively. The switching functions are derived for these conditions in the same manner as described above. Similarly, the other line voltages are obtained. Hence the overall switching function for the line voltages, V_{ab} and V_{ca} are given by the following equations,

$$\begin{aligned}
V_{ab} &= +V_{dc} \\
&= (A+B+C+D+E+F).B1.B6 + C.B1.\overline{B3}.\overline{B4}.\overline{B6} + D.\overline{B1}.\overline{B3}.\overline{B4}.B6 + \\
&\quad D.B1.\overline{B3}.\overline{B4}.\overline{B6} + D.\overline{B1}.\overline{B3}.\overline{B4}.\overline{B6} + E.\overline{B1}.\overline{B3}.\overline{B4}.B6 + \\
&\quad E.\overline{B1}.\overline{B3}.\overline{B4}.\overline{B6} + E.B1.\overline{B3}.\overline{B4}.\overline{B6} + F.\overline{B1}.\overline{B3}.\overline{B4}.B6
\end{aligned} \tag{B.12}$$

$$\begin{aligned}
V_{ab} &= -V_{dc} \\
&= (A+B+C+D+E+F).B3.B4 + A.\overline{B1}.\overline{B3}.\overline{B4}.\overline{B6} + A.\overline{B1}.B3.\overline{B4}.\overline{B6} + \\
&\quad A.\overline{B1}.\overline{B3}.B4.\overline{B6} + B.\overline{B1}.\overline{B3}.\overline{B4}.\overline{B6} + B.\overline{B1}.B3.\overline{B4}.\overline{B6} + \\
&\quad B.\overline{B1}.\overline{B3}.B4.\overline{B6} + C.\overline{B1}.B3.\overline{B4}.\overline{B6} + F.\overline{B1}.\overline{B3}.B4.\overline{B6}
\end{aligned} \tag{B.13}$$

$$
\begin{aligned}
V_{ca} &= +V_{dc} \\
&= (A+B+C+D+E+F).B4.B5 + A.\overline{B1}.\overline{B2}.\overline{B4}.B5 + B.\overline{B1}.\overline{B2}.\overline{B4}.\overline{B5} + \\
&\quad B.\overline{B1}.\overline{B2}.B4.\overline{B5} + B.\overline{B1}.\overline{B2}.\overline{B4}.B5 + C.\overline{B1}.\overline{B2}.\overline{B4}.\overline{B5} + \\
&\quad C.\overline{B1}.\overline{B2}.B4.\overline{B5} + C.\overline{B1}.\overline{B2}.\overline{B4}.B5 + D.\overline{B1}.\overline{B2}.B4.\overline{B5}
\end{aligned} \tag{B.14}
$$

$$
\begin{aligned}
V_{ca} &= -V_{dc} \\
&= (A+B+C+D+E+F).B1.B2 + A.B1.\overline{B2}.\overline{B4}.\overline{B5} + D.\overline{B1}.B2.\overline{B4}.\overline{B5} + \\
&\quad E.\overline{B1}.\overline{B2}.\overline{B4}.\overline{B5} + E.B1.\overline{B2}.\overline{B4}.\overline{B5} + E.\overline{B1}.B2.\overline{B4}.\overline{B5} + \\
&\quad F.\overline{B1}.\overline{B2}.\overline{B4}.\overline{B5} + F.B1.\overline{B2}.\overline{B4}.\overline{B5} + F.\overline{B1}.B2.\overline{B4}.\overline{B5}
\end{aligned} \tag{B.15}
$$

The phase voltages are then obtained from the line voltages by,

$$V_{as} = \frac{V_{ab} - V_{ca}}{3} \tag{B.16}$$

$$V_{cs} = \frac{V_{ab} + 2V_{ca}}{3} \tag{B.17}$$

$$V_{bs} = -(V_{as} + V_{cs}) \tag{B.18}$$

Reversal of rotation is achieved by a phase sequence reversal of the stator currents in the induction motors. The switching functions derived above are valid for any phase sequence which is of significant importance for four quadrant operation of the motor drive system.

Appendix C

LIST OF SYMBOLS

A_e Gain of the PWM controller

B Coefficient of viscous friction

f_B Base frequency

f_c PWM switching frequency

i_{as} Actual value of A phase current

i^*_{as} Commanded value of A phase current

i_{bs} Actual value of B phase current

i^*_{bs} Commanded value of B phase current

i_{cs} Actual value of C phase current

i^*_{cs} Commanded value of C phase current

i_f Actual value of field current

i^*_f Actual value of field current

i_{dr} Actual value of d axis rotor current

i_{ds} Actual value of d axis stator current

i^*_{ds} Commanded value of d axis stator current

i_{qr} Actual value of q axis rotor current

i_{qs} Actual value of q axis stator current

i^*_{qs} Commanded value of q axis stator current

i_s Stator phase current

i_t Actual value of torque current

i^*_t Actual value of torque current

I_{asn}	Normalized value of A phase stator current
I_b	Base value of current
I_{fn}	Normalized value of field current
I_{max}	Maximum current limit
I_{tn}	Normalized value of torque current
J	Moment of inertia
K_d	Derivative constant
K_i	Integral constant
K_p	Proportional constant
K_t	Torque constant
L_a	Equivalent inductance
L_m	Mutual inductance
L_r	Rotor inductance
L_s	Stator inductance
N_s	Rated speed
p	Derivative operator
P	Number of poles
P_a	Airgap power
P_o	Rated output power
$Psirn$	Normalized value of rotor flux
R_r	Rotor resistance
R_s	Stator resistance
T_b	Base value of torque
T_e	Actual value of electromagnetic torque
T_e^*	Commanded value of electromagnetic torque
T_{en}	Normalized value of electromagnetic torque

T_l	Load torque
T_{max}	Maximum torque limit
$Thetar$	Angular value of rotor position
v_{as}	Actual value of A phase voltage
v_{as}^*	Commanded value of A phase voltage
v_{bs}	Actual value of B phase voltage
v_{bs}^*	Commanded value of B phase voltage
v_{cs}	Actual value of C phase voltage
v_{cs}^*	Commanded value of C phase voltage
v_{dr}	Actual value of d axis rotor voltage
v_{ds}	Actual value of d axis stator voltage
v_{ds}^*	Commanded value of d axis stator voltage
v_{qr}	Actual value of q axis rotor voltage
v_{qs}	Actual value of q axis stator voltage
v_{qs}^*	Commanded value of q axis stator voltage
V_{asn}	Normalized value of A phase stator voltage
V_b	Base value of voltage
V_{dc}	DC link voltage
V_{ll}	line to line voltage
V_r	Rated voltage
W_{rn}	Normalized value of rotor speed
α	Triggering angle for the rectifier
Δi	Current window for hysteresis controller
θ_f	Field angle
θ_r	Actual value of angular rotor position
θ_r^*	Commanded value of angular rotor position

θ_{sl}	Actual value of slip angle
θ^*_{sl}	Commanded value of slip angle
θ_{sc}	Stator phasor angle with the current vector
θ_{sv}	Stator phasor angle with the voltage vector
θ_{tc}	Torque angle with the current vector
θ_{tv}	Torque angle with the voltage vector
ψ_{dr}	Actual value of d axis rotor flux
ψ_{ds}	Actual value of d axis stator flux
ψ_{qr}	Actual value of q axis rotor flux
ψ_{qs}	Actual value of q axis stator flux
ψ_r	Actual value of rotor flux
ψ^*_r	Commanded value of rotor flux
ω_b	Base value of speed
ω_e	Synchronous speed
ω_r	Actual value of rotor speed
ω^*_r	Commanded value of rotor speed
ω_{sl}	Actual value of rotor speed
ω^*_{sl}	Commanded value of rotor speed

VITA

Aravind S. Bharadwaj was born in Madras, India on May 21, 1964. He received the B.E. degree with Honors in Electronics and Communication Engineering from Madurai Kamaraj University, India in 1985 and the M.S. degree in Electrical Engineering from Virginia Polytechnic Institute and State University (VPI&SU) in 1987. He joined the Ph.D. program at VPI&SU in the winter quarter of 1988. His research interests are in the area of motion control systems and power electronics in which he has published several papers in international conferences and refereed journals. He is a member of IAS, PES and IES of IEEE and received the outstanding student member award in 1985. He will be joining the GM Research Labs soon after graduation to pursue his research in the area of power electronics. His hobbies include tennis, jogging and travel.

Aravind S. Bharadwaj